

AD-A193 831

DIESEL COMBUSTION FUNDAMENTALS PHASE 1 VOLUME 1  
TECHNICAL REPORT(U) MISSOURI UNIV-ROLLA DEPT OF  
MECHANICAL AND AEROSPACE ENGINEERING R T JOHNSON

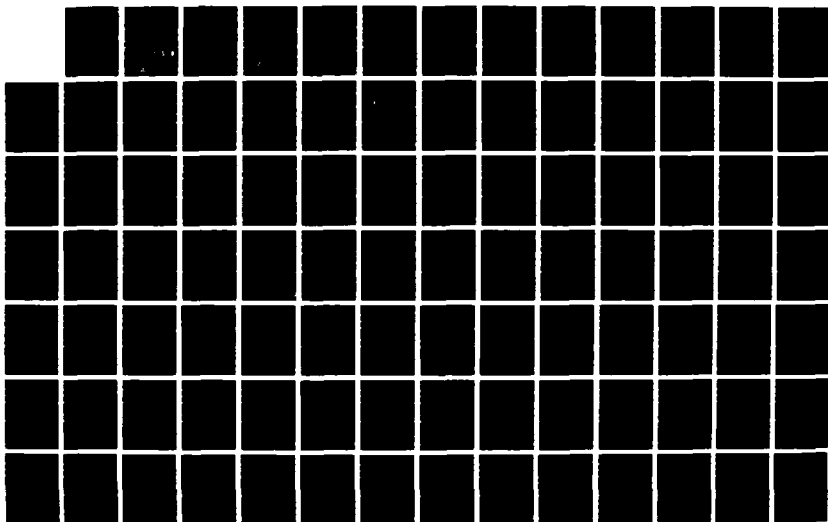
1/2

UNCLASSIFIED

JUL 87

F/G 21/2

NL





MICROCOPY RESOLUTION TEST CHART  
 5-1-61

AD-A193 831

Department of  
**Mechanical and Aerospace Engineering**

**DIESEL COMBUSTION FUNDAMENTALS  
PHASE I**

by

**R.T. Johnson  
Professor**

**FINAL REPORT**

**APPROVED FOR PUBLIC RELEASE; DISTRIBUTION UNLIMITED**

**Prepared for**

**The Coordinating Research Council, Inc.  
219 Perimeter Center Parkway  
Atlanta, Georgia 30346**

**Project CM-126**

**July, 1987**

**DTIC  
ELECTE  
MAY 11 1988  
S H D**

**VOLUME I—TECHNICAL REPORT**



**University of Missouri-Rolla**

**88 5 10 158**

NOTE: Since the Appendices of this report are voluminous, it has purposely been prepared without them to serve as a summary of the project. If you need the additional detail present in the Appendices, please request them from Mr. Alan E. Zengel, 219 Perimeter Center Parkway, Atlanta, GA 30346. (Phone 404-396-3400)



---

Department of  
**Mechanical and Aerospace Engineering**

---

**DIESEL COMBUSTION FUNDAMENTALS  
PHASE I**

BY

**R. T. JOHNSON  
PROFESSOR**

**FINAL REPORT**

PREPARED FOR

**THE COORDINATING RESEARCH COUNCIL, INC.  
219 PERIMETER CENTER PARKWAY  
ATLANTA, GEORGIA 30346**

**PROJECT CM-126**

**JULY, 1987**



**University of Missouri-Rolla**

---

DIESEL COMBUSTION FUNDAMENTALS  
PHASE I

by

R. T. Johnson  
Professor,  
Department of Mechanical and Aerospace Engineering  
University of Missouri - Rolla  
Rolla, Missouri 65401

FINAL REPORT

Prepared for  
The Coordinating Research Council, Inc.  
219 Perimeter Center Parkway  
Atlanta, Georgia 30346

Project CM-126

## FORWARD

The research project described in this report was performed for the Coordinating Research Council, under the guidance of the Light Duty Diesel Combustion Group, at the University of Missouri - Rolla in the Mechanical and Aerospace Engineering Department. The project was initiated in Early 1984 and completed in June, 1987. A significant number of people were involved with the project and not all can be recognized here, however, some of the more important contributors are:

### CRC Staff:

Alan E. Zengel, Secretary and General Manager  
Gayle H. Greenwood, Recording Secretary

### Light Duty Diesel Combustion Group (members specifically involved):

#### Committee Chairmen;

Garbis H. Meguerian  
Research Department  
Amoco Oil Company (Retired)

Joseph M. Perez  
Research Department  
Caterpillar Tractor Company (Retired)\*  
\* Now with National Bureau of Standards

Michael McMillan  
Fuels and Lubricants Department  
General Motors Research

#### Assistance with Statistical Analyses;

Fredric Rakowsky  
Research Department  
Amoco Oil Company



#### Assistance with Fuel Properties Organization;

William Marshall  
NIPER

#### Assistance in Obtaining DOE Fuels;

Ralph D. Fleming  
U.S. Department of Energy (retired)\*  
\* Currently a consultant

#### Assistance in Obtaining CEC Fuels;

E. G. Barry  
Mobil Oil Company

Accession For	
NTIS GRA&I	<input checked="" type="checkbox"/>
DTIC TAB	<input type="checkbox"/>
Unannounced	<input type="checkbox"/>
Justification	
By	
Distribution/	
Availability Codes	
Dist	Avail and/or Special
A-1	

Special Assistance from others:

Collation of Fuel Properties Data;

Don Seizinger  
NIPER

Assistance with Equipment and Instrumentation;

Raymond Keller  
President  
AVL of North America

Richard K. Riley  
Research Department  
Phillips Petroleum Company

University of Missouri - Rolla Faculty, Staff, and Students:

Richard T. Johnson, Project Directory and Principal Investigator  
Kenneth R. Schmid, Teaching Associate and Technical Consultant  
Marcus Merrideth, Student Research Assistant  
Michael Luetkemeyer, Student Research Assistant

Other members of the Light Duty Diesel Combustion Group:

W. A. Buscher, Jr.	Texaco
J. A. Dystrup	Caterpillar
R. T. Holmes	Shell
J. W. Horst	Mercedes-Benz
C. E. Hunter	Ford Motor Company
M. C. Ingham	Chevron Research
R. Y. Iwamoto	Unocal
R. F. Klein	Volkswagen
B. J. Kraus	Exxon Research & Engineering
D. L. Lenane	Ethyl Petroleum Additives
K. Mitchell	Shell of Canada
D. Noble	Perkins Engines
R. F. Parker	John Deere
P. Polss	Du Pont
R. Primus	Cummins Engine
J. R. Regueiro	Chrysler
D. C. Siegla	General Motors Research Lab.
J. S. Smith	Sun R&M
R. D. Tharby	PetroCanada
G. D. Webster	National Research Council, Canada

## Table of Contents

<u>Page</u>	
Forward .....	ii
Table of Contents .....	iv
List of Figures .....	vi
List of Tables .....	xi
Summary .....	xii
1. Introduction .....	1
1.1 Review of the Cetane Rating Procedure .....	1
1.2 Basic Approach for this Project .....	4
1.3 General Conduct of the Work .....	5
2. Fuels .....	6
2.1 History of Fuel Selection .....	6
2.2 Summary Properties of Fuels .....	8
3. Equipment .....	11
3.1 Engine Test Apparatus .....	11
3.2 Emissions Measurement Instrumentation .....	14
3.2.1 Gaseous Emissions .....	14
3.2.2 Smoke and Particulate Measurements .....	16
3.3 Combustion Instrumentation .....	18
3.4 Computer Data Acquisition Equipment .....	22
4. Test Program .....	25
4.1 Test and Operating Conditions .....	25
4.2 Test and Operating Procedures .....	28
4.2.1 System Start-up .....	28
4.2.2 Optimum Injection Timing .....	29
4.2.3 Performance and Emissions Measurements .....	30
4.2.4 Particulates Sampling .....	32
4.2.5 Data Acquisition for Combustion Analysis .....	35
4.2.6 Required Maintenance .....	37
4.3 Test Sequence .....	38
5. Data Reduction Methods .....	42
5.1 Engine Performance .....	42
5.2 Specific Emissions .....	44
5.3 Combustion Characteristics and Parameters .....	45
5.4 Data Quality Measures .....	51
6. Results .....	55
6.1 Fuel Property Information .....	55
6.2 Detailed Results for Cetane Engine .....	55
6.2.1 Calculated Data, Cetane Engine .....	55
6.2.2 Graphical Results, Cetane Engine .....	60
6.3 Example Detailed Results for Ricardo Engines .....	71
6.4 Summary Graphical Results for Cetane Engine .....	81
6.4.1 Test Condition and Engine Variable Effects, Cetane Engine ....	89

## Table of Contents (cont'd)

### Page

6.4.2 Fuel Effects, Cetane Engine .....	111
6.4.3 Statistical Relationships .....	124
6.5 Summary Graphical Results for Ricardo Engines .....	133
6.5.1 Test Condition and Engine Variable Effects, Ricardo Engines ..	140
6.5.2 Fuel Effects, Ricardo Engines .....	142
6.6 Comparison of Results from Cetane and Ricardo Engines .....	144
6.7 Ranking of Fuels .....	146
7. Conclusions and Recommendations .....	149
References .....	151

### Appendices\*

A. Review of Detailed Results Data for Cetane Engine	
B. Summary Tabulated Data from Cetane Engine Test Program	
C. Data for DOE/Ricardo Fuel #1	
D. Data for DOE/Ricardo Fuel #2	
E. Data for DOE/Ricardo Fuel #3	
F. Data for DOE/Ricardo Fuel #4	
G. Data for CAPE-32 Fuel #5	
H. Data for CAPE-32 Fuel #6	
I. Data for CEC Fuel #1	
J. Data for CEC fuel #2	
K. Data for CEC fuel #2A	
L. Data for CEC fuel #3	
M. Data Prepared from DOE/Ricardo Program	

\* Note: Appendices are listed here for reference only. Due to the volume of material in these sections, they are contained in two separately bound volumes.

## List of Figures

Fig. No.	Title	Page
1-1	Schematic of Cetane Rating Cylinder & Head Assembly for ASTM-CFR Engine	3
3-1	Comparison of Cetane, Direct Injection, and Indirect Injection Combustion Systems	12
3-2	Modified Cetane Engine Test Apparatus	13
3-3	Schematic, Emissions Instrumentation and Sample Systems	15
3-4	Schematic, Mini-Dilution Tunnel System	17
3-5	Schematic, Cetane Head Transducer Installations	19
3-6	Changes in Fuel Injector for Lift Transducer	21
3-7	High Speed Data Acquisition and Processing System	23
4-1	Determination of Optimum Injection Timing for Cetane Engine	31
4-2	Sample Laboratory Data Sheet for Engine Performance and Emissions	33
4-3	Sample Laboratory Data Sheet for Particulates Measurements	36
5-1	dP/d $\theta$ Data Illustrating Determination of Start of Combustion	49
5-2	Determination of Diesel Combustion Analysis Parameters	52
5-3	Determination of End of Premixed Combustion Mode	53
5-4	Motoring Test Confirming Pressure Transducer Response	54
6-1	Example Laboratory Data Sheet for Cetane Engine Performance and Emissions	57
6-2	Example Laboratory Data Sheet for Cetane Engine Particulates Measurements	58
6-3	Example Calculated Results Sheet for Performance and Emissions, Cetane Engine	59
6-4	Example Calculated Results Sheet for Combustion Parameters, Cetane Engine	61
6-5	Example Calculated Results for Data Quality Check, Cetane Engine	62

# List of Figures(continued)

Fig. No.	Title	Page
6-6	Example Plotted Results, Main Chamber Pressure, Full Cycle Data, Cetane Engine	63
6-7	Example Plotted Results, Main Chamber Pressure Variance, Full Cycle Data, Cetane Engine	64
6-8	Example Plotted Results, Log-Pressure vs Log-volume, Main Chamber, Full Cycle Data, Cetane Engine	66
6-9	Example Plotted Results, Crank Case Pressure, Full Cycle Data, Cetane Engine	67
6-10	Example Plotted Results, Pre-Chamber Pressure, High Speed Data System, Cetane Engine	68
6-11	Example Plotted Results, Main Chamber Pressure, High Speed Data System, Cetane Engine	69
6-12	Example Plotted Results, Pre-Chamber Pressure Derivative, High Speed Data System, Cetane Engine	70
6-13	Example Plotted Results, Injector Lift and Pressure, High Speed Data System, Cetane Engine	72
6-14	Example Plotted Results, Estimated Bulk Gas Temperature, High Speed Data System, Cetane Engine	73
6-15	Example Plotted Results, Normalized Apparent Heat Release, Cetane Engine	74
6-16	Example Plotted Results, Normalized Rate of Heat Release (ROHR), Cetane Engine	75
6-17	Example Plotted Results, Normalized Derivative of ROHR, Cetane Engine	76
6-18	Example Calculated Results Sheet for Performance and Emissions, Ricardo IDI Engine	78
6-19	Example Calculated Results Sheet for Combustion Parameters, Ricardo IDI Engine	79
6-20	Example Plotted Results, Log-Pressure vs Log-volume, Main Chamber, Ricardo IDI Engine	80
6-21	Example Plotted Results, Main Chamber Pressure, Ricardo IDI Engine	82
6-22	Example Plotted Results, Main Chamber Pressure Derivative, Ricardo IDI Engine	83



# List of Figures(continued)

Fig. No.	Title	Page
6-23	Example Plotted Results, Injector Lift and Pressure, Ricardo IDI Engine	84
6-24	Example Plotted Results, Estimated Bulk Gas Temperature, Ricardo IDI Engine	85
6-25	Example Plotted Results, Normalized Apparent Heat Release, Ricardo IDI Engine	86
6-26	Example Plotted Results, Normalized Rate of Heat Release (ROHR), Ricardo IDI Engine	87
6-27	Example Plotted Results, Normalized Derivative of ROHR, Ricardo IDI Engine	88
6-28	Cetane Engine, DOE #1 Fuel, Emissions, Fuel Consumption, and Air/Fuel Ratio	90
6-29	Cetane Engine, DOE #2 Fuel, Emissions, Fuel Consumption, and Air/Fuel Ratio	91
6-30	Cetane Engine, DOE #3 Fuel, Emissions, Fuel Consumption, and Air/Fuel Ratio	92
6-31	Cetane Engine, DOE #4 Fuel, Emissions, Fuel Consumption, and Air/Fuel Ratio	93
6-32	Cetane Engine, CEC #1 Fuel, Emissions, Fuel Consumption, and Air/Fuel Ratio	94
6-33	Cetane Engine, CEC #2 Fuel, Emissions, Fuel Consumption, and Air/Fuel Ratio	95
6-34	Cetane Engine, CEC #2A Fuel, Emissions, Fuel Consumption, and Air/Fuel Ratio	96
6-35	Cetane Engine, CEC #3 Fuel, Emissions, Fuel Consumption, and Air/Fuel Ratio	97
6-36	Cetane Engine, CAPE #5 Fuel, Emissions, Fuel Consumption, and Air/Fuel Ratio	98
6-37	Cetane Engine, CAPE #6 Fuel, Emissions, Fuel Consumption, and Air/Fuel Ratio	99
6-38	Cetane Engine, DOE #1 Fuel, Combustion Parameters	101
6-39	Cetane Engine, DOE #2 Fuel, Combustion Parameters	102
6-40	Cetane Engine, DOE #3 Fuel, Combustion Parameters	103

# List of Figures(continued)

Fig. No.	Title	Page
6-41	Cetane Engine, DOE #4 Fuel, Combustion Parameters	104
6-42	Cetane Engine, CEC #1 Fuel, Combustion Parameters	105
6-43	Cetane Engine, CEC #2 Fuel, Combustion Parameters	106
6-44	Cetane Engine, CEC #2A Fuel, Combustion Parameters	107
6-45	Cetane Engine, CEC #3 Fuel, Combustion Parameters	108
6-46	Cetane Engine, CAPE #5 Fuel, Combustion Parameters	109
6-47	Cetane Engine, CAPE #6 Fuel, Combustion Parameters	110
6-48	Cetane Engine, DOE #1 Fuel, Combustion Analysis Parameters	112
6-49	Cetane Engine, DOE #2 Fuel, Combustion Analysis Parameters	113
6-50	Cetane Engine, DOE #3 Fuel, Combustion Analysis Parameters	114
6-51	Cetane Engine, DOE #4 Fuel, Combustion Analysis Parameters	115
6-52	Cetane Engine, CEC #1 Fuel, Combustion Analysis Parameters	116
6-53	Cetane Engine, CEC #2 Fuel, Combustion Analysis Parameters	117
6-54	Cetane Engine, CEC #2A Fuel, Combustion Analysis Parameters	118
6-55	Cetane Engine, CEC #3 Fuel, Combustion Analysis Parameters	119
6-56	Cetane Engine, CAPE #5 Fuel, Combustion Analysis Parameters	120
6-57	Cetane Engine, CAPE #6 Fuel, Combustion Analysis Parameters	121
6-58	DOE/Ricardo IDI Engine, DOE Fuels 1-4, Emissions, Fuel Consumption, and Air/Fuel Ratio	134
6-59	DOE/Ricardo DI Engine, DOE Fuels 1-4, Emissions, Fuel Consumption, and Air/Fuel Ratio	135
6-60	DOE/Ricardo IDI Engine, DOE Fuels 1-4, Combustion Parameters	136
6-61	DOE/Ricardo DI Engine, DOE Fuels 1-4, Combustion Parameters	137

List of Figures(continued)

Fig. No.	Title	Page
6-62	DOE/Ricardo IDI Engine, DOE Fuels 1-4, Combustion Analysis Parameters	138
6-63	DOE/Ricardo DI Engine, DOE Fuels 1-4, Combustion Analysis Parameters	139

## List of Tables

Table No.	Title	Page
2-1	Fuel Property Data Determined by SouthWest Research	9
4-1	Cetane Engine Test Conditions	27
4-2	Particulate Dilution Tunnel Operating Conditions	27
4-3	Interpretation of Data Set Identifier Code	34
4-4	Test Sequence for Each Fuel	39
4-5	Summary of Test Runs	39
6-1	Summary Fuel Properties	56
6-2	Correlation Coefficients for Fuel Properties Used as Independent Variables	126
6-3	Linear Regression Results for Cetane Engine, Full Load Optimum Injection Timing	128
6-4	Linear Regression Results for Cetane Engine, Medium Load Optimum Injection Timing	129
6-5	Linear Regression Results for Cetane Engine, Medium Load Retarded Injection Timing	130
6-6	Linear Regression Results for Cetane Engine, Light Load Optimum Injection Timing	131
6-7	Fuels - Results Matrix for Use in Ranking Fuels	147
6-8	Ranking of Ten Test Fuels	148

## Summary

The general goal of the CM-126 project on "Diesel Combustion Fundamentals" was to operate the Cooperative Fuel Research engine for rating diesel fuels (cetane engine) at conditions more representative of modern diesel engines and determine if results could be obtained that would better predict fuel behavior in modern engines. This goal was pursued by installing extensive instrumentation and data acquisition facilities on a cetane engine and evaluating the performance, emissions and combustion characteristics of ten different diesel fuels that had a wide range of different properties.

After substantial experimental investigation, operating conditions for the cetane engine were established using an engine speed of 1200 rpm and a compression ratio of 20:1. The engine speed was sufficient to eliminate data reproducibility problems encountered at the standard cetane rating speed of 900 rpm. The 20:1 compression ratio was selected as a compromise between nominal values for DI and IDI engines. Detailed test, operation, and maintenance procedures were established to provide consistent results from the cetane engine.

The ten fuels used in the program were selected from other research programs dealing with diesel combustion that had either been completed or were in progress. Of particular interest were four fuels from a U.S. Department of Energy sponsored program at Ricardo Consulting Engineers, Ltd. and four fuels from a program coordinated by CEC in Europe. Both of these programs involved engine test work, and the potential for direct comparison of results between programs was very high.

The ten fuels were evaluated in the cetane engine, and substantial performance, emissions, and combustion data were taken and analyzed. Results, in the form of specific emissions, imep, and combustion parameters determined from apparent heat release computations, were prepared and examined. Similar data reduction was performed using information from Ricardo on the performance of the Ricardo DI and IDI engines using four of the selected test fuels.

After review of the results generated from the cetane engine test programs and the results determined using data from the DOE/Ricardo program, the following limited conclusions were drawn:

1. The cetane engine can be operated at conditions more representative of current design diesel engines and provides consistent results for engine performance, emissions, and combustion characteristics.
2. The results obtained indicate that the cetane number is a good indicator of fuel behavior in the cetane engine.
3. Comparison of results between the cetane engine and the Ricardo engines indicated that the fuel performance in the cetane engine was not necessarily a good indicator of how that fuel would behave in the Ricardo engines or other commercial engines that they represent. As might be expected, the cetane results showed

greater similarities to the results for the Ricardo IDI engine than for the DI engine.

Since no comparisons have been made with data resulting from the CEC program in Europe, these conclusions must be recognized as limited in scope. It is recommended that this CRC program be followed by another program that will make these comparisons to the CEC data when it becomes available, further refine the data analysis methods as needed, and investigate cetane engine operation at low intake air temperatures. The behavior of primary and secondary reference materials at these temperatures should also be examined.

## 1. Introduction

The combustion quality of fuels for compression ignition engines (diesel fuels for diesel engines) has long been measured and ranked using the ASTM standard D-613, "Ignition Quality of Diesel Fuels". ASTM D-613 is more commonly known as the "cetane rating procedure", and it provides a single number measure of combustion quality referred to as the "cetane" number. Fuels with lower "combustion quality" have a lower cetane number when rated with the ASTM D-613 procedure. Generally, acceptable combustion quality for a diesel fuel can be expected for fuels with a cetane number between 40 and 55. Nominally, number 2 diesel fuels in the United States have a cetane number in the mid to low 40's. Diesel fuels with a cetane number in the mid to low 30's would be expected to have poor combustion performance in diesel engines.

Experience with atypical diesel fuels, such as those containing vegetable oils, oil from shale, oil from tar sands, or even heavy crude oils (references 1-1 through 1-11) has indicated that the combustion performance of these fuels was in many instances not well predicted by the cetane number. In some instances, Trevits(1-4), Needham(1-8), Siebers(1-9), and Ryan(1-11), the combustion performance of a fuel having a "low" cetane number has been substantially better than might be expected from the cetane rating of that fuel. This is cause for some concern since it is anticipated that the character of diesel fuels will change as heavy crude oils and other sources provide a larger fraction of the liquid fuels used for transportation. Although there is some disagreement concerning the timing of these changes in the transportation liquid fuel supply, there is little argument that the changes will occur.

When the problem of accurately describing the combustion quality of a diesel fuel from a laboratory test is combined with the exhaust emissions constraints for diesel engines, it is clear that the cetane test, as now constituted, does not provide information adequate to describe the combustion performance of a diesel fuel in commercial diesel engines. Unfortunately, no clear method or test procedure is currently available to adequately address these problems. Also, the cetane rating is a legally accepted measurement of diesel fuel quality with a world-wide installed equipment base. With these facts in mind, the Light Duty Diesel Combustion Committee of the Coordinating Research Council formulated a moderate research program to study the feasibility of modifying the operating conditions and instrumentation of the cetane engine to determine if it could provide information directly applicable to commercial diesel engines. This report describes the conduct and results of that program, "Diesel Combustion Fundamentals - Phase I", designated CRC project CM-126.

### 1.1 Review of the Cetane Rating Procedure

A brief review of the cetane rating procedure is appropriate in order to establish a background for understanding the changes in equipment and test procedures employed in this project. The review will begin with the test apparatus since it is fundamental to the test procedure and rating.

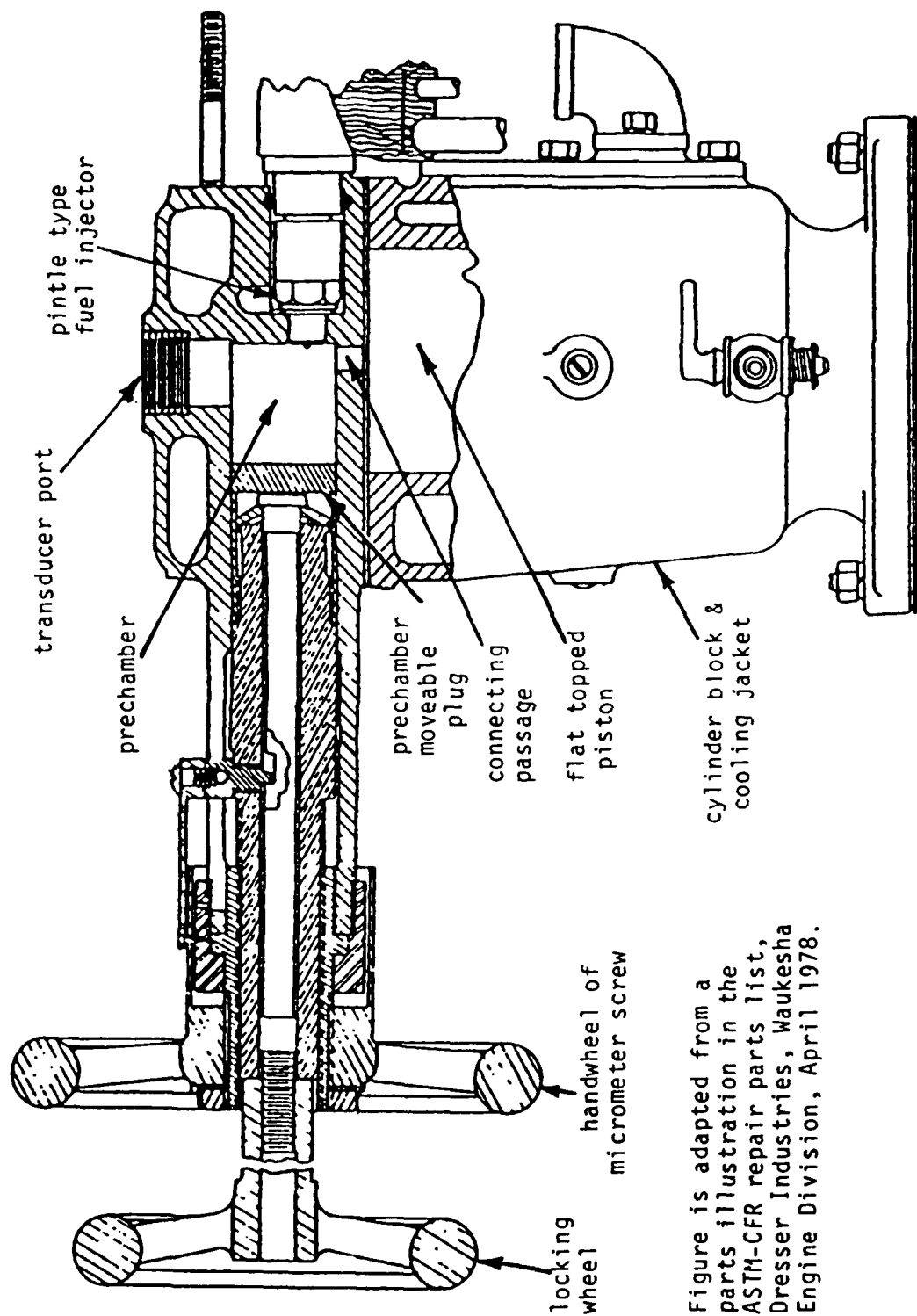
The heart of the experimental apparatus is an ASTM Cooperative Fuel Research (CFR) engine manufactured by the Waukesha Engine Company. This single-cylinder engine consists of a standard crankcase with appropriate counter balancing for the single piston and sufficient strength and durability to survive engine operation at heavy knock and other adverse operating conditions. A separate cylinder and head assembly is fitted to the crankcase depending upon the tests to be performed. For cetane rating, a unique cylinder and head assembly is used. (See Figure 1-1 for illustration of the following details.) This assembly consists of a relatively simple cylinder block with integral cooling jacket and a rather unusual cylinder head. The cylinder head provides a flat top to the main combustion chamber that contains the flat topped piston. This main combustion chamber is attached to a pre-chamber of rather novel design. The pre-chamber is shaped in the form of a small cylinder placed on its side at the end and to one side of the top of the main cylinder. It is connected to the main chamber with a small rectangular passage that is tangent to the wall of the small cylinder and exits on a diameter of the top of the main chamber. At one end of this small cylinder is the pintle type fuel injector. The other end of the small cylinder is a moveable plug attached to a large micrometer screw for accurate location in the bore of the small cylinder. There is a port in the side of the small cylinder (the top of the cylinder head) where a transducer sensitive to rate of change of pressure is installed.

Instrumentation for the engine consists of the transducer for sensing rate of change of pressure, an instrumented fuel injector that generates a signal proportional to rate of change of lift, and inductance pickups mounted to sense TDC and 13 degrees before TDC from the engine flywheel. An electronic readout device uses the injector and pressure signals (which have been amplified and filtered to appear as electronic spikes) as discrete markers for identifying start of injection and start of combustion, respectively. The timing information from the flywheel inductive pickups is used to locate the start of injection relative to TDC and the delay period before ignition (start of combustion). Injection timing is shown as crank angle degrees before TDC and ignition delay is shown as the number of crank angle degrees after injection. Thus, when the engine is firing an operator has a convenient indication of injection timing and ignition delay.

As with other ASTM fuel rating procedures, cetane rating relies on operating the engine at a standard reference condition with the unknown fuel and comparing some measurable variable to values obtained with two reference fuels blended to "bracket" the operation with the unknown. For the cetane test, the standard test condition is when the injection advance and the corresponding ignition delay are both 13 degrees. In other words, injection is 13 degrees before TDC and ignition is at TDC. Of course, other conditions such as engine speed = 900 RPM, inlet air temperature = 150°F (65.6°C), fuel flow = 13 ml/min must also be maintained.

In order for the engine to be operated at standard test conditions with the three different fuels (unknown, low reference, and high reference), the compression ratio must be changed to force firing at TDC. This change in compression ratio is measured as a micrometer reading from the handwheel that controls the moveable plug motion. It is usu-





Note: Figure is adapted from a parts illustration in the ASTM-CFR repair parts list, Dresser Industries, Waukesha Engine Division, April 1978.

Figure 1-1  
Schematic of Cetane Rating Cylinder & Head Assembly for ASTM-CFR Engine

ally referred to as the handwheel setting. Each reference fuel is made up of a volume blend of n-cetane (cetane number = 100) and heptamethylnonane (cetane number = 15), and the cetane number of the blend is determined in direct proportion to the volume fractions in the blend. Thus, the cetane numbers of the reference blends bracket the cetane number of the unknown fuel, and its cetane number is reported as the linear interpolation of the handwheel settings for all three fuels and the known cetane numbers of the reference blends. The procedure is essentially the same when secondary reference fuels (T and U series provided by Phillips Specialty Chemicals) are used, although a calibration mixing table is supplied giving the cetane numbers for volume fractions of the secondary reference fuels.

The cetane rating process is time consuming and takes a good deal of care and experience on the part of the operator to obtain accurate and reproducible ratings. It is not unrealistic to observe differences of up to one cetane number for tests on the same fuel in the same engine with the same operator but done several days apart. The net result of the process is a single number that can be used for a relative comparison between different fuels.

## 1.2 Basic Approach for this Project

The basic concept behind the CRC Diesel Combustion Fundamentals project was to study the feasibility of obtaining more useful information about diesel combustion from the cetane engine. The general approach was to use more modern instrumentation on the engine and operate it at conditions that were more representative of those encountered in current design diesel engines. Independent variables to be investigated included engine speed, fuel injection timing, and fuel properties such as distillation characteristics and aromatic content. Dependent variables to be measured included gaseous and particulate emissions, power output and fuel consumption, and combustion characteristics such as ignition delay.

A primary goal for the project was to compare emissions, performance, and combustion characteristics from the cetane engine operating at more realistic conditions with emissions, performance, and combustion characteristics from diesel engines that employ current technology and design. This goal was an optimistic one since the scope of the project was only to include a test program using the cetane engine. The approach used to overcome this limitation in the experimental program was to use fuels from other test programs that had either been completed or were in progress. Of particular interest were programs that could provide test data for direct comparison with the results of this work. Three such programs were identified, and the original experimental plan called for testing fuels from each of these programs with the intention of making a comparison of results from the cetane engine with results from the engines used in those programs.

The three programs originally identified were:

1. A U.S. Department of Energy sponsored program performed at Ricardo Consulting Engineers in England entitled "Investigation

Into Alternative Fuel Rating Techniques".(1-12) This program will be referred to in abbreviated terms as the DOE/Ricardo program.

2. A CRC sponsored program conducted by Southwest Research Institute entitled "Study of the Effects of Fuel Composition, and Injection and Combustion System Type and Adjustment, on Exhaust Emissions from Light-Duty Diesels".(1-13) The CRC project identification was CAPE-32-80. This program will be referred to in abbreviated terms as the CAPE-32 program.
3. A program at NIPER that was in the startup phase. The program was to use several fuels especially blended for properties including aromatic content. Multi-cylinder engine tests were to be performed to include emissions, performance, and measurement of some combustion characteristics.

In the final test program for this project, fuels from the DOE/Ricardo program and the CAPE-32 program were used. Fuels to be blended for the NIPER program were not available when needed, and they were replaced by four fuels from a program being conducted under the auspices of the Coordinating European Council. Specific details of the changes and description of the set of ten fuels used are included in section 2 dealing with fuels.

### 1.3 General Conduct of the Work

Monthly progress reports on the project were prepared and distributed to members of the CRC Light Duty Diesel Combustion group. Additional information was provided and exchanged on an individual basis by correspondence and telephone conversations. Direction from the project group was provided at several meetings and a few teleconferences. The data compilation, analysis, and presentation reflect a consensus of the project group and an attempt to respond to individual requests insofar as possible. For some aspects of the work, subcommittees made up of a few members have been available as an advisory group to assist in dealing with problems as they arise.

## 2. FUELS

One of the primary goals developed in the formulation of this project was to compare performance and emissions results from the cetane engine with performance and emissions results from diesel engines that reflect current technology and design. A major variable in this comparison process was to be a series of fuels selected to have a range of properties that would allow identification of fuel property effects on the performance and emissions from an operating engine. Since the scope of this program was confined to gathering experimental data from the cetane engine, the fuels to be used were selected from other test programs that had either been completed or were already in progress.

### 2.1 History of Fuel Selection

During the planning stages of this program the CRC Light-Duty Diesel Combustion Committee identified fuels from three different programs that could be made available for this project.

A program sponsored by the U.S. Department of Energy with Ricardo Consulting Engineers of England was nearing completion. This project, referred to as the DOE/Ricardo project, involved single cylinder engine tests of eight different fuels with widely varying properties. Four of these fuels were made up entirely of normal petroleum products. The remaining four fuels involved alternative fuel components such as sunflower oil, methanol, coal liquid, and partially upgraded shale oil. The four fuels made up entirely of petroleum were considered to be the most suitable for this program. Preliminary arrangements were made to make suitable quantities of these four fuels available for the CRC project on light-duty diesel combustion.

The second potential source of fuels for this project was the CAPE-32 program conducted by Southwest Research Institute. This work was sponsored by the Coordinating Research Council as project CAPE-32-80. A nominally orthogonal fuel set was prepared for this project by controlling aromatic content, 10% distillation point and 90% distillation point. Six of the fuels from this set were available for use in this test program. The major problem with using these fuels for the cetane engine test program was that the results would have to be compared to vehicle test data generated in the CAPE-32 program.

The third source for fuels to be used in this test program was an engine test program planned at NIPER to evaluate the combustion and performance characteristics of a set of fuels blended for specific properties. This evaluation program was to be done using multi-cylinder current design diesel engines. The exact properties of the fuels was not yet defined, however, there was to be significant variation in aromatic content to study the influence of this fuel variable.

Once the CRC diesel combustion program was initiated, arrangements to obtain the appropriate fuels from these three programs were begun. Sufficient quantities of the DOE fuels from the Ricardo program were obtained through arrangements with Ricardo in England. Although there were some delays in shipping and importing these fuels into the country, they did not represent a problem in so far as the project itself was

concerned. The fuels obtained from Ricardo were DOE #1, DOE #2, DOE #3, and DOE #4. These identification numbers refer to the fuel identification numbers used in the DOE/Ricardo program.

Similarly, other arrangements were made with Southwest Research Institute to obtain six fuels from the CAPE-32 program. The fuels obtained were designated test fuels 1, 2, 5, 6, 7, and 8 in that program. Sufficient quantities of these fuels were obtained in reasonable time so that no delays were encountered in this combustion study program. The fuels are hereafter identified to as CAPE #1, CAPE #2, etc..

After several delays it became obvious that problems were being experienced in fuel preparation for the NIPER program. It finally became obvious that these fuels would not be available in the time frame necessary for this research work and so the fuels were dropped from the CM-126 project.

Fortunately, the Coordinating European Council was conducting a fuel analysis project (CF 26) in Europe to evaluate the behavior of a wide variety of diesel fuels in a wide variety of diesel engines and vehicles. Several parts of this program were laboratory engine tests of these fuels, many with instrumentation similar to that to be used in this program with the cetane engine. Upon official request from CRC, samples of four fuels from this program were made available for use in this study. The CEC identification numbers for these fuels were 1, 2, 2A, and 3. The CRC Light-Duty Diesel Combustion Committee selected these fuels as covering the range of properties most likely to be of interest in this program.

The final selection of fuels tested reflected the need to fit the program within the time and resources available and to provide information that would have the most versatility in terms of analysis and comparisons to other programs. The following ten fuels were the final selections for evaluation in this program.

- |           |             |
|-----------|-------------|
| 1. DOE #1 | 6. CEC #2   |
| 2. DOE #2 | 7. CEC #2A  |
| 3. DOE #3 | 8. CEC #3   |
| 4. DOE #4 | 9. CAPE #5  |
| 5. CEC #1 | 10. CAPE #6 |

The four DOE fuels and the four CEC fuels were selected because of the availability of engine test data similar to that provided in this program. Since one of the major objectives in this program was to make as direct a comparison as possible between performance and emissions of the cetane engine and current design diesel engines, the priority for testing these fuels was very high.

Since the CAPE-32 program focused on vehicle tests rather than engine tests, it was felt that comparisons to the cetane engine tests would be less meaningful than for the fuels for which engine test data were available. For this reason, the primary savings in time and effort to meet the program resources was obtained by eliminating four of the CAPE-32 fuels. The remaining two fuels, number 5 and number 6, were

selected as having comparable 10% and 90% distillation points but widely differing aromatic content.

## 2.2 Properties of Fuels

As previously mentioned, there was substantial fuel property information available for the fuels used in this test program. Tests were performed by a variety of laboratories to identify and quantify properties that are not normally reported. Unfortunately, these tests were not performed for all the fuels used in this program so they could not be used effectively in determining fuel property effects on engine performance and emissions. The combined measured properties of the ten fuels used in this test program are given in Table 2-1. Appropriate footnotes are included at the end of the table to identify data that were not generated by Southwest Research Institute.

Examination of Table 2-1 shows that two different properties measurements were made for DOE fuel #1. Both of these determinations were made at Southwest Research Institute. The information in the first column was made when the DOE fuels were prepared for the Ricardo program before shipment to England for testing. The second measurement was made near the conclusion of this test program after the fuel had been re-drummed in England and shipped back to the United States. Thus, even though most of the property data was measured at Southwest Research, it was determined over a period of several years. During this period, the fuels were shipped and re-drummed several times, and discrepancies are to be anticipated. For this work the original values of fuel properties measured for the DOE #1 fuel were used. It was felt that this analysis would be more consistent with the values determined for the DOE #2, 3 and 4 fuels which were not re-analyzed for this program.

Table 2-1

CRC Program CM-126

FUEL PROPERTY DATA DETERMINED BY SOUTHWEST RESEARCH

Sheet 1 of 2

FUELS :		DOE/Ricardo Fuels				CEC Fuels				CRC CAPE-32	
		DOE 1/ *	DOE 2	DOE 3	DOE 4	CEC 1	CEC 2	CEC 2A	CEC 3	CAPE 5	CAPE 6
Property	method										
Gravity, °API	D 287	35.7/35.8	29.2	31.7	48.1	35.8	32.9	29.9	29.9	36.2	27.5
Specific gravity, 60°F	D 287	0.846/-	0.881	0.867	0.788	-	-	-	-	0.844	0.890
Distillation, °F, v%	D 86										
IBP		372/420	427	362	184	365	366	378	364	400	378
5%		402/439	467	388	184	385	379	391	384	440	436
10%		420/457	487	406	200	408	411	410	411	462	456
15%		432/470	499	419	212	430	436	433	432	-	-
20%		445/480	508	430	220	451	455	449	447	493	486
30%		467/498	523	455	237	487	481	477	473	512	503
40%		485/514	536	484	254	513	506	499	504	530	518
50%		502/530	551	512	281	536	532	522	523	546	534
60%		516/545	567	542	320	560	555	551	551	565	553
70%		532/560	587	574	392	586	582	580	577	585	574
80%		549/569	611	612	485	612	610	610	608	609	603
90%		572/578	653	664	535	647	647	648	645	641	641
95%		590/592	700	708	565	668	668	665	669	671	671
FBP		616/600	763	724	594	683	688	690	687	708	696
Recovery, %		99.0/98	98.0	98.5	98.5	97	96	99	97	-	-
Residue, %		1.0/1	2.0	1.5	1.0	1	1	0.5	1	-	-
Cetane Number	D 613	50.1/47.3	41.6	40.7	36.2	49.8	48.0	43.2	39.4	53.1	33.9
Cetane Index	D 967	47.1/-	42.2	42.0	14.8	-	-	-	-	52.8	38.2
Viscosity, cSt @ 40°C	D 445	2.40/2.39	4.37	2.76	0.91	3.16	3.01	2.84	2.90	-	-
Pour point, °C	D 97	-18 0.0	-10 14	-15 5	-39 138	-31 <sup>1</sup> -24	-35 <sup>1</sup> -31	-43 <sup>1</sup> -45	-44 <sup>1</sup> -47	-	-

\* Second evaluation of DOE 1 fuel sample obtained after DOE/Ricardo program.

1 From CEC CF-26 fuel properties data (FTP.38.2438)

Table 2-1 (continued)

CRC Program CM-126

FUEL PROPERTY DATA DETERMINED BY SOUTHWEST RESEARCH

Sheet 2 of 2

FUELS :		DOE/Ricardo Fuels				CEC Fuels				CRC CAPE-32	
Property	method	DOE 1/*	DOE 2	DOE 3	DOE 4	CEC 1	CEC 2	CEC 2A	CEC 3	CAPE 5	CAPE 6
Hydrocarbon type, v %	D 1319										
Saturates		70.8/61.2	62.5	52.2	80.8	54.0	44.9	34.7	33.5	74.2	42.1
Olefins		1.2/2.3	1.0	0.5	0	2.7	2.5	2.3	2.3	1.3	0
Aromatics		28.0/36.5	36.5	47.3	19.2	43.3	52.6	63.0	64.1	24.5	57.9
Aromatic carbon, m%											
monocyclic		16.66	15.9	23.66	8.81	-	-	-	-	18.1	42.7
dicyclic		5.86	7.7	11.41	4.31	-	-	-	-	12.5	24.5
tricyclic		9.79	6.8	10.48	4.09	-	-	-	-	5.4	16.4
		1.01	1.4	1.77	0.41	-	-	-	-	0.2	1.8
Elemental analysis											
C, m%	D 3178	86.69	86.82	87.27	86.04	86.51	86.71	87.51	87.21	86.3	87.4
H, m%	mod @	12.96	12.62	12.19	13.63	13.21	12.61	12.01	12.11	13.6	12.1
S, m%	D 262	0.20	0.22	0.38	0.07	0.256	0.272	0.293	0.298	0.24	0.47
O, m%		0.45	0.33	0.058	0.020	-	-	-	-	-	-
N, m%		0.004	0.017	0.015	0.001	-	-	-	-	0.003	0.016
Heat of combustion											
BTU/lb											
Mj/kg											
Gross	D 240	19503	19316	19269	19886	19563	19378	19150	19206	19611 <sup>2</sup>	19077 <sup>2</sup>
Net		45.36	44.93	44.82	46.25	45.50 <sup>1</sup>	45.07 <sup>1</sup>	44.54 <sup>1</sup>	44.67 <sup>1</sup>	45.62	44.37
		18321	18165	18148	18643	18356	18226	18054	18100	18370	17973
		42.61	42.25	42.21	43.36	42.69	42.39	41.99	42.09	42.73	41.80
Flash point, °F	D 93	-	94/201	47/116	-	74/165	77/171	80/176	76/169	-	-

\* Second evaluation of DOE 1 fuel sample obtained after DOE/Ricardo program.

@ Modified for liquid samples

1 From CEC CF-26 fuel properties data (FTP.38.2438)

2 Measurements made by Galbraith Laboratories, Inc., Knoxville, TN.



### 3. EQUIPMENT

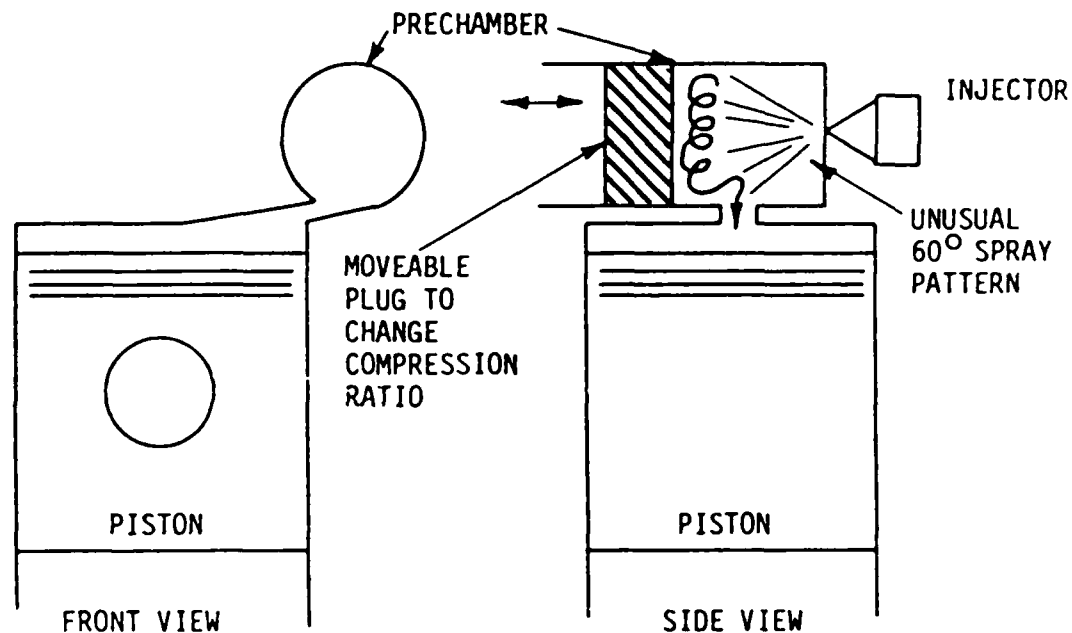
#### 3.1 Engine Test Apparatus

The Cooperative Fuel Research (CFR) engine used in the ASTM D-613 diesel fuel rating procedure was the major item of equipment of interest in this study. The CFR engine used for rating diesel fuels is commonly called the cetane engine and will generally be referred to as such throughout this report. As previously indicated, both the ASTM rating procedure and the cetane engine have been called into question as to whether the cetane number provided from the rating procedure provides an adequate description of the combustion quality of diesel fuels in current design compression ignition engines. Figure 3-1 illustrates that the combustion system for the cetane engine is significantly different than the general arrangement for current design direct injection and indirect injection combustion systems.

One of the major objectives of this test program was to operate the cetane engine at conditions more representative of a current design diesel engines to determine if it could provide performance and emissions results that might be comparable to these engines. Modifications to the cetane engine and test apparatus had to be made to accomplish this end. Figure 3-2 schematically illustrates many of the major modifications made to the engine system for this program. Major changes include the following:

1. The simple air inlet and heating system has been replaced with a controlled air supply system that provides dry oil-free air at precisely controllable pressure and temperature conditions to the engine. This system provided dramatically improved consistency of inlet air conditions as well as the ability to measure inlet air flow.
2. The volumetric fuel flow burette system of the ASTM test procedure has been replaced with a mass balance measuring system. This system provides both improved precision of fuel flow measurement as well as the ability to accurately accommodate fuels of differing energy density.
3. The synchronous motor normally used to control the speed of the cetane engine by absorbing or delivering power has been removed and replaced with a 15 hp speed controlled electric dynamometer. The dynamometer provides the ability to accurately measure the power being produced by the cetane engine. This associated speed control for the dynamometer system provides improved speed regulation for the engine. Nominal control is plus or minus 1 rpm, and plus or minus 2 rpm is representative of worst cases observed in operation.
4. The exhaust stilling chamber for the cetane engine has been modified to provide access for three emissions probes. A pressure regulating valve has also been placed in the exhaust system downstream from the stilling chamber to provide control of exhaust pressure when needed. The three emission probes placed in the exhaust stilling tank are located at different positions

THE UNUSUAL SIZE, SHAPE, AND GEOMETRY OF THE PRECHAMBER MAKE THIS ENGINE UNIQUE AND POSSIBLY UNREPRESENTATIVE OF DIESEL ENGINES



WAUKESHA ASTM-CETANE ENGINE COMBUSTION SYSTEM

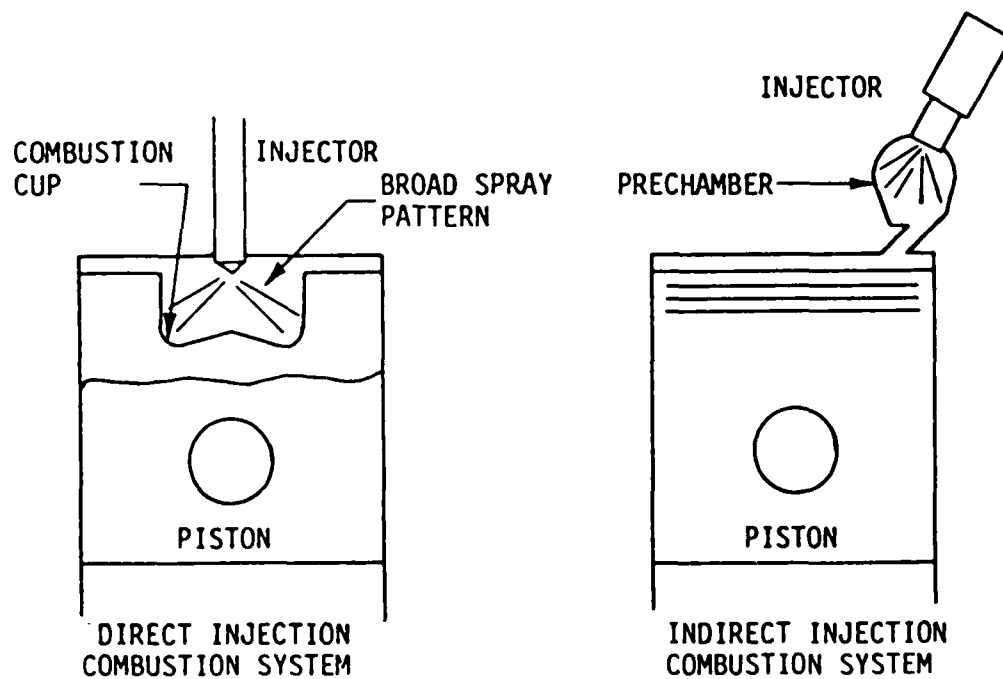


Figure 3-1 Comparison of Cetane, Direct Injection, and Indirect Injection Combustion Systems

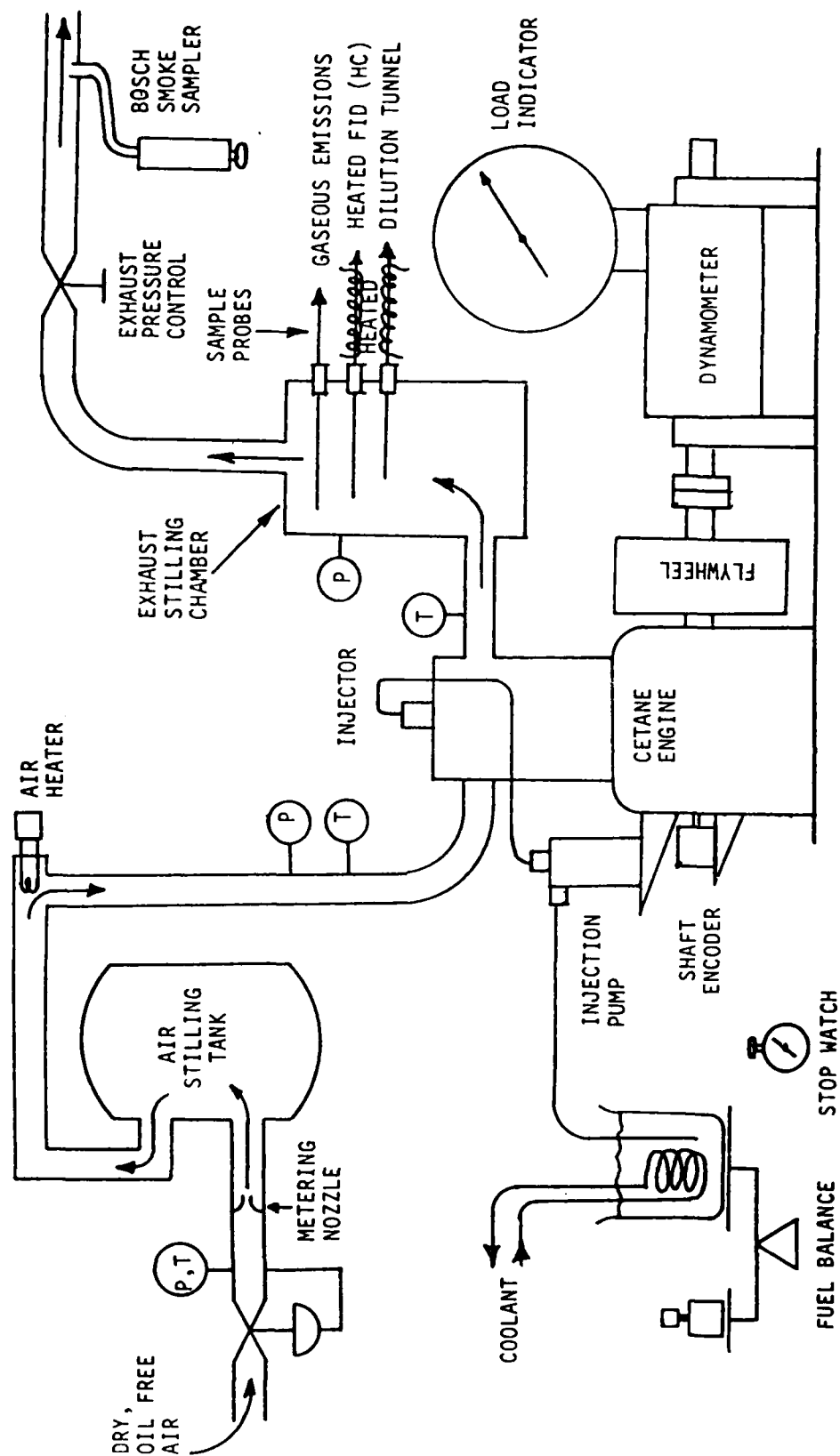


Figure 3-2 Modified Cetane Engine Test Apparatus

in the tank so they will not interfere with each other. In addition, each probe consists of a tube of length somewhat less than the diameter of the tank. The end of the tube has been sealed and several sampling holes have been drilled into the sides of the tube for sampling at different radial locations in the stilling chamber. It was felt that this type of probe would provide an averaging effect across the inside of the stilling chamber to eliminate any variations in results due to flow patterns that might be developed. The sample line for gaseous emissions was unheated. The sample line for the heated FID hydrocarbon instrument was maintained at a temperature of 350°F (176.7°C). The separate short sample line for the dilution tunnel was also heated. A Bosch smoke sampler was installed in the exhaust system downstream from the exhaust pressure control valve.

5. Pressure gauges and thermocouples were also installed at numerous points in the engine systems to monitor operating conditions. A precision pressure gauge and thermocouple for temperature measurement were installed immediately upstream of the critical flow metering nozzle for the engine air supply system. Accurate pressure gauges and thermocouples were placed to measure inlet manifold pressure and temperature, exhaust port temperature, and stilling chamber pressure. Other gauges to monitor coolant temperature, oil temperature, fuel temperature, and ambient conditions were also installed.

These modifications to the cetane engine system provided dramatically improved control of many of the experimental variables as well as improved instrumentation for accurately measuring the operating conditions of the engine.

### 3.2 Emissions Measurement Instrumentation and Apparatus

#### 3.2.1 Gaseous Emissions

Figure 3-3 is a simplified schematic diagram of the system used to measure gaseous emissions from the engine exhaust. The exhaust gas constituents measured in this program were: carbon monoxide (CO), carbon dioxide (CO<sub>2</sub>), oxides of nitrogen (NO<sub>x</sub>), oxygen (O<sub>2</sub>), and unburned hydrocarbons (HC).

The instruments for measuring CO and CO<sub>2</sub> emissions were Beckman model 864 non-dispersive infrared analyzers. A Thermolectron company model 10A chemiluminescent analyzer was used for measurements of oxides of nitrogen emissions. Oxygen levels in the exhaust were measured with a Beckman model 742 amperometric analyzer. These instruments were installed in a bench apparatus and supplied with a sample from one of the engine stilling chamber probes by an appropriate water trapping and filter system. The internal connections of the instrument bench allowed each of these instruments to be checked for zero and span values frequently during daily operation. One or more span gases connected with concentrations near the range of values expected from the engine were connected to each instrument.

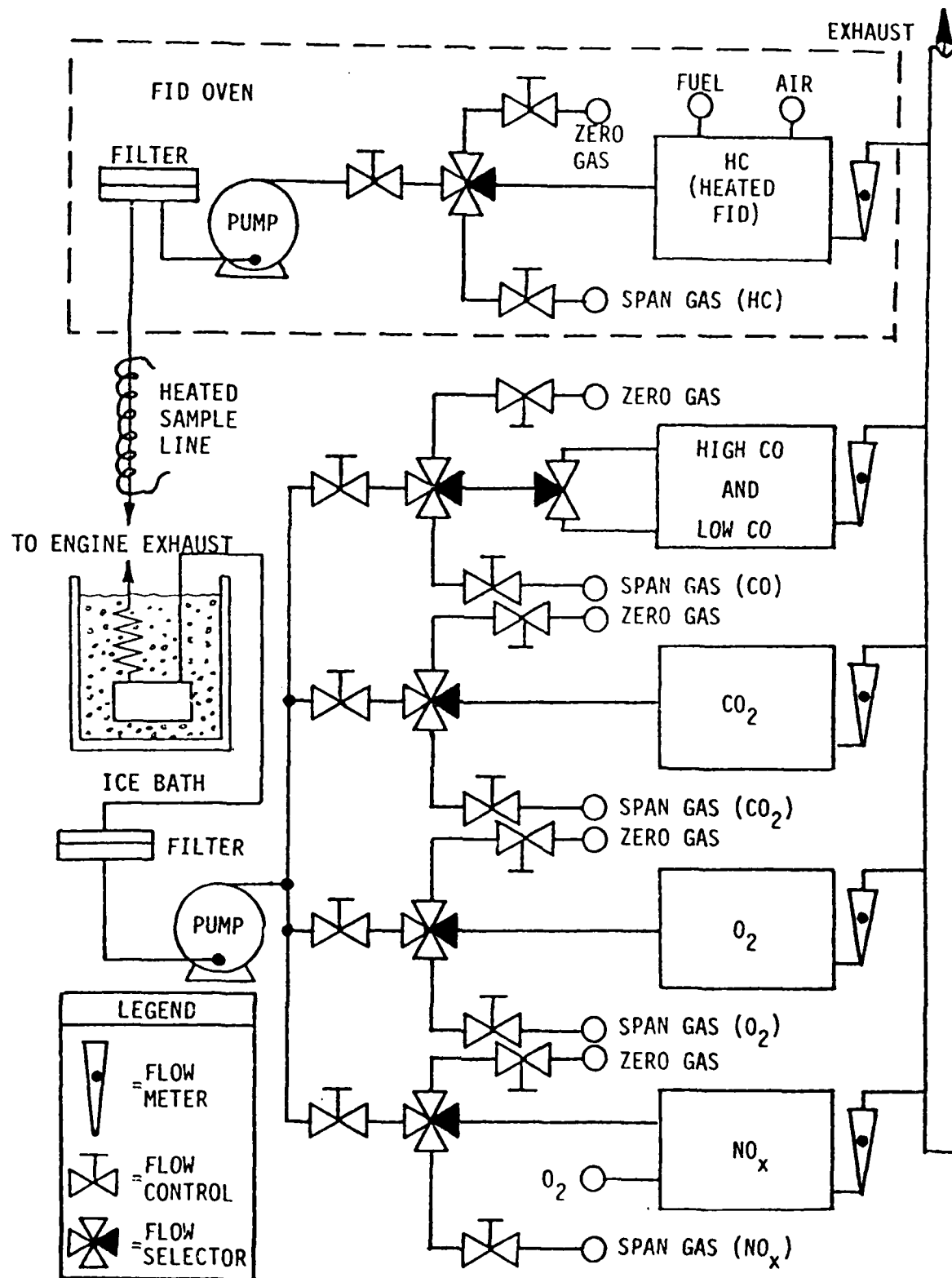


Figure 3-3 Schematic, Emissions Instrumentation and Sample Systems

A Beckman model 402 Heated Flame Ionization Detector (HFID) instrument was used for measuring unburned hydrocarbons in the engine exhaust. An entirely separate portable apparatus is used with this instrument. The apparatus includes fuel and combustion gases for the instrument as well as appropriate zero and calibration gases. The portability of the instrument allows it to be installed near the engine being tested and minimizes the length of heated sample line.

### 3.2.2 Smoke and Particulate Measurements

The measurement of smoke and particulate emissions from a diesel engine is an important and often difficult task. For the purpose of this report smoke will refer to a measurement of opacity or optical density of the undiluted exhaust gas. The system available for this project was a Robert Bosch model EFAW65A spot-type smoke meter. This meter uses a sampling device that draws a fixed volume of exhaust gas at a controlled flow rate through a special filter. A spot of soot forms on the filter, and the light absorbance of the soot is measured with a instrument containing a controlled light source and a photo detection cell. The instrument measures a reading that is proportional to the density of the soot spot, and thus to the density of the smoke in the exhaust. The units are arbitrary and are identified as Bosch units. The reading is referred to as the Bosch Smoke Number.

The term particulate emissions refers to measurements intended to capture the particulate matter in the diesel exhaust for mass measurements and other types of analyses. Of greatest interest is particulate matter that has been exposed to a cooling and dilution process approximating that of the exhaust plume leaving the exhaust pipe and mixing with the atmosphere. The fact that diesel exhaust contains unburned HC emissions of high boiling point materials and sulfates from fuel sulfur leads to a condensation and absorption of these materials on the carbon particles in the exhaust during the cooling and dilution process into the atmosphere. A dilution tunnel is used to cool and dilute the exhaust under controlled conditions so that the particulate material recovered will be representative of that likely to occur during the normal exhaust process to the atmosphere.

In the interest of space, cost, and experimental reproducibility, a mini-dilution tunnel, patterned after one described by MacDonald et al. (3-1) was used for sampling of particulate emissions. A schematic for this mini-dilution tunnel system is shown in Figure 3-4. The system collects a portion of the exhaust from a sample probe in the exhaust stilling chamber of the engine. Aspiration of this exhaust material through a short heated line is provided by a critical flow nozzle located at the beginning of the dilution section of the tunnel. Dry, oil-free compressed air is supplied to the upstream side of this converging-diverging critical flow nozzle. The dilution air is heated to provide a filter sample temperature of approximately 125°F (51.7°C). The supersonic nozzle discharges into a straight section of pipe that provides for a fully turbulent mixing of the exhaust sample and dilution air. The diluted exhaust is sampled something over 10 diameters downstream from the nozzle exit. Sampling involves drawing a known amount of diluted gas through a 47 millimeter Teflon coated filter that has been previously weighed. A separate analyzer is used to measure the CO<sub>2</sub>

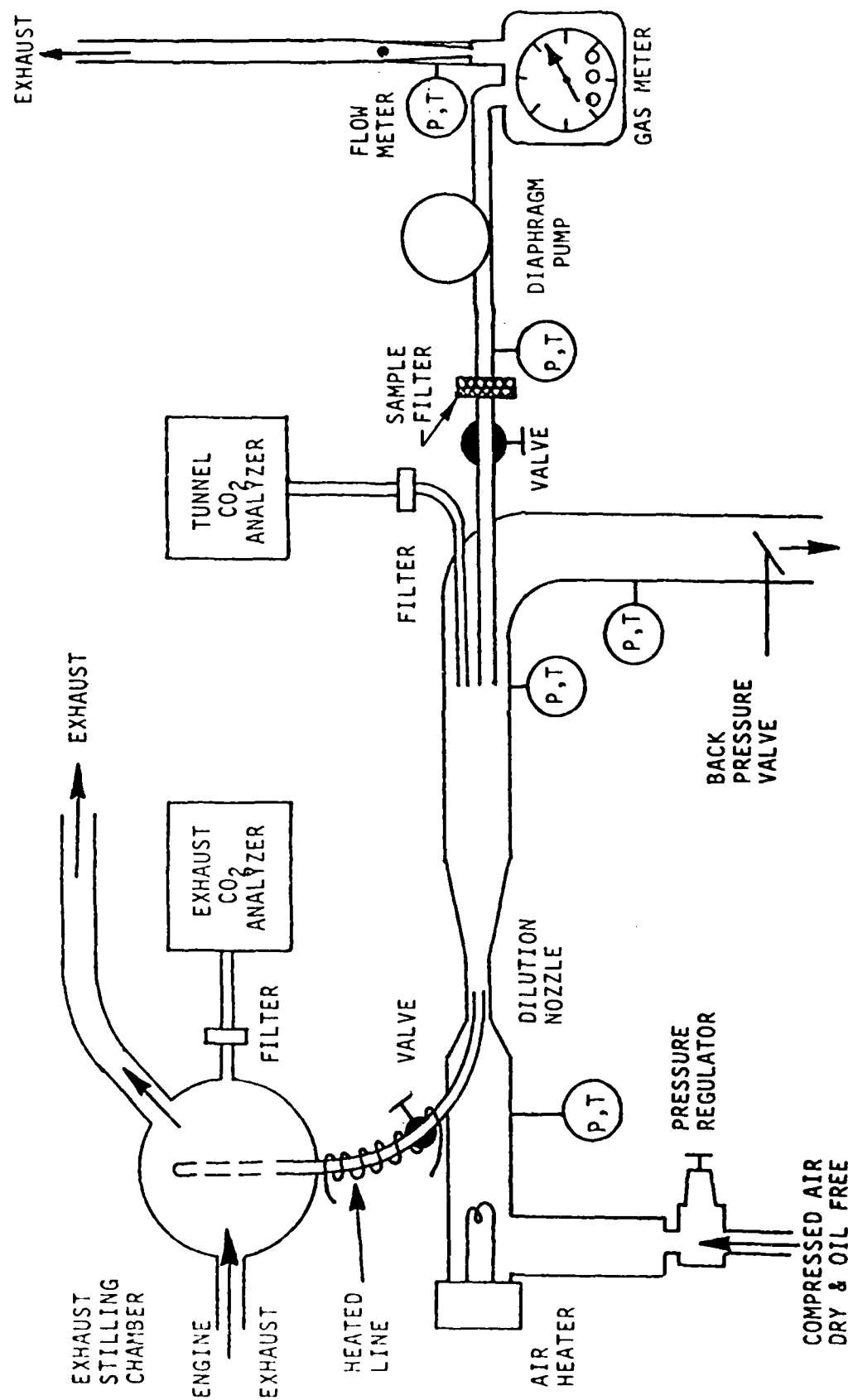


Figure 3-4 Schematic, Mini-Dilution Tunnel System

level of the dilute exhaust at the location in the tunnel from which the particulate sample is drawn. By comparing the level of  $\text{CO}_2$  in the dilute exhaust to the level of  $\text{CO}_2$  in the engine exhaust and correcting for background  $\text{CO}_2$  and the presence of water vapor, the dilution ratio provided by the tunnel can be calculated. Changes in the dilution ratio can be easily made during operation by changing the dilution air supply pressure upstream of the supersonic nozzle. Back pressure in the dilution tunnel is carefully adjusted to one inch of water with a butterfly valve in the exhaust of the tunnel system. Instrumentation for pressure and temperature measurement in various portions of the dilution tunnel system provide the information necessary to operate the tunnel properly and to perform the computations necessary for determining the mass of particulates collected per cubic meter of engine exhaust flowing. The nominal dilution ratio used for this test program was 10:1.

### 3.3 Combustion Instrumentation

A major requirement of the program was to make transient measurements of the cylinder pressure, pre-chamber pressure, and fuel injector behavior during the combustion process. These measurements would give some insight into the combustion process in the cetane engine. Instrumentation for cetane rating does not provide a direct measurement of cylinder or pre-chamber pressure or injector lift characteristics. Measurement of cylinder pressure, pre-chamber pressure, and injector lift provides information that can be directly compared to data from other engines. This information is also used in the computation of combustion parameters describing the fractions of premixed and diffusion burning.

Modifications were made to the cylinder head for the cetane engine to place an AVL 8QP505CA pressure transducer in a position to measure main chamber pressure. The pressure pickup hole in the pre-chamber was large enough to fabricate an adapter that would allow both a Kistler model 6001 pressure transducer and a small optical window to be mounted in the pre-chamber. Both modifications are shown schematically in Figure 3-5.

Considerable problems were encountered in obtaining proper operation of the AVL pressure transducer for measuring main chamber pressure. Initially, the problems were related to proper sealing for the electrical connections in the system. After these problems were resolved, a major problem developed in that the transducer diaphragm failed catastrophically after approximately 50 hours of operation. The major concern was that there was no obvious cause for this failure. There was some evidence of corrosion around the weld seams of the diaphragm; however, even analysis by the manufacturer could not provide a clear indication of what caused the failure. The transducer being used initially was an AVL 8QP500CA. This transducer was replaced by a model 8QP505CA which was a new style of transducer for this application. The major differences between the two transducers was that the model 8QP505CA was equipped with a combustion shield to protect the sealing diaphragm from direct exposure to the combustion chamber. Once installed, no further problems were experienced with the main cylinder pressure transducer system.



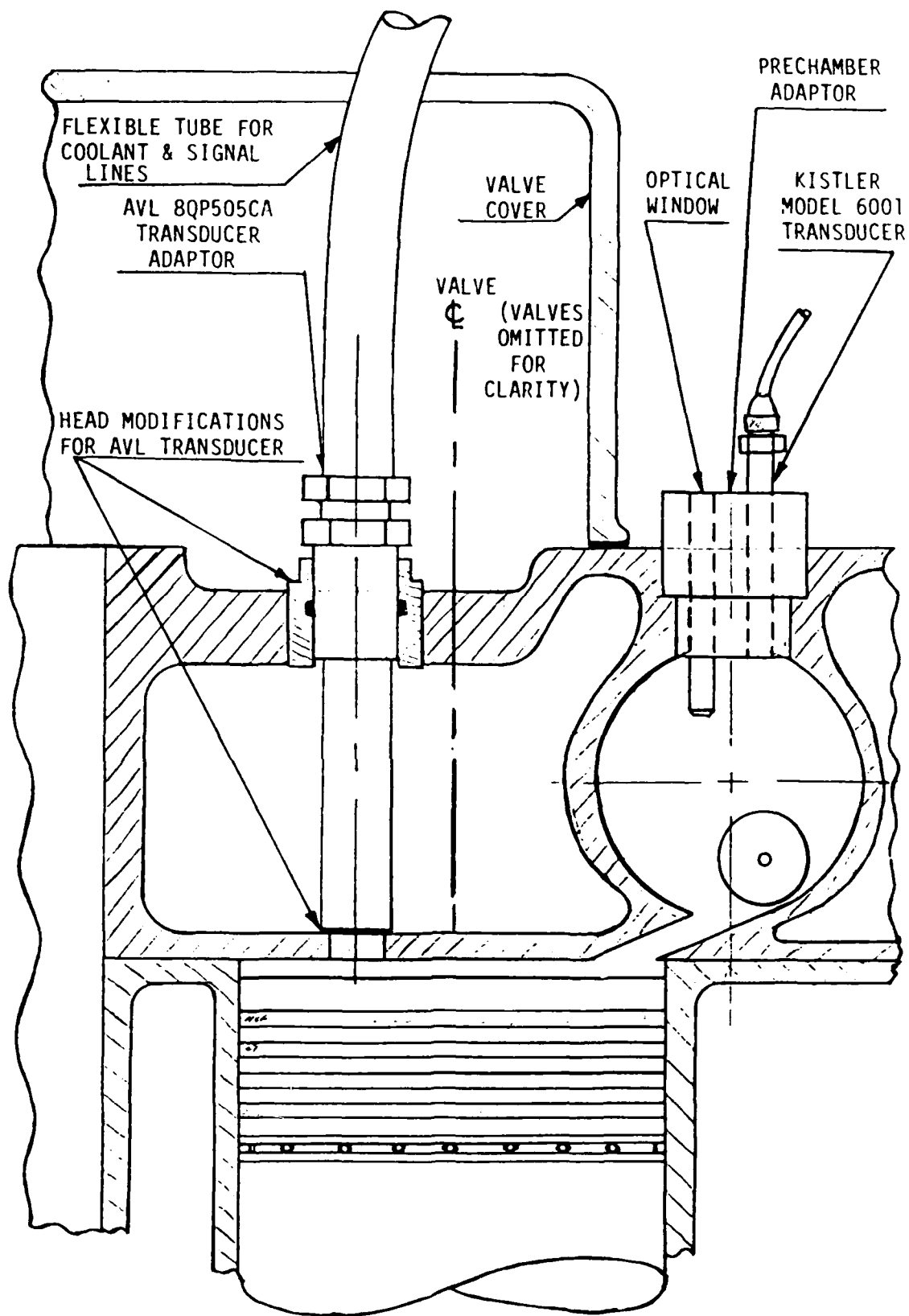
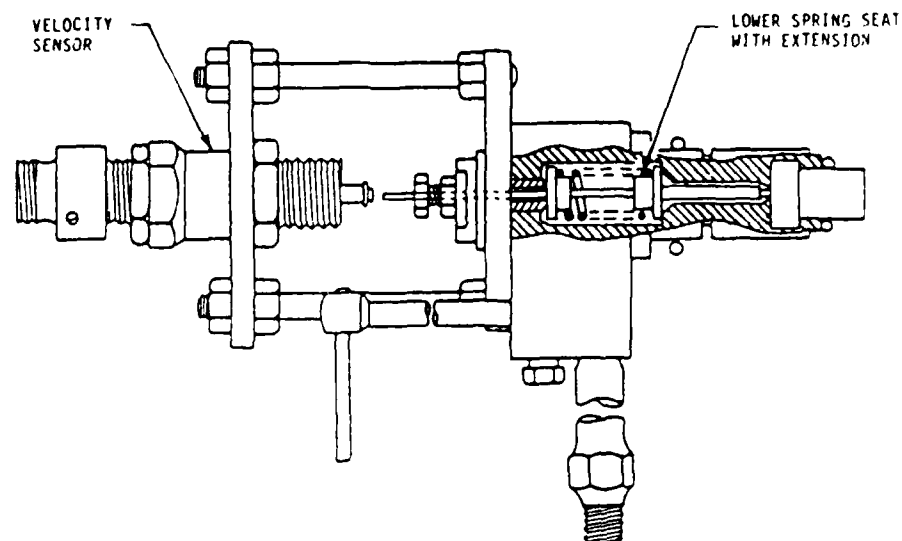


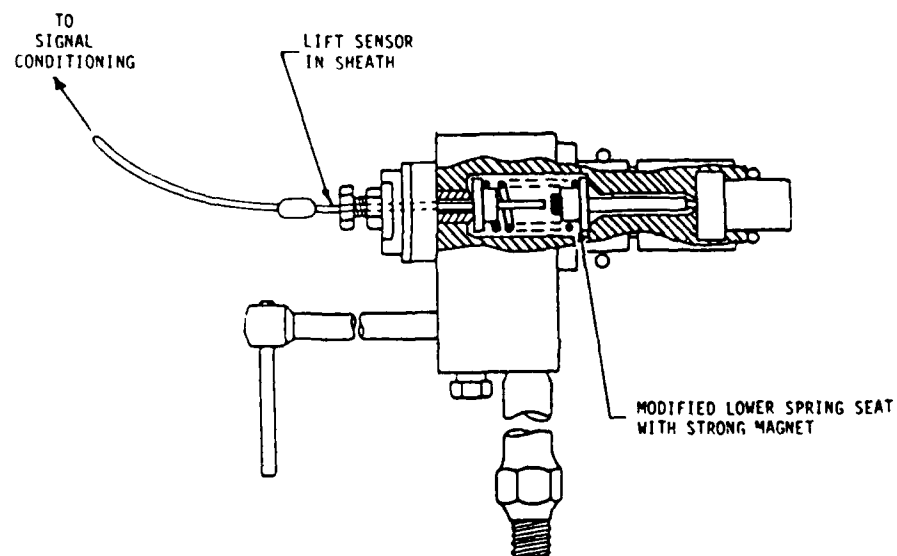
Figure 3-5 Schematic, Cetane Head Transducer Installations

One of the initial objectives in the project was to measure the start of combustion by sensing illumination since it was thought this might be a more sensitive process than inferring the start of combustion from pressure data. The optical window in the pre-chamber adapter was prepared for just this function. Unfortunately, determining the start of combustion by sensing illumination did not provide satisfactory results in this application. There were two major reasons for discontinuing the use of this sensor system. First, the location of the window was such that it did not see a large enough volume of the pre-chamber to insure that luminosity from the start of combustion would appear in the field of view. Within the range that the pre-chamber adapter and the optical window could be adjusted or modified, several different positions for placing the window were tried. Unfortunately, the positions that provided better results in terms of field of view did not receive adequate cleaning action from the flame and the window would soot up after a few minutes of operation. When the optical window was located in a position that it received cleaning action from the flame, it was not located appropriately to view start of combustion. The second major problem that was encountered was that the lifetime of the quartz window appeared to be on the order of 50 hours of operation. Since each window represented a considerable expense in terms of purchase cost and shop time to modify it for this application, combustion luminosity measurements were terminated.

The modifications to the cetane engine head allowed modern design pressure transducers to be placed for measuring both pre-chamber and main chamber pressures during combustion. The next step in improving the instrumentation of the engine was to modify the fuel injector for a modern transducer that would measure injector lift rather than something proportional to rate of change of lift that the current cetane instrumentation provides. The approach used for this modification is shown by the two portions of Figure 3-6. The upper figure of Figure 3-6 illustrates the approach used with the standard cetane engine instrumentation to determine rate of change of lift. Essentially, the lower spring seat of the injector return spring has a long extension that passes through the spring and the adjustment nut of the injector and extends beyond the end of the injector body to a point near the pole piece of a coil type pickup. The velocity of the end of this extension relative to the pole piece induces a current in the coil pickup that is related to the velocity of injector lift. This method is appropriate for determination of start of injection; however, it provides no information about the injector lift characteristic that might be used in determination of instantaneous fuel flow. This system was replaced by using a Hall effect microsensor manufactured by Wolff Controls Corporation. This sensor system uses a tiny but very powerful magnet attached to the lower spring seat of the injector needle return spring. A microsensor that slips inside a sheath less than 3 mm in diameter is located near the end of this magnet with appropriate clearance under full lift conditions. With an appropriate power supply, this system provides a strong, noise-free signal that is proportional to injector lift. The lower portion of Figure 3-6 illustrates how the injector was modified to incorporate this new lift measurement system. The system has been very reliable, and no problems have been experienced with its operation.



NORMAL CETANE RATING INJECTOR LIFT SENSING



MODIFIED INJECTOR LIFT SENSING

Figure 3-6 Changes in Fuel Injector for Lift Transducer

In order to estimate the approximate instantaneous fuel flow into the combustion chamber, not only needle lift information is needed but the pressure difference across the injector must also be known. The pre-chamber pressure transducer will provide the downstream pressure on the injector. In order to measure fuel pressure upstream of the injector, an AVL 7QP2000A pressure transducer was installed at the inlet of the modified fuel injector using a model DG10006 injection line adapter. This system provided a reasonably close coupled upstream pressure transducer that did not require major modifications to the fuel injector itself. Once initially calibrated, virtually no problems were encountered with this system.

An initial desire in the test program was to measure engine blowby during the test program to determine if sufficient wear was occurring in the engine to influence the results. Measurement of blowby in the CFR engine would be difficult due to the construction of the engine and its crankcase. However, since the intent was a quality check of the upper cylinder condition, a variable reluctance pressure transducer was installed to measure crankcase pressure on a dynamic basis. The sensitivity of this transducer was such that any significant blowby would appear as a distortion of the pressure in the crankcase. This system worked satisfactorily throughout the test program, and no indication of increased blowby or upper cylinder wear was encountered.

### 3.4 Computer Data Acquisition Equipment

The requirements for computing combustion parameters related to premixed combustion and diffusion combustion could only be met by using a computer data acquisition system to record the appropriate pressure and injector lift information. The requirements for this computer data acquisition system were relatively difficult. In terms of data quality analysis, it was desirable to acquire approximately 100 consecutive cycles to provide estimates of the average cycle and a statistically meaningful deviation from the average cycle. Even with samples taken only once each crank angle degree, a large amount of fast access memory is required to store information for 100 consecutive cycles. Unfortunately, a resolution of one sample for each crank angle degree is not nearly adequate to capture the detail needed during the combustion process. Samples every one or two-tenths of a degree would be more appropriate for the pressure and injector lift measurements near top dead center during the combustion process. These requirements of high sampling rates and storage of a large number of cycles tend to be mutually exclusive. For this program, a hybrid data acquisition system has been developed using an IBM model XT personal computer system equipped with a data acquisition subsystem and a Norland model 2001 processing digital oscilloscope. A schematic of this system is shown in Figure 3-7.

The hybrid data acquisition shown in Figure 3-7 relies on two major features. The first feature is a laboratory data system that performs signal conditioning and switching functions for the transient sensors used in the experiment. The second important feature of the system is a communication link between the Norland processing digital oscilloscope and the IBM personal computer. The personal computer can also access a

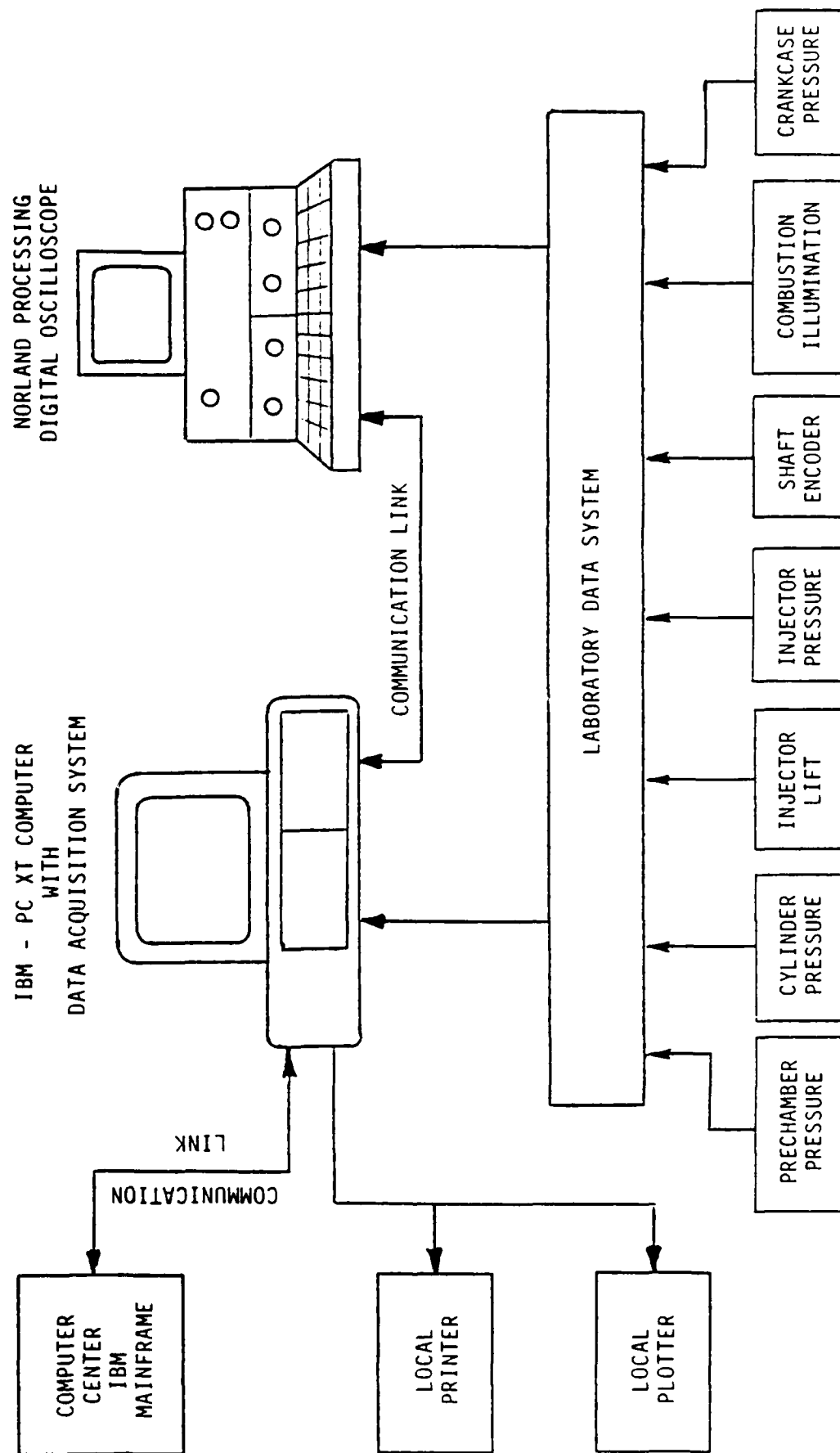


Figure 3-7 High Speed Data Acquisition and Processing System

local printer, a local plotter, and a communication link with the main-frame IBM computer in the UMR Computer Center.

In operation, the laboratory data system routes all channels of information to the data acquisition subsystem in the IBM personal computer. Sampling of the appropriate information is determined by appropriate software written for the personal computer. The personal computer system is used to sample data every crank angle degree for the 720 degrees in each cycle. It can acquire up to 143 consecutive cycles of pressure data. The shaft encoder attached to the engine crankshaft provides clock pulses every crank angle degree that are used to drive the sampling of the personal computer data acquisition system. Appropriate software logic uses the top dead center pulses from the shaft encoder and the level of the cylinder pressure to ensure that data acquisition starts at TDC when the valves are open. After the cycle data has been acquired, a graphic display showing the average of the first ten cycles provides for an immediate quality check of the data. If the graphic display indicates that the data is reasonable, then the memory image of the data is stored on the diskette that contains all the data for the particular test condition.

The Norland processing digital oscilloscope is used to acquire data at the sample intervals from the 0.1 to 0.2 crank angle degrees for a range of approximately 100 crank angle degrees during the combustion process. The laboratory data system uses information from the shaft encoder and cylinder pressure measurement to trigger the Norland processing digital oscilloscope exactly 40 crank angle degrees before top dead center. In this way, data taken using the processing digital oscilloscope can be directly correlated with data taken using the personal computer system. The laboratory data system allows any two channels of information to be switched to the Norland processing digital oscilloscope for high speed data acquisition. Pre-chamber pressure and cylinder pressure are recorded with the Norland processing oscilloscope at the same time that the cylinder pressure is being acquired using the personal computer data acquisition system. Other channels of information are measured using the processing oscilloscope in quick succession until all channels of interest have been measured. The processing oscilloscope is set to average 50 cycles of information, and some data smoothing and processing is done using the features of the processing oscilloscope. The processed data are then sent to the personal computer through the communication link and stored on the data diskette for the given test condition.

The personal computer system is used as the primary control device for the entire data acquisition operation. Extensive software has been prepared to prompt the operator for entry of appropriate laboratory data. This software also computes other useful information such as air-fuel ratio and dilution ratio for use in engine and system adjustments, and stores all information in an organized fashion on the diskette for the given data run. The personal computer system is also used extensively in the data reduction process and in preparing printed and plotted output.

#### 4.0 TEST PROGRAM

One of the major goals of this research program was to operate the cetane engine at more realistic conditions to determine if the performance, emissions, and combustion characteristics would be more representative of current design diesel engines. The two most fundamental changes made in the engine operating conditions were to increase the compression ratio and operate the engine at an optimum injection timing point.

The original work statement for this project specified a compression ratio of 20:1. This compression ratio represents a substantial increase over the nominal compression ratio used in rating diesel fuel. For a nominal number 2 diesel fuel the compression ratio used for cetane rating is in the range of 12:1 to 15:1. The value of 20:1 compression ratio represents a compromise between compression ratios for DI engines, nominally in the range of 16:1 to 19:1, and compression ratios for IDI engines, nominally in the range of 22:1 to 24:1.

The cetane rating procedure uses a fixed injection timing of 13 °BTDC. The ignition delay of the given fuel is forced to be 13 crank angle degrees by adjusting the compression ratio such that combustion begins at TDC. Bracketing the compression ratio of the unknown fuel with different compression ratios for reference fuel blends is used to estimate the cetane number of the unknown fuel. Since the compression ratio for this program was fixed, the procedure of using a fixed injection timing of 13 °BTDC would have little meaning in terms of optimum combustion. For this reason, optimum injection timing was established as one of the major reference test conditions. The use of optimum timing would also allow study of the effects of a fixed number of crank angle degrees injection retard on the engine performance, emissions, and combustion characteristics.

Many other minor changes in the operating procedures and conditions were used in this test program. The details of these changes in test conditions and operating procedures are included in the following sections.

##### 4.1 Test and Operating Conditions

The initial test plan called for taking a complete set of data at 900 rpm for all test fuels. Additional data were to be taken at two higher engine speeds in an effort to determine how engine speed might influence results from the cetane engine. Previous experience with the cetane engine operating at 900 rpm had indicated that significant problems could be anticipated in obtaining consistent data, particularly in the measurement of HC emissions and mass particulates. By careful refining of the test procedures, it was possible to obtain reasonable consistency during this test program, particularly with the 20:1 compression ratio. Data for all four fuels from the DOE/Ricardo program had been taken when operational problems with the engine were observed. The operational problems were traced to a failure of the roller cam follower in the fuel injection pump. The roller cam follower was replaced, and after break-in operation a qualification data run was performed to determine if the engine was providing results consistent

with previous data. Unfortunately, the results obtained using the new cam were sufficiently different from previous results to create a significant data discrepancy. Also, emission data results using the new cam were not nearly as consistent as those obtained using the previous cam. Additional tests indicated that the cetane rating capability of the engine was essentially the same for the new cam as it had been for the old cam. Thus, the changes in the new cam that caused the difference in emissions results from the engine were subtle enough that they had no apparent effect on the cetane rating capabilities of the engine.

After a substantial amount of time had been invested in trying to resolve the problems of inconsistent emission measurement results from the new cam, it was concluded that the 900 rpm operating condition was a marginal condition for this engine and very slight changes in the engine or in the operating procedure would produce a significant variation in results. This conclusion is reinforced by the significant problems encountered in previous test programs in trying to obtain consistent emissions data from this engine at the 900 rpm operating condition.

The 900 rpm operating speed was selected because it is the speed used in the ASTM D-613 rating procedure. Since this speed is not indicative of a nominal operating condition for a current design light-duty diesel engine, a new set of operating conditions at 1200 rpm was established. A series of preliminary tests at full, medium, and light loads indicated that this operating speed provided considerably better operational stability of the engine and more consistent emissions results. The 1200 rpm operating speed was also convenient in that it would allow direct comparison to data from the DOE/Ricardo program taken at 1200 rpm.

The specific details of the 1200 rpm operating condition for the engine are given in Table 4-1. Three load conditions corresponding to full, medium, and light load were established. The air-fuel ratio was used to set these load conditions with 20:1, 30:1, and 40:1 corresponding to full, medium, and light load, respectively. The other operating conditions shown in Table 4-1 are basically self-explanatory with the possible exception of Injector Coolant Temperature. The cetane engine uses the standard boiling-water condenser system to maintain the temperature of the coolant used for cooling the cylinder and head. The fuel injector has a separate cooling system supplied by a parallel leg from the condenser coolant loop of the boiling-water condenser cooling system. By controlling the flow through this leg, the separate water jacket around the fuel injector is controlled to a temperature of 100°F (37.8°C). This arrangement provides improved viscosity control in the fuel injection process.

The operating conditions for the mini-dilution tunnel used for mass particulates sampling are given in Table 4-2. The air pressure upstream of the sample aspiration nozzle was subject to some variability since it was used to adjust the dilution ratio in the tunnel. Gradual buildup of soft carbon in the sample probe caused minor changes in sample flow drawn into the tunnel, thus requiring changes in tunnel flow to maintain the dilution ratio. The remaining mini-dilution tunnel operating conditions are self explanatory.



Table 4-1

## Cetane Engine Test Conditions

Compression Ratio	= 20:1
Engine Speed	= 1200 RPM
Injection Timing	= Optimum or 5° Retarded
Fuel Flow	= Mass flow to provide nominal Air/Fuel ratios of 20:1, 30:1, and 40:1
Inlet Air Temperature	= 150 °F $\pm$ 1 °F
Inlet Air Pressure	= 14.4 psia $\pm$ 0.1 psia
Inlet Air Humidity	= Less than -10 °F Dew Point
Exhaust Pressure	= 0 to 1 inch of water in stilling chamber
Oil Temperature	= 150 °F $\pm$ 5 °F
Coolant Temperature	= 211 to 212 °F (dependent on barometric pressure)
Injector Coolant Temperature	= 100 °F $\pm$ 1 °F

Table 4-2

## Particulate Dilution Tunnel Operating Conditions

Air Pressure Upstream of Sample Aspiration Nozzle	= 30 to 40 psia (depending on sample line condition)
Back Pressure in Tunnel	= 1 inch of water
Nominal Dilution Ratio	= 10:1 -0.5 to +0.8
Temperature at Sample Point in Tunnel	= 150 °F $\pm$ 1 °F
Temperature at Particulate Filter	= 125 °F -5°F to +2°F
Sample Flow Through Particulate Filter	= 75 cfh $\pm$ 5 cfh

The loss of time and resources encountered by discarding the data taken at 900 rpm led to a reevaluation of the work that could be completed in this program. It was established that a complete set of data at the 1200 rpm operating condition would be a reasonable expectation for the remaining time and resources. For this reason, test conditions at other engine speeds were eliminated from the program.

#### 4.2 Test and Operating Procedures

The use of the cetane engine over the past several years for research projects with diesel fuels has allowed the accumulation of a significant amount of experience with this device used to measure performance and emissions. One of the major problems in using the cetane engine for this type of work has been the difficulty in obtaining consistent and reproducible results from one day's operation to the next. Two different commercial engines, one with a DI combustion system and the second with a IDI combustion system, have been tested using the same dynamometer and emission measurement system and found to provide substantially more consistent results than the cetane engine. The DI engine was a John Deere 3164D, modified for single cylinder operation. The IDI engine was a single cylinder Kubota, model EA-450N. More details about these engines are given in references (4-1, 4-2, and 4-3).

In addition to giving more consistent test results, these engines require little or no daily maintenance other than fluid checks and scheduled oil changes. The cetane engine, on the other hand, requires substantial daily maintenance to achieve reasonable consistency in emissions results. The following sections are devoted to outlining the test procedures used for this project. Special attention has been given to describing the specialized procedures used with the cetane engine that have been developed over the last several years.

##### 4.2.1 System Startup

At the beginning of each day's operation the cetane engine was started with the dynamometer and operated using a nominal number 2 diesel fuel normally used for diesel certification testing. The normal period required to bring the engine to operating stability was approximately 1 hour. During this time the compression plug was moved and reset to the handwheel reading required for the 20:1 compression ratio. This procedure was necessary to avoid seizure of the plug due to carbon deposits. The crankcase of the engine is made up of several large castings, and at least one hour of operation is required before the oil temperature has stabilized. Oil temperature stability and the associated viscosity control are important because of the high mechanical frictional losses for the cetane engine.

During the warm-up period the engine is operated at a full-load condition corresponding to 20:1 air-fuel ratio. After the engine has been warmed up for approximately one-half hour, the emissions instruments are used to set the air-fuel ratio to 20:1. During this period the computer data acquisition system and the processing digital oscilloscope have been used to maintain injection timing near the optimum value. For the next 15 to 30 minutes data traces for pre-chamber pressure, cylinder pressure, injector lift, and injector pressure are

examined to ensure that the engine is operating in a consistent fashion. Nominal emissions measurements are also being made with particular attention being given to HC emissions and to Bosch smoke readings since these variables seem to be most sensitive to problems with the fuel injection system of the engine. If a problem is obvious, the engine is shut down immediately and the appropriate corrective action is taken. Many times, simply removing the injector nozzle and cleaning it will resolve problems.

At the beginning of the warm-up period, the engine is operated directly from room air. A simple solenoid valve instantaneously switches operation between room air and the high pressure air system used to provide controlled pressure and inlet humidity conditions. When the warm-up period is concluded, the engine is switched over to the high pressure air system, and the fuel is changed over from the warm-up fuel to the test fuel to be used. The engine is normally operated for an additional 20-30 minutes with the test fuel and the high pressure air system before data is recorded. During this time, fine adjustments are being made to establish the 20:1 air-fuel ratio and optimum injection timing. Because of a problem associated with taking motoring data, the inlet air pressure for the engine is set at the value observed while operating the engine from room air.

During the period that the engine is warming up, high pressure humidity controlled air is passed through the mini-dilution tunnel. The inlet air heater is controlled by a temperature sensor at the sampling point in the tunnel to bring the temperature of the flowing gas to 150°F (65.6°C) at that point. During this warm-up operation, heated air is also drawn through the particulate sample system to bring all the parts of this system to an equilibrium temperature condition. The short sample line between the exhaust stilling chamber for the engine and the aspirating nozzle of the tunnel is also heated during this period of time, even though no sample is flowing through yet. Typical warm-up time for the mini-dilution tunnel is 30-45 minutes.

The normal operating time to bring both the engine and the mini-dilution tunnel to equilibrium conditions and stabilize operation with the test fuel at the desired conditions is approximately one and one-half hours. At the end of this period, data taking for the test fuel at full load conditions commences. Once the engine and mini-dilution tunnel system have been fully warmed up with a given test fuel, the time required to change operating conditions of load or injection timing is approximately one-half hour. These warm-up and changeover constraints leave enough time for testing at 4 different operating conditions in a total 8-10 hour period.

#### 4.2.2 Optimum Injection Timing

One of the more commonly used approaches for determining optimum injection timing for a diesel engine is to vary the injection timing at a given engine speed and measure the fuel consumption and power output from the engine. Typically, the engine will exhibit a minimum specific fuel consumption in lb/hp-hr for some value of injection timing. Since

this point typically represents maximum efficiency for a given speed and load condition, it is considered to be the optimum injection timing.

The nature of the cetane engine is such that changes in fuel flow and power output are very small over a wide range of injection timing values. Therefore, it is very difficult to identify a minimum specific fuel consumption and its associated injection timing. Changes in injection timing of several degrees have virtually no reproducible effect on fuel consumption or power output. For this reason, a different approach was needed to consistently determine optimum injection timing for the cetane engine.

A study of the timing sensitivity of diesel engines shown in various papers and in previous programs using commercial engines indicated that the rapid cylinder pressure rise due to combustion started before TDC for engines operating at optimum timing. These observations led to the following procedure used in this test program to determine an estimate of optimum injection timing for the cetane engine.

The Norland processing digital oscilloscope was used to study how changes in injection timing altered the relationship between the pressure in the pre-chamber and the TDC marker from the shaft encoder. After considerable experimentation, a method was devised that would provide consistent results for engine operation and  $\text{NO}_x$  emissions. The sensitivity of the  $\text{NO}_x$  emissions to injection timing was quite useful in arriving at a method to provide consistent results.

The processing features of the Norland processing digital oscilloscope allowed a rapid computation of the pressure derivative while the engine was operating. Adjustment of the injection timing to place the first derivative maximum (after the first derivative minimum) at TDC gave consistent day to day results for engine performance and oxide of nitrogen emissions. The speed of operation of the Norland processing digital oscilloscope was such that the derivative operation could be done quickly enough to use the device as a tool for setting the injection timing. Figure 4-1 illustrates the appearance of the pre-chamber pressure derivative at the conditions assumed for optimum injection timing.

#### 4.2.3 Performance and Emissions Measurements

Once the engine and mini-dilution tunnel systems were fully warmed up and operational, several sets of data were gathered at each steady state test condition. Software prepared specifically for use in this laboratory was used with the microcomputer data acquisition system to prompt a test operator to enter the information needed. This prompting involved requesting information about the test fuel, important fuel properties, nominal operating conditions for the engine, and data from the performance and emissions measuring instruments. For this program, five separate measurements were made for the emissions and performance data. Many features of the software provided information to the operator concerning system performance. For example, air-fuel ratios calculated on a carbon basis and an oxygen basis were shown at the end of each data entry panel. Any major discrepancies in these numbers would indicate to the operator some problem in the emissions measuring system.

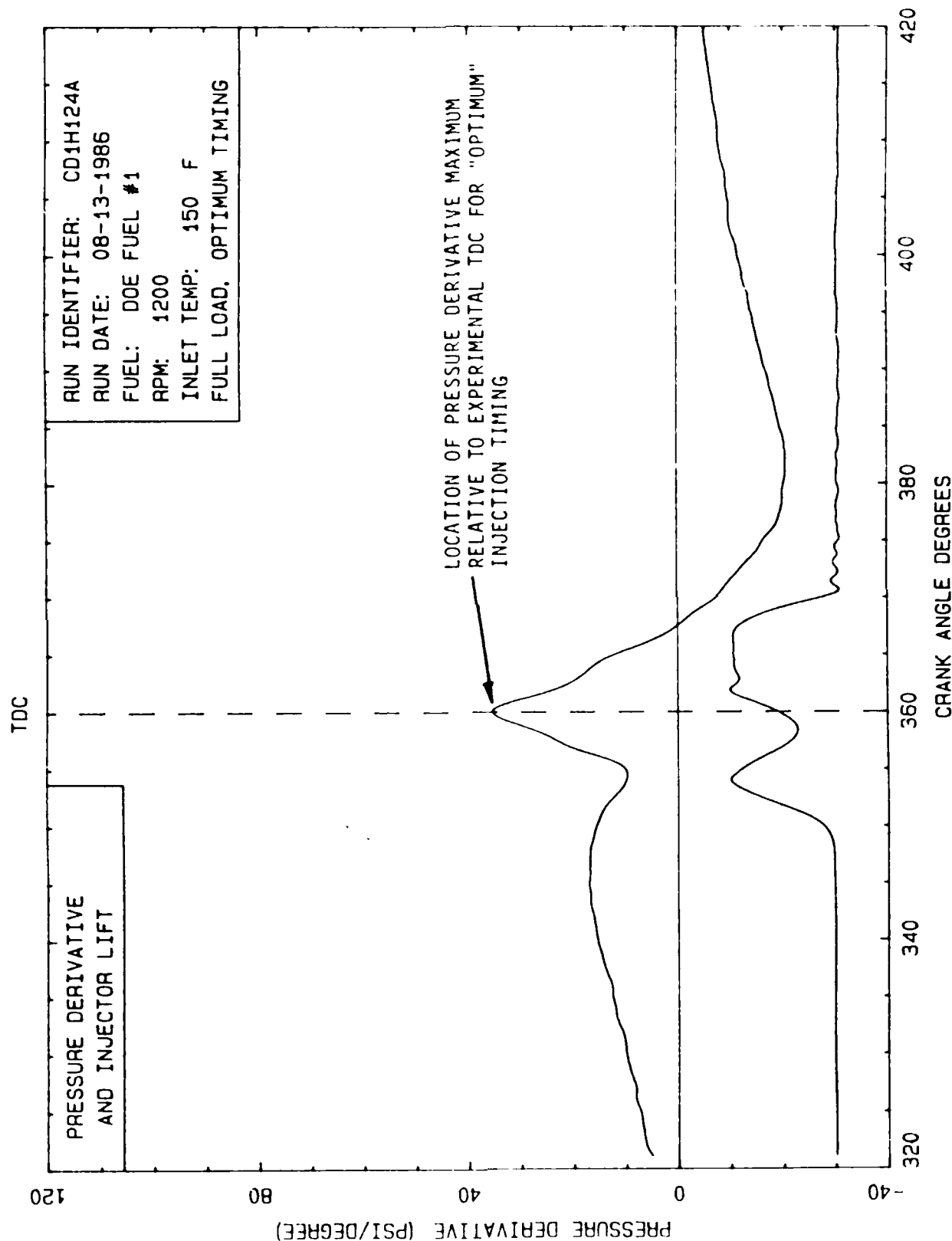


Figure 4-1 Determination of Optimum Injection Timing for Cetane Engine

The five consecutive sets of emissions and performance data were taken over a period of approximately 1 hour. If particulates data were also being taken with the mini-dilution tunnel, each of the five data sets had a corresponding particulates data set. The 1-hour period and the five separate data sets were felt to give a good indication of the consistency and stability of the engine operation at the particular test condition. The laboratory data sheet, shown in Figure 4-2, provides a printed record of the calibrated data from the emissions and performance instrumentation as well as an average value and a standard deviation for the five data runs. The average values are used in data processing software employed to calculate performance terms and specific emissions.

Each laboratory data sheet is identified at the top with several pieces of record keeping information. In the upper left-hand corner of the data sheet is the date on which the particular printout was prepared. Immediately below this date are the initials of the laboratory operators. In the upper right-hand corner of the data sheet is the data set identification which describes the fuel and test conditions, and immediately below it is the run date on which the laboratory data was taken. A more thorough explanation of the coding used for the data set identifier is given in Table 4-3.

During each data taking run, very minor adjustments may be made to the engine system to maintain constant operating conditions. For example, minor adjustments may be made to the inlet manifold pressure or temperature to keep them within the very close limits established in the operating conditions. Any changes made were allowed to stabilize before an additional data set was taken.

#### 4.2.4 Particulates Sampling

For those test conditions that also involved obtaining a mass particulates sample, the following procedures were used with the mini-dilution tunnel.

Before the start of each day's operations a number of Pallflex type T60A20 47mm Teflon coated filters were weighed to the nearest 10 micrograms. The filters had been stored in a desiccator for at least 24 hours prior to weighing, and a sufficient number of filters were weighed for all the anticipated data runs plus a few extra in case a filter was dropped or damaged. All filters were carefully handled with tweezers, and each filter was placed in a plastic box which was labeled with the initial filter weight, the date, and the initials of the person who weighed the filter. After particulates were collected on each filter in the mini-dilution tunnel, tweezers were used to carefully remove the filter without disturbing the particulate matter and place it back in the marked plastic box. An identification number was then placed on the box label to exactly correlate this particulate sample with the data record information entered into the laboratory computer system. The filters in their boxes were then placed in a desiccator for a 24-hour period and weighed again to determine the total weight of filter plus particulate matter. This weight, the date the filter was re-weighed, and the initials of the person weighing the filter were then entered on the box label. The difference between the initial filter weight and the

Data Sheet  
SINGLE CYLINDER DIESEL ENGINE

Date: 11-07-1986  
Operator: MWL & MEM

Data set: B:CD1H124A  
Run date: 07-30-1986

I. Fuel Characteristics:

- a) Fuel Number : DOE-1
- b) Fuel Description : PHILLIPS D-2
- c) Physical Properties : LHV = 18321 , Y = 1.78 , X = .00039

II. Operating Conditions:

- a) Barometric Pressure : 28.88 in. Hg. at 96 Deg. F
- b) Nozzle Number : 16
- c) Engine Speed : 1200 RPM
- d) Air Intake Temperature : 150 Deg. F
- e) Oil Temperature : 155 Deg. F
- f) Coolant Temperature : 212 Deg. F
- g) Critical Flow Nozzle Temperature : 96 Deg. F
- h) Critical Flow Nozzle Pressure : 46.4 Psia
- i) Manifold Pressure : 14.4 Psia
- j) Exhaust Pressure : 0 in. water
- k) Injection Advance Setting : 9.4 Deg. BTDC

III. Exhaust Emissions and Test Conditions:

Run Number	1	2	3	4	5	Avg/Dev (%)
a) HC (ppm, C1)	260	220	230	220	210	228/ 8.44
b) NOx (ppm)	510	520	510	510	520	514/ 1.07
c) CO (%)	0.146	0.107	0.109	0.119	0.110	0.118/13.71
d) CO2 (%)	10.9	10.9	10.9	10.9	10.9	10.9/ 0.00
e) O2 (%)	5.9	6.0	5.8	6.0	5.9	5.9/ 1.41
f) Bosch Smoke	5.5	5.3	5.3	5.4	5.6	5.4/ 2.41
g) Fuel Flow (min) for .1 lbm	3.032	2.985	2.967	2.967	2.977	2.985/ 0.90
h) Firing Force (lb)	13.8	13.8	13.8	13.8	13.8	13.8/ 0.00
i) Fuel Temp. (Deg. F)	95	96	96	96	96	96/ 0.47
j) Exhaust Temp. (Deg. F)	783	779	782	787	792	785 / 0.64
k) Motoring Force :	11 lbf	(zero = 0 , 11 lb cal. = 10 )				

IV. Comments:

HANDWHEEL SETTING = .947

Figure 4-2 Sample Laboratory Data Sheet for Engine  
Performance and Emissions

Table 4-3

Interpretation of Data Set Identification Code

DATA SET CODE NAME WITH NO EXTENSIONS OR PREFIXES

	C	D	1	H	1	2	4	A
ENGINE	FUEL	INLET AIR TEMP.	SPEED (RPM IN HUNDREDS)	LOAD (FRACTION, FULL LOAD)	INJECTION TIMING			
C = CETANE R = RICARDO (IDI) Q = RICARDO (DI)	C2 = BASE D1 = DOE #1 D2 = DOE #2 D3 = DOE #3 D4 = DOE #4 E1 = CEC #1 E2 = CEC #2 E3 = CEC #3 E4 = CEC #2A K5 = CAPE #5 K6 = CAPE #6	H = HOT C = COLD	09 = 900 12 = 1200 15 = 1500 18 = 1800	1 = 1/4 2 = 2/4 3 = 3/4 4 = 4/4	A = OPT. TIMING C = -5 CA° RETARD			

For this example:

CD1H124A

- C - Cetane engine being tested
- D1 - DOE #1 fuel
- H - Heated inlet air
- 12 - 1200 RPM engine speed
- 4 - Full load (4/4)
- A - Optimum injection timing



final filter weight was recorded as the mass of particulate matter collected.

As indicated in a previous section, the mini-dilution tunnel was fully warmed up and stabilized during the warm-up and stabilization process for the engine itself. Once the data taking process was begun, the laboratory software also provided prompting information for the dilution tunnel and particulate measurements. Using the information from the first of the five consecutive data runs, the exhaust CO<sub>2</sub> reading, the tunnel CO<sub>2</sub>, and the background CO<sub>2</sub> reading for the air in the tunnel were entered and the nominal dilution ratio computed and displayed. Adjustment of the upstream pressure from the dilution nozzle allowed some adjustment of the dilution ratio to keep it near the desired value of 10:1. When particulates data were being taken, at the end of each data entry panel for the emissions and performance information a second panel would appear requesting the appropriate information for the dilution tunnel and particulates measurement. A printout of this data sheet is illustrated in Figure 4-3. The date and run identification information shown at the top of this data sheet are identical to those shown for the emissions and performance data sheet. The software used to generate this information not only shows the values recorded in the laboratory, it computes both corrected sample volume and mass particulates in milligrams per cubic meter of dilute exhaust. As with the emissions and performance data, the mass particulates values are shown for each run number as well as an average and a standard deviation. The average value for mass particulate shown on the data sheet is used in calculation of mass particulates on a mass per unit energy basis.

#### 4.2.5 Data Acquisition for Combustion Analysis

As indicated in the equipment description in Section 3, the IBM personal computer system was used as the controlling device for the acquisition and storage of high speed transient data. Substantial menu driven software has been developed to prompt the operator for the correct method and sequence of taking pressure, injector lift, and other data pertinent to the combustion analysis process.

Once the data acquisition software was initiated, a series of instructions were displayed on the screen giving the operator information about how to set up the instrumentation and the Norland processing digital oscilloscope to take data. The first data taking operation involved using the data acquisition system contained in the IBM-PC to sample and store over 100 consecutive cycles of main chamber pressure data. Simultaneous with the data acquisition being performed by the IBM-PC, the Norland processing digital oscilloscope was acquiring high resolution data for main and pre-chamber pressures and storing them in memory segments of the processing oscilloscope. Simultaneous measurement of the main-chamber pressure by both the Norland processing oscilloscope and the IBM-PC system for full cycle measurements provided a test of the data consistency from both systems. After the full cycle pressure data had been acquired with the IBM-PC system, a memory image of the data was stored on the data run diskette for further processing at a later time. The IBM-PC data acquisition was then used to measure

Particulates Data Sheet  
SINGLE CYLINDER DIESEL ENGINE

Date: 11-07-1986  
Operator : MWL & MEM

Data set: B:CD1H124A  
Run date: 07-30-1986

V. Dilution Tunnel Data :

- a) Dilution Nozzle Pressure : 17 psig
- b) Tunnel Back Pressure : 1 in. H<sub>2</sub>O
- c) Background CO<sub>2</sub> Reading : 10 = 367 ppm
- d) Tunnel CO<sub>2</sub> Reading : 60 = 9648 ppm
- e) Dilution Ratio : 10.7

VI. Particulates Data :

Run Number	1	2	3	4	5
a) Filter No.	D14A-1	D14A-2	D14A-3	D14A-4	D14A-5
b) Sample Temp (°F)	150	150	150	150	150
c) Filter Temp (°C)	49	50	50	50	51
d) Sample Flow (cfh)	75	75	75	75	75
e) Initial Filter Wt (mg)	64.56	63.70	64.86	67.09	64.79
f) Final Filter Wt. (mg)	77.98	75.89	78.47	81.71	77.78
g) Filter Wt. Dif. (mg)	13.42	12.19	13.61	14.62	12.99
h) Initial Dry Test (ft <sup>3</sup> )	747.79	755.87	763.02	770.81	779.27
i) Final Dry Test (ft <sup>3</sup> )	755.87	763.02	770.81	779.27	786.64
j) Dry Test Diff. (ft <sup>3</sup> )	8.08	7.15	7.79	8.46	7.37
k) Dry Test Temp (°C)	34	35	35	35	35
l) Dry Test Press. (psi)	0.45	0.45	0.45	0.45	0.45
m) Sample Volume (cu M)	0.2175	0.1919	0.2091	0.2270	0.1978

VII. Mass Particulates (mg/m<sup>3</sup>)

Run No.	1	2	3	4	5	Avg.	Dev. (%)
mg/m <sup>3</sup>	61.7	63.5	65.1	64.4	65.7	64.1	2.4

Figure 4-3 Sample Laboratory Data Sheet for  
Particulates Measurements

and record the crankcase pressure data used as a quality check for blowby and upper cylinder conditions.

The software prompted the operator with instructions for processing the Norland data. Specific instructions were given for using the process features of the oscilloscope to smooth the data to remove spikes caused by the sampling process. Also, instructions were provided for taking the derivative of the pre-chamber pressure data and storing the result in an additional memory area of the oscilloscope. The three data segments corresponding to pre-chamber pressure, main-chamber pressure, and derivative of pre-chamber pressure were then sequentially transferred from the Norland memory to the IBM-PC and then to the run data diskette. All data files were stored on the diskette with a file name consisting of the run identification code and an appropriate extension for identifying the specific data contained in the file.

Once the data acquisition process was begun, the menu system prompted the operator to switch appropriate data channels to the Norland processing oscilloscope, take appropriate data, smooth the data (if needed), and then transfer and store the data on the run diskette for further processing. Additional data acquisition runs with the Norland processing oscilloscope included the simultaneous recording of injector pressure and injector lift and a separate recording of the TDC marker for synchronization of the Norland and IBM-PC data as well as providing a precise timing reference. The process of taking and storing all the combustion data files required approximately 15-20 minutes. In so far as possible the process was automated with the IBM-PC controller to minimize the influence of operator technique or error in recording these data.

The final operation in the combustion analysis data acquisition process was to take pre-chamber pressure data and dynamometer scale force for motoring operation of the engine. The dynamometer control system was not sufficiently sophisticated to change instantaneously from firing to motoring operation, and there was a transient period of approximately 30 seconds before data could be taken. If the transient period was significantly longer than 30 seconds, the engine was restarted and temperature stabilized before another motoring run was attempted. The engine was operated using room air because the high pressure air system introduced additional dynamics and time lags in the transient between firing and motoring operation. This problem is why the high pressure air system is set at nominal atmospheric conditions for each data test run.

#### 4.2.6 Required Maintenance

As previously indicated, the maintenance required for satisfactory results from the cetane engine is substantially greater than that needed for a typical modern design diesel engine. One of the most critical maintenance operations for the cetane engine is cleaning of the fuel injector nozzle. The small lift (0.004 to 0.006 inches) and short pintle configuration lead to rapid fouling of the injector nozzle. Even a small deposit accumulation on the face of the nozzle will affect the spray pattern. For this reason, the injector nozzle must be removed from the engine and cleaned after approximately 8 hours of operation.

Thus, the injector nozzle for the engine was cleaned before each day's data taking. Once the injector tip had been cleaned it was reassembled with the injector body and tested for opening pressure and nozzle spray pattern. If the observed spray pattern was not a symmetrical cone with a reasonably fine fog of fuel, the injector was disassembled and the tip re-cleaned. This process was repeated until an appropriate spray pattern, droplet size and opening pressure were obtained. The injector was then installed in the engine and the warm-up process begun.

After 30 hours of operation the crankcase oil in the engine and the oil filter were changed. At this time the compression plug for the engine was also removed and cleaned of carbon deposits to avoid seizure in the bore of the combustion chamber. The lubricating oil used was Shell Rotella, SAE 30W.

Another item of equipment requiring regular maintenance and observation was the mini-dilution tunnel sample system. At the end of each operating day, the exit of the tunnel was sealed and the upstream pressure used to back flush the heated sample line from the exhaust stilling chamber to the aspirating nozzle. Even with this daily routine, occasionally the sample line had to be removed and the soft carbon deposits mechanically removed. The need for this process was indicated by changes required in the upstream aspiration nozzle pressure needed to maintain the nominal 10:1 dilution ratio.

#### 4.3 Test Sequence

The initial plan for the project was to run a semi-random test sequence mixing fuels, loads, and injection timing in an attempt to minimize any effects on the results that might be related to a certain sequence of test events. Unfortunately, when the test conditions had to be changed because of the problems associated with the roller cam follower in the fuel pump, there was insufficient time or resources to carry out this semi-random test procedure.

The test sequence shown in Table 4-4 was developed with the assistance of several key members of the CRC Light-Duty Diesel Combustion Committee. The sequence shown in Table 4-4 addresses not only the time and resource constraints but several other problems encountered during preliminary testing. The fact that the test sequence is organized into two test days that represent 8-10 hours of engine operation for each day reflects the fact that the injector nozzle must be cleaned after each 8-10 hours of operation. It should also be noted that not all test runs involve taking mass particulate data. This compromise reflects problems encountered with the amount of time required for collecting particulate data, especially at light load conditions. It should also be noted that operating conditions are alternated between heavy and lighter loads during each day's test sequence. This arrangement was intended to minimize effects that might appear due to the operational history of the engine and emission sampling systems. Retarded timing was only used at the medium load condition since it was felt that this case would be most sensitive to changes in emissions results due to timing and, would provide sufficient load that mass particulates sampling would not be extremely time consuming.

Generally speaking, few problems were encountered with this test sequence from an operational point of view. In a preliminary review of the data results there does not appear to be a consistent day-to-day change due to this operational sequence either. Table 4-5 summarizes all the cetane engine data runs included in this report.

Table 4-4  
Test Sequence for Each Fuel

DAY 1			DAY 2		
LOAD	TIMING	PARTICULATES	LOAD	TIMING	PARTICULATES
FULL	OPTIMUM	YES	FULL	OPTIMUM	NO
LIGHT	OPTIMUM	NO	MEDIUM	OPTIMUM	YES
MEDIUM	OPTIMUM	YES	LIGHT	OPTIMUM	NO
LIGHT	OPTIMUM	NO	MEDIUM	RETARDED	YES

Table 4-5  
Summary of Test Runs

Note: All tests were performed at an engine speed of 1200 RPM and a compression ratio of 20:1. Measurements of HC, CO, CO<sub>2</sub>, NO<sub>x</sub>, and Bosch Smoke were made for all runs. Mass particulates data were taken only for the runs indicated.

FUEL & RUN DATE	ENGINE CONDITIONS LOAD      A/F	PARTICULATES DATA (YES OR NO)	COMMENTS
DOE #1			
8/13/86	FULL      20.1:1	YES	from prev. test
8/14/86	FULL      19.9:1	NO	
7/30/86	FULL      19.7:1	YES	
8/13/86	MEDIUM    30.2:1	YES	retarded timing from prev. test
8/14/86	MEDIUM    30.0:1	YES	
8/14/86	MEDIUM    30.1:1	YES	
7/30/86	LIGHT      41.0:1	YES	
8/13/86	LIGHT      40.1:1	NO	
8/13/86	LIGHT      40.1:1	NO	
8/14/86	LIGHT      40.1:1	NO	
DOE #2			
8/11/86	FULL      20.3:1	NO	from prev. test
8/12/86	FULL      20.1:1	YES	
7/31/86	FULL      20.2:1	YES	
8/11/86	MEDIUM    30.1:1	YES	makeup run
8/12/86	MEDIUM    30.1:1	YES	
9/06/86	MEDIUM    30.3:1	YES	

Thus, the injector nozzle for the engine was cleaned before each day's data taking. Once the injector tip had been cleaned it was reassembled with the injector body and tested for opening pressure and nozzle spray pattern. If the observed spray pattern was not a symmetrical cone with a reasonably fine fog of fuel, the injector was disassembled and the tip re-cleaned. This process was repeated until an appropriate spray pattern, droplet size and opening pressure were obtained. The injector was then installed in the engine and the warm-up process begun.

After 30 hours of operation the crankcase oil in the engine and the oil filter were changed. At this time the compression plug for the engine was also removed and cleaned of carbon deposits to avoid seizure in the bore of the combustion chamber. The lubricating oil used was Shell Rotella, SAE 30W.

Another item of equipment requiring regular maintenance and observation was the mini-dilution tunnel sample system. At the end of each operating day, the exit of the tunnel was sealed and the upstream pressure used to back flush the heated sample line from the exhaust stilling chamber to the aspirating nozzle. Even with this daily routine, occasionally the sample line had to be removed and the soft carbon deposits mechanically removed. The need for this process was indicated by changes required in the upstream aspiration nozzle pressure needed to maintain the nominal 10:1 dilution ratio.

#### 4.3 Test Sequence

The initial plan for the project was to run a semi-random test sequence mixing fuels, loads, and injection timing in an attempt to minimize any effects on the results that might be related to a certain sequence of test events. Unfortunately, when the test conditions had to be changed because of the problems associated with the roller cam follower in the fuel pump, there was insufficient time or resources to carry out this semi-random test procedure.

The test sequence shown in Table 4-4 was developed with the assistance of several key members of the CRC Light-Duty Diesel Combustion Committee. The sequence shown in Table 4-4 addresses not only the time and resource constraints but several other problems encountered during preliminary testing. The fact that the test sequence is organized into two test days that represent 8-10 hours of engine operation for each day reflects the fact that the injector nozzle must be cleaned after each 8-10 hours of operation. It should also be noted that not all test runs involve taking mass particulate data. This compromise reflects problems encountered with the amount of time required for collecting particulate data, especially at light load conditions. It should also be noted that operating conditions are alternated between heavy and lighter loads during each day's test sequence. This arrangement was intended to minimize effects that might appear due to the operational history of the engine and emission sampling systems. Retarded timing was only used at the medium load condition since it was felt that this case would be most sensitive to changes in emissions results due to timing and, would provide sufficient load that mass particulates sampling would not be extremely time consuming.

Generally speaking, few problems were encountered with this test sequence from an operational point of view. In a preliminary review of the data results there does not appear to be a consistent day-to-day change due to this operational sequence either. Table 4-5 summarizes all the cetane engine data runs included in this report.

Table 4-4  
Test Sequence for Each Fuel

DAY 1			DAY 2		
LOAD	TIMING	PARTICULATES	LOAD	TIMING	PARTICULATES
FULL	OPTIMUM	YES	FULL	OPTIMUM	NO
LIGHT	OPTIMUM	NO	MEDIUM	OPTIMUM	YES
MEDIUM	OPTIMUM	YES	LIGHT	OPTIMUM	NO
LIGHT	OPTIMUM	NO	MEDIUM	RETARDED	YES

Table 4-5  
Summary of Test Runs

Note: All tests were performed at an engine speed of 1200 RPM and a compression ratio of 20:1. Measurements of HC, CO, CO<sub>2</sub>, NO<sub>x</sub>, and Bosch Smoke were made for all runs. Mass particulates data were taken only for the runs indicated.

FUEL & RUN DATE	ENGINE CONDITIONS LOAD      A/F	PARTICULATES DATA (YES OR NO)	COMMENTS
DOE #1			
8/13/86	FULL      20.1:1	YES	from prev. test
8/14/86	FULL      19.9:1	NO	
7/30/86	FULL      19.7:1	YES	
8/13/86	MEDIUM   30.2:1	YES	
8/14/86	MEDIUM   30.0:1	YES	retarded timing from prev. test
8/14/86	MEDIUM   30.1:1	YES	
7/30/86	LIGHT     41.0:1	YES	
8/13/86	LIGHT     40.1:1	NO	
8/13/86	LIGHT     40.1:1	NO	
8/14/86	LIGHT     40.1:1	NO	
DOE #2			
8/11/86	FULL      20.3:1	NO	from prev. test
8/12/86	FULL      20.1:1	YES	
7/31/86	FULL      20.2:1	YES	
8/11/86	MEDIUM   30.1:1	YES	
8/12/86	MEDIUM   30.1:1	YES	makeup run
9/06/86	MEDIUM   30.3:1	YES	

Table 4-5 (Continued)  
Summary of Test Runs

FUEL & RUN DATE	ENGINE CONDITIONS LOAD            A/F	PARTICULATES DATA (YES OR NO)	COMMENTS
DOE #2 8/11/86 8/11/86 8/12/86 8/12/86 7/31/86	MEDIUM    30.0:1 LIGHT       40.3:1 LIGHT       40.1:1 LIGHT       40.4:1 LIGHT       40.5:1	YES NO NO NO YES	retarded timing    from prev. test
DOE #3 8/15/86 8/18/86 8/01/86 8/15/86 8/18/86 8/15/86 8/15/86 8/15/86 8/18/86	FULL        20.0:1 FULL        20.1:1 FULL        20.9:1 MEDIUM     30.0:1 MEDIUM     30.2:1 MEDIUM     30.0:1 LIGHT       40.0:1 LIGHT       39.7:1 LIGHT       40.0:1	YES NO YES YES YES YES NO NO NO	  from prev. test  retarded timing    
DOE #4 8/19/86 8/20/86 8/04/86 8/19/86 8/20/86 9/02/86 9/06/86 8/19/86 8/19/86 8/20/86 8/04/86	FULL        20.0:1 FULL        19.9:1 FULL        20.2:1 MEDIUM     29.9:1 MEDIUM     30.0:1 MEDIUM     30.0:1 MEDIUM     30.1:1 LIGHT       40.1:1 LIGHT       40.3:1 LIGHT       39.9:1 LIGHT       40.0:1	YES NO YES YES YES YES YES NO NO NO YES	  from prev. test  rerun, retarded rerun, retarded    from prev. test
CEC #1 12/02/86 12/04/86 12/04/86 12/02/86 12/04/86 12/02/86 12/02/86 12/04/86	FULL        20.1:1 FULL        20.2:1 MEDIUM     30.2:1 MEDIUM     30.1:1 MEDIUM     30.1:1 LIGHT       39.9:1 LIGHT       39.7:1 LIGHT       39.7:1	YES NO YES YES YES NO NO NO	   retarded timing    
CEC #2 12/06/86 12/11/86 12/06/86 12/11/86 12/11/86	FULL        20.1:1 FULL        20.2:1 MEDIUM     29.9:1 MEDIUM     29.8:1 MEDIUM     29.9:1	YES NO YES YES YES	   retarded timing



Table 4-5 (Continued)  
Summary of Test Runs

FUEL & RUN DATE	ENGINE CONDITIONS LOAD                  A/F	PARTICULATES DATA (YES OR NO)	COMMENTS
CEC #2 12/06/86 12/06/86 12/11/86	LIGHT      40.0:1 LIGHT      39.9:1 LIGHT      39.9:1	NO NO NO	
CEC #2A 10/28/86 10/30/86 10/28/86 10/30/86 10/30/86 10/28/86 10/28/86 10/30/86	FULL        19.9:1 FULL        20.1:1 MEDIUM    30.1:1 MEDIUM    30.0:1 MEDIUM    29.9:1 LIGHT       40.1:1 LIGHT       40.1:1 LIGHT       40.0:1	YES NO YES YES YES NO NO NO	retarded timing
CEC #3 12/13/86 12/18/86 12/13/86 12/18/86 12/18/86 12/13/86 12/13/86 12/18/86	FULL        20.0:1 FULL        20.1:1 MEDIUM    30.0:1 MEDIUM    30.0:1 MEDIUM    30.0:1 LIGHT       39.9:1 LIGHT       39.9:1 LIGHT       40.1:1	YES NO YES YES YES NO NO NO	retarded timing
CAPE #5 9/13/86 9/20/86 9/13/86 9/20/86 9/20/86 9/13/86 9/13/86 9/20/86	FULL        20.0:1 FULL        20.0:1 MEDIUM    30.1:1 MEDIUM    30.0:1 MEDIUM    30.0:1 LIGHT       40.1:1 LIGHT       40.3:1 LIGHT       40.1:1	YES NO YES YES YES NO NO NO	retarded timing
CAPE #6 9/27/86 9/28/86 9/27/86 9/28/86 9/28/86 9/27/86 9/27/86 9/27/86	FULL        20.2:1 FULL        19.9:1 MEDIUM    30.0:1 MEDIUM    30.0:1 MEDIUM    30.0:1 LIGHT       39.9:1 LIGHT       39.9:1 LIGHT       39.9:1	YES NO YES YES YES NO NO NO	retarded timing

## 5. Data Reduction Methods

As indicated in preceding sections, virtually all of the data taken in the laboratory were stored on the data diskette for the test run. Manually read data, such as readings from the engine operation console and the emissions instruments, was entered through menu driven software that prompted the operator for a specific reading. Machine read data, such as cylinder pressure and injector lift, were taken using the data acquisition system and stored directly on the diskette. Thus, essentially all the information needed for data reduction was contained on the data diskette.

A significant amount of computer software was written for the IBM-PC to read the laboratory data from the data diskette, compute the appropriate results, and output the information. The form of this output included results files on the data diskette, screen displays on the computer, printed output, and plots showing the results in graphical form. Where appropriate, the data reduction proceeds automatically without operator intervention. During all phases of the data reduction process, intermediate values and quality check plots are displayed on the screen to assist the operator in identifying any problems or discrepancies that may occur. The software can be run in a manually controlled mode that lets the operator locate specific problem areas so that they can be resolved.

Some portions of the data reduction process require operator input for selecting the location of critical points in the process. For example, the software uses several rules to locate start of combustion and the end of premixed combustion. Occasionally, when the data contains higher frequency components or certain features are not well defined, the software does not locate the "correct" point. The operator can enter different values for the independent variable (usually sample point) until he feels that the graphical display of the selected location is correct. This value is then accepted, and the program proceeds with additional data reduction.

For purposes of discussion, the data reduction process has been broken down into three segments: engine performance, specific emissions, and combustion characteristics and parameters. Generally, the order of these segments is the order in which the computation process proceeds. Any exceptions are related to convenience in programming or the need for a specific sequence of computational steps. Since the software is a series of sequential programs, there are checks to insure that the programs are being run in the right order.

### 5.1 Engine Performance

Engine performance is generally related to the power output and fuel consumption of the engine. In the laboratory, variables such as engine speed, dynamometer scale force, fuel flow, and various pressures and temperatures are controlled and/or recorded. As previously mentioned, all this information is stored on the data diskette for later data reduction.

The computations for engine performance results are relatively simple and straight forward. Torque and power are determined from the equations:

$$T = F \times L \quad (5.1)$$

$$hp = \frac{(F \times N) \times L}{5252} \quad (5.2)$$

Where: T = torque in lb-ft  
 hp = power in horsepower  
 F = dynamometer scale force in lb  
 N = engine RPM  
 L = dynamometer force arm (1 foot)  
 5252 = dynamometer constant

Appropriate conversion factors are used to compute the torque in N-m and the power in kw. Both English and metric values are provided in the printed results. Values for brake, friction, and indicated conditions are computed. Because of the high mechanical frictional losses of the CFR engine and the fact that the engine was unthrottled, no attempt was made to separate mechanical and pumping loop friction. The values measured during motored operation are treated as frictional. Indicated values are then the sum of these frictional values plus the brake values determined while the engine was firing.

Mean effective pressure is determined directly from the computed values for torque and the displacement volume of the engine. English units are used for the computation, and the angle through which the torque acts is assumed to be  $4\pi$  radians, corresponding to a four-stroke cycle. After the torque is multiplied by the  $4\pi$  angle, the resulting ft-lb of energy are converted to in-lb and divided by the displacement volume in cubic inches to yield mean effective pressure in psi. Values for brake, friction, and indicated are determined. Metric equivalents in kPa are also computed using the appropriate conversion term.

Fuel flow in the laboratory is recorded as the minutes and seconds to consume a known mass of fuel in pounds. Fuel flow is computed by converting the minutes and seconds to decimal minutes and dividing the fuel mass consumed by the decimal time giving lb/min of fuel flow. Once the fuel flow has been computed, division by the power output (indicated or brake) yields the specific fuel consumption in lb/(hp-hr). Conversion to metric units yields  $\mu\text{gm/J}$  (micrograms/Joule). The specific fuel consumption and the Lower Heating Value (LHV) of the fuel are used to compute engine efficiency. Values are determined for both brake and indicated cases.

Air-fuel ratio is computed using two different approaches for this test program. One is based upon the exhaust gas emissions measurements, and the other is based upon measurement of fuel flow and air flow. For the computation based upon fuel and air flow, the absolute pressure and temperature upstream from the flow metering nozzle in the air supply system are used with the classic relation for critical flow nozzles and experimentally determined flow coefficient to compute the air flow in

lb/min. This value is divided by the computed fuel flow in lb/min to determine the air-fuel ratio based upon air and fuel flow measurement.

## 5.2 Specific Emissions

In the laboratory, the exhaust gas emissions are observed from the laboratory instruments and entered into the laboratory computer system through the aid of menu driven prompting software. The software has appropriate calibration information so that direct instrument readings are converted into mole percent values and displayed for operator confirmation. Once accepted, the calibrated values for emissions data are stored on the data diskette for further reduction.

The CO, CO<sub>2</sub>, NO<sub>x</sub>, and O<sub>2</sub> levels are measured on a "dry" basis in that the sample is passed through a refrigerated trap system to remove the majority of water from the gas stream. The HC emissions are measured on a "wet" basis since the sample is held at 350°F (176.7°C) until it has passed through the flame ionization sensor, thereby keeping the exhaust water in a gaseous state. Data from the Bosch smoke meter were observed directly in the laboratory and the average of at least 3 consecutive samples averaged and then recorded. Particulate data from the mini-dilution tunnel were observed and recorded as described in the section dealing with laboratory procedures.

During the data reduction process, the HC emission concentration was corrected to a "dry" basis so that it could be used in computations with the other exhaust emissions which were measured on a dry basis. One of the first uses of the emissions data was to compute the air-fuel ratio by balancing carbon atoms in an equilibrium equation describing the oxidation of the fuel to the exhaust constituents measured. The approach used was patterned after a method described by Stivender (5-1). The air-fuel ratio determined by this process is said to be "carbon based". When both carbon and oxygen atoms are balanced, the resulting air-fuel ratio is said to be "oxygen based". These computations were actually done by the laboratory data acquisition software so that the values could be used in laboratory operations to set engine operating conditions and check on the consistency of operation of the emissions instruments.

Specific emissions were also computed using an approach based on a method developed by Stivender(5-1). This approach assumes a fuel molecule of the form:



Where:  $y$  = Hydrogen/Carbon mole ratio  
 $x$  = Oxygen/Carbon mole ratio

and the molecular weight of the fuel (MF) can be expressed as:

$$\text{MF} = 12.01 + 1.008y + 16x \quad (5.3)$$

The carbon containing exhaust constituents are expressed as mole percentages represented by the abbreviations HC, CO, and CO<sub>2</sub>. The mole percent of a given emission is described by XX and the molecular weight

of that material is  $MW_{XX}$ . Specific fuel consumption is abbreviated SFC (using either brake or indicated values). With this nomenclature the specific emissions can be expressed as

$$\text{specific } XX = \text{SFC} \cdot \frac{MW_{XX}}{MF} \cdot \frac{(XX)}{(HC + CO + CO_2)} \quad \text{in } lb_{XX}/(hp\text{-}hr). \quad (5.4)$$

More typical units of grams/(hp-hr) are obtained by multiplying by 454 grams/lb. Suitable conversions yield metric units of  $\mu\text{gm}/J$ . Also, grams of XX per kilogram of fuel is determined by deleting the SFC term above and making the appropriate decimal change. Results are reported in all three forms.

Several assumptions were made to compute the mass particulate emissions. The first assumption is that the engine exhaust can be described as an ideal gas with properties roughly comparable to air. This approximation can be in error, particularly at the lower air-fuel ratios. However, it does provide a consistent and simple approach to computing the exhaust density used in determining the mass particulate emissions. The second assumption is that the mass of the exhaust can be described in terms of the mass fuel flow into the engine by the following:

$$\text{mass of exhaust/mass of fuel} = (1 + \text{AIR/FUEL}) \quad (5.5)$$

Using these assumptions and data for exhaust temperature, exhaust pressure, dilution ratio, specific fuel consumption, and particulate mass per  $m^3$  of exhaust, the specific particulates in gm/hp-hr are determined. Appropriate computations are made to also calculate this information on a  $\mu\text{gm}/J$  basis and a gm/kg of fuel basis.

### 5.3 Combustion Characteristics and Parameters

Laboratory data required to determine various combustion parameters included both information from the steady-state measurements for performance and emissions and the following cyclic data:

1. main chamber firing cylinder pressure (full-cycle data and high-speed data)
2. pre-chamber firing pressure (high-speed data)
3. injector lift (high-speed data)
4. injector pressure (high-speed data)
5. TDC marker (high-speed data)
6. time derivative of pre-chamber pressure (high-speed data)
7. pre-chamber motoring pressure (high-speed data)

Full-cycle data are taken at one degree increments and have 720 samples for a single cycle. Normally, over 90 consecutive cycles are included in the data file. High-speed data consist of 1024 data points taken at 0.1 to 0.2 degree increments beginning at 40 degrees BTDC. Each high speed data point is the average of 50 samples at that angular position.

Unless specifically stated otherwise, the computations and determinations described in the following paragraphs were performed with the

IBM-PC laboratory computer system without manual data entry or assistance. Some segments of the computational sequence prompt the operator to accept the result determined by the computer or to enter what the operator feels is a more correct answer based upon his experience. The interactive nature of this process allows the operator to try several values until he feels that the correct result has been reached.

The full cycle data for main chamber pressure are read from a memory image file, calibrated in psi, and the ensemble average and standard deviation of pressure for each crank angle degree is computed. The average pressure when the piston is at bottom dead center is equated to the inlet manifold pressure and the average data shifted accordingly to account for the fact that the quartz transducer does not have an absolute calibration. Study of log pressure vs. log volume plots for different arbitrary values for inlet pressure indicated that this approach gave satisfactory results.

It is a well known fact that the location of TDC for an engine operating at speed and load can be different from the value determined by static measurement. (The TDC marker of the shaft encoder was located precisely, but by static measurements.) Unfortunately, a difference of only a few crank angle degrees can make a significant difference in cycle computations relating to mean effective pressure and heat release. For this reason, an estimate of the location of dynamic TDC must be made. One approach to making this estimate was to compute the net area under the full cycle pressure-volume data, convert this information to indicated mean effective pressure (imep), and compare it to imep determined from dynamometer scale measurements. This comparison was accomplished by shifting the data, in  $0.1\text{ CA}^\circ$  increments, from  $4^\circ\text{BTDC}$  to  $6^\circ\text{ATDC}$ , computing the imep for each case, and selecting the shift that yielded the smallest difference between imep from the area computation and imep from the dynamometer measurements. The shift determined from this comparison was typically in the range from 1 to  $3\text{ CA}^\circ$ .

High speed data for pre-chamber and main chamber pressure were calibrated in psi and adjusted for absolute value by forcing the first data point ( $40^\circ\text{BTDC}$ ) to have the same pressure value as the corresponding data point for the full cycle main chamber pressure data that had already been calibrated and adjusted for absolute value. Although there may be some difference in the pressure between the main and pre chambers at this point, it was felt that the difference would be small, particularly at the lower engine speeds used in this program. Comparison of the pre-chamber and main chamber pressures during compression seems to verify this assumption in that there is virtually no divergence of the pressure curves from  $40^\circ\text{BTDC}$  until injection.

The TDC marker data were used to accurately correlate the high speed data samples, which were taken on a time sampling basis, with the angular rotation of the engine in  $\text{CA}^\circ$ . The exact time for each sample is passed from the Norland processing oscilloscope when the data is being stored on diskette. This time per sample is used with the fact that the TDC marker is at exactly  $40\text{ CA}^\circ$  after the first data sample to determine the exact angular value for each sample. This angular value is used in all cases when processing the high speed data.

Problems in consistency and resolution with the pressure shift determined from full cycle data by matching imeps from dynamometer and P-V area lead to a method that could use the high resolution data from the high speed data acquisition. This method is based upon the work of Douaud and Eyzat (5-2). The basic concept is to use the extreme sensitivity of the compression index for a motored engine near dynamic TDC. By minimizing the changes in the compression index, a location for dynamic TDC can be determined to about  $0.1 \text{ CA}^\circ$ . In essence, the method assumes that if the angular phasing is correct the slope of the log-pressure vs. log-volume plot will be a constant in the vicinity of TDC. A technique using least-squares fitting of straight line segments in the vicinity of TDC was used to measure variations in this slope. The appropriate phase shift was accomplished by shifting the data, in  $0.1 \text{ CA}^\circ$  increments, from  $4^\circ \text{BTDC}$  to  $6^\circ \text{ATDC}$ , computing an error term for differences in the least-squares slopes, and selecting the shift that yielded the smallest error term. The shift determined, using this approach, was between 1 and  $2 \text{ CA}^\circ$  and provided significantly more consistent results than the imep matching method. For this reason, it was used in shifting all data for plotting and heat release computations. The values for the compression index (exponent of  $P \cdot V^n$ ) determined from this computation are used in estimating motoring pressure for computation of heat release parameters.

After considerable effort, it was determined that the measured pre-chamber pressure for motoring operation was quite satisfactory for determining a consistent value for dynamic TDC, but it was not satisfactory to be used with firing pressure data to determine the pressure change due to combustion. The shape of the motored data did not change drastically, but minor fluctuations caused significant changes in the heat release characteristics estimated from the difference in pressure between firing and motoring operation. For this reason, a calculated motoring pressure data set was developed. This data set used the values for compression index determined from the computation for dynamic TDC and computed a motoring pressure shape using the  $P \cdot V^n$  relationship. A least-squares two parameter linear fit was used to force the motor shape to coincide with the compression portion of the firing data from  $20^\circ \text{BTDC}$  to  $5^\circ \text{BTDC}$ . Once the parameters were determined for a best fit in this region, the entire motored data set was adjusted using them. This process gave very consistent calculated motoring data that was still based on experimental measurements.

The injector lift data was calibrated to a relative value. The base line of data before lift began was assigned a value of 0, and the peak lift was assigned a value of 20. All intermediate values were scaled accordingly. This approach was used since the installation of the lift transducer allowed some movement of the sensing element within the probe sheath. Slight changes in the nominal distance from the sensor to the magnet caused measurable changes in the calibration, and since the injector was disassembled and cleaned each day it was unrealistic to try to maintain a calibration for this system. The relative calibration approach worked well and no problems were encountered.

The injector pressure (also measured with a crystalline transducer) was calibrated in psi and then shifted to absolute calibration by estimating that the lowest pressure reached after injection was approxi-

mately 10 psia. Of the several approaches attempted to determine the absolute calibration of this transducer, this method produced the most consistent results over a range of operating loads and injection timing.

The pre-chamber pressure derivative was calibrated from the pre-chamber pressure transducer calibration factor and the derivative relationship. Since the derivative function describes slopes, no absolute shift of the resulting data was needed. The derivative was converted to  $dP/d\theta$  form using the angle/sample time relationship.

The estimate of the compression index determined from the motoring data was also used to develop a very crude estimate of the bulk gas temperature in the combustion chamber during the compression process. In essence, a polytropic process was assumed for the compression using the inlet air temperature at BDC as the starting point. Although not highly accurate, this approach did provide a means to compare how engine and fuel variables might influence the compression temperature.

Once all laboratory data had been properly calibrated and shifted, results were written to diskette files for use in plotting and in computing various combustion parameters. A separate file was established for each of the calibrated variables. This approach made it more convenient for following programs to select and read only the information needed for the portion of the data manipulation they addressed. Separate files also made trouble-shooting problems considerably easier during the data reduction process.

Combustion characteristics and parameters were computed from the calibrated and shifted data. One of the first items determined was the start of fuel injection (SOI). Because there is no sharp distinctive point at which the injector needle begins to rise, an arbitrary definition for start of injection was needed. Because this system has been used with another engine having a considerably less regular injection lift pattern, an average lift was computed using data points forward from the peak level until the value was less than 90% of the peak level. Start of injection was defined as when the lift curve first reached 20% of this average lift. End of injection was defined as the point after peak value when the lift dropped below 10% of the average lift or when the injector pressure fell equal to or below the pre-chamber pressure, whichever occurred first. These points are illustrated in figure 5-1.

The start of combustion is defined from the  $dP/d\theta$  data. Comparison of  $dP/d\theta$  for firing and motored data clearly illustrates that the minimum immediately before the peak value for firing data is the start of the combustion process (SOC). This point is illustrated in figure 5-1. The operator has the option to accept the estimate of this point determined by the computer software or to select a different point. Each time a different point is selected, the graphical display showing the derivative and the selected location of the minimum is shown. The computation does not advance until the operator accepts the new value. Ignition delay is simply the angular difference between the SOI and SOC based upon these definitions.



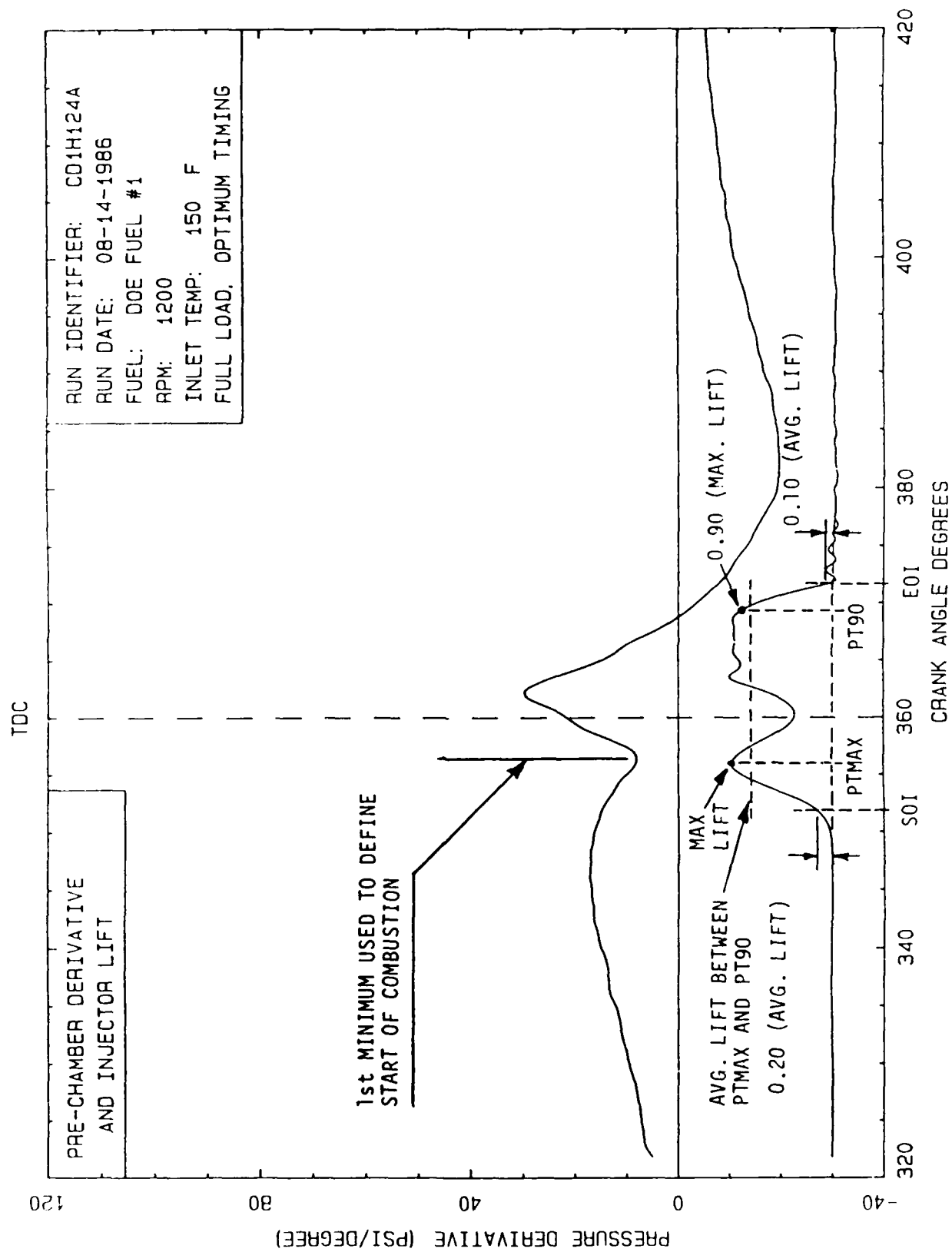


Figure 5-1 dP/dθ Data Illustrating Determination of Start of Combustion

Several other parameters were determined directly from measurements from the results data. They include the following:

1. Pre-chamber pressure at start of combustion
2. Maximum pre-chamber pressure and associated  $CA^\circ$
3. Maximum rate of change of pre-chamber pressure in  $psi/CA^\circ$
4. Estimated bulk gas temperature at SOI

A very simplified approach based on the work of Rassweiler and Withrow (5-3) was used to estimate heat release during the combustion process. Their work indicates that during combustion, the change in cylinder pressure from one point to the next is made up of a component due to the change in cylinder volume and a component due to combustion. Calculated motoring data provides the pressure component due to cylinder volume change so that the component due to combustion can be determined by a simple subtraction operation. The end of combustion is defined as the angular position at which the combustion component of the pressure change becomes zero or negative. Since no attempt is made to account for the heat transfer from the gas to the walls, the heat release information determined is called "apparent heat release" to indicate that is not determined from a comprehensive combustion analysis. From this information, terms comparable to cumulative heat release, Rate of Heat Release (ROHR) and the derivative of ROHR were determined. All were put on a normalized basis so that there would be no confusion that these were actual heat release values and so that the relative shapes of the curves could be easily compared.

The curves determined from the apparent heat release information were used to compute three combustion parameters described by Wade, et. al. (5-4). The computation of these parameters uses the assumption that the diesel combustion process can be approximately described as having an initial mode of combustion similar to the spark ignition engine where fuel and air are mixed together in combustible proportions and the flame propagates through the mixture. This mode is called premixed combustion. It is followed by the diffusion mode of combustion where the fuel is still diffusing into the air in the cylinder and combustion is occurring in regions of this process where the local mixture will support combustion. The three parameters determined were:

- |                                      |  |
|--------------------------------------|--|
| Premixed Combustion - Fraction (PCF) | The fraction of the total apparent heat release which occurs at the end of the premixed combustion mode.   |
| Premixed Combustion - Index (PCI)    | The ratio of the cumulative apparent heat release to the cumulative available heat release at the end of the premixed mode.  |
| Diffusion Combustion - Index (DCI)   | The ratio of the average apparent rate of heat release in the diffusion mode to the average available rate of heat release, excluding the heat release in the premixed mode. |

Figure 5-2 illustrates the computation of these three parameters. Since it is obvious that the key item in these computations is the accurate location of the end of premixed combustion, figure 5-3 is included to illustrate how this location is determined for both IDI and DI engines. Both of these figures are reproduced from reference 5-4. The computer software does select a point as the end of premixed combustion based upon criterion 1 or criterion 2 as shown in figure 5-3. Unfortunately, the minima shown for the rate of change of ROHR is not always as obvious as that shown in the figure. For this reason, the operator must always accept the computer determination of the end of premixed combustion and may select a different point if appropriate. Again, this is an iterative process that allows the operator to try several different values before accepting a final value.

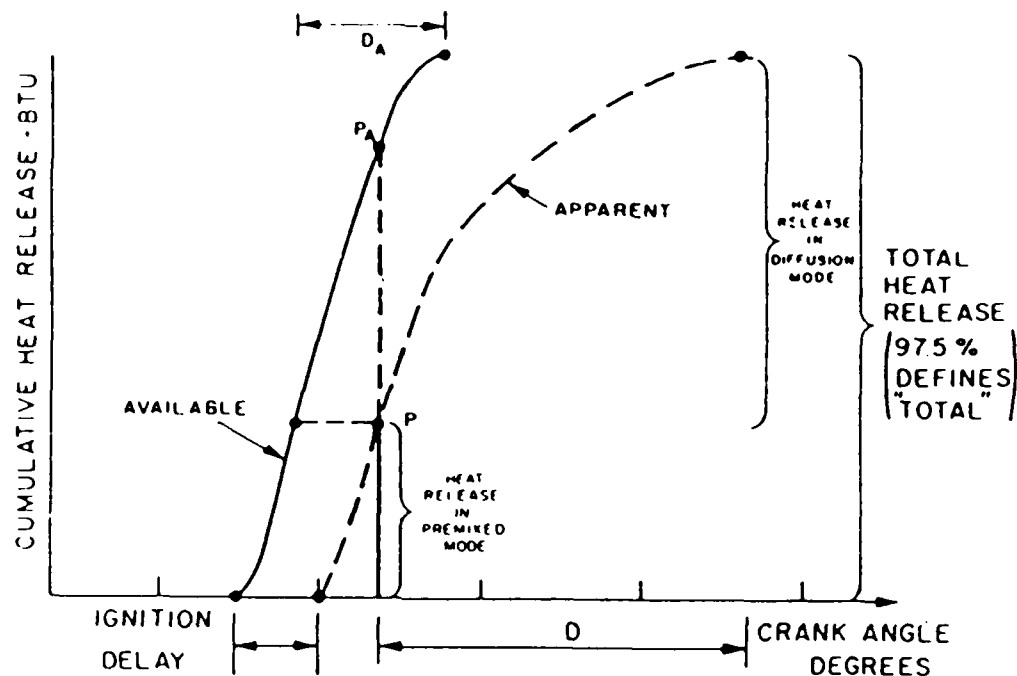
The available energy shown in figure 5-2 is the cumulative fuel energy present in the cylinder for any given moment. It is determined directly from the estimated fuel flow across the injector. The fuel flow is assumed to be proportional to the injector lift (approximate flow area) and the square root of the difference between the injector pressure and the pre-chamber pressure. The flow coefficient is computed for each data run using the average measured mass flow of fuel as the known parameter. Once the coefficient has been computed, the instantaneous flow at each sample point is determined.

#### 5.4 Data Quality Measures

A variety of measures were taken to ensure the quality and consistency of the data presented. In the laboratory, pressure data were displayed on the laboratory computer screen in graphical form to allow the operator to determine if the data taking operation had been successful. The use of the processing digital oscilloscope provided a continual visual check on the quality and consistency of data being taken and recorded. The nature of this system allowed replacement data to be taken if some random problem was discovered in the laboratory data. In addition, transducer calibrations were checked periodically both for static and dynamic performance. The log-pressure vs log-volume plot for motoring operation shown in figure 5-4 is for data taken at the conclusion of the test program after several hundred hours of operation with the AVL 8QP505A pressure transducer. The linear relationship for compression and expansion, particularly at lower pressure levels, is a good indicator of the condition and stability of this transducer.

During the data reduction process, numerous intermediate answers were displayed for operator review and acceptance to determine that all data were being processed properly and that answers were at least "reasonable". As previously mentioned, plots of crankcase pressure were used to determine if any change in blowby or upper cylinder condition occurred during the program. Also, log-pressure vs log-volume plots were prepared to provide a visual indication of phasing accuracy and the use of a reasonable value for absolute pressure calibration.

Although many measures were taken to ensure the quality of laboratory data, computed results were carefully examined and compared to determine if any data inconsistencies existed. If there was a major discrepancy or other problem, additional runs were performed.



### DIESEL COMBUSTION PARAMETERS

IGNITION DELAY (ID) = CRANK ANGLE DEGREES BETWEEN  
START OF INJECTION (AVAILABLE  
HEAT RELEASE) AND START OF  
COMBUSTION (APPARENT HEAT RELEASE)

PREMIXED COMBUSTION FRACTION (PCF) = FRACTION OF TOTAL APPARENT HEAT  
RELEASE AT END OF PREMIXED  
COMBUSTION MODE  $= \frac{P}{\text{TOTAL}}$

PREMIXED COMBUSTION INDEX (PCI) =  $\frac{\text{CUMULATIVE APPARENT HEAT RELEASE AT END OF PREMIXED MODE}}{\text{CUMULATIVE AVAILABLE HEAT RELEASE AT END OF PREMIXED MODE}} = \frac{P}{P_A}$

DIFFUSION COMBUSTION INDEX (DCI) =  $\frac{\text{AVERAGE APPARENT RATE OF HEAT RELEASE IN DIFFUSION MODE} \left( \frac{HR_{\text{DIFFUSION}}}{D} \right)}{\text{AVERAGE AVAILABLE RATE OF HEAT RELEASE EXCLUDING PREMIXED MODE} \left( \frac{HR_{\text{DIFFUSION}}}{D_A} \right)} = \frac{D_A}{D}$

Figure 5-2 Determination of Diesel Combustion  
Analysis Parameters (From Reference 5-4)

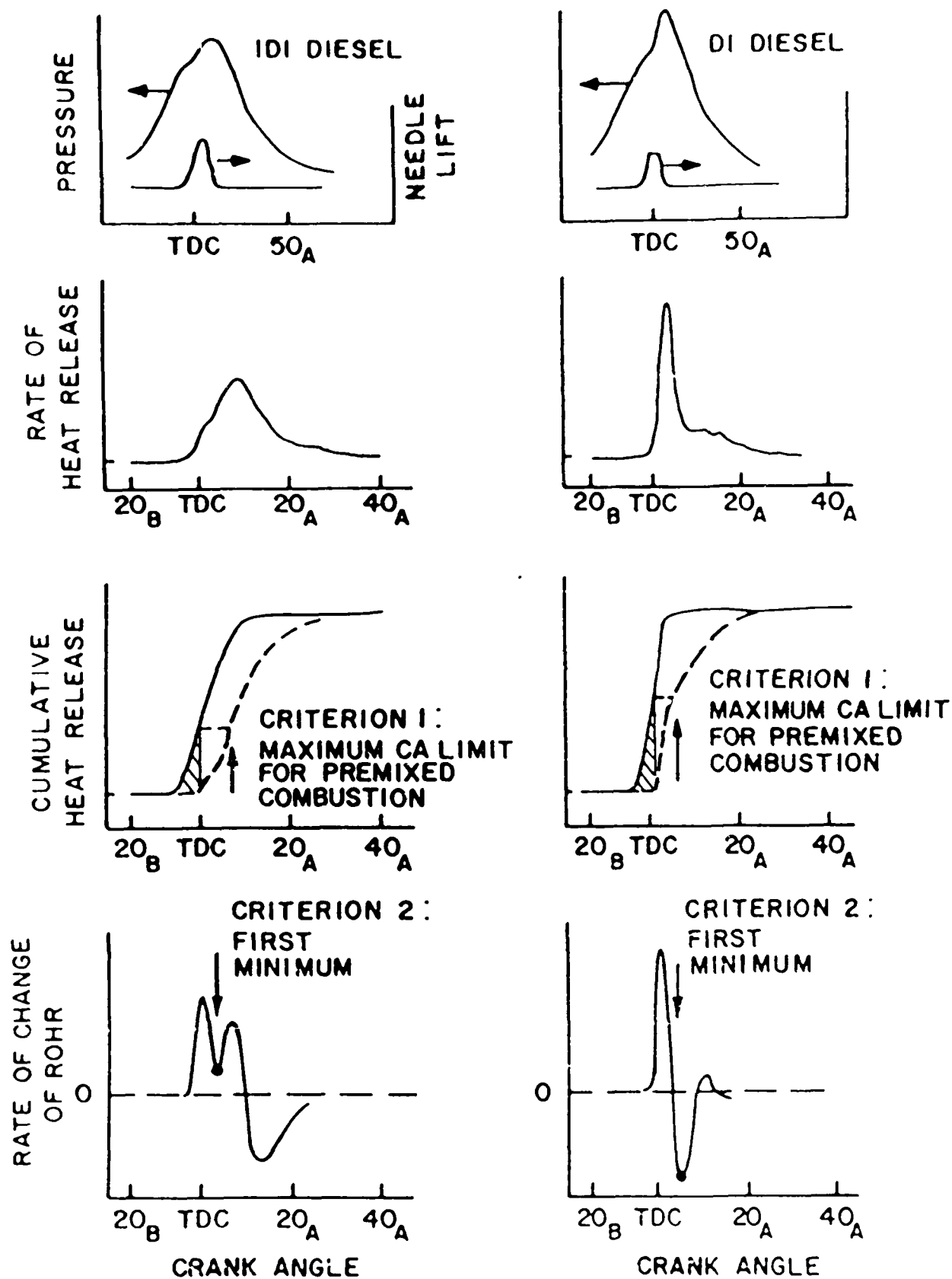


Figure 5-3 Determination of End of Premixed Combustion Mode (From Reference 5-4)

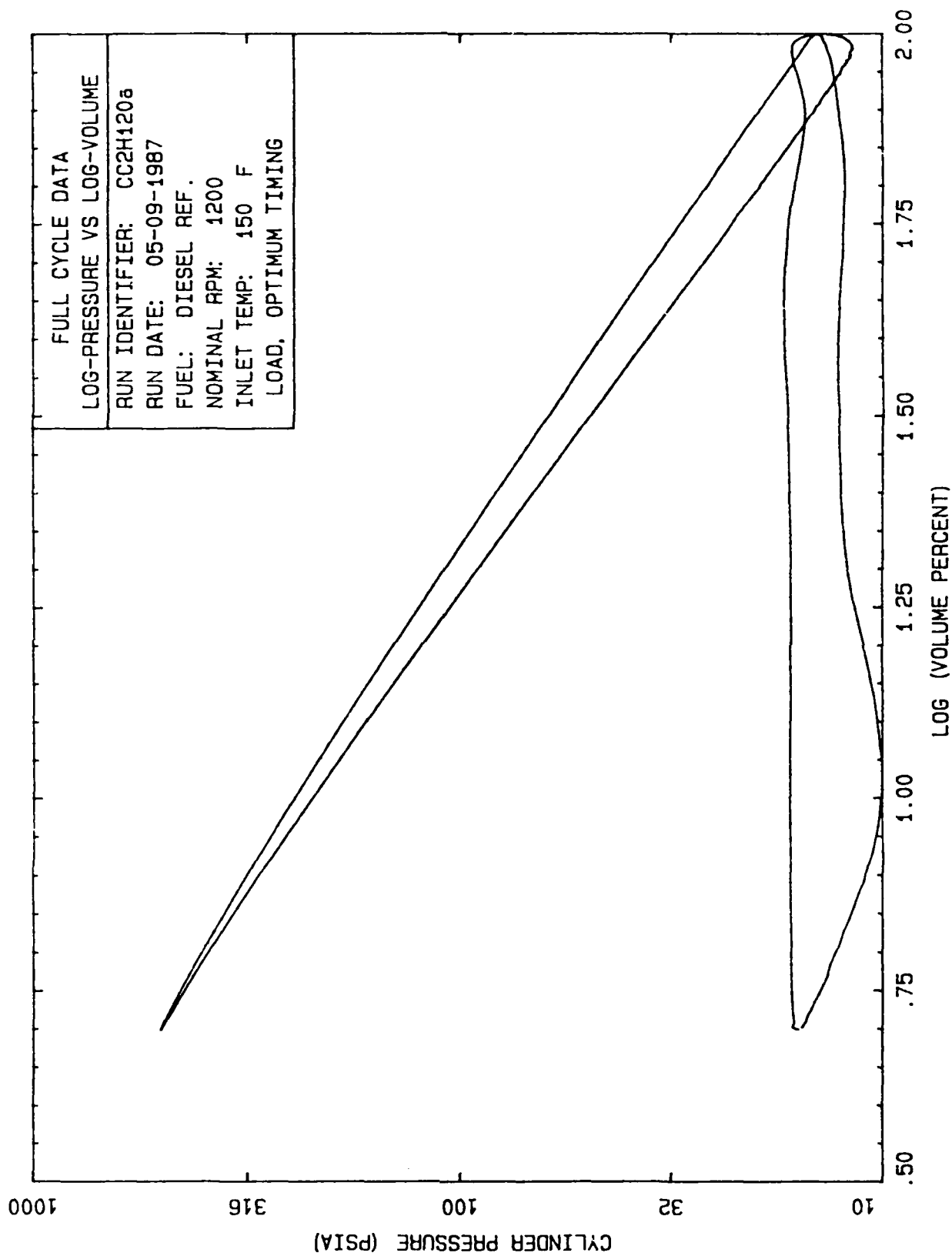


Figure 5-4 Motoring Test Confirming Pressure Transducer Response

## 6. Results

The results section also contains a complete example of the calculated data and plotted results that were generated for each fuel at each test condition. Complete sets of these calculated data are included in the appendices since they are too voluminous for inclusion in the body of the report.

Since all the detailed calculated results are not included in the body of the report, summary graphical results were prepared for all the test conditions for each fuel examined. A substantial portion of this section is devoted to the presentation and discussion of these results.

Considerable effort was devoted to reducing and presenting data from the DOE/Ricardo program in a format that could be directly compared with results from this test program. Summary graphical results are presented in the same format as that used for cetane engine results and appropriate comparisons are made where possible.

### 6.1 Fuel Property Information

As previously mentioned, there was substantial fuel property information available for the fuels used in this test program. Unfortunately, these tests were not performed for all the fuels used in this program so they could not be used effectively in determining fuel property effects on engine performance and emissions. Table 6-1 has been prepared to summarize the normal fuel properties information previously presented in section 2. This summary information is presented here for ready reference in correlating fuel properties with engine performance, emissions, and combustion characteristics.

### 6.2 Example Detailed Results for Cetane Engine

For each fuel tested at each operating condition, considerable detailed information about the performance and emissions of the engine was measured. This information was processed to provide a variety of calculated and graphical results. The tabular and graphical information for each data run fill approximately 16 pages. Since it was not practical to include all this information in the body of this report, an example of the tabulated and graphical information is described.

#### 6.2.1 Calculated Data, Cetane Engine

Figures 6-1 and 6-2 are reproductions of the laboratory data sheets for engine performance and particulate emissions, respectively. They were previously described in section 4 of this report. They are included here to illustrate the complete data package for each test run, from laboratory data sheets to plotted results. All figures use data set CD1H124A, taken August 13, 1986. This data set is for the DOE #1 fuel at full load with optimum injection timing.

Figure 6-3 is an example of the calculated results for engine performance and emissions. Section 1 of the calculated results displays the operating conditions under which the data were taken. Section 2 gives the calculated results. The engine performance results for

Table 6-1  
SUMMARY FUEL PROPERTY DATA<sup>1</sup>

FUELS :		DOE/Ricardo Fuels				CEC Fuels				CRC CAPE-32	
		DOE 1/ *	DOE 2	DOE 3	DOE 4	CEC 1	CEC 2	CEC 2A	CEC 3	CAPE 5	CAPE 6
Property	method										
Gravity, °API	D 287	35.7/35.8	29.2	31.7	48.1	35.8	32.9	29.9	29.9	36.2	27.5
Distillation, °F, %	D 86										
IBP		372/420	427	362	184	365	366	378	364	400	378
10%		420/457	487	406	200	408	411	410	411	462	456
90%		572/578	653	664	535	647	647	648	645	641	641
FBP		616/600	763	724	594	683	688	690	687	708	696
Cetane Number	D 613	50.1/47.3	41.6	40.7	36.2	49.8	48.0	43.2	39.4	53.1	33.9
Viscosity, cSt @ 40°C	D 445	2.40/2.39	4.37	2.76	0.91	3.16	3.01	2.84	2.90	-	-
Hydrocarbon type, V %	D 1319										
Saturates		70.8/61.2	62.5	52.2	80.8	54.0	44.9	34.7	33.5	74.2	42.1
Olefins		1.2/2.3	1.0	0.5	0	2.7	2.5	2.3	2.3	1.3	0
Aromatics		28.0/36.5	36.5	47.3	19.2	43.3	52.6	63.0	64.1	24.5	57.9
Mole ratios y and x											
y, H/C mole ratio		1.78	1.66	1.73	1.90	1.818	1.732	1.634	1.653	1.88	1.65
x, O/C mole ratio		0.0004	0.0005	0.0029	0.0002	0.0	0.0	0.0	0.0	0.0	0.0
Sulfur content, m%	D 262	0.20	0.22	0.38	0.07	0.256	0.272	0.293	0.298	0.24	0.47
Heat of combustion											
BTU/lb											
Mj/lb											
Gross	D 240	19503	19316	19269	19886	19563	19378	19150	19206	19611	19077
Net		45.36	44.93	44.82	46.25	45.50	45.07	44.54	44.67	45.62	44.37
		18321	18165	18148	18643	18356	18226	18054	18100	18370	17973
		42.61	42.25	42.21	43.36	42.69	42.39	41.99	42.09	42.73	41.80

\* Second evaluation of DOE 1 fuel sample obtained after DOE/Ricardo program.

<sup>1</sup> See table 2-1 for additional fuel property information.



Data Sheet  
SINGLE CYLINDER DIESEL ENGINE

Date: 11-07-1986  
Operator: MEM & MWL

Data set: B:CD1H124A  
Run date: 08-13-1986

I. Fuel Characteristics:

- a) Fuel Number : DOE-1
- b) Fuel Description : PHILLIPS D-2
- c) Physical Properties : LHV = 18321 , Y = 1.78 , X = .00039

II. Operating Conditions:

- a) Barometric Pressure : 28.93 in. Hg. at 87 Deg. F
- b) Nozzle Number : 16
- c) Engine Speed : 1200 RPM
- d) Air Intake Temperature : 150 Deg. F
- e) Oil Temperature : 154 Deg. F
- f) Coolant Temperature : 212 Deg. F
- g) Critical Flow Nozzle Temperature : 84 Deg. F
- h) Critical Flow Nozzle Pressure : 46.4 Psia
- i) Manifold Pressure : 14.5 Psia
- j) Exhaust Pressure : 0 in. water
- k) Injection Advance Setting : 9.5 Deg. BTDC

III. Exhaust Emissions and Test Conditions:

Run Number	1	2	3	4	5	Avg/Dev (%)
a) HC (ppm, C1)	210	190	190	190	220	200/ 7.07
b) NOx (ppm)	520	480	500	490	490	496/ 3.06
c) CO (%)	0.081	0.078	0.074	0.074	0.083	0.078/ 5.21
d) CO2 (%)	10.8	10.8	10.8	10.8	10.6	10.8/ 0.83
e) O2 (%)	5.8	5.8	5.8	5.8	5.8	5.8/ 0.00
f) Bosch Smoke	5.3	5.0	5.0	4.8	5.3	5.1/ 4.27
g) Fuel Flow (min) for .1 lbm	3.070	3.062	3.080	3.052	3.062	3.065/ 0.34
h) Firing Force (lb)	13.7	14.0	13.9	13.9	13.9	13.9/ 0.79
i) Fuel Temp. (Deg. F)	85	86	86	86	87	86/ 0.82
j) Exhaust Temp. (Deg. F)	772	776	774	776	769	773 / 0.38
k) Motoring Force :	10.9	1bf	(zero = 0	, 11 lb cal. = 11	)	

IV. Comments:

HANDWHEEL SETTING 0.947 - TIMING CHANGED TO 10.1

Figure 6-1 Example Laboratory Data Sheet for Cetane Engine  
Performance and Emissions

Particulates Data Sheet  
SINGLE CYLINDER DIESEL ENGINE

Date: 11-07-1986  
Operator : MEM & MWL

Data set: B:CD1H124A  
Run date: 08-13-1986

V. Dilution Tunnel Data :

- a) Dilution Nozzle Pressure : 17 psig
- b) Tunnel Back Pressure : 1 in. H<sub>2</sub>O
- c) Background CO<sub>2</sub> Reading : 9 = 330 ppm
- d) Tunnel CO<sub>2</sub> Reading : 61 = 9935 ppm
- e) Dilution Ratio : 10.3

VI. Particulates Data :

Run Number	1	2	3	4	5
a) Filter No.	D14A-6	D14A-7	D14A-8	D14A-9	D14A-10
b) Sample Temp (°F)	150	150	150	150	150
c) Filter Temp (°C)	48	49	49	50	50
d) Sample Flow (cfh)	75	75	75	75	75
e) Initial Filter Wt (mg)	75.62	77.68	76.39	76.60	77.67
f) Final Filter Wt. (mg)	89.51	89.71	88.29	88.11	89.61
g) Filter Wt. Dif. (mg)	13.89	12.03	11.90	11.51	11.94
h) Initial Dry Test (ft <sup>3</sup> )	637.91	646.42	654.83	662.68	670.40
i) Final Dry Test (ft <sup>3</sup> )	646.42	654.83	662.68	670.40	677.79
j) Dry Test Diff. (ft <sup>3</sup> )	8.51	8.41	7.85	7.72	7.39
k) Dry Test Temp (°C)	34	34	34	34	34
l) Dry Test Press. (psi)	0.50	0.50	0.50	0.50	0.50
m) Sample Volume (cu M)	0.2303	0.2276	0.2124	0.2089	0.2000

VII. Mass Particulates (mg/m<sup>3</sup>)

Run No.	1	2	3	4	5	Avg.	Dev. (%)
mg/m <sup>3</sup>	60.3	52.9	56.0	55.1	59.7	56.8	5.6

Figure 6-2 Example Laboratory Data Sheet for Cetane Engine  
Particulates Measurements

# EMISSIONS DATA CALCULATED RESULTS

Date: 11-01-1986  
Fuel: DOE-1, PHILLIPS D-2

Data Set: CD1H124A  
Run Date: 08-13-1986

## 1. Operating Conditions

RPM:	1200	Inlet Air Temp.:	150 °F
Load:	FULL	Inlet Pressure:	14.50 psia
Injection Timing:	9.5 °BTDC	Fuel Flow Rate:	0.0326 lb/min

Carbon Based Air/Fuel Ratio: 20.1

## 2. Calculated Results

The following results were computed using the average values of the measured variables for the data runs.

### A. Performance

	Brake	Friction	Indicated
Torque, lb-ft (N-m):	13.9 (18.8)	10.9 (14.8)	24.8 (33.6)
Power, hp (kw):	3.17 (2.37)	2.49 (1.86)	5.66 (4.22)
Mean Effective Pressure, psi (kPa):	56.1 (387)	44.1 (304)	100.2 (691)
Specific Fuel Consumption, lb/hp-hr (µgm/J):	0.617 (104.2)	---- (---)	0.346 ( 58.4)
Efficiency, % :	22.5	----	40.2

### B. Emissions Results Based on Indicated Power

	gm/ihp-hr	µgm/J	gm/kg fuel
Hydrocarbons:	0.289	0.108	1.845
Carbon Monoxide:	2.29	0.85	14.59
Oxides of Nitrogen (NOx):	2.39	0.89	15.24
Mass Particulates:	1.371	0.512	8.76

### C. Emissions Results Based on Brake Power

	gm/bhp-hr	µgm/J	gm/kg fuel
Hydrocarbons:	0.516	0.192	1.845
Carbon Monoxide:	4.08	1.52	14.59
Oxides of Nitrogen (NOx):	4.26	1.59	15.24
Mass Particulates:	2.448	0.913	8.76

### D. Bosch Smoke: 5.1 Bosch units

Figure 6-3 Example Calculated Results Sheet for Performance and Emissions, Cetane Engine

torque, power, mean effective pressure, specific fuel consumption, and efficiency are presented in section 2A. Notice that brake, friction and indicated values are given in both English and metric units. Section 2B gives the specific emissions based upon indicated power output. Values for unburned Hydrocarbons, Carbon Monoxide, Oxides of Nitrogen, and Mass Particulates are shown in units of gm/ihp-hr,  $\mu\text{gm/J}$ , and gm/kg of fuel. Section 2C provides similar results for brake specific emissions.

Figure 6-4 is an example of the calculated combustion parameters for the given data set. It includes a significant amount of information that is derived from the experimental data shown in the plots of the following section. In practice, the computer software determines these parameters from the reduced data directly. The plots provided in the following section are primarily an aid to assist in visualizing the results and determining if any errors may have occurred.

Figure 6-5 is an example of quality checks performed to test for data consistency by calculating specific results using more than one approach employing independent data. Air-fuel ratio determined from measured fuel flow and measured air flow is compared to the air-fuel ratio determined from exhaust emissions measurements. Nominal differences are less than 3% with exceptions usually traceable to discrepancies in air flow measurement. Indicated mean effective pressure is computed using dynamometer force arm measurements and compared to the imep determined from the area under the P-V diagram. This area is determined using the phase shift from the imep matching method with main chamber pressure data and from the slope method using the pre-chamber pressure data. Comparisons using the shift determined from main chamber pressure are usually within 1%. Comparison using the shift determined from the pre-chamber slope method are usually within 10%. Considering the fact that different transducers are used and the pre-chamber data must be synchronized with the main chamber pressure data, these differences are considered acceptable.

#### 6.2.2 Graphical Results, Cetane Engine

Data taken using the data acquisition systems involves a large number of data points that have little meaning in numerical form. Therefore, graphical results are most useful for interpreting these data. Three types of graphical data are included in the presentations. The first series of plots display full cycle information calculated from data taken with the IBM-PC data acquisition system. The second series of plots display information calculated from the high speed data acquired with the Norland processing oscilloscope. The third type of graphical presentations display information related to heat release determined from the high speed data acquired for the Norland oscilloscope.

Figure 6-6 is a full cycle plot of the main chamber pressure as a function of  $\text{CA}^\circ$ . This plot is the ensemble average of over 90 consecutive pressure cycles. Only 100  $\text{CA}^\circ$  of the information about TDC are displayed so that the results can be directly compared to those obtained from the high speed Norland system. Also, the area of greatest interest is in the vicinity of TDC where the combustion process begins and proceeds. Figure 6-7 is the estimate of the standard deviation for the

COMBUSTION PARAMETERS  
CALCULATED RESULTS

Date: 11-10-1986  
Fuel: DOE-1, PHILLIPS D-2

Data Set: CD1H124A  
Run Date: 08-13-1986

1. Operating Conditions

RPM:	1200	Inlet Air Temp.:	150 °F
Load:	FULL	Inlet Pressure:	14.50 psia
Injection Timing:	9.5 °BTDC	Fuel Flow Rate:	0.0326 lb/min

Carbon Based Air/Fuel Ratio: 20.1

2. Calculated Results

The following results were computed using the approach described by Wade and Hunter in their paper, 'Analysis of Combustion Performance of Diesel Fuels', presented at the CRC Workshop on Diesel fuel Combustion Performance, Atlanta, Georgia, September 14, 1983.

The combustion parameter data used in the computations were determined by manual observation and measurement of the pressure and heat release information contained in the plotted data results for in cylinder measurements

- a) Dynamic Injection Timing : 9.1 °BTDC
- b) Prechamber Pressure at SOC : 543 psi
- c) Crank Angle degrees at SOC : 354.8 Crank Angle Degrees
- d) Ignition Delay : 3.9 Crank Angle Degrees
- e) Combustion Period in CA ° : 21.2 Crank Angle Degrees
- f) Prechamber Peak Pressure : 791 psi
- g) Peak Pressure crank angle : 367.5 Crank Angle Degrees
- h) Prechamber Peak Rate of Pressure Rise : 35.4 psi/CA°
- i) Main Chamber Peak Pressure : 767 psi
- j) Angle at maximum ROHR : 360.8 Crank Angle Degrees
- k) Est. Bulk Gas Temp. at injection : 1065 °R
- l) Premixed Combustion Fraction (PCF): 0.070
- m) Premixed Combustion Index (PCI) : 0.164
- n) Diffusion Combustion Index (DCI) : 0.868

Figure 6-4 Example Calculated Results Sheet for Combustion Parameters, Cetane Engine

DATA QUALITY CHECK  
CALCULATED RESULTS

Date: 01-03-1987  
Fuel: DOE-1, PHILLIPS D-2

Data Set: B:CD1H124A  
Run Date: 08-13-1986

OPERATING CONDITIONS

RPM:	1200	Inlet Air Temp.:	150 °F
Load:	FULL	Inlet Pressure:	14.50 psia
Injection Timing:	10.0 °BTDC	Fuel Flow Rate:	0.0326 lb/min

Carbon Based Air/Fuel Ratio: 20.1

DATA QUALITY CHECK ITEMS

1. IMEP determined from dynamometer force arm measurements : 100.2 psi
2. IMEP determined from shifted main chamber pressure data : 100.5 psi
3. Dif. between dynamometer measured and main chamber IMEP's : 0.3 %
4. IMEP determined by using data shift from prechamber : 91.5 psi
5. Dif. between dynamometer measured and prechamber shift IMEP's : -8.7 %
6. A/F ratio based on fuel flow and air flow measurements : 19.8
7. Dif. between carbon based and flow measured A/F ratios : -1.2 %

Figure 6-5 Example Calculated Results for Data Quality Check,  
Cetane Engine

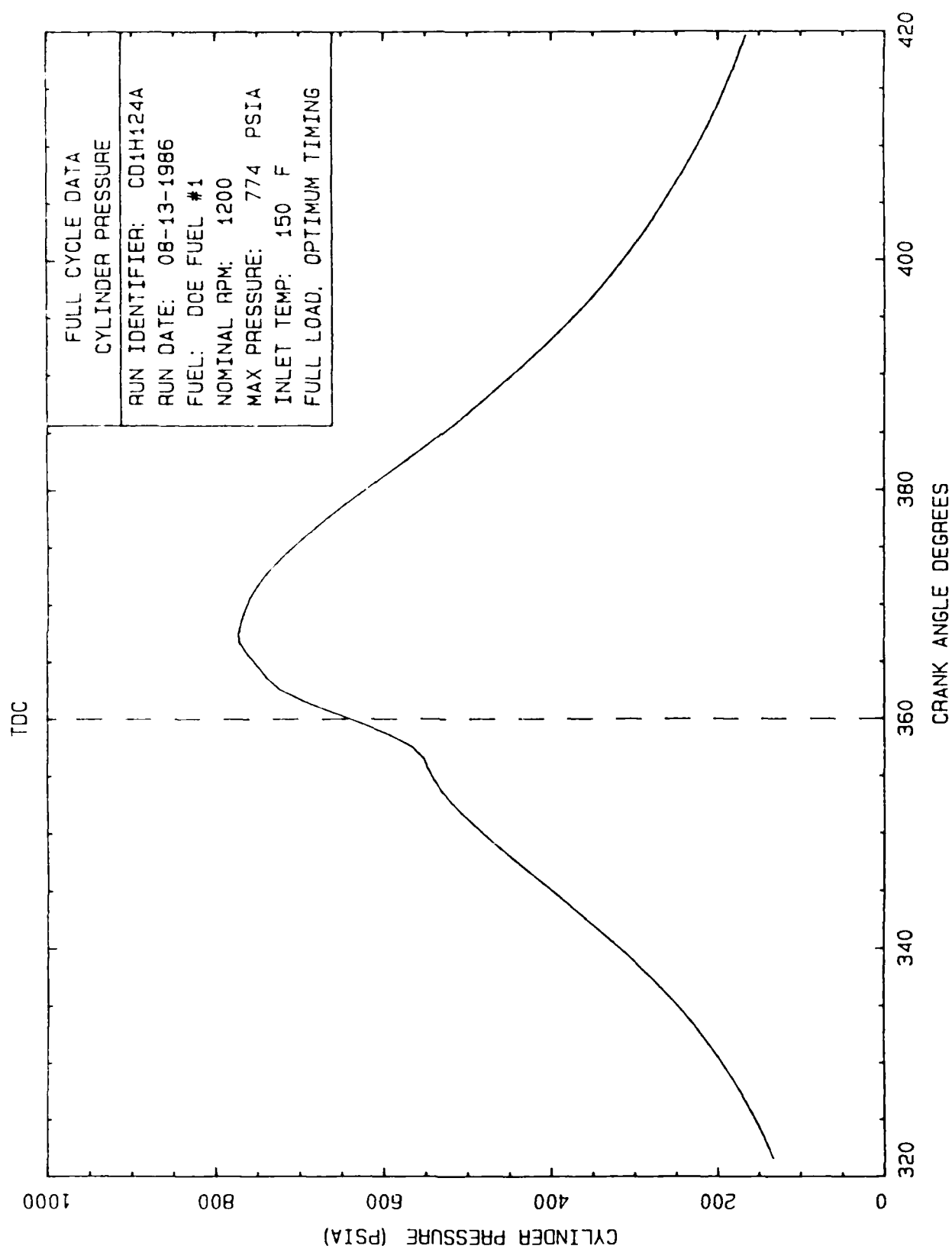


Figure 6-6 Example Plotted Results, Main Chamber Pressure, Full Cycle Data, Cetane Engine

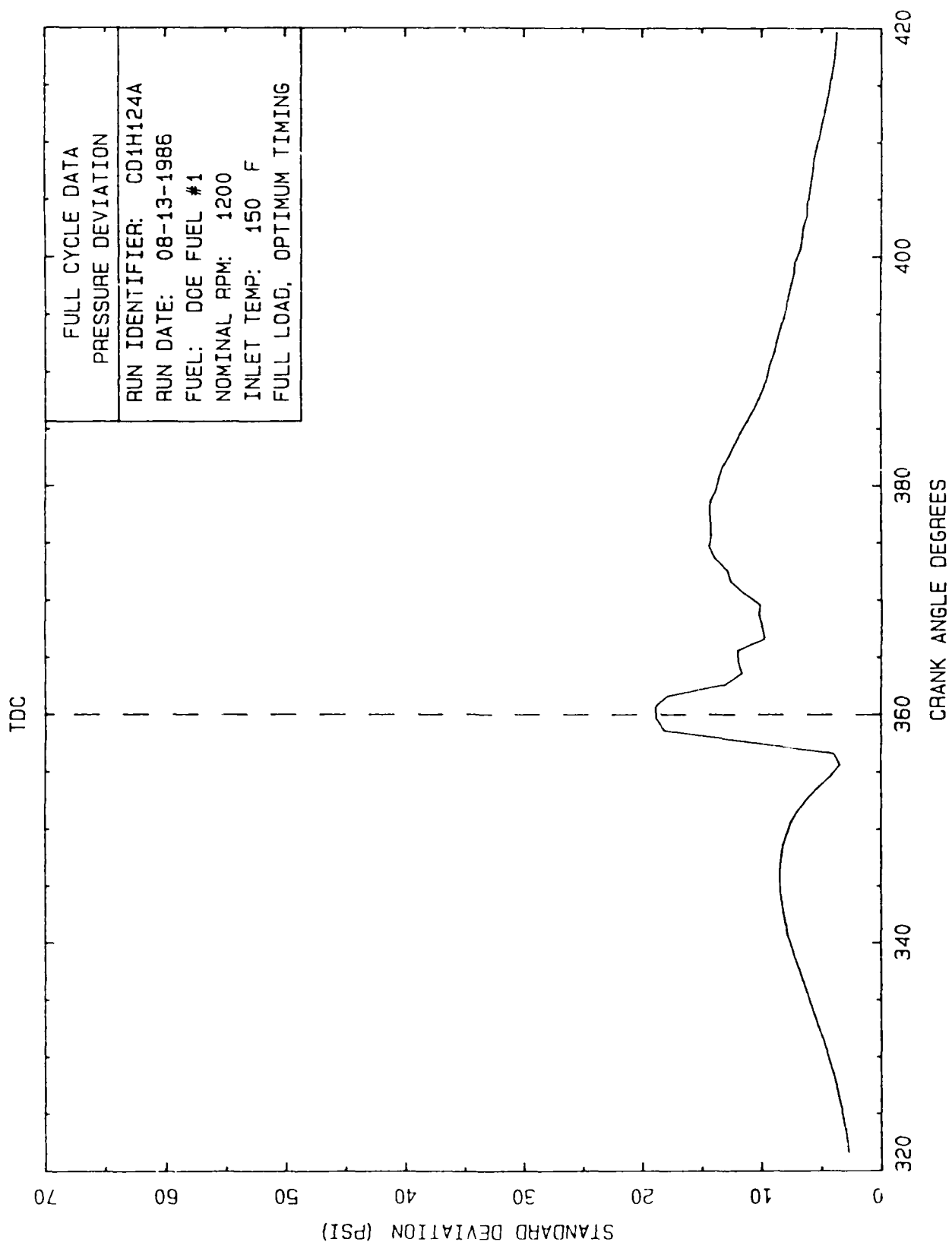


Figure 6-7 Example Plotted Results, Main Chamber Pressure Variance, Full Cycle Data, Cetane Engine



ensemble average of full cycle data. This information is also quite useful in the vicinity of TDC in that it gives a direct indication of the variability of the combustion process over a reasonable number of cycles.

Figure 6-8 shows the ensemble average of the main chamber pressure data for a complete cycle. The log-pressure vs log-volume format for the information is quite useful in determining data quality and characteristics for the run. A relatively straight compression line and appropriately shaped pumping loop usually indicate that the system is working properly and there is no reason to be suspicious of the data. Also, other characteristic features of the plot, such as the shape near TDC during the combustion process and the linear nature of the expansion process as the piston covers the lower part of its travel, provide indications of the operating conditions and data quality. The consistent shape of the pumping loop at the lower part of the figure is also a good indicator that the transducer system is functioning well since these data are from measurements representing about 1% of the transducer's dynamic range.

The crankcase pressure shown plotted in figure 6-9 is one of the data quality checks performed for each data run. The purpose of this measurement is to observe, over the period of the test program, any changes in the crankcase pressure that would indicate increased blowby or other upper cylinder problems with the engine. The characteristic shape of this figure did not change for any of the observed data sets, indicating that blowby and upper cylinder problems did not occur during the test program. For this reason, the individual plots for each data set are not included in the appendix information in an effort to consolidate already voluminous material.

Figure 6-10 is the first of several figures displaying the calibrated results from data gathered with the Norland high speed data acquisition system. The pre-chamber pressure and the calculated estimate of the motored pressure (both plotted to the same scale) are shown in this figure. The figure provides a quick visual indication of the general pressure shape due to combustion and also indicates the quality of the calculated estimate of the motored pressure.

Figure 6-11 is a duplication of the main chamber pressure measurement shown in figure 6-6. The difference is that the data shown in figure 6-11 were taken with the Norland high speed data acquisition system with a resolution of 0.1 to 0.2 CA°. Those shown in figure 6-6 were taken with the IBM-PC data acquisition system which has a resolution of 1 CA°. Comparison of the two figures indicates good correlation between the data acquisition systems.

The derivative of the pre-chamber pressure is shown in figure 6-12. Two pieces of information were drawn from this data - the start of combustion, as previously defined, and the peak rate of pressure change, as determined from the largest maximum from the plot. An unscaled plot of the injector lift data is included in this figure to provide a reference between start of injection and start of combustion.

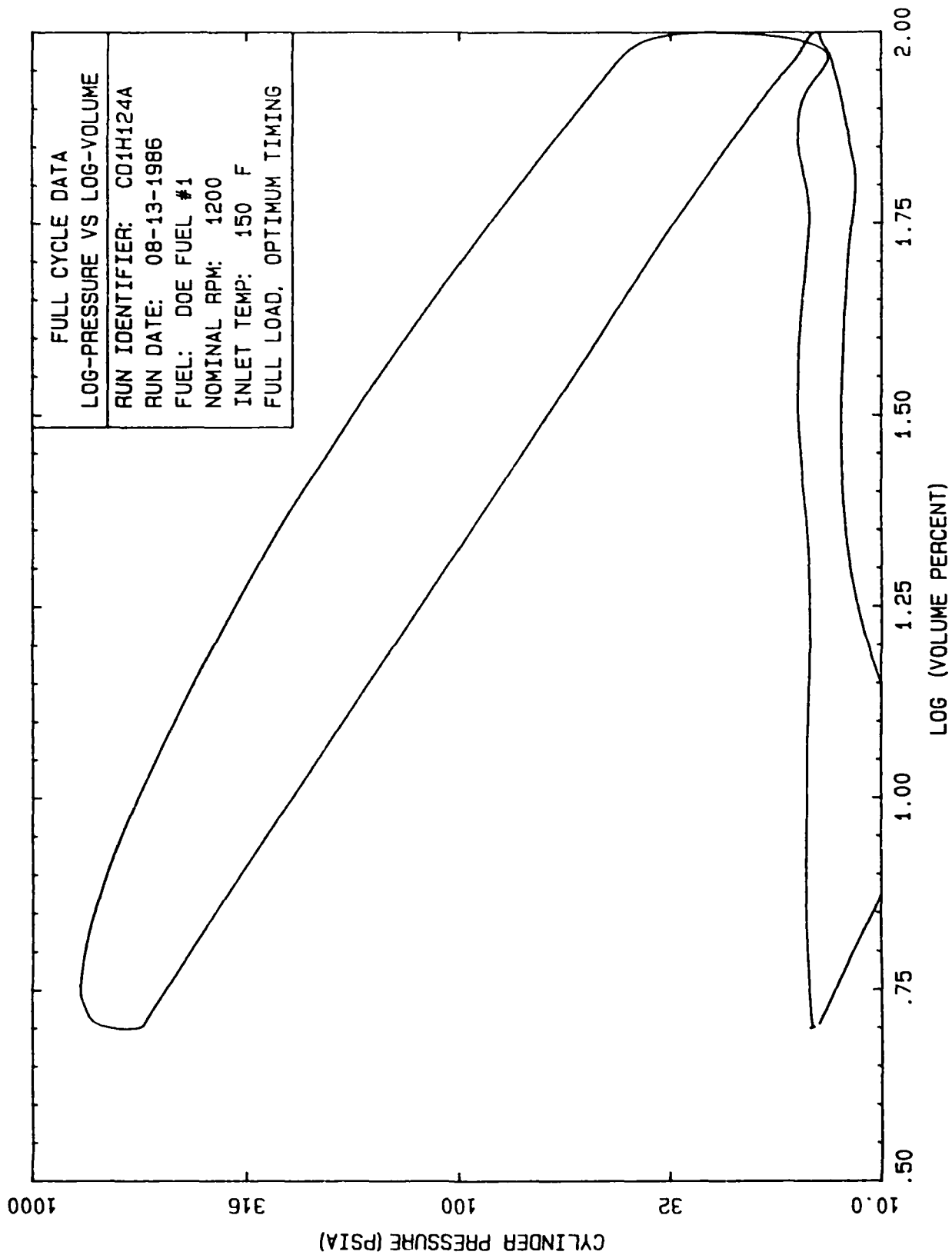


Figure 6-8 Example Plotted Results, Log-Pressure vs Log-volume, Main Chamber, Full Cycle Data, Cetane Engine

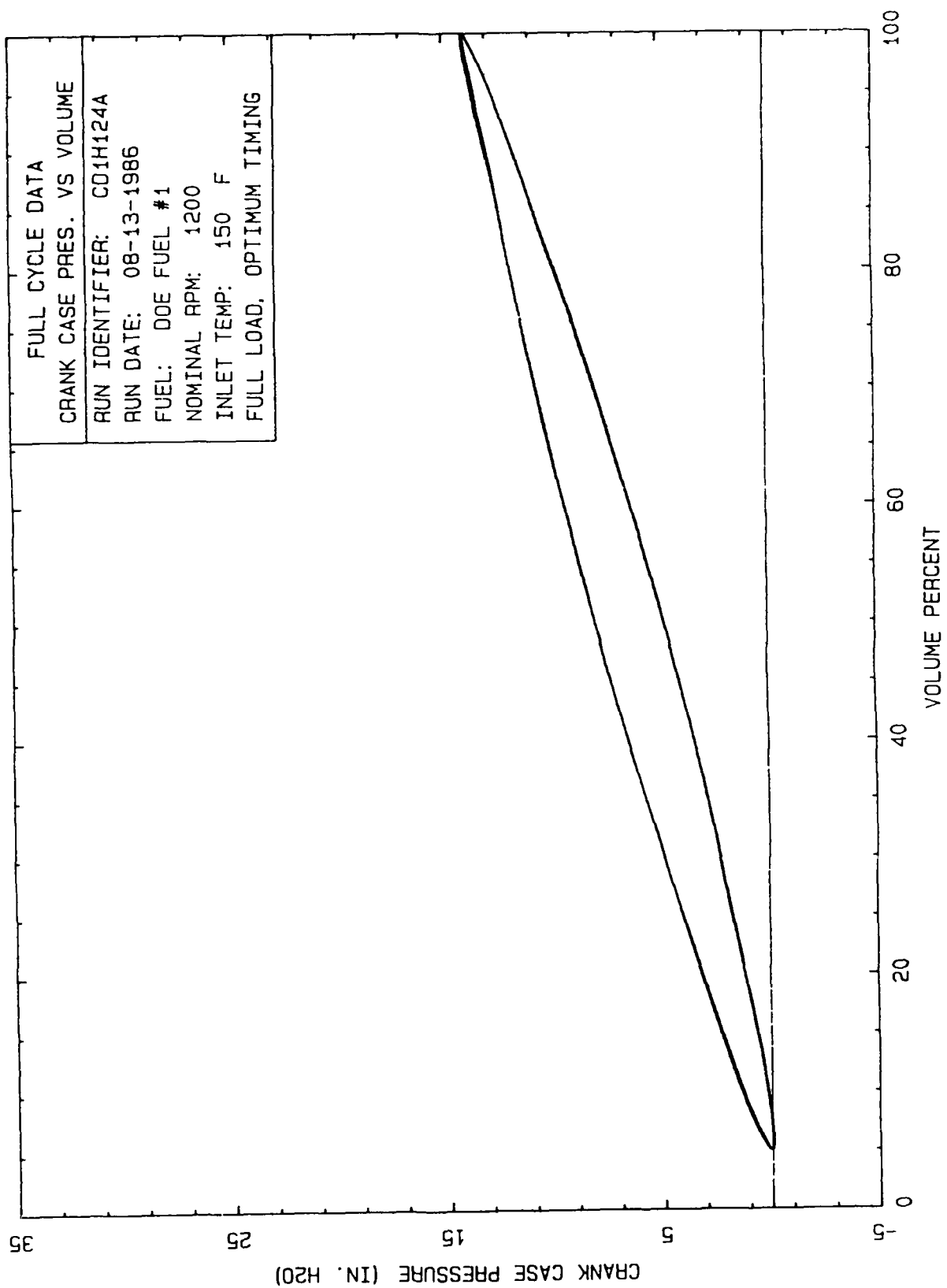


Figure 6-9 Example Plotted Results, Crank Case Pressure, Full Cycle Data, Cetane Engine

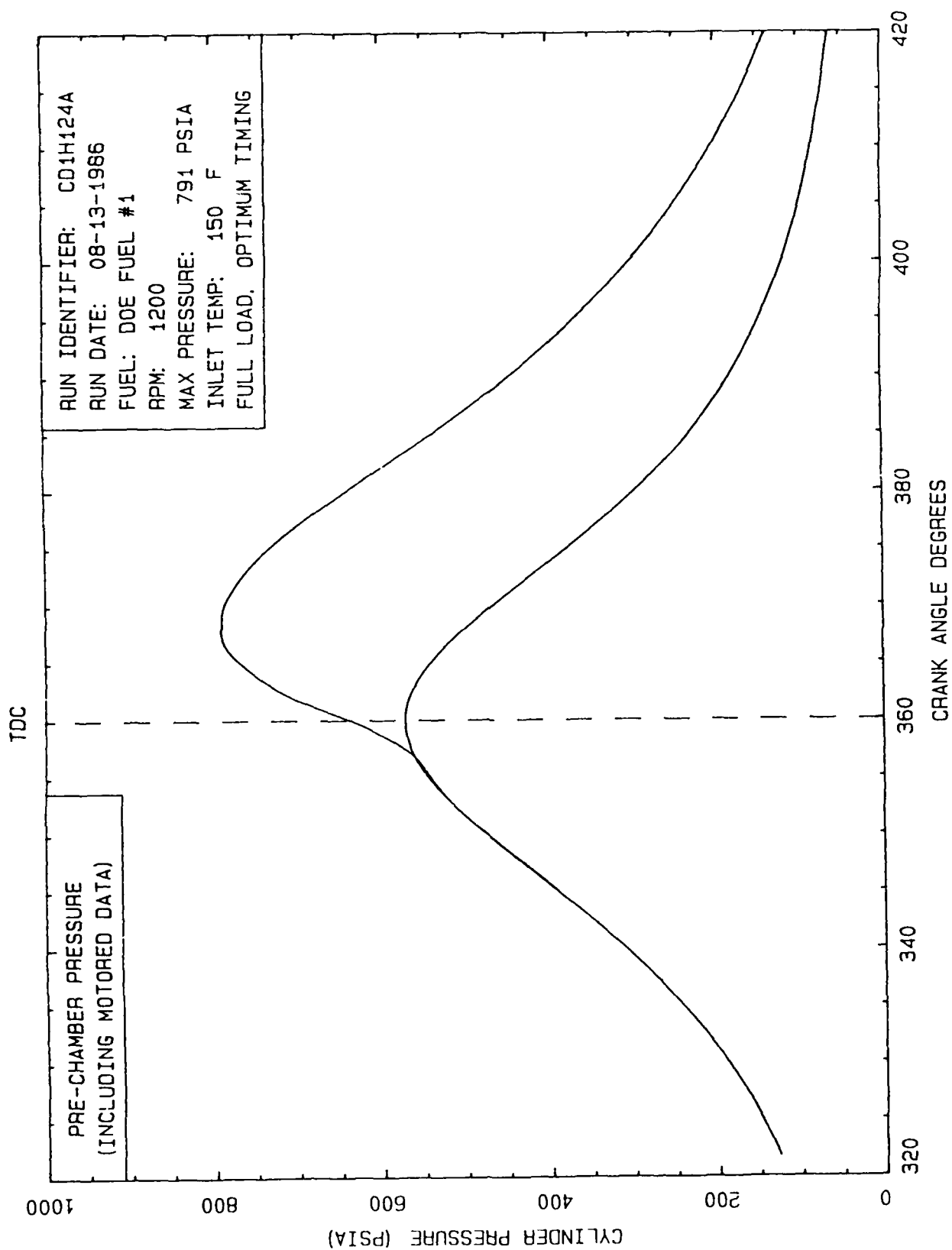


Figure 6-10 Example Plotted Results, Pre-Chamber Pressure, High Speed Data System, Cetane Engine

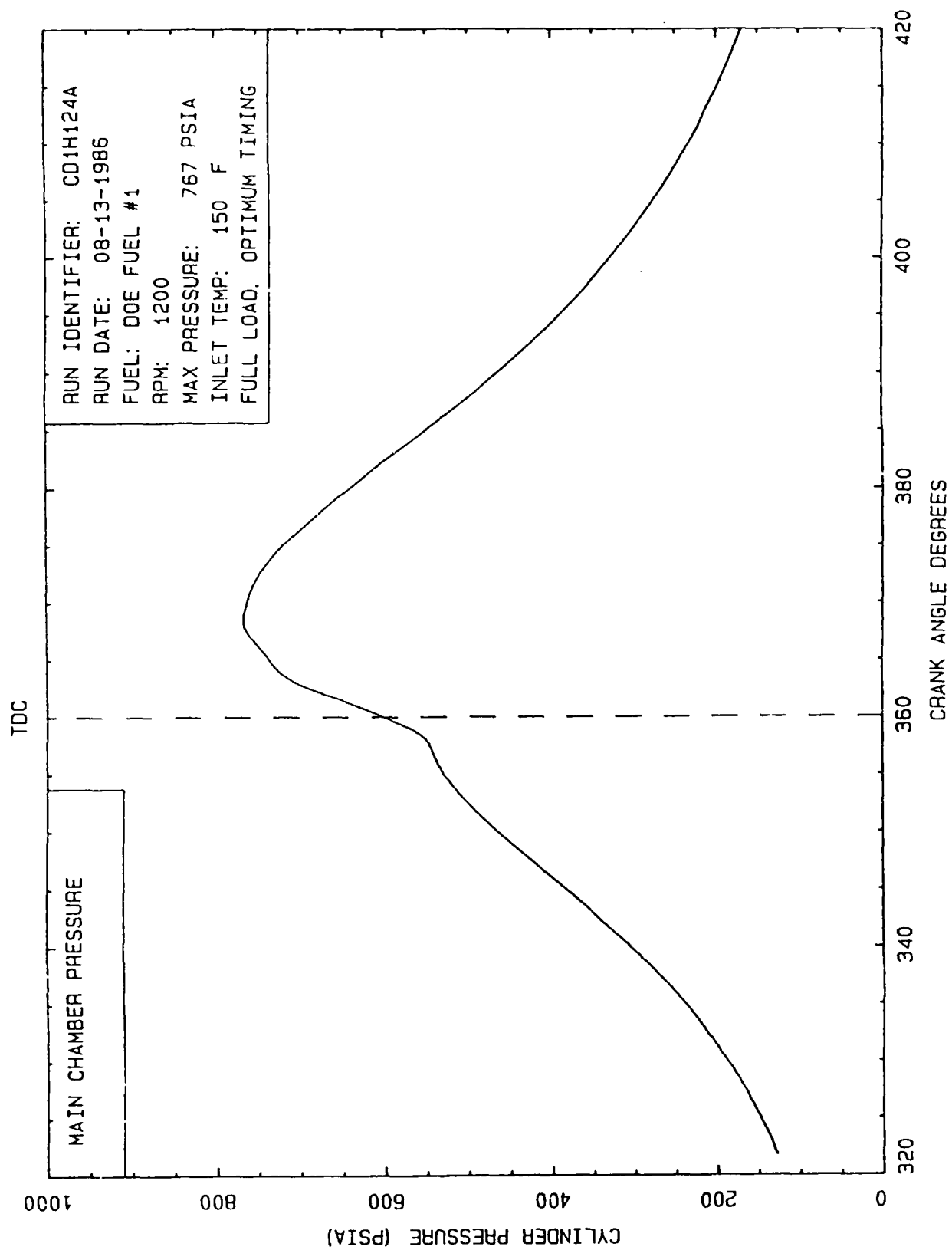


Figure 6-11 Example Plotted Results, Main Chamber Pressure, High Speed Data System, Cetane Engine

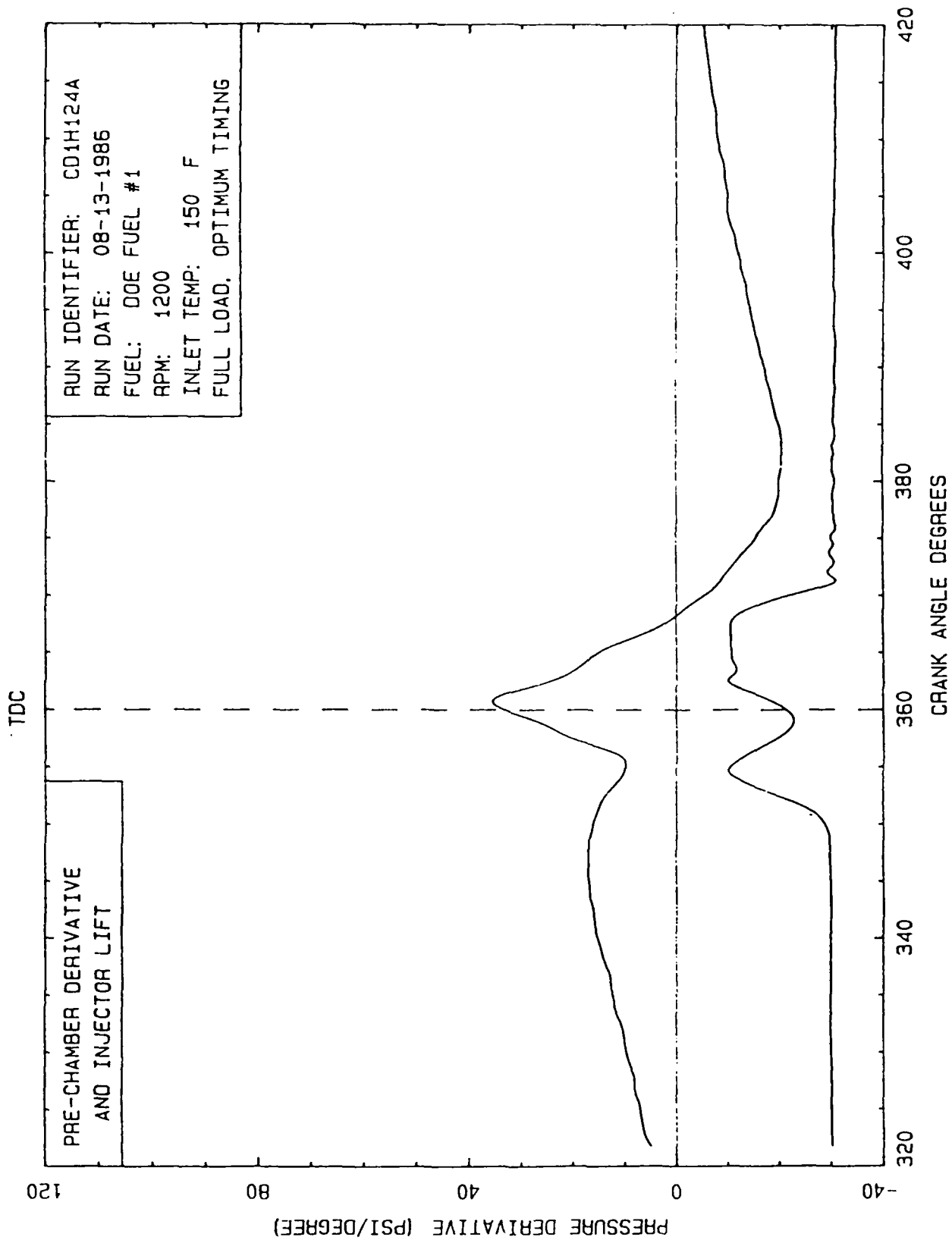


Figure 6-12 Example Plotted Results, Pre-Chamber Pressure Derivative, High Speed Data System, Cetane Engine

Three different sets of data are shown in figure 6-13. They are the injector lift data, the injector pressure data, and the pre-chamber pressure data. The pressure data are plotted to the same scale and the injector lift data is unscaled. This figure was prepared primarily to aid in visualizing the variables that have a major influence on fuel flow across the injector nozzle. The injector lift data is related to the instantaneous flow area and the difference between injector and pre-chamber pressures is the pressure drop across this flow area. The instantaneous values of the variables are used to estimate the instantaneous fuel flow into the combustion chamber. This information is used to compute the fuel energy available for combustion at any given time, a term needed in the determination of computed combustion parameters PCF, PCI, and DCI.

The estimated bulk gas temperature during the final stages of the compression process is shown in figure 6-14. The intended value of this term was to investigate if injection timing changes were sufficient to significantly change the air temperature into which fuel was injected. Experience with the data has indicated that there is greater variability in temperature due to slight changes in apparent gas properties (compression index) than any induced by injection timing changes.

Figures 6-15, 6-16, and 6-17 are plots of apparent heat release information computed from the results information just described. Figure 6-15 shows the fractional energy available on a cumulative basis and is similar to cumulative heat release. The solid line represents cumulative heat release due to combustion. The dashed line represents the cumulative fuel energy available in the combustion chamber and was computed from the information described in figure 6-13. As described in section 5, this cumulative energy information is used in the computation of the combustion parameters PCF, PCI, and DCI.

Figure 6-16 presents the normalized Rate of Heat Release (R.O.H.R.). In essence, this is the result determined directly from the pressure change due only to combustion as described in section 5. It is included as useful reference information.

Figure 6-17 is a display of the normalized derivative of R.O.H.R. This information is used in conjunction with the cumulative heat release information of figure 6-15 to determine the end of the pre-mixed combustion mode. The exact rules for determining the end of premixed combustion are described in section 5. In the example shown in figure 6-17, there is a clear relative minimum of the derivative, indicating the end of the pre-mixed combustion mode. In several cases for the cetane engine and the Ricardo IDI engine, this relative minimum was not readily obvious. In those cases the end of premixed combustion was manually selected, usually at an inflection point on the derivative curve that preceded the criterion that all fuel energy had been delivered to the combustion chamber.

### 6.3 Example Detailed Results for Ricardo Engines

The original objective in reducing the data from the DOE/Ricardo program was to process the information using the same assumptions and computational approaches as those used in reducing the data from the

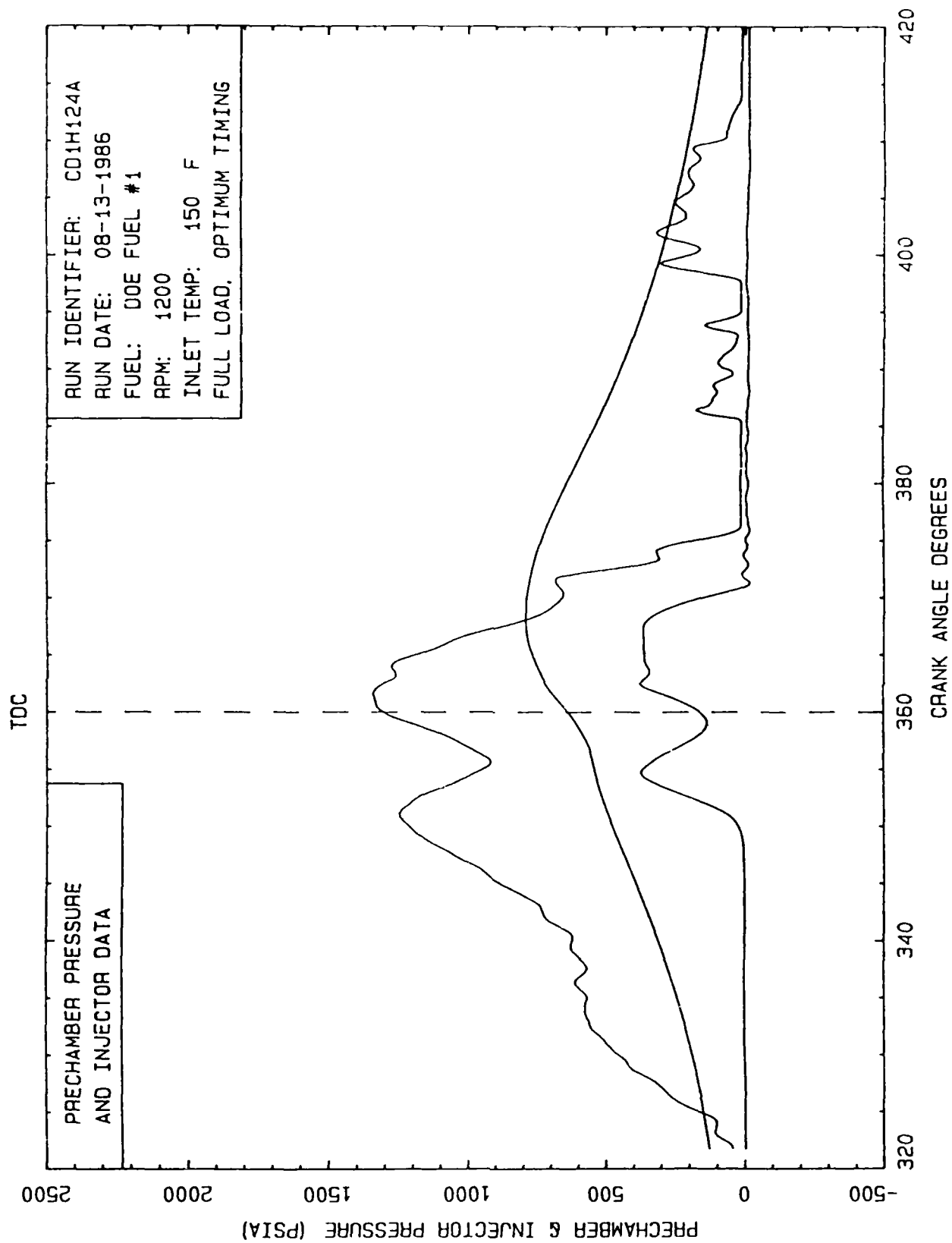


Figure 6-13 Example Plotted Results, Injector Lift and Pressure, High Speed Data System, Cetane Engine



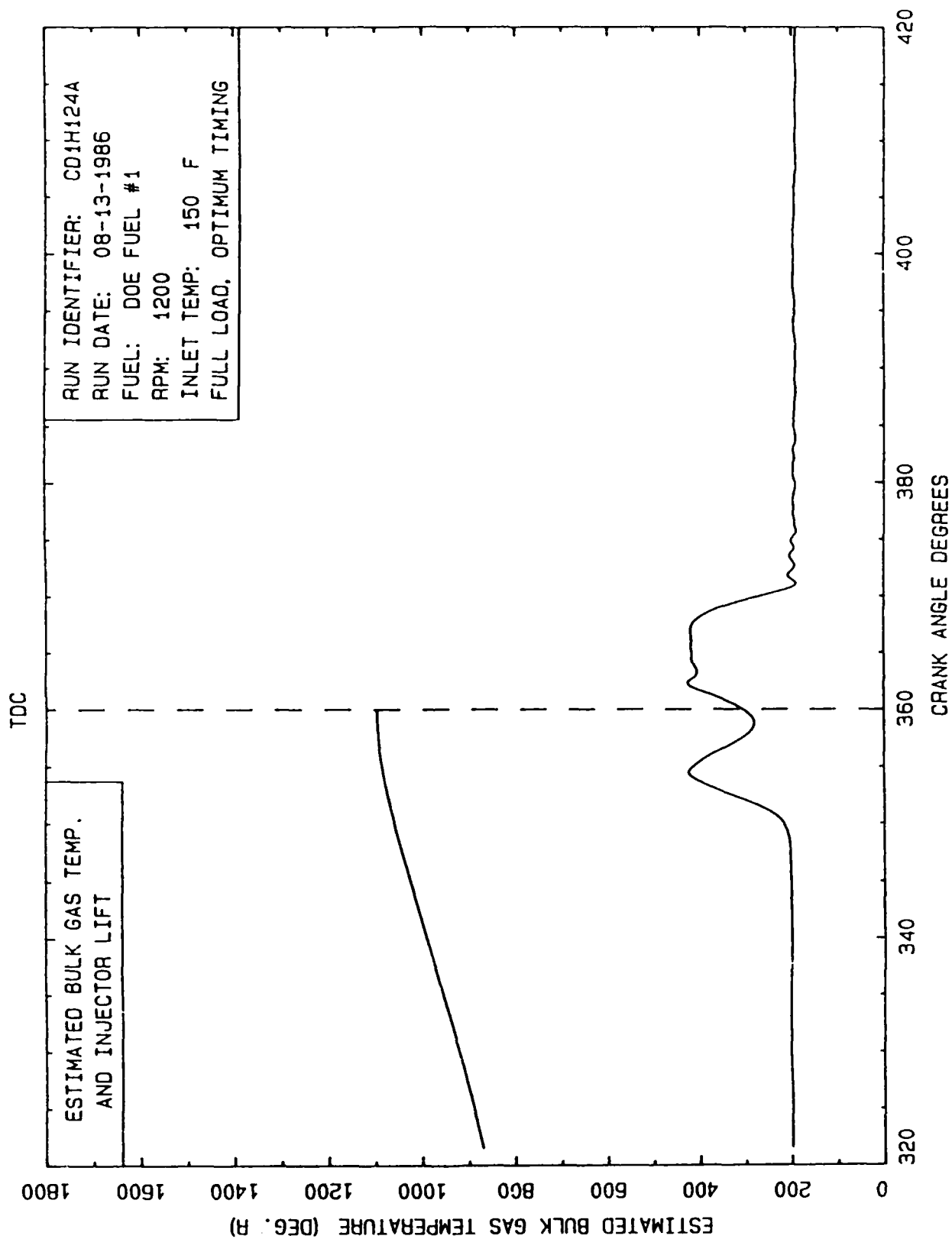


Figure 6-14 Example Plotted Results, Estimated Bulk Gas Temperature, High Speed Data System, Cetane Engine

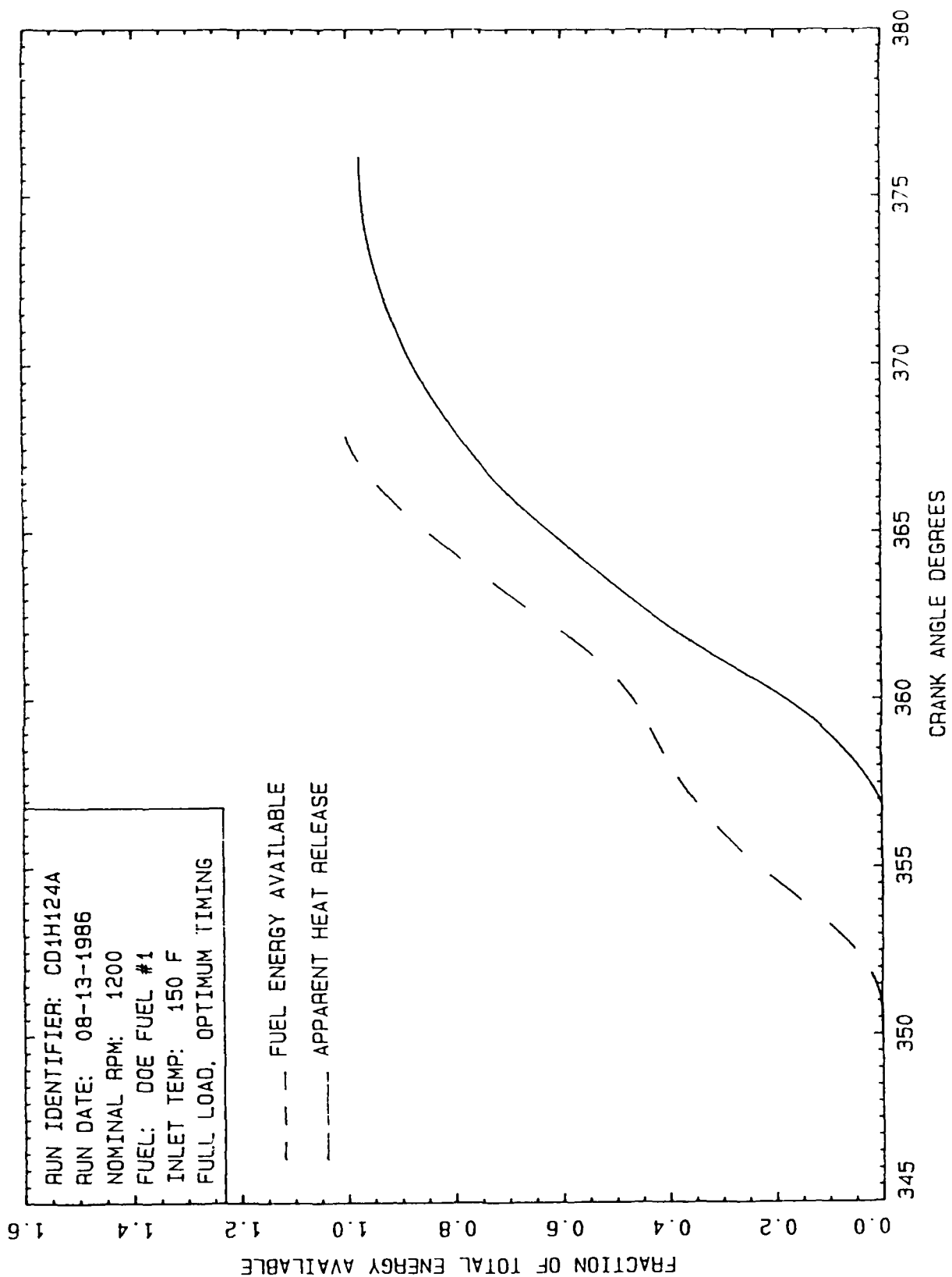


Figure 6-15 Example Plotted Results, Normalized Apparent Heat Release, Cetane Engine

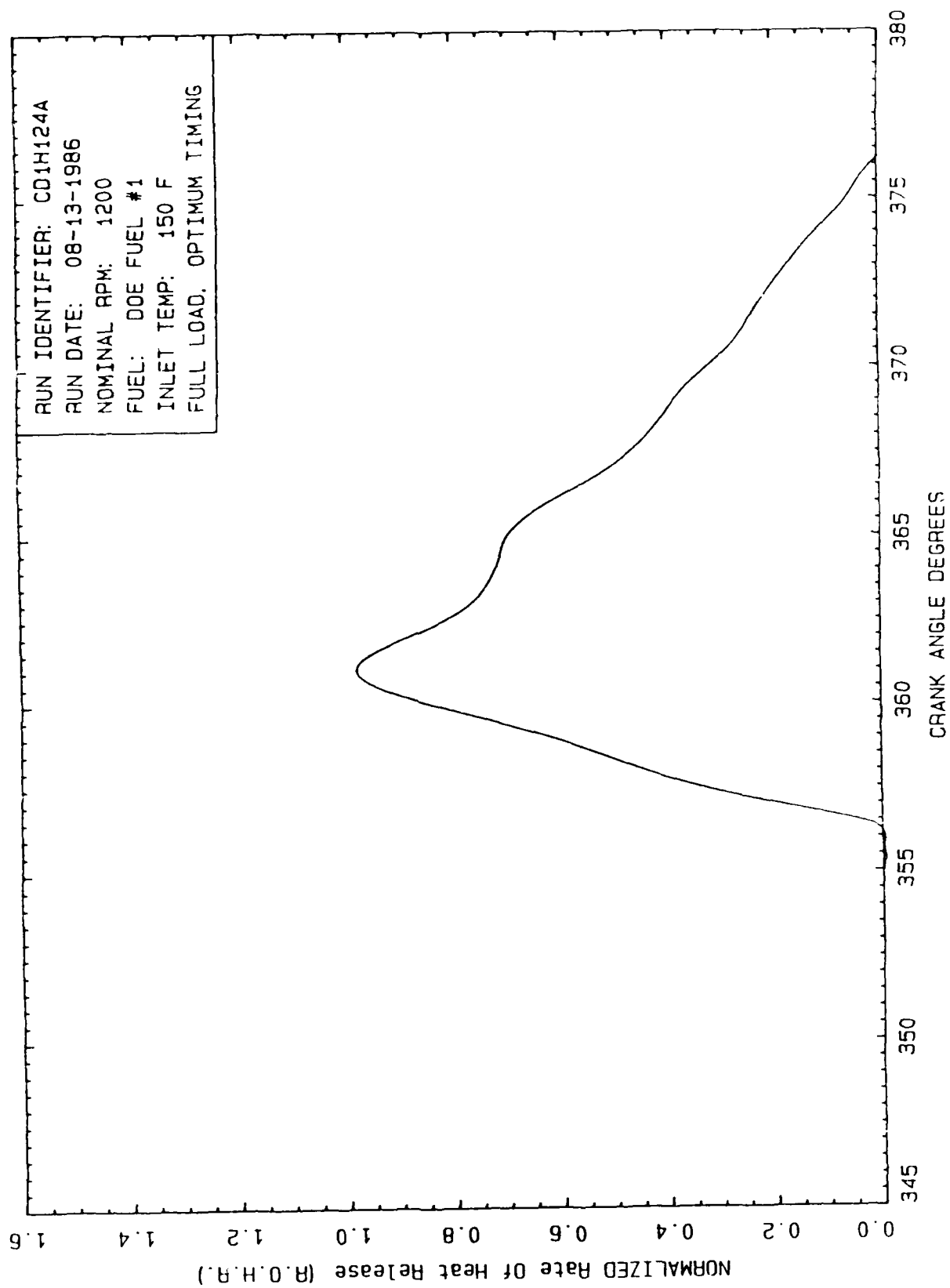


Figure 6-16 Example Plotted Results, Normalized Rate of Heat Release (ROHR), Cetane Engine

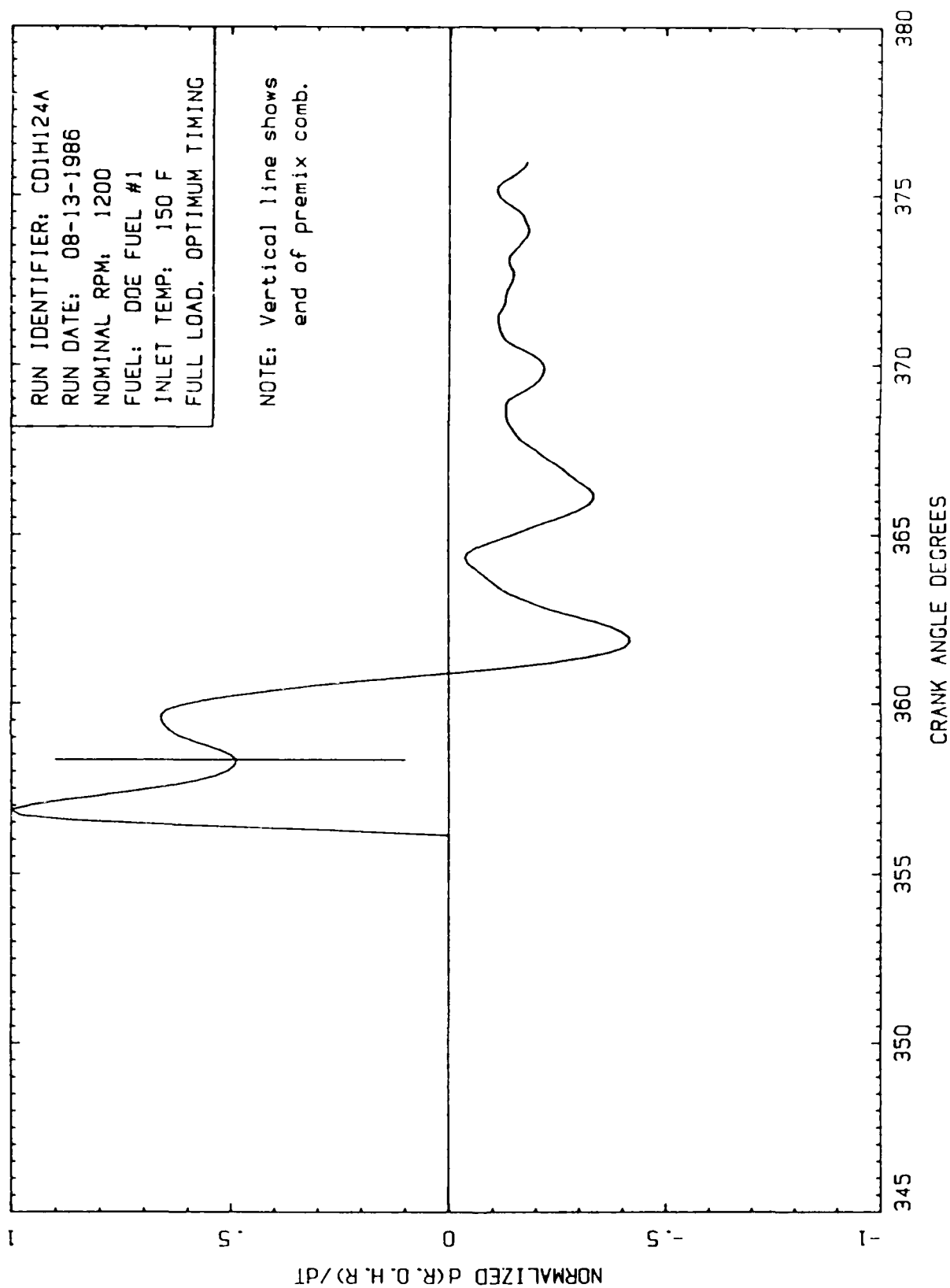


Figure 6-17 Example Plotted Results, Normalized Derivative of ROHR, Cetane Engine

cetane engine. Preliminary reduction of the DOE/Ricardo data into a form that could be used directly by the data processing software for the cetane engine was the original goal. In most major aspects, this goal was achieved. The primary differences are related to information not available in the DOE/Ricardo data.

No frictional measurement data was available to be used in computing results on an indicated basis. In fact, only brake specific data for emissions was available in the DOE/Ricardo report (1-12). Cylinder pressure and injector lift data were available; however, no injector pressure data were available. These differences required some minor modification to the available computer software used for data reduction and plotting; however, the changes were not substantial and did not represent any alteration of the logic or algorithms used in the data reduction process.

All data for emissions, fuel consumption, and air-fuel ratio were manually read from the graphical data contained in the DOE/Ricardo report and entered into a preparatory computational program. The high speed data for cylinder pressure and injector lift were converted from the hex format in which they were received and calibrated using calibration information supplied by Ricardo (6-1). Plots of specific data files showed good agreement with similar information shown in the Ricardo report indicating that this portion of the data reduction method was satisfactory. Once this fact had been established, the DOE/Ricardo data were processed to provide results files for pressure and injector lift similar to those determined for the cetane engine data. Injector pressure was estimated by assuming a simple sine wave shape for the pressure data and computing parameters to force this shape to fit the opening pressure, peak pressure, and closing characteristics assumed. Tests with sine wave, triangle wave, and square wave estimates for injector pressure shape indicated that the sine wave approach provided the most consistent results. Hence, all data presented in this report assume the sine wave injector pressure shape for the data from the Ricardo engines. Appropriate results files were also created for this estimated injector pressure data.

Once calibrated pressure data were available, imep data were obtained from determination of the area under the P-V data for each Ricardo data run. These imep estimates were used in preparing the calculated results shown in the following figures for engine performance and emissions.

Since no original data for emissions or engine performance terms were available, no original laboratory data sheets are available for the DOE/Ricardo information. Figure 6-18 presents an example of the performance and emissions results taken from the DOE/Ricardo report and pressure data and into information directly comparable to that provided for the cetane engine. Figure 6-19 shows example data for the computed combustion parameter information that can also be directly compared to data for the cetane engine.

The example data of figure 6-20 shows the full cycle log-pressure vs log-volume data presented in a format directly comparable to results from the cetane engine. This format also provides a good visual check

# EMISSIONS DATA CALCULATED RESULTS

Date: 06-01-1987  
Fuel: DOE #2, LOW QUAL MID DIST

Data Set: B:RD2H124A  
Run Date: RICARDO IDI

## 1. Operating Conditions

RPM:	1200	Inlet Air Temp.:	150 °F
Load:	FULL	Inlet Pressure:	14.50 psia
Injection Timing:	9.0 °BTDC	Fuel Flow Rate:	0.0383 lb/min

Carbon Based Air/Fuel Ratio: 19.8

## 2. Calculated Results

The following results were computed using the average values of the measured variables for the data runs.

### A. Performance

	Brake	Friction	Indicated
Torque, lb-ft (N-m):	21.5 (29.2)	3.7 ( 5.0)	25.2 (34.2)
Power, hp (kw):	4.92 (3.67)	0.84 (0.63)	5.76 (4.29)
Mean Effective Pressure, psi (kPa):	87.0 (600)	14.8 (102)	101.9 (702)
Specific Fuel Consumption, lb/hp-hr (µgm/J):	0.467 ( 78.9)	---- (---)	0.399 ( 67.4)
Efficiency, % :	30.1	----	35.2

### B. Emissions Results Based on Indicated Power

	gm/ihp-hr	µgm/J	gm/kg fuel
Hydrocarbons:	0.127	0.047	0.704
Carbon Monoxide:	0.89	0.33	4.93
Oxides of Nitrogen (NOx):	1.72	0.64	9.51
Mass Particulates:	0.573	0.214	3.17

### C. Emissions Results Based on Brake Power

	gm/bhp-hr	µgm/J	gm/kg fuel
Hydrocarbons:	0.149	0.056	0.704
Carbon Monoxide:	1.04	0.39	4.93
Oxides of Nitrogen (NOx):	2.01	0.75	9.51
Mass Particulates:	0.671	0.250	3.17

### D. Bosch Smoke: 3.6 Bosch units

Figure 6-18 Example Calculated Results Sheet for Performance and Emissions, Ricardo IDI Engine

AD-A193 831

DIESEL COMBUSTION FUNDAMENTALS PHASE 1 VOLUME 1  
TECHNICAL REPORT(U) MISSOURI UNIV-ROLLA DEPT OF  
MECHANICAL AND AEROSPACE ENGINEERING R T JOHNSON

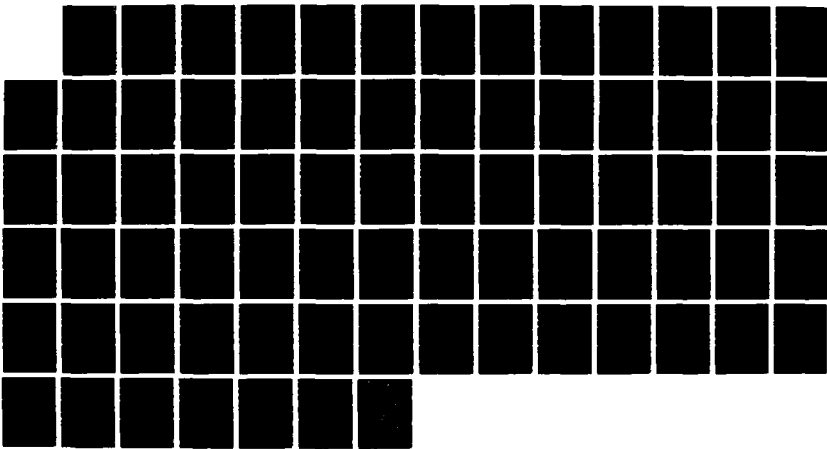
2/2

UNCLASSIFIED

JUL 87

F/G 21/2

NL





MICROCOPY RESOLUTION TEST CHART

U.S. GOVERNMENT PRINTING OFFICE: 1963 O - 348-101



COMBUSTION PARAMETERS  
CALCULATED RESULTS

Date: 06-01-1987  
Fuel: DOE #2, LOW QUAL MID DIST

Data Set: RD2H124A  
Run Date: JAN. 1985

1. Operating Conditions

RPM:	1200	Inlet Air Temp.:	150 °F
Load:	FULL	Inlet Pressure:	14.50 psia
Injection Timing:	9.0 °BTDC	Fuel Flow Rate:	0.0383 lb/min

Carbon Based Air/Fuel Ratio: 19.8

2. Calculated Results

The following results were computed using the approach described by Wade and Hunter in their paper, 'Analysis of Combustion Performance of Diesel Fuels', presented at the CRC Workshop on Diesel fuel Combustion Performance, Atlanta, Georgia, September 14, 1983.

The combustion parameter data used in the computations were determined by manual observation and measurement of the pressure and heat release information contained in the plotted data results for in cylinder measurements

- a) Dynamic Injection Timing : 7.4 °BTDC
- b) Cylinder Pressure at SOC : 709 psi
- c) Crank Angle degrees at SOC : 357.0 Crank Angle Degrees
- d) Ignition Delay : 4.4 Crank Angle Degrees
- e) Combustion Period in CA ° : 20.2 Crank Angle Degrees
- f) Peak Cylinder Pressure : 909 psi
- g) Peak Pressure crank angle : 368.4 Crank Angle Degrees
- h) Peak Rate of Pressure Rise : 34.0 psi/CA°
- i) Angle at maximum ROHR : 363.5 Crank Angle Degrees
- j) Est. Bulk Gas Temp. at injection : 1102 °R
- k) Premixed Combustion Fraction (PCF): 0.126
- l) Premixed Combustion Index (PCI) : 0.247
- m) Diffusion Combustion Index (DCI) : 0.879

Figure 6-19 Example Calculated Results Sheet for Combustion Parameters, Ricardo IDI Engine

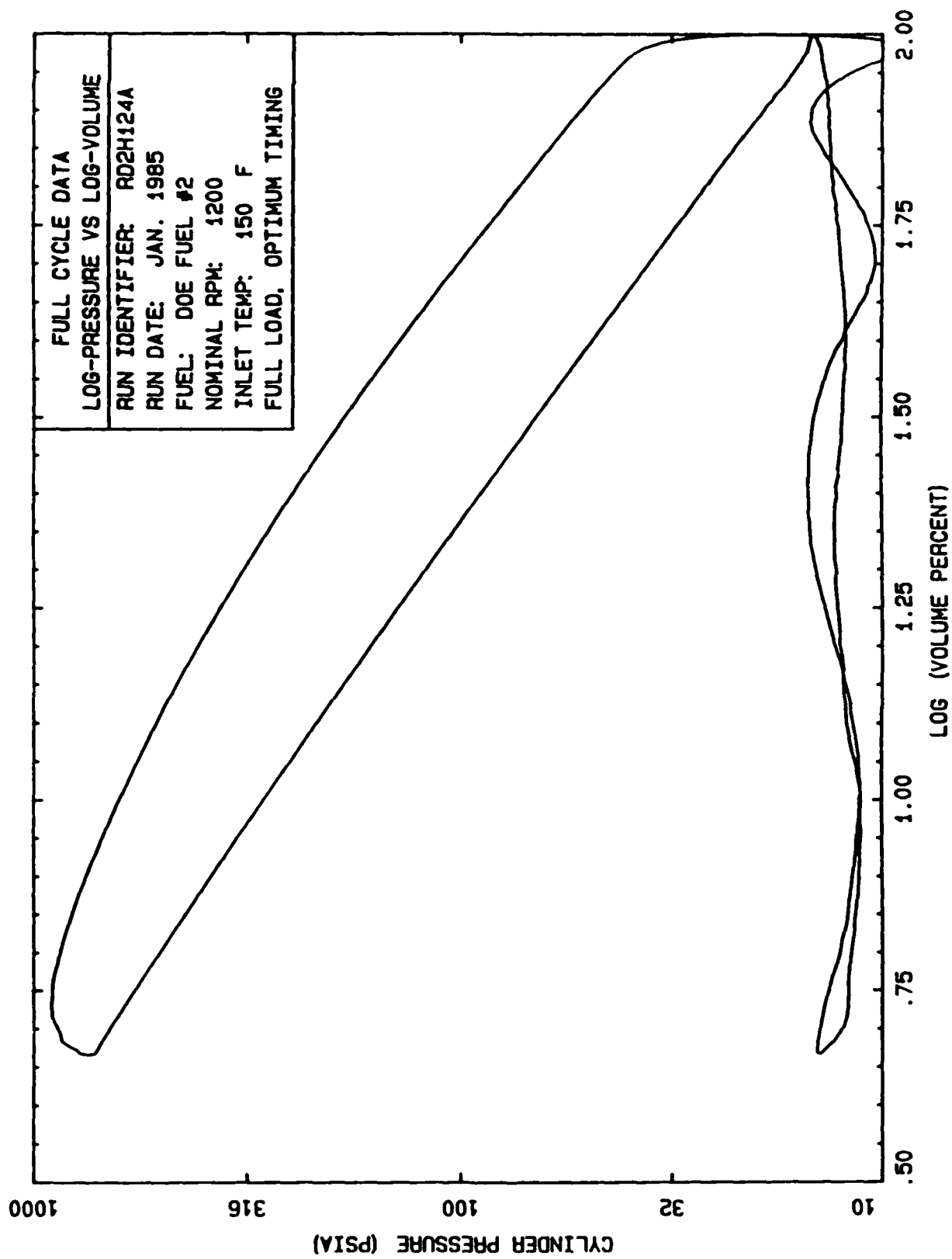


Figure 6-20 Example Plotted Results, Log-Pressure vs Log-volume, Main Chamber, Ricardo IDI Engine

on the quality and consistency of the pressure data from the DOE/Ricardo program and helps to locate any errors or discrepancies that occur in the data reduction process.

An example of main chamber pressure data with estimated motoring results is shown in figure 6-21. The motoring estimate is calculated using the  $P \cdot V^n$  relationship. The value for  $n$  is determined from the slope of the log-pressure vs log-volume relationship during the compression process. For the Ricardo IDI engine this data is not directly comparable to the data for the cetane engine since it is for main chamber measurements rather than pre-chamber measurements.

The derivative of main chamber pressure example is shown in figure 6-22. This derivative is calculated from smoothed pressure data. As with the cetane engine data, the first minimum of the derivative before the peak value is used to determine the start of combustion. In some instances, there are several small peaks in the derivative before the maximum value is reached. When necessary, the start of combustion was manually selected as the first minimum of this group.

Figure 6-23 shows examples of the injector lift, estimated injector pressure, and main chamber pressure for the Ricardo IDI engine. Although not entirely accurate, it was assumed that the pressure differences between the pre-chamber and main chamber were small enough to be neglected in computing the approximate fuel flow into the engine using the injector lift and pressure difference method previously described. The figure clearly shows the sine wave shape assumed for the injector pressure shape.

An example of the plot for estimated bulk gas temperature for the Ricardo IDI engine is shown in figure 6-24. This information is subject to the same assumptions and limitations that apply to the data for the cetane engine.

Figures 6-25, 6-26, and 6-27 are example plots of apparent heat release, apparent R.O.H.R, and the derivative of R.O.H.R. These figures are directly comparable to figures 6-15, 6-16, and 6-17, respectively for the cetane engine. The ability to make this type of comparison was the major impetus in reducing the DOE/Ricardo data with the methods used for this project.

#### 6.4 Summary Graphical Results for Cetane Engine

For each of the ten fuels tested in this program, eight distinct data runs were made. Each of these data runs is described by tabular data and graphs exceeding 15 pages of information. It is not reasonable to expect to examine this volume of information and be able to draw conclusions from the individual run data. For this reason, it was imperative that some form of graphical summary information be prepared. Figures 6-28 through 6-57 are this graphical summary information.

For each of the ten test fuels, there are three separate pages of graphical information. The first page displays selected data dealing with engine performance, emissions, and fuel consumption. The second page presents combustion parameters such as combustion period and peak

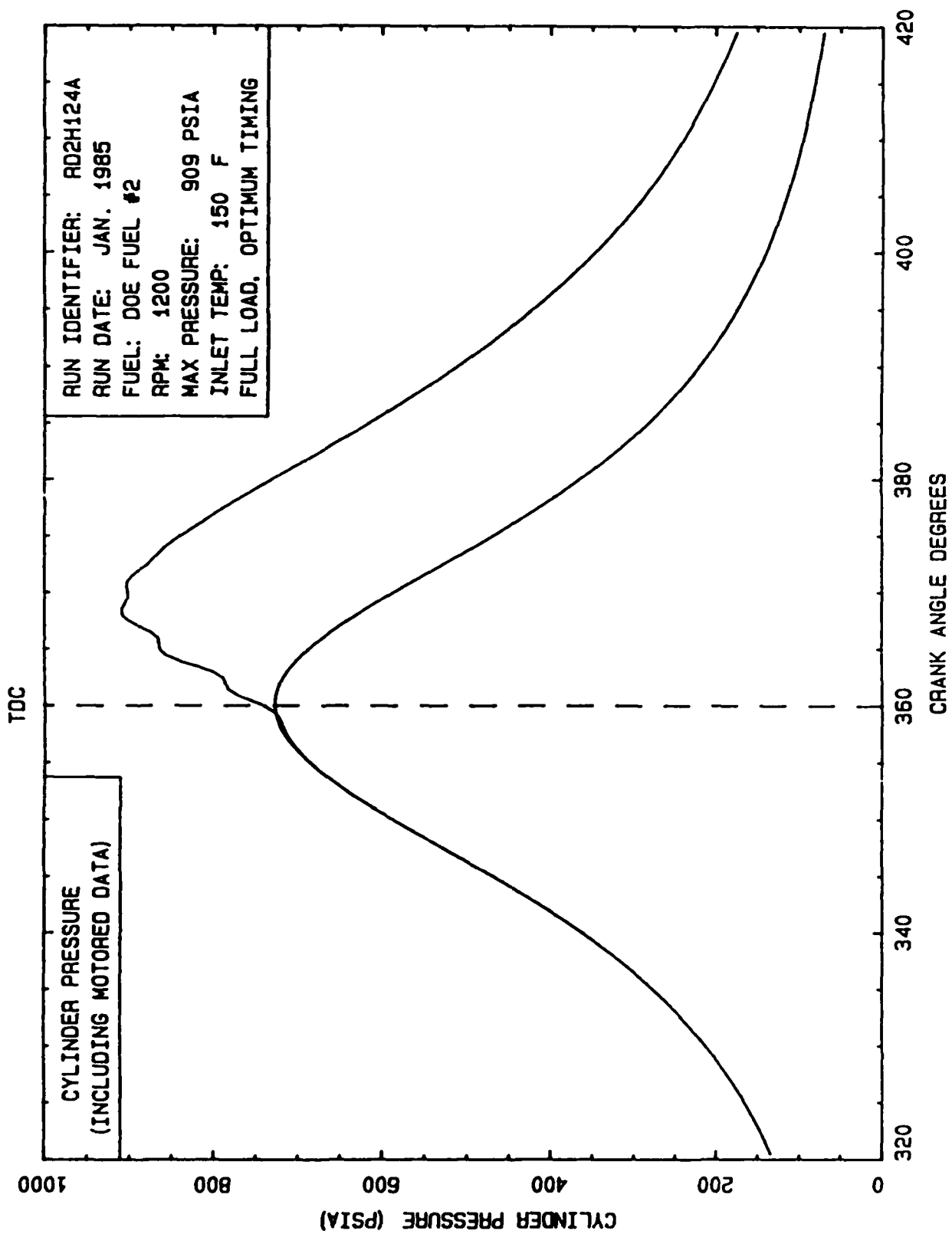


Figure 6-21 Example Plotted Results, Main Chamber Pressure, Ricardo IDI Engine

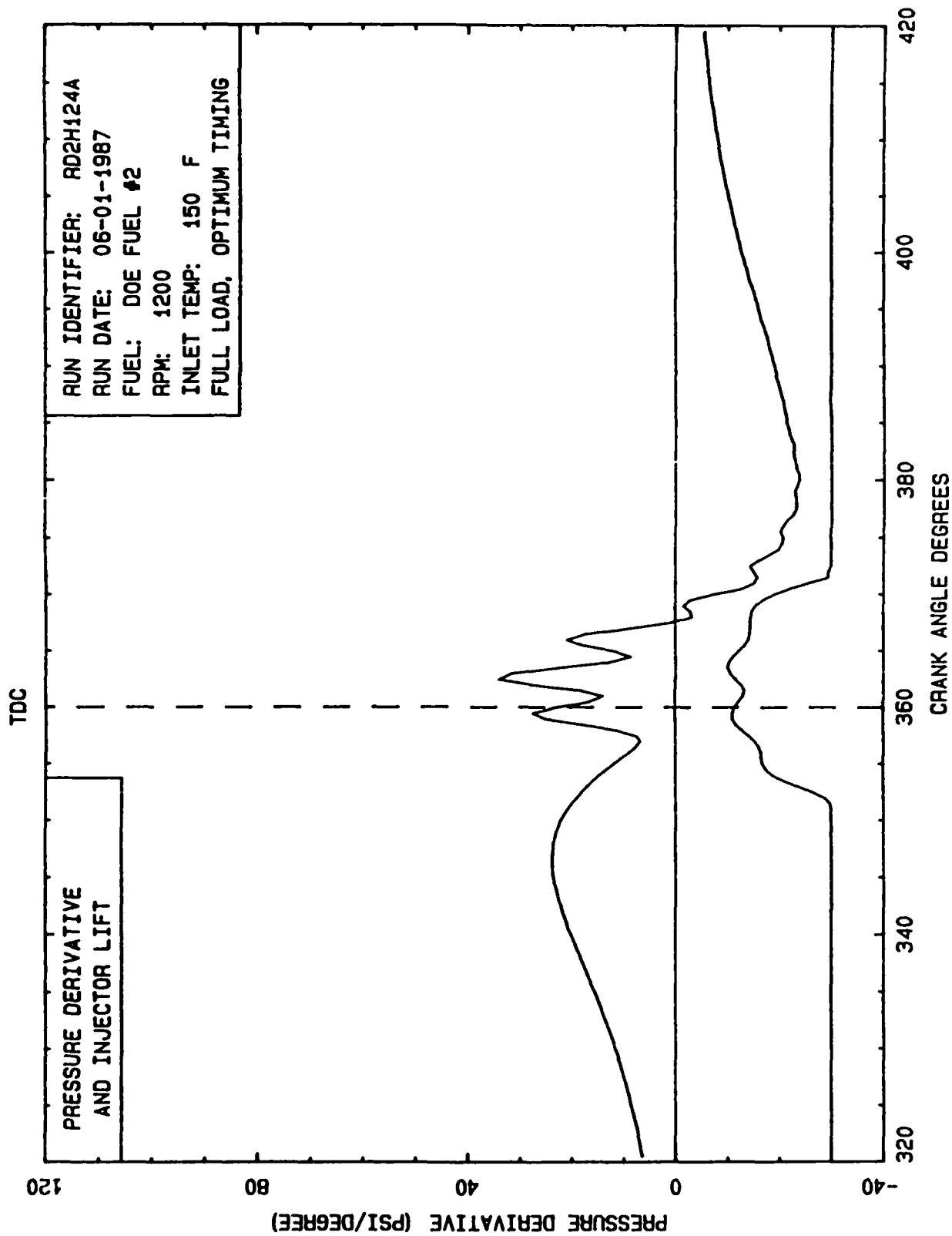


Figure 6-22 Example Plotted Results, Main Chamber Pressure Derivative, Ricardo IDI Engine

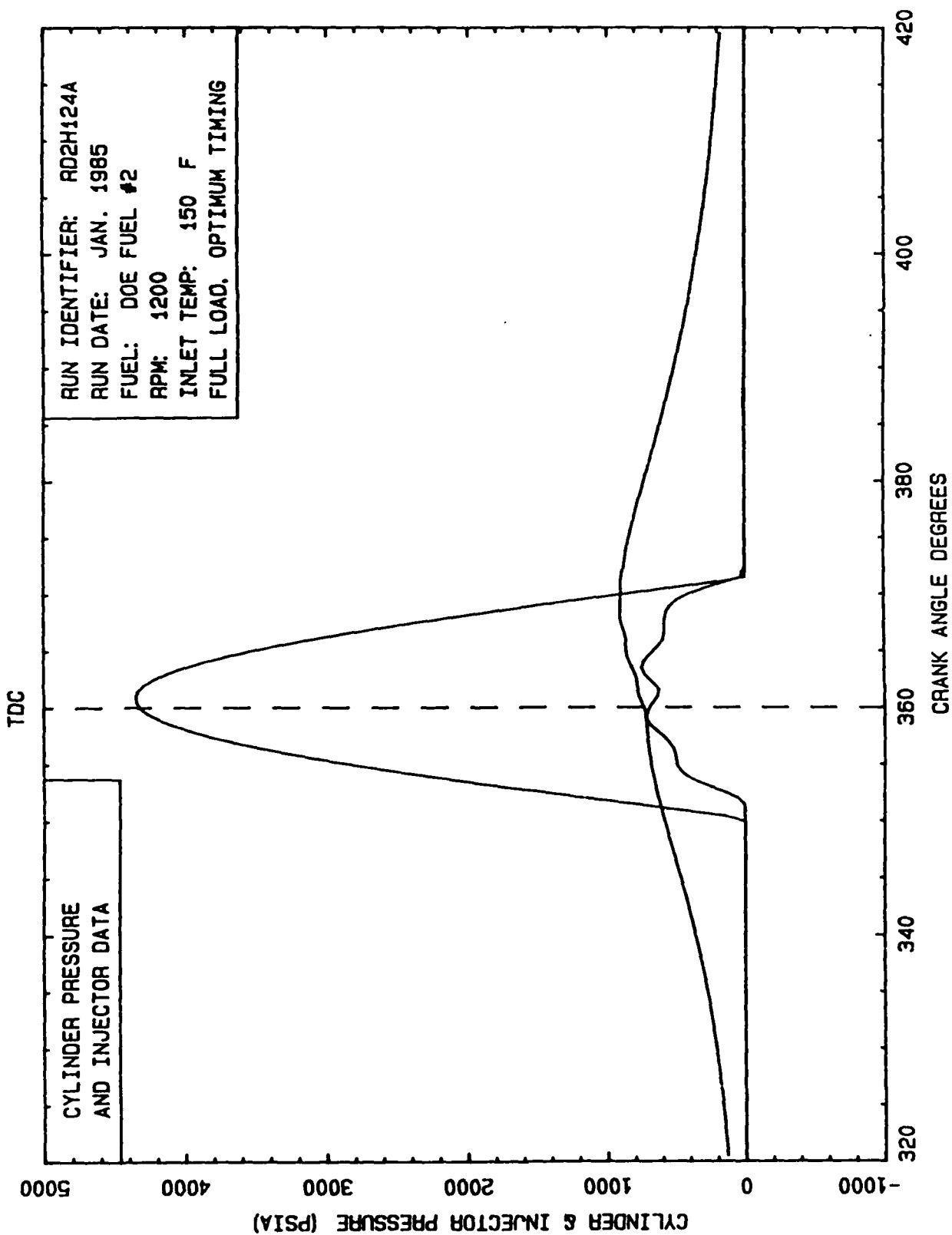


Figure 6-23 Example Plotted Results, Injector Lift and Pressure, Ricardo IDI Engine

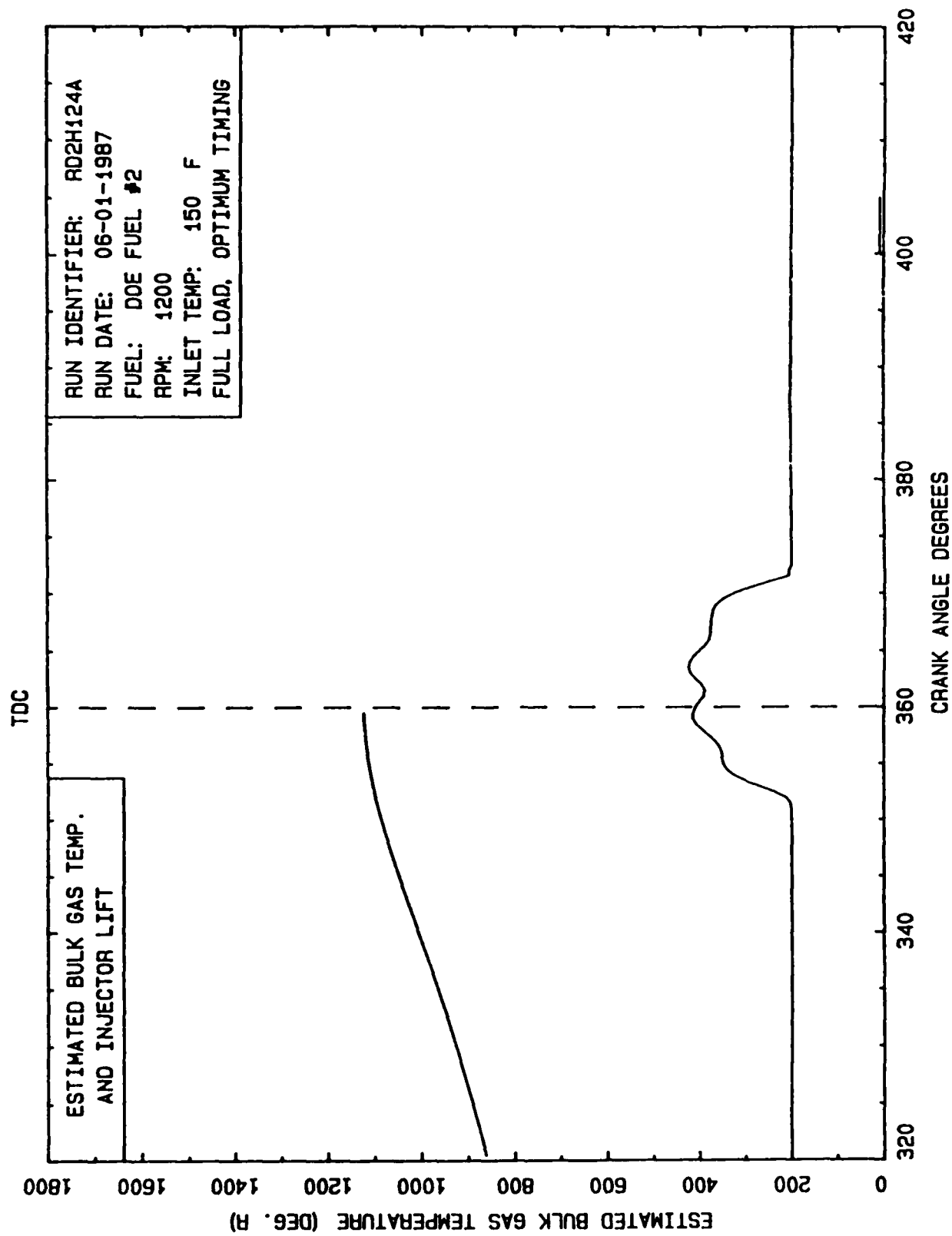


Figure 6-24 Example Plotted Results, Estimated Bulk Gas Temperature, Ricardo IDI Engine

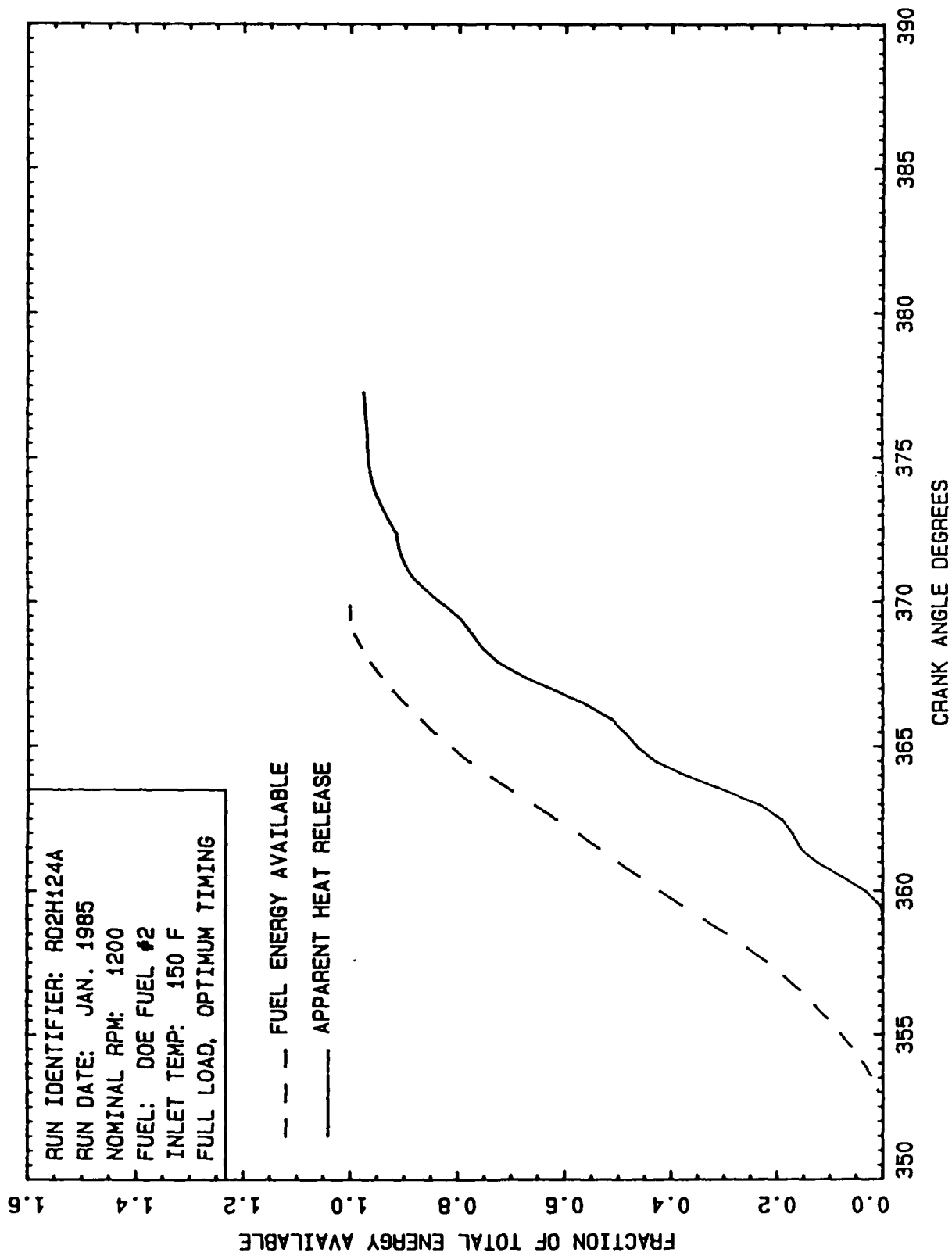


Figure 6-25 Example Plotted Results, Normalized Apparent Heat Release, Ricardo IDI Engine



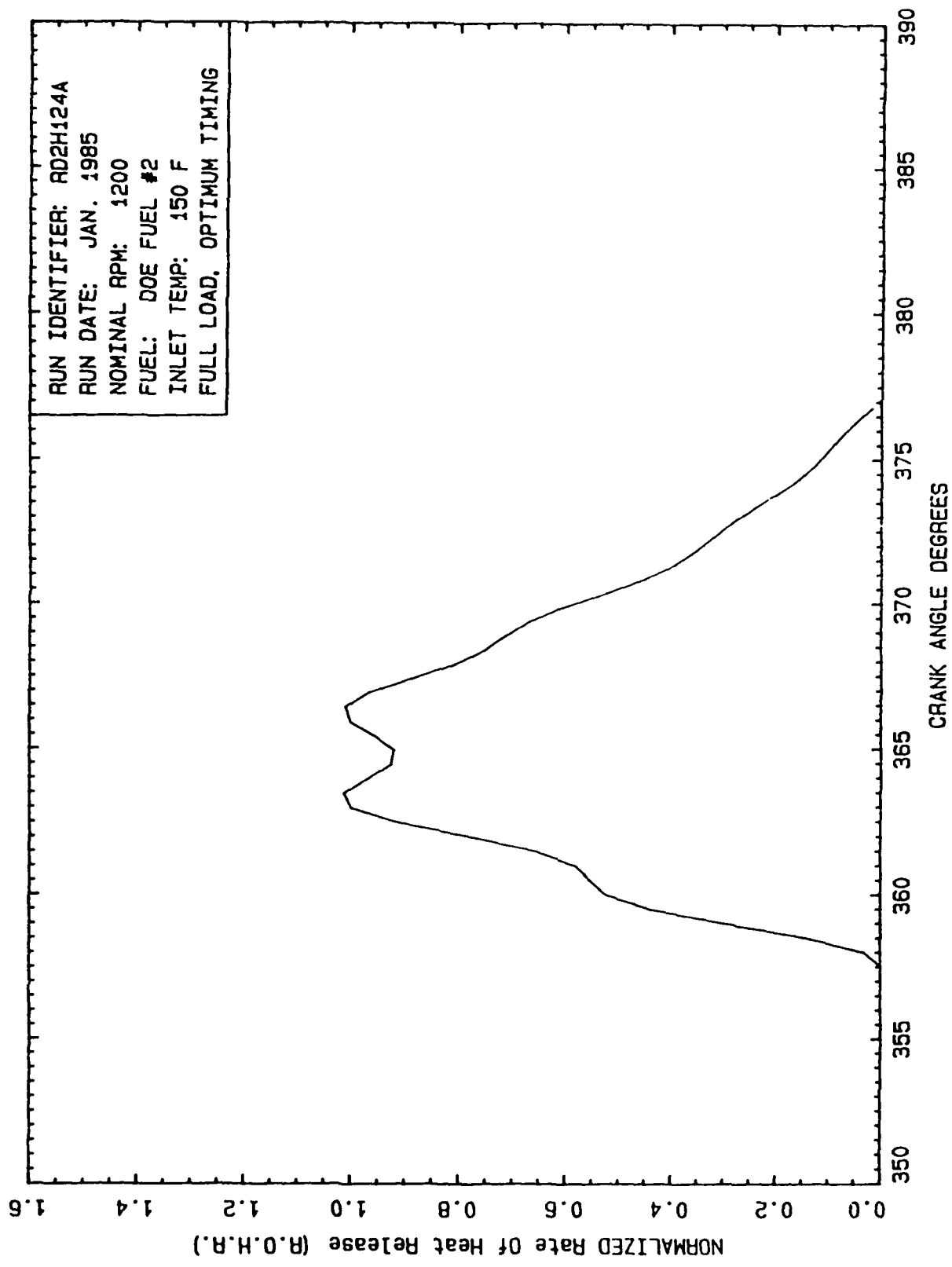


Figure 6-26 Example Plotted Results, Normalized Rate of Heat Release (ROHR), Ricardo IDI Engine

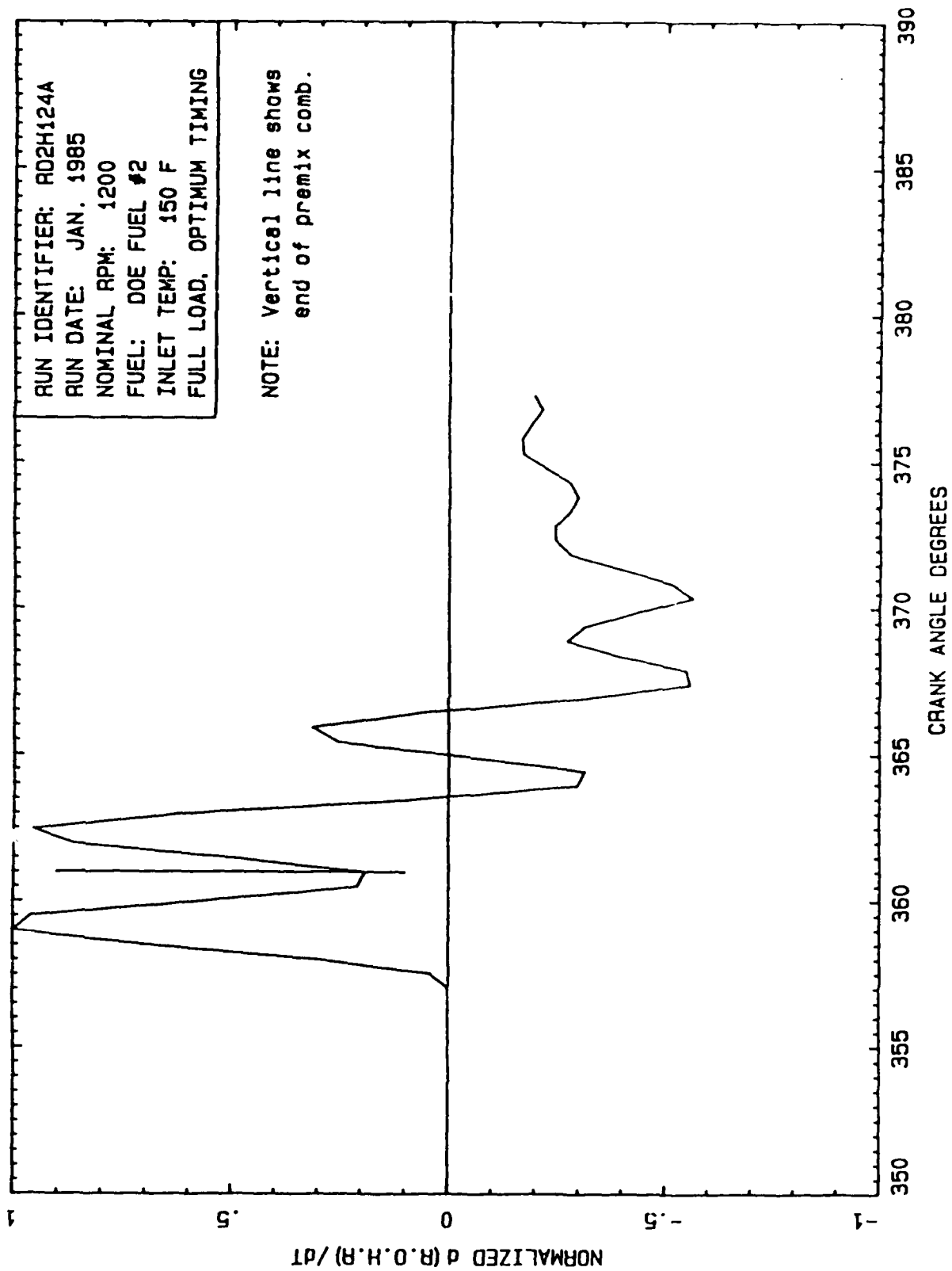


Figure 6-27 Example Plotted Results, Normalized Derivative of ROHR, Ricardo IDI Engine

cylinder pressure. The third page is used to display the calculated combustion parameters: ignition delay, Pre-mixed Combustion Fraction (PCF), Pre-mixed Combustion Index (PCI), and Diffusion Combustion Index (DCI). The independent variable in all cases is imep, used as an indication of engine load. The data are coded so that first and second day runs can be differentiated, and retarded timing and additional runs are obvious. The pages for each fuel have been grouped so that the first pages for all the fuels are grouped together and in the order that the fuels are described in table 6-1. The second and third pages are grouped in the same fashion. It was felt that this organization would be useful in making comparisons to determine fuel-related effects.

#### 6.4.1 Test Condition and Engine Variable Effects, Cetane Engine

The graphical summary results were first examined to determine effects that were due primarily to test conditions or engine variables so that these effects would be easy to distinguish from fuel-related changes. Comments in the following paragraphs were developed after significant study and comparison of figures 6-28 through 6-37.

For all cases, the air-fuel ratio trend was as expected, showing a decrease with increasing imep and very little variation between tests at the same conditions. As should be anticipated, retarded injection timing has no effect on air-fuel ratio. Two anomalies were noted for the CAPE #6 fuel at medium and light load. In these cases, the air-fuel ratio determined from measurement of fuel flow and air flow differed significantly from the carbon based air-fuel measurement. This discrepancy was attributed to problems in accurately measuring fuel and air flow. These measurement problems were related to the relatively poor operation of the engine with this fuel at the medium and light load conditions.

Specific Oxides of Nitrogen Emissions (ISNO<sub>x</sub>) behaved as expected, decreasing with increasing imep (load). The richer overall air-fuel ratio and the larger power output (larger denominator for specific emissions) at higher loads explain this trend. The 5 CA° retard in injection timing at medium load produced a significant reduction in ISNO<sub>x</sub> emissions.

ISFC (indicated specific fuel consumption) generally increased with increasing imep, and the 5 CA° retard at medium load had little effect on this variable. This result is not what would be generally expected. Usually ISFC decreases with load at optimum injection timing conditions. The answer lies in the fact that the internal friction for the cetane engine is very large, particularly when compared to light load brake output. This large term added to the denominator in the ISFC computation significantly distorts the result. Additional problems were noted in the values of ISFC for medium and light load using the CAPE #6 fuel. As indicated in the discussion of air-fuel ratio characteristics, medium and light load results for the CAPE #6 fuel were questionable because of poor engine operation.

The mass particulates emissions (ISPart) generally increased with increasing imep or load. This result is expected with diesel engines. The 5 CA° retard and medium load also tended to cause an increase in

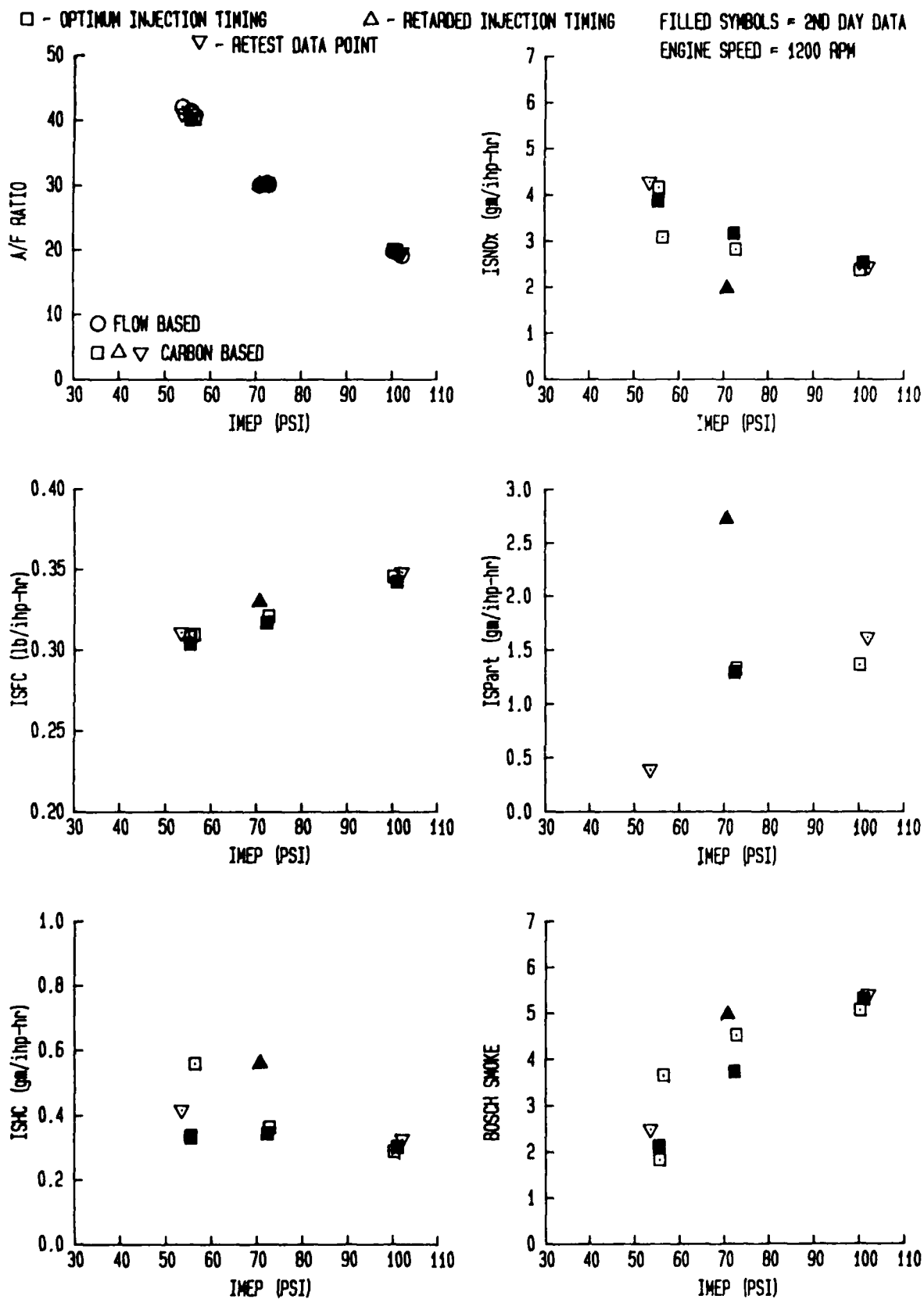


FIGURE 6-28      CETANE ENGINE      FUEL : DOE-1  
 EMISSIONS, FUEL CONSUMPTION, AND AIR-FUEL RATIO

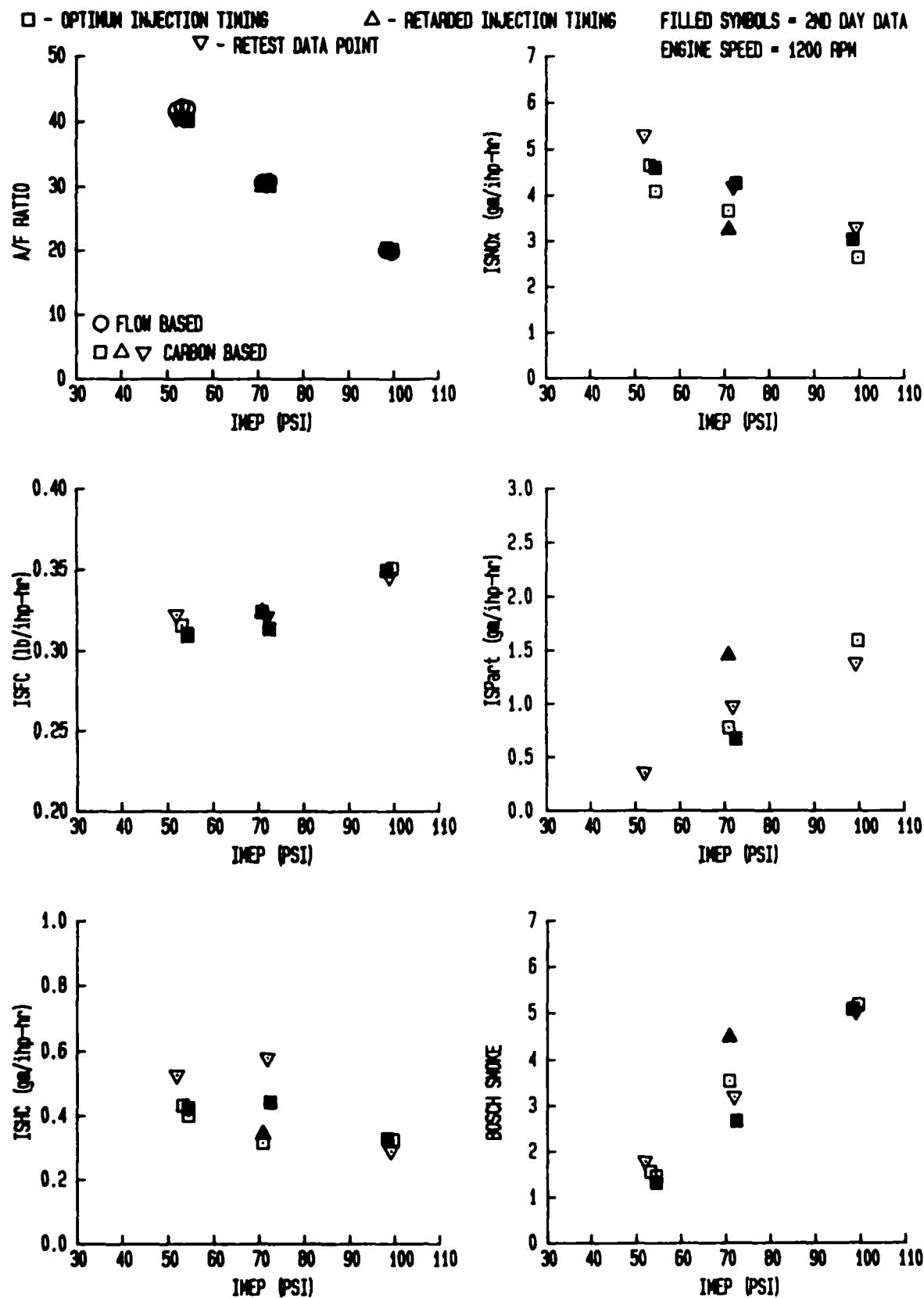


FIGURE 6-29      CETANE ENGINE      FUEL : DOE-2  
 EMISSIONS, FUEL CONSUMPTION, AND AIR-FUEL RATIO

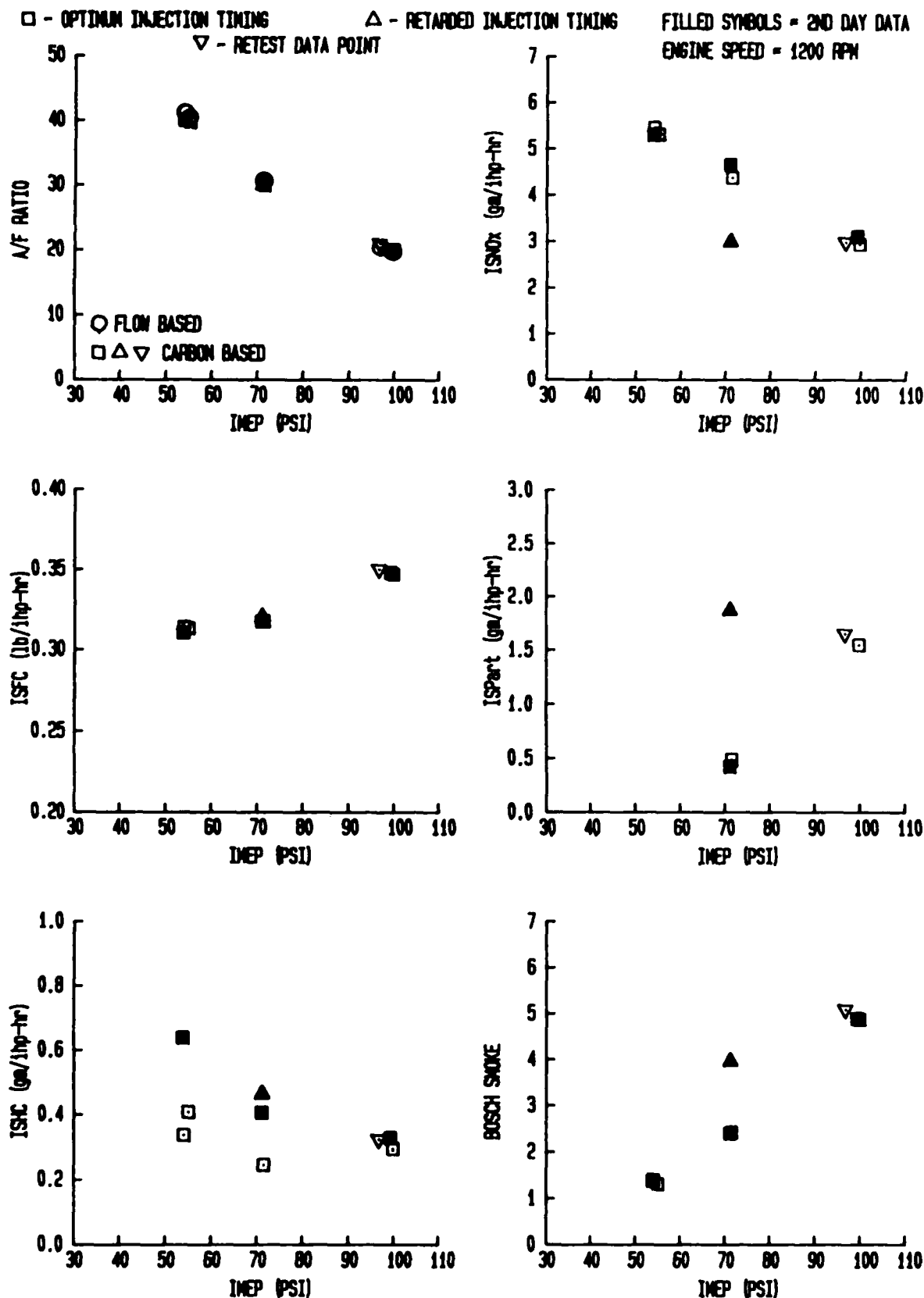


FIGURE 6-30      CETANE ENGINE      FUEL : DOE-3  
 EMISSIONS, FUEL CONSUMPTION, AND AIR-FUEL RATIO

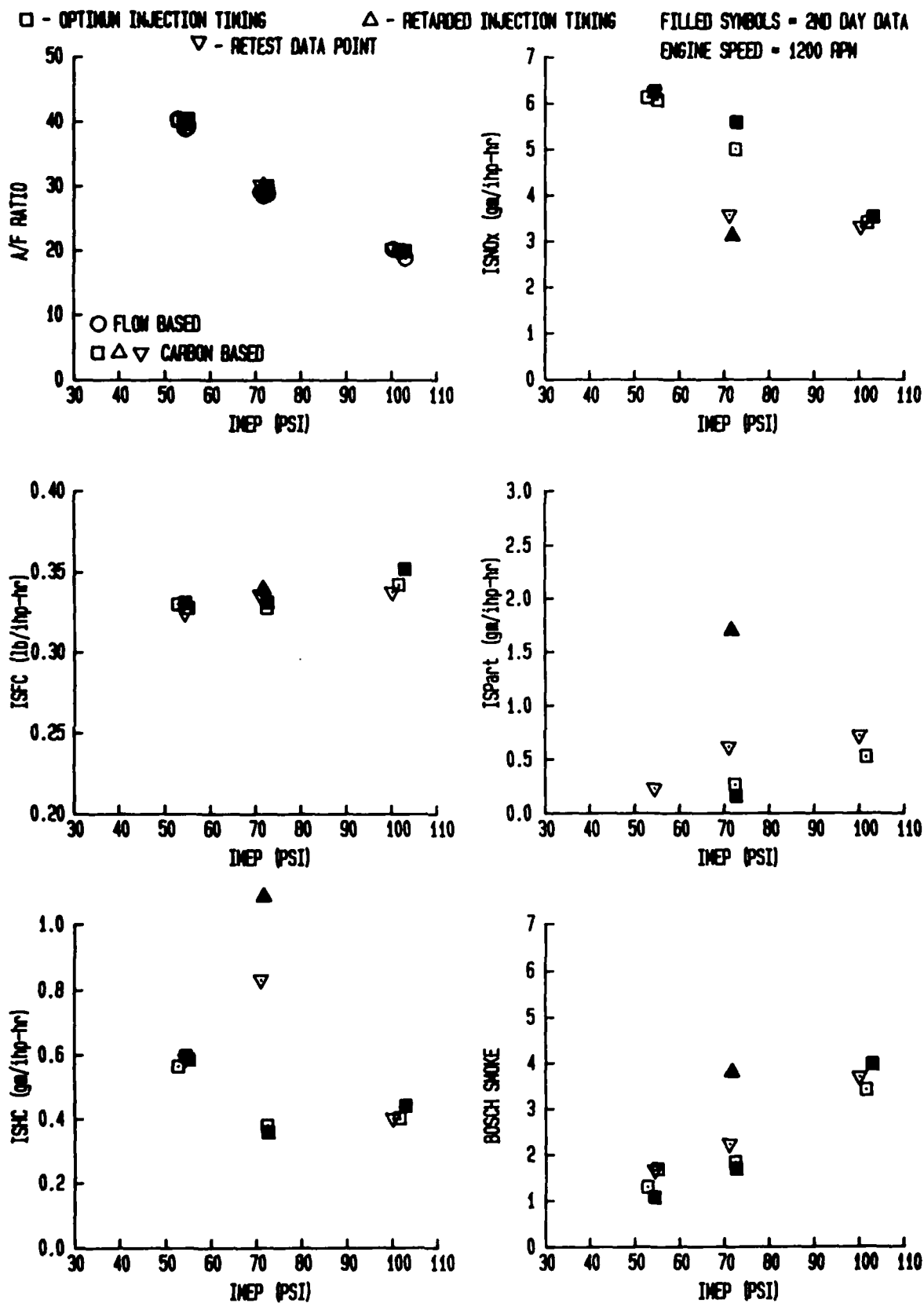


FIGURE 6-31      CETANE ENGINE      FUEL : DOE - 4  
 EMISSIONS, FUEL CONSUMPTION, AND AIR-FUEL RATIO

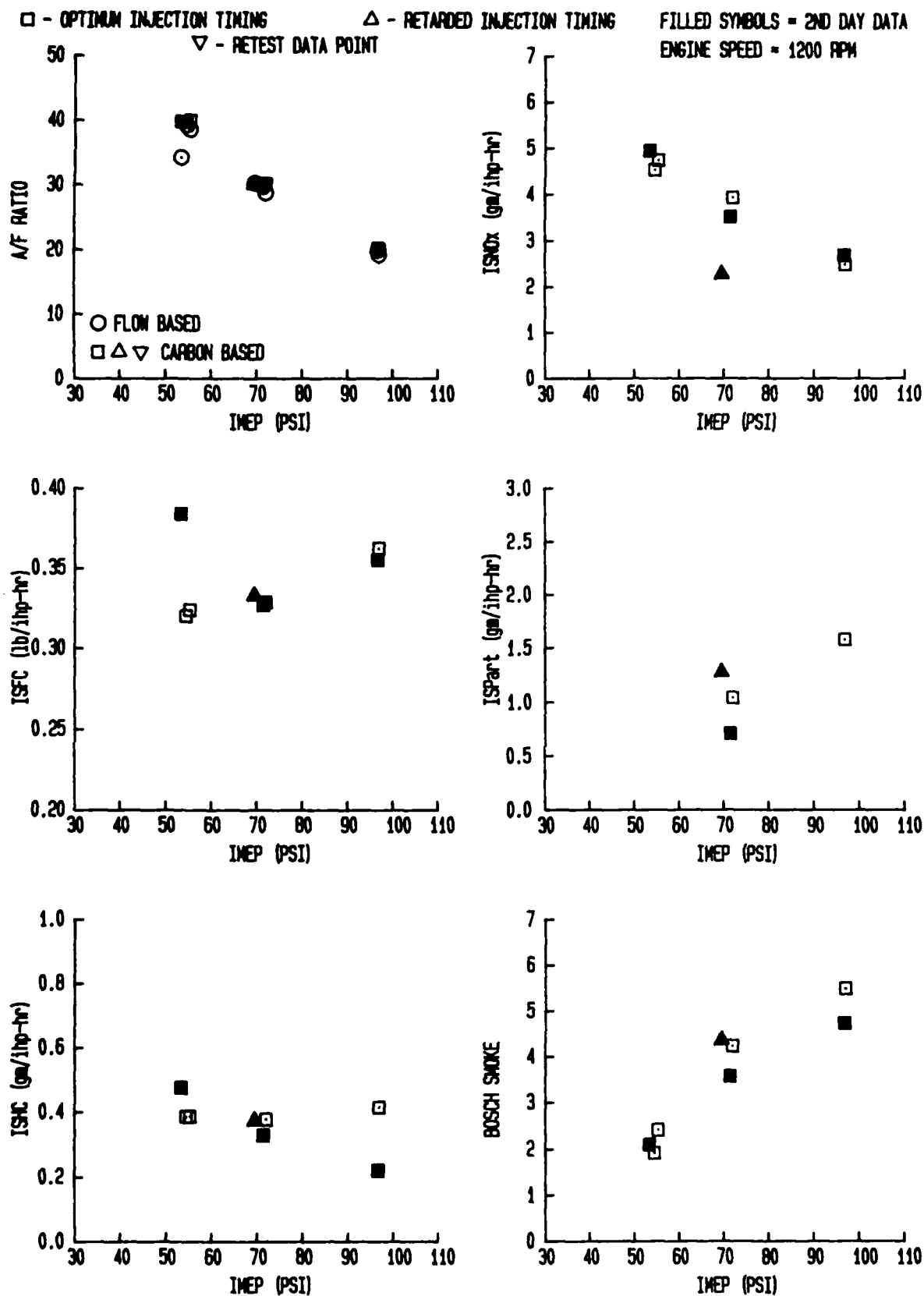


FIGURE 6-32      CETANE ENGINE      FUEL : CEC #1  
 EMISSIONS, FUEL CONSUMPTION, AND AIR-FUEL RATIO



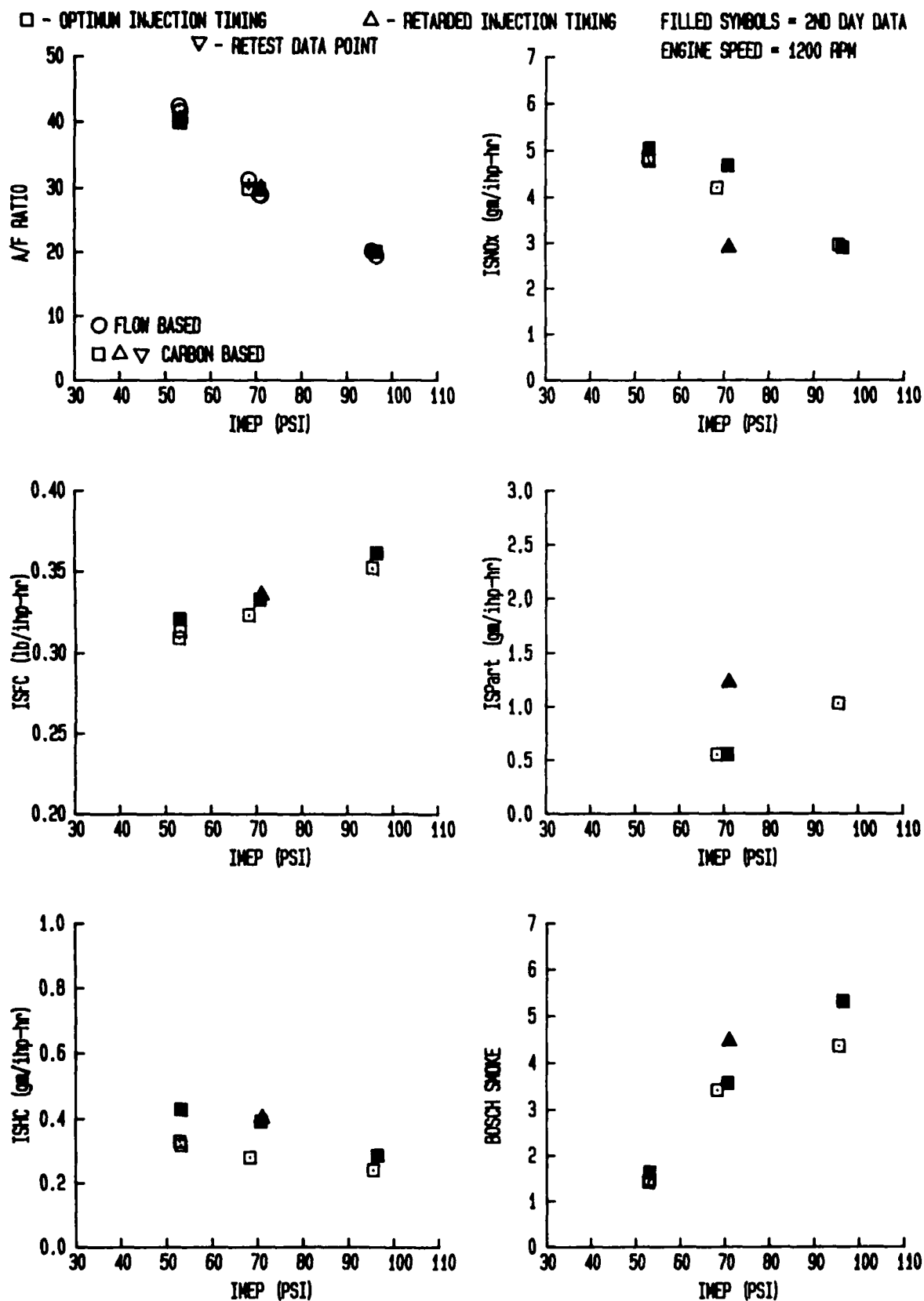


FIGURE 6-33      CETANE ENGINE      FUEL : CEC #2  
 EMISSIONS, FUEL CONSUMPTION, AND AIR-FUEL RATIO

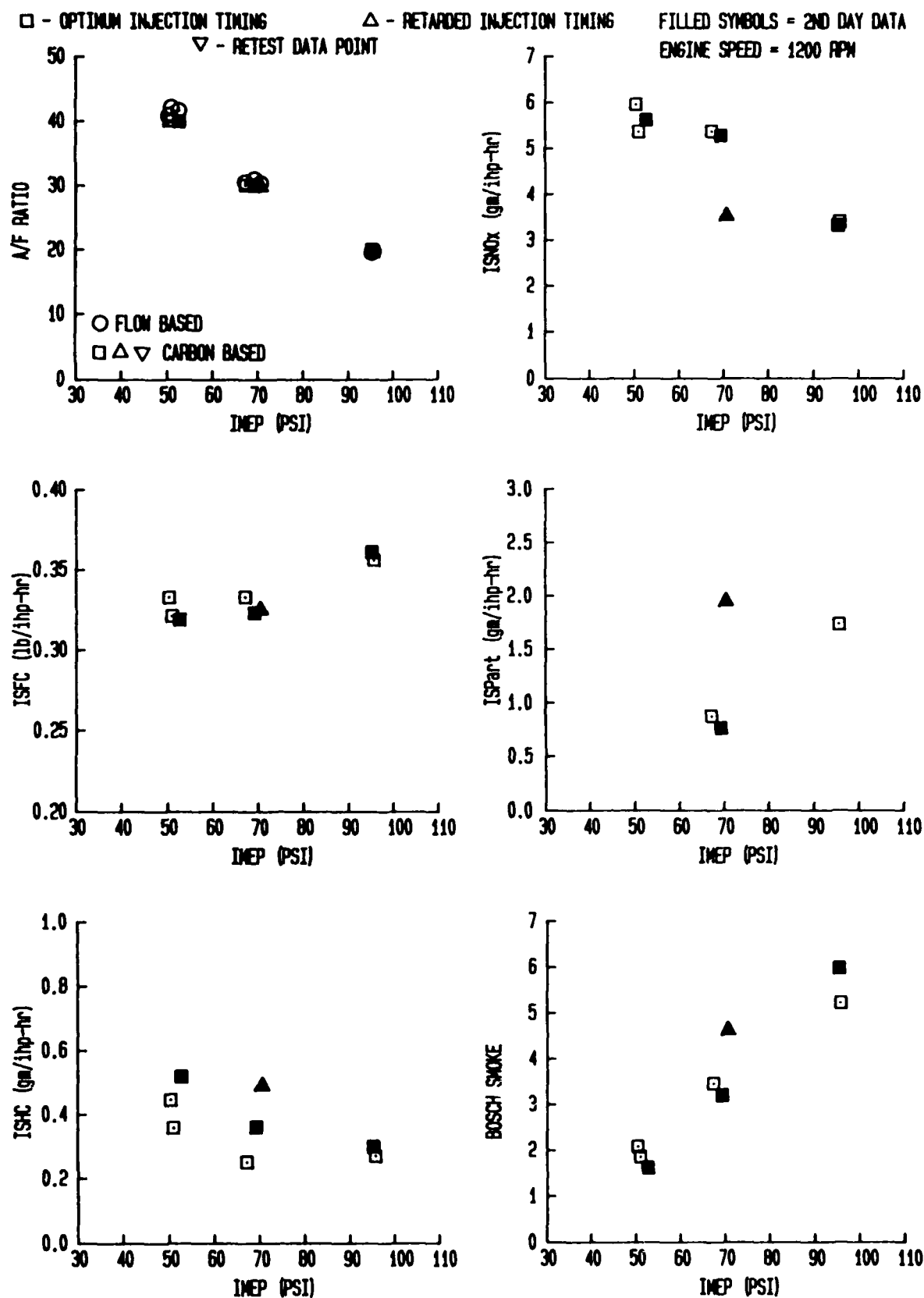


FIGURE 6-34      CETANE ENGINE      FUEL : CEC-2A  
 EMISSIONS, FUEL CONSUMPTION, AND AIR-FUEL RATIO

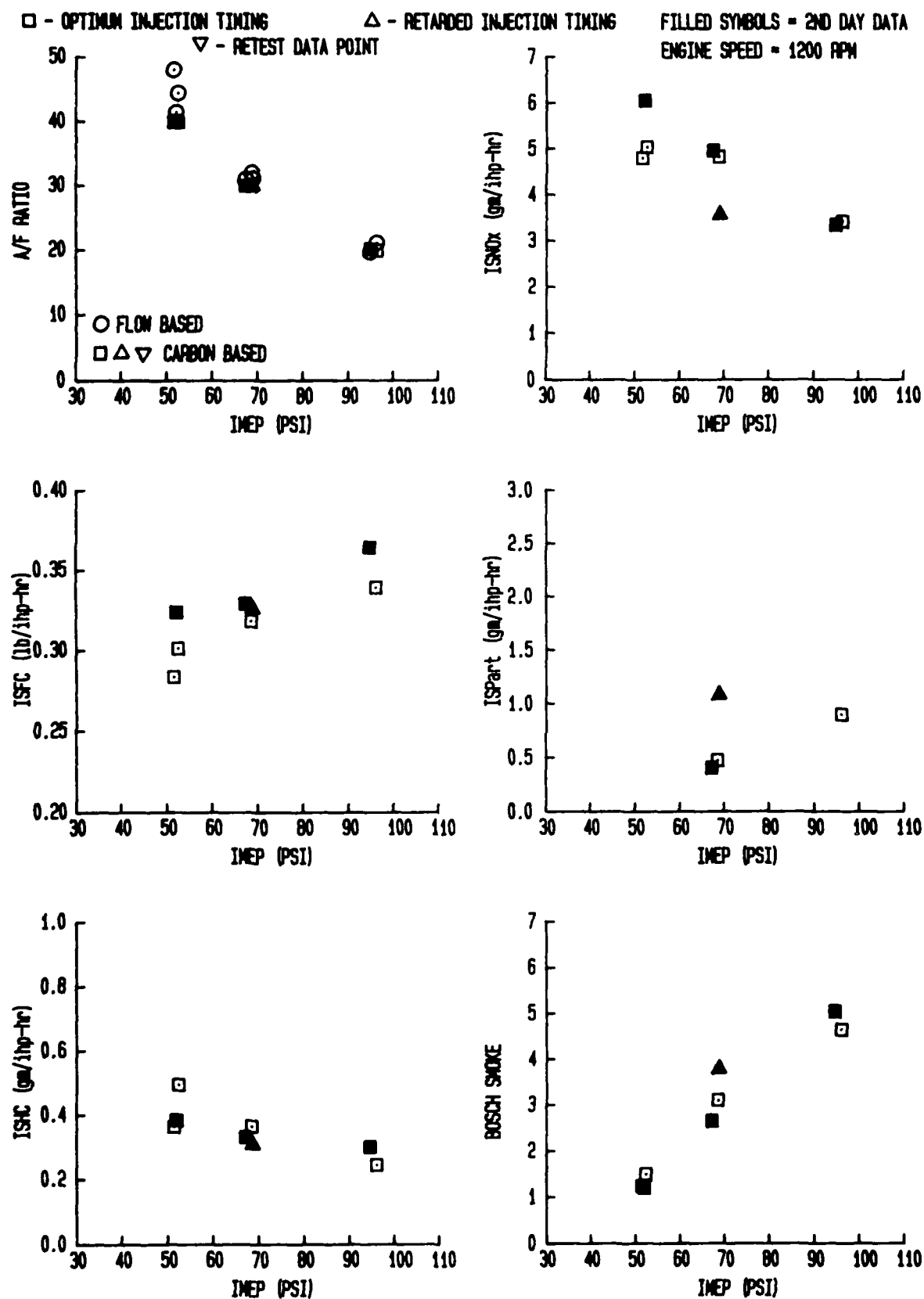


FIGURE 6-35      CETANE ENGINE      FUEL : CEC #3  
 EMISSIONS, FUEL CONSUMPTION, AND AIR-FUEL RATIO

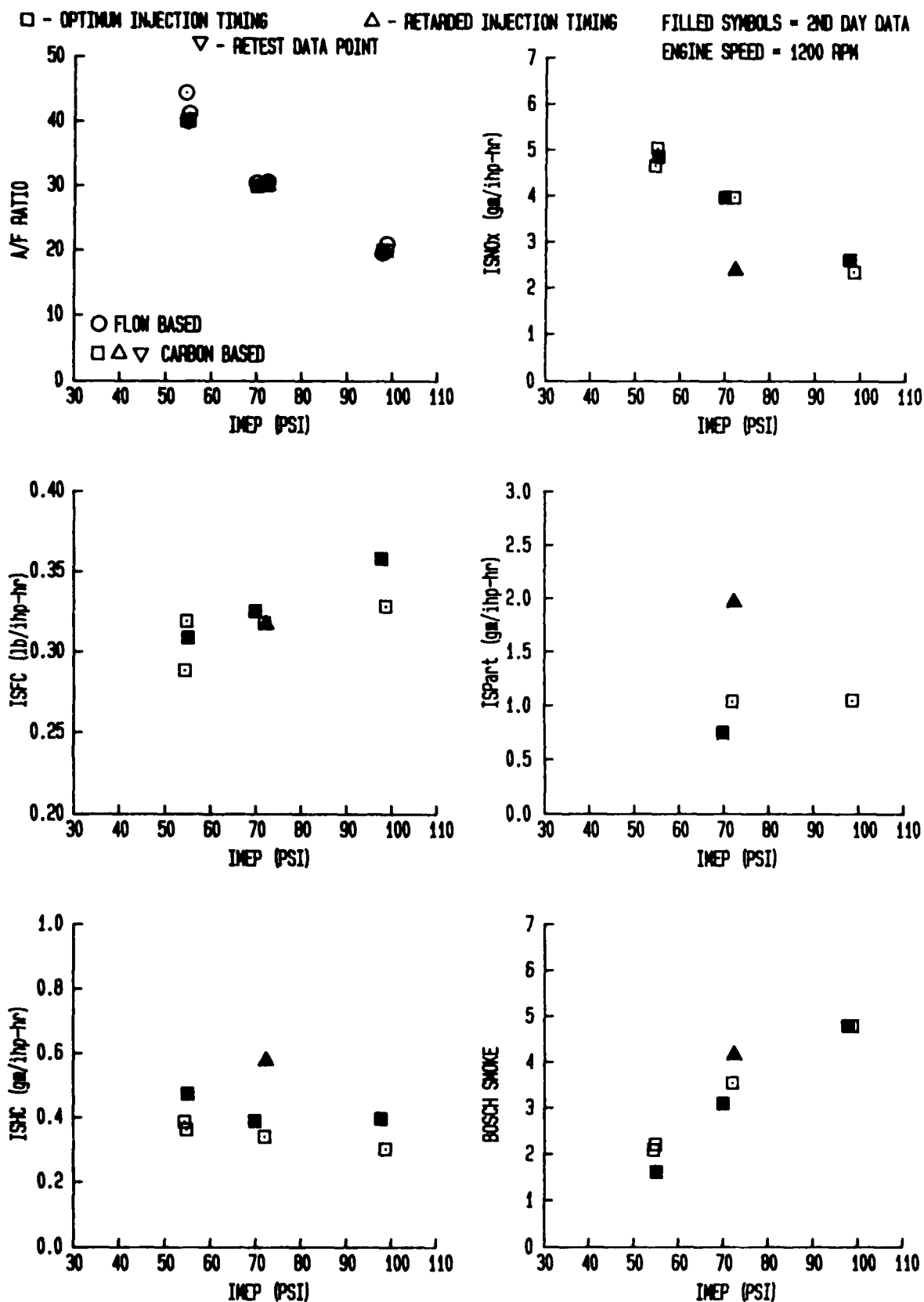


FIGURE 6-36      CETANE ENGINE      FUEL : CAPE #5  
 EMISSIONS, FUEL CONSUMPTION, AND AIR-FUEL RATIO

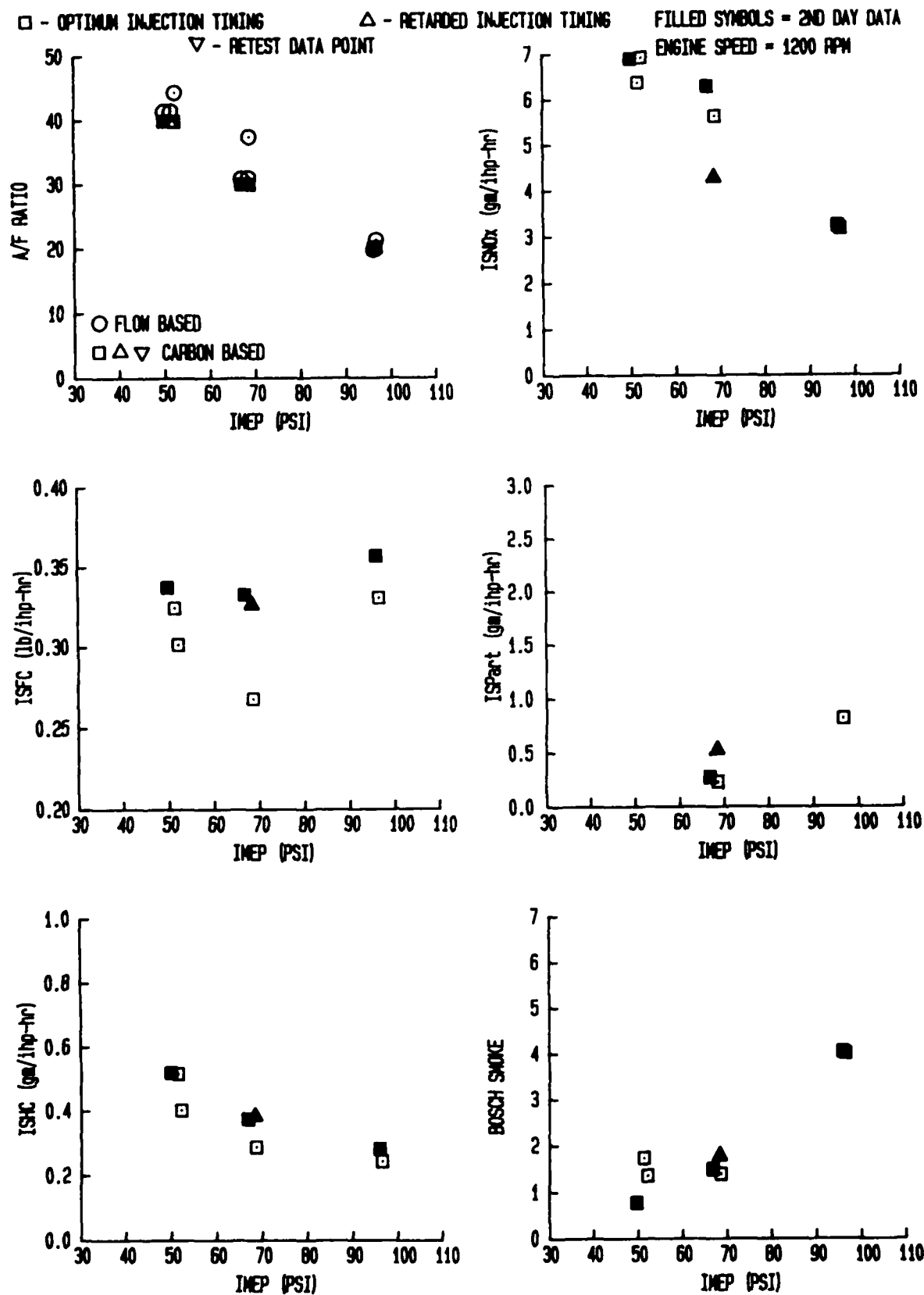


FIGURE 6-37      CETANE ENGINE      FUEL : CAPE #6  
 EMISSIONS, FUEL CONSUMPTION, AND AIR-FUEL RATIO

ISPart emissions. The increase due to retard is more pronounced with some fuels than others.

Hydrocarbon emissions (ISHC) show some reduction with increasing load (imep). It is hard to accurately assess the effects of test and operating conditions on ISHC emissions since they display wider variability from day-to-day, even when operating with the same fuel at the same test conditions. It is assumed that this problem is related to the fact that the injector nozzle tip must be removed and cleaned after approximately 8 hours of operation. Even though the same injector tip is being used, the cleaning and reassembly operations seem to cause differences that can appear in ISHC emissions.

The Bosch smoke data are consistent with the mass particulate emissions in that they show a consistent increase in the Bosch smoke number with increasing load (imep). There was also a small, but consistent increase in the Bosch smoke number for the 5 CA° retarded condition at medium load. As previously mentioned, these results were anticipated based upon past behavior of diesel engine systems.

The second group of graphical results for the cetane engine deals with combustion parameters that have a direct physical meaning. The discussion in the following paragraphs refers to information in figures 6-38 through 6-47.

The combustion period in CA° changes as expected. The period increased with load (imep). This behavior is indicative of the increased amount of fuel that must be burned at the higher load conditions and the nominally constant characteristics of flame speed and combustion chamber geometry.

The rate of pressure rise data for the pre-chamber pressure of the cetane engine shows a generally wide distribution of values with load for all fuels. If there is sensitivity of this data to load (imep), it is toward a slight decrease in rate with increasing load. However, the wide scatter of data does not strongly support this observation. Retarded timing, on the other hand, produces a significant reduction in the rate at medium load. The reduction is on the order of 50% or more.

Peak Pressure data for pressure in the pre-chamber is more consistent than the rate of pressure rise data; however, it is relatively insensitive to load. As might be expected, there is a slight increase in peak pressure with load. The retarded injection timing condition at medium load causes a significant reduction in peak pressure accompanied by a slight loss in imep.

The estimate of the bulk gas temperature at SOI (Start of Injection) shows a wide variation in the data. The nominal trend is that the temperature is relatively insensitive to load. This should be the case since the temperature is more related to the gas properties and the compression process than to load for an unthrottled engine.

The third set of graphical results deals primarily with combustion parameters that are computed from heat release characteristics. The

□ - OPTIMUM INJECTION TIMING

△ - RETARDED INJECTION TIMING

▽ - RETEST DATA POINT

FILLED SYMBOLS = 2ND DAY DATA

ENGINE SPEED = 1200 RPM

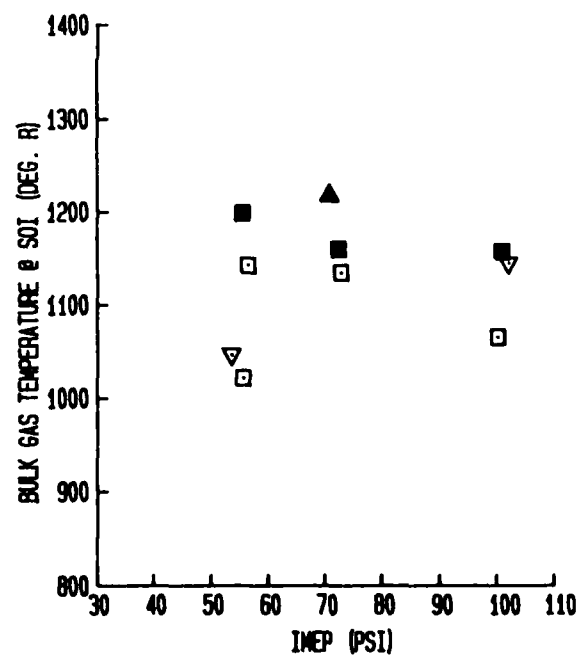
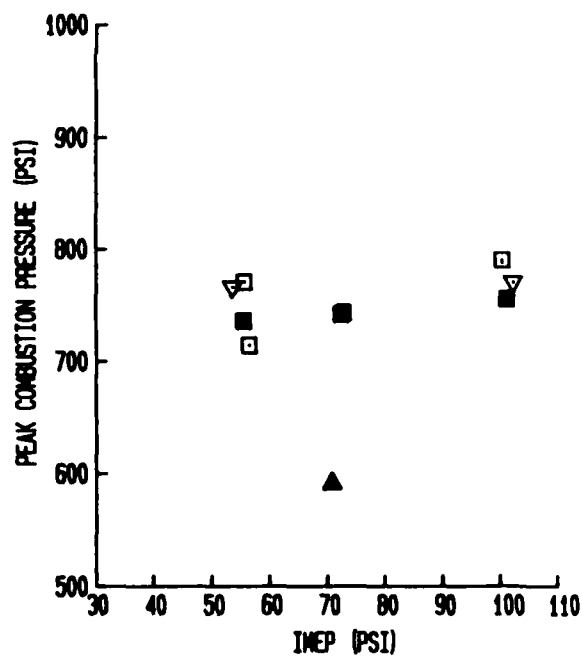
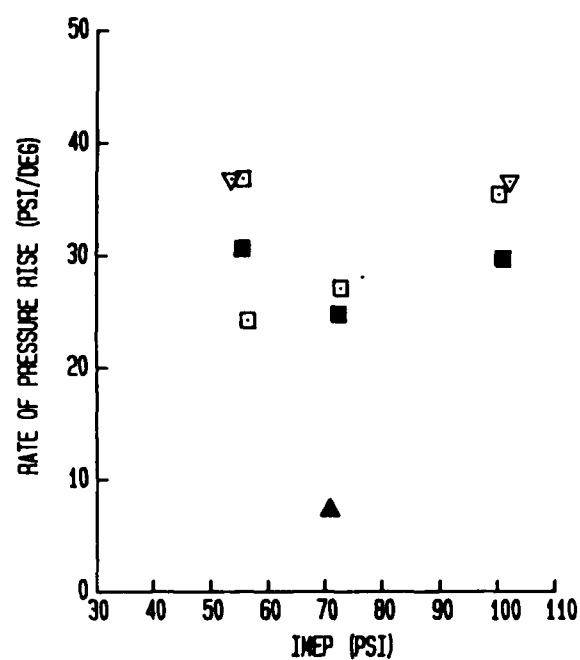
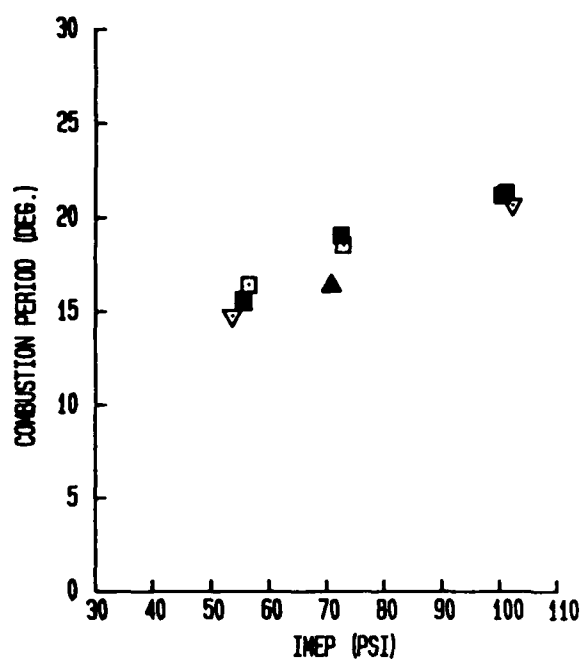


FIGURE 6-38

CETANE ENGINE

FUEL : DOE-1

COMBUSTION PARAMETERS

□ - OPTIMUM INJECTION TIMING

△ - RETARDED INJECTION TIMING

FILLED SYMBOLS = 2ND DAY DATA

▽ - RETEST DATA POINT

ENGINE SPEED = 1200 RPM

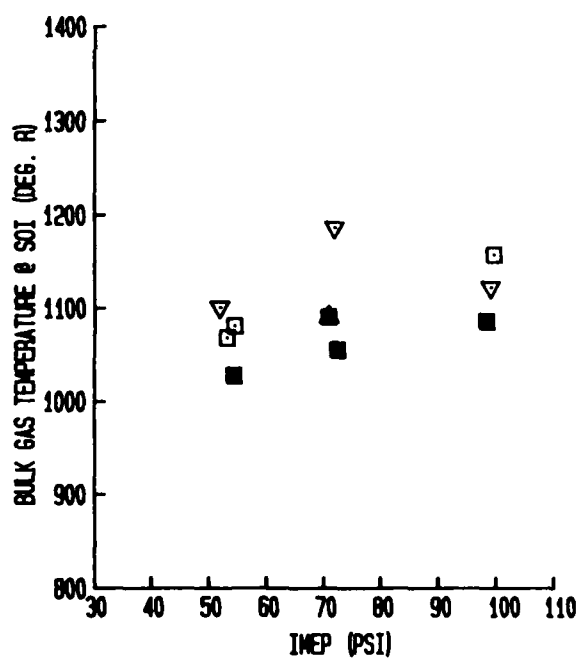
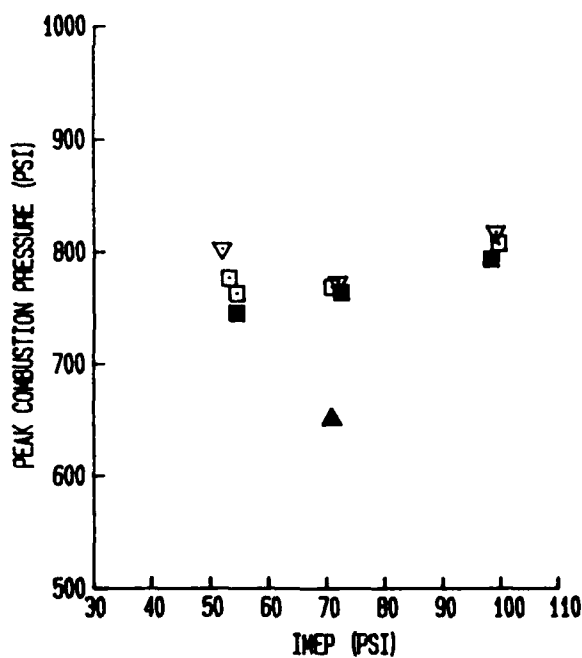
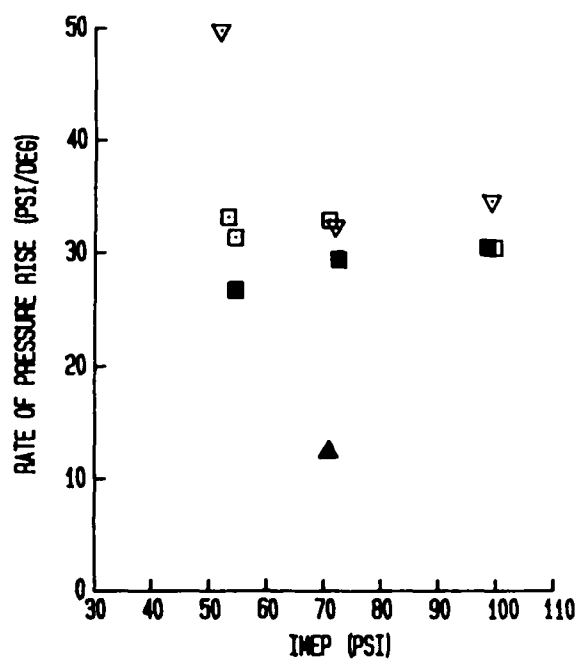
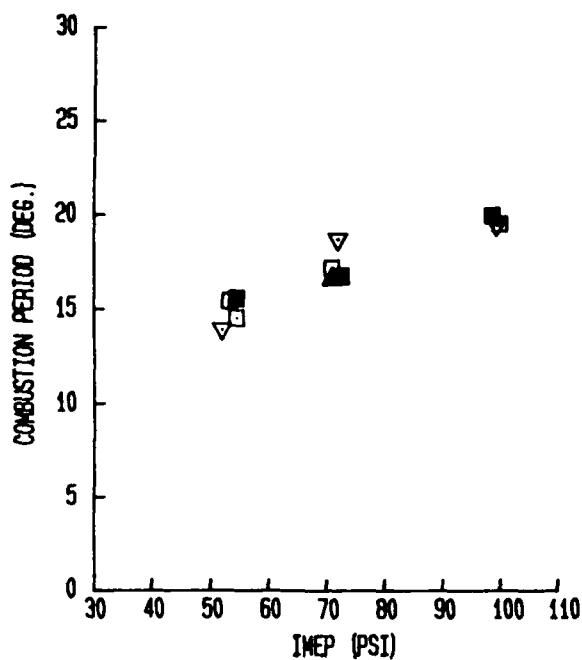


FIGURE 6-39

CETANE ENGINE

FUEL : DOE-2

COMBUSTION PARAMETERS



□ - OPTIMUM INJECTION TIMING      △ - RETARDED INJECTION TIMING      FILLED SYMBOLS = 2ND DAY DATA  
 ▽ - RETEST DATA POINT      ENGINE SPEED = 1200 RPM

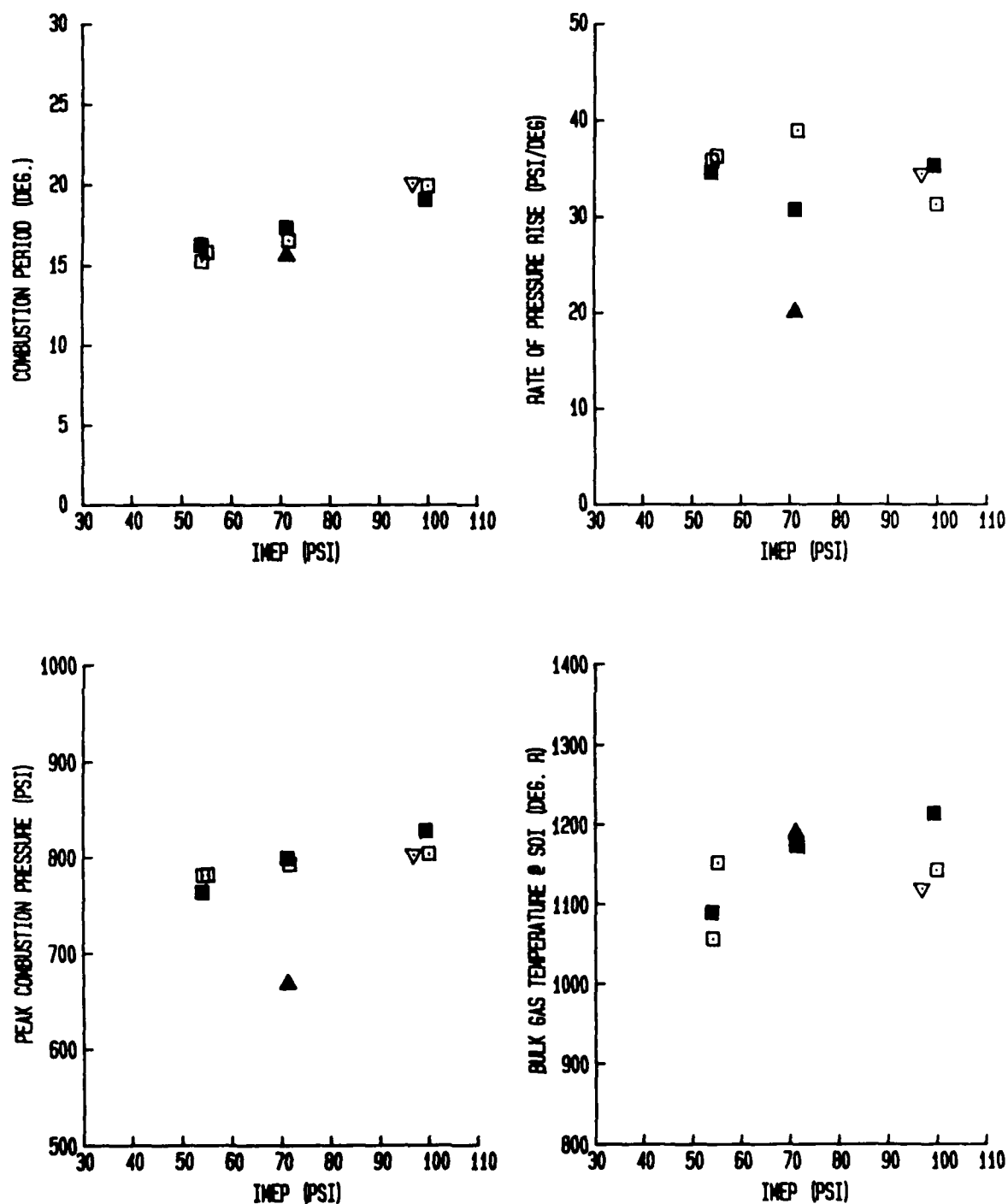


FIGURE 6-40

CETANE ENGINE

FUEL : DOE-3

COMBUSTION PARAMETERS

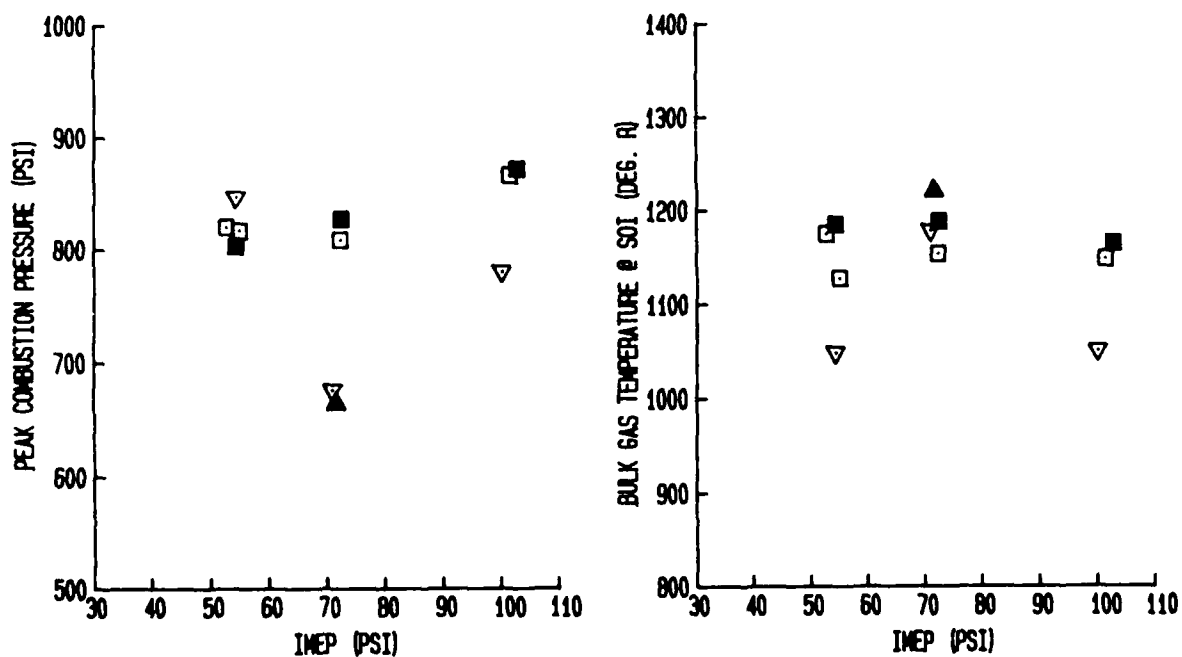
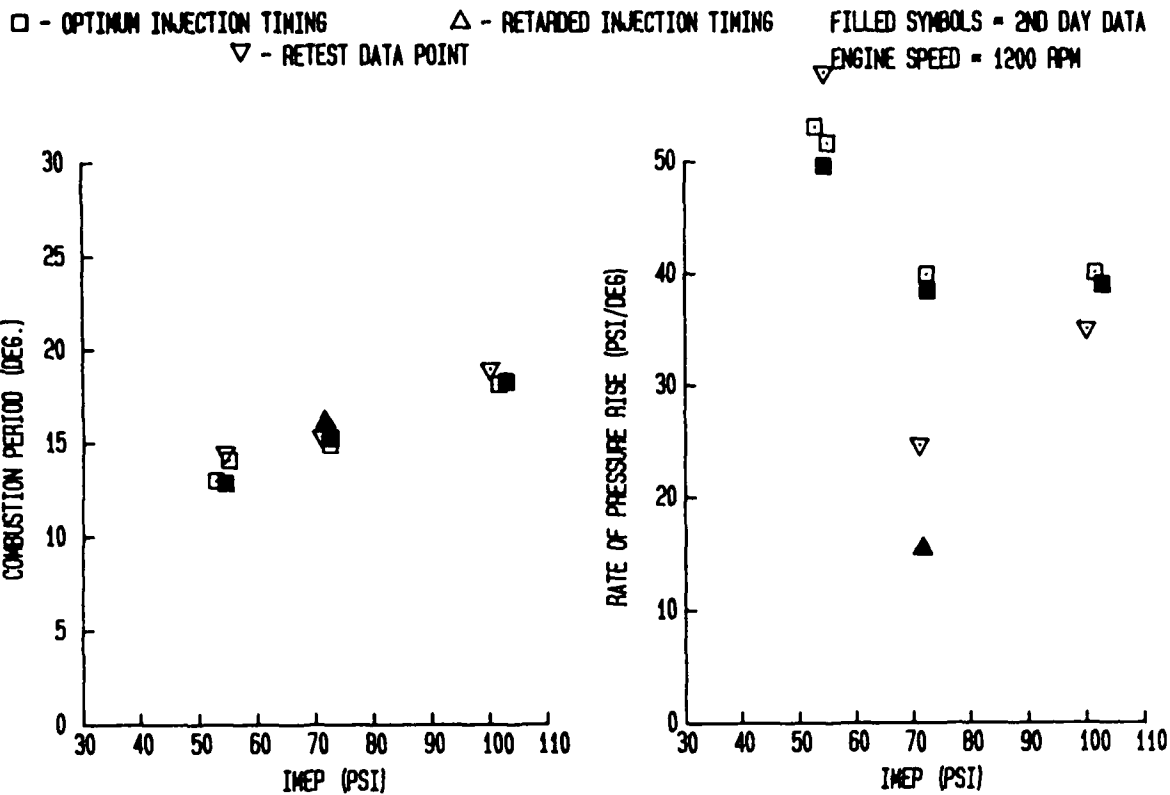


FIGURE 6-41

CETANE ENGINE

FUEL : DOE - 4

COMBUSTION PARAMETERS

□ - OPTIMUM INJECTION TIMING

△ - RETARDED INJECTION TIMING

FILLED SYMBOLS = 2ND DAY DATA

▽ - RETEST DATA POINT

ENGINE SPEED = 1200 RPM

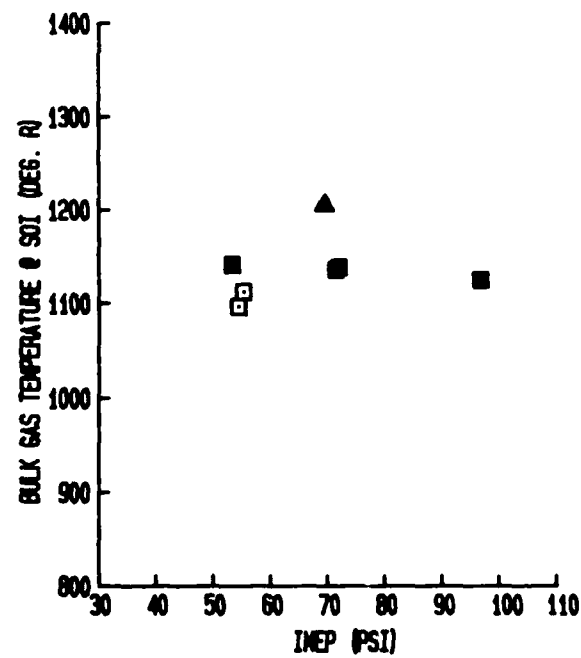
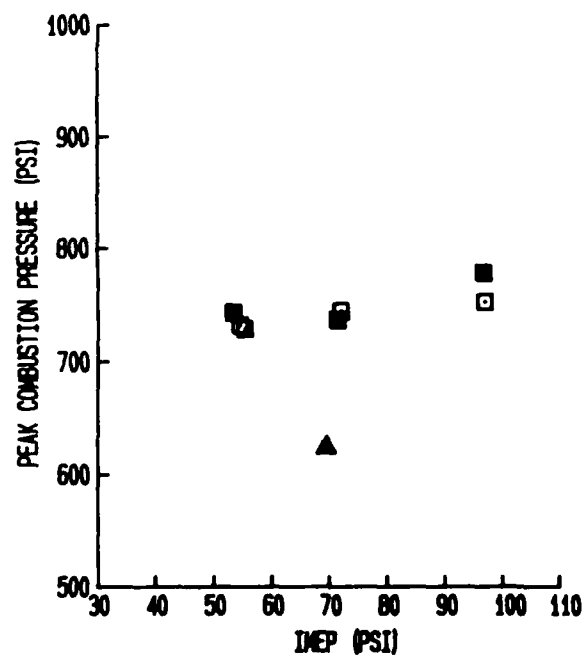
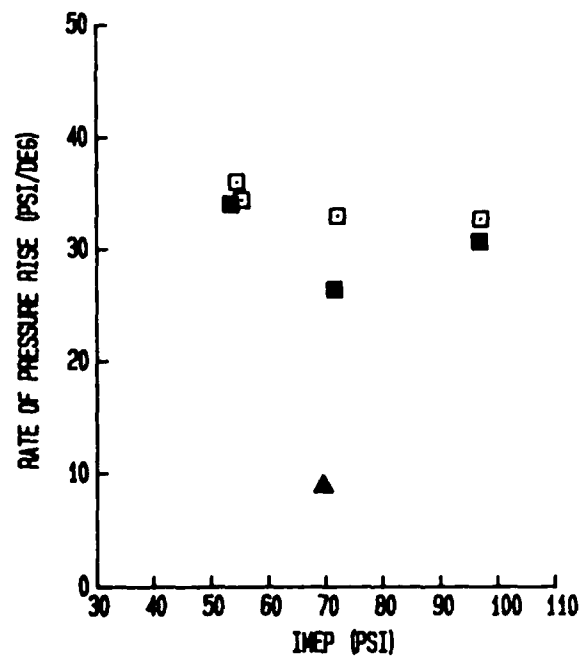
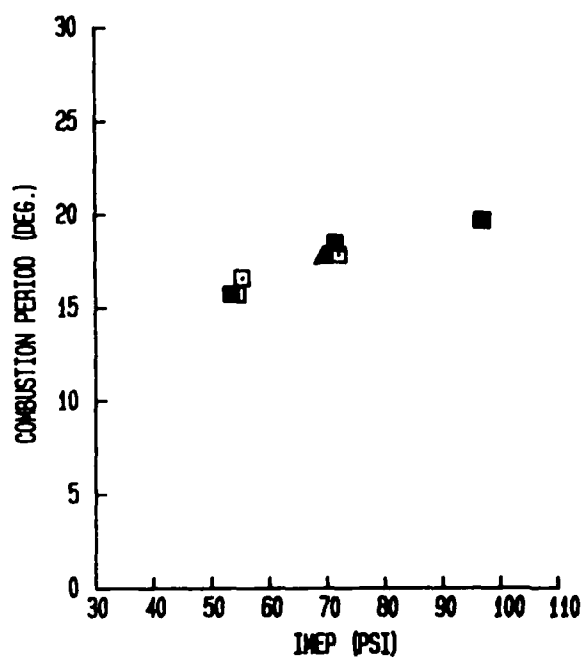


FIGURE 6-42

CETANE ENGINE

FUEL : CEC #1

COMBUSTION PARAMETERS

□ - OPTIMUM INJECTION TIMING

△ - RETARDED INJECTION TIMING

FILLED SYMBOLS = 2ND DAY DATA

▽ - RETEST DATA POINT

ENGINE SPEED = 1200 RPM

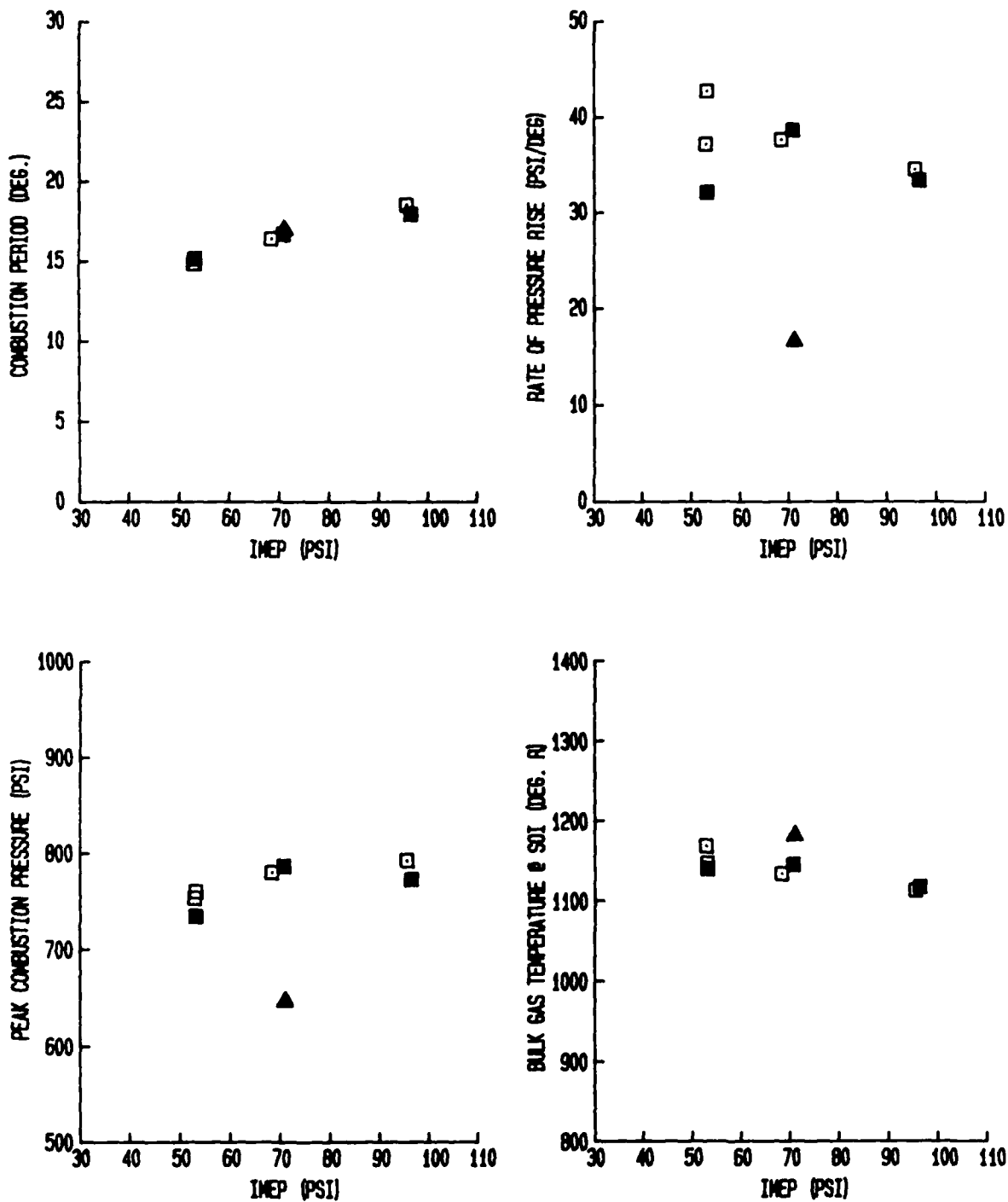


FIGURE 6-43

CETANE ENGINE

FUEL : CEC #2

COMBUSTION PARAMETERS

□ - OPTIMUM INJECTION TIMING      △ - RETARDED INJECTION TIMING      FILLED SYMBOLS = 2ND DAY DATA  
 ▽ - RETEST DATA POINT      ENGINE SPEED = 1200 RPM

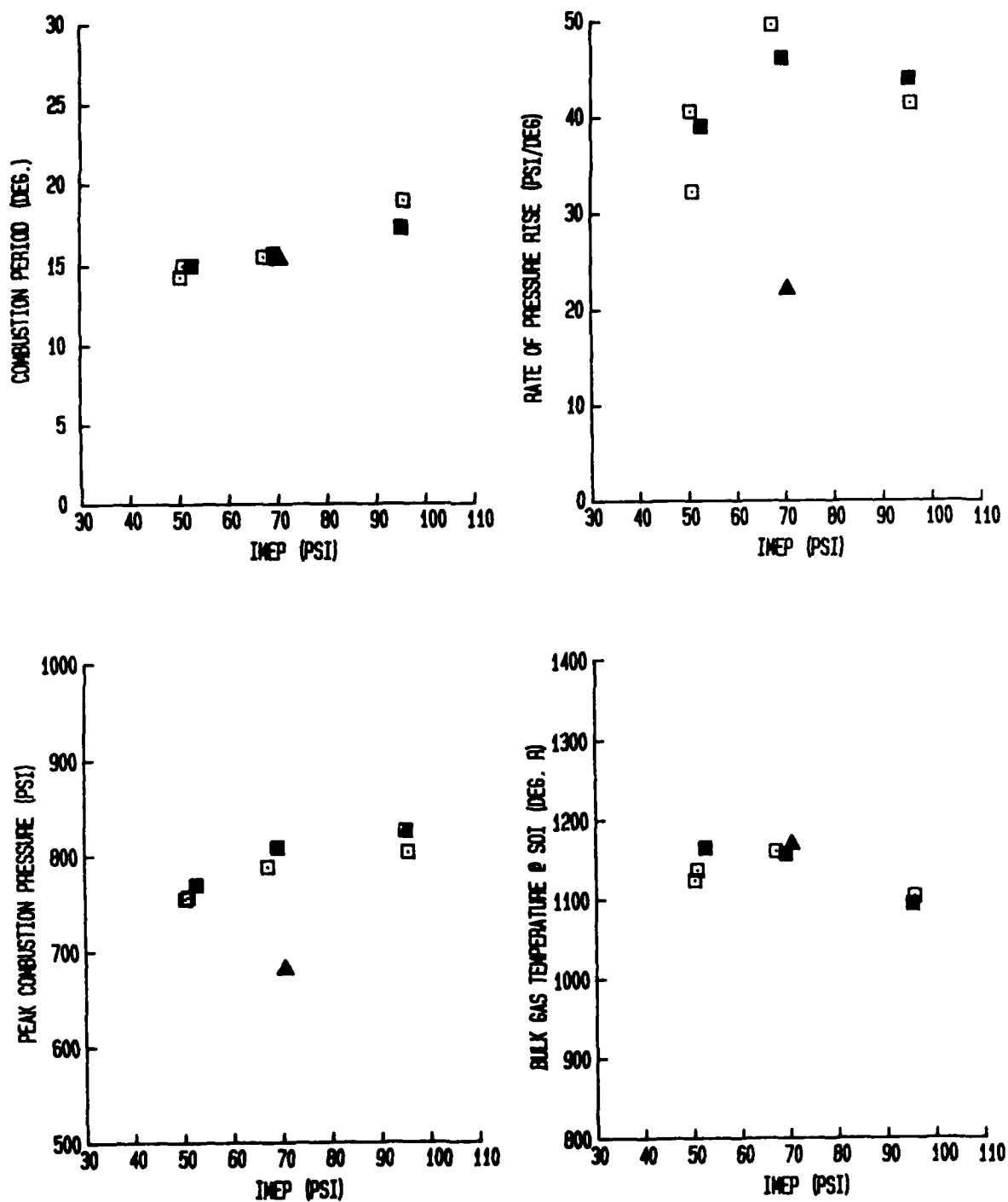


FIGURE 6-44

CETANE ENGINE

FUEL : CEC-2A

COMBUSTION PARAMETERS

□ - OPTIMUM INJECTION TIMING

△ - RETARDED INJECTION TIMING

▽ - RETEST DATA POINT

FILLED SYMBOLS = 2ND DAY DATA

ENGINE SPEED = 1200 RPM

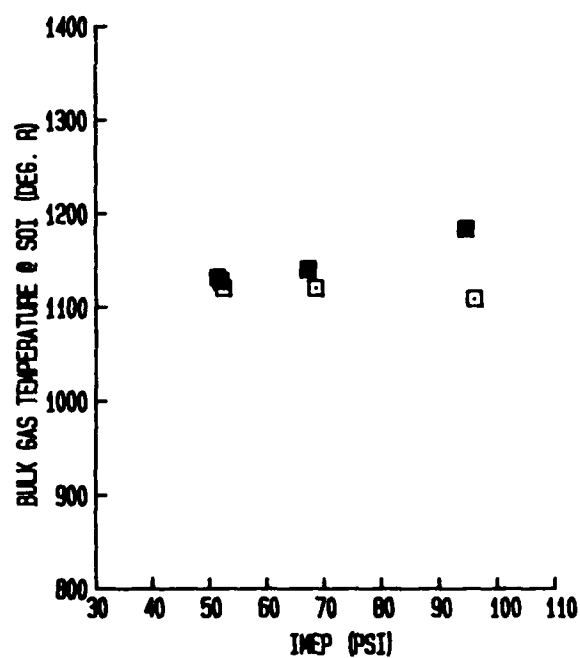
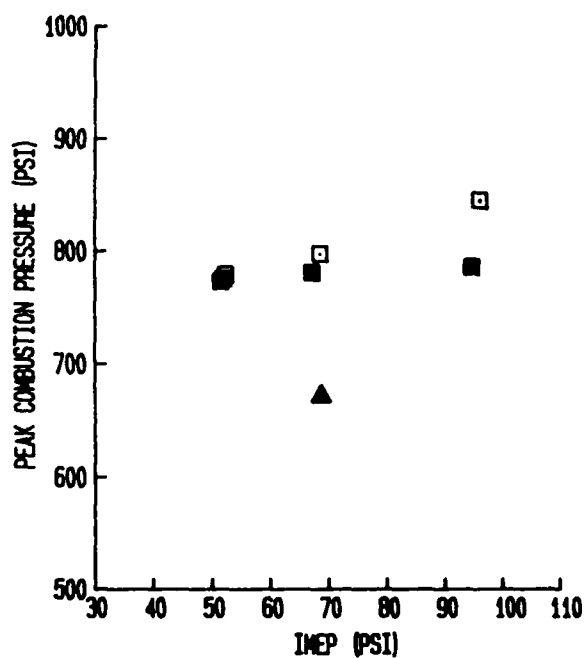
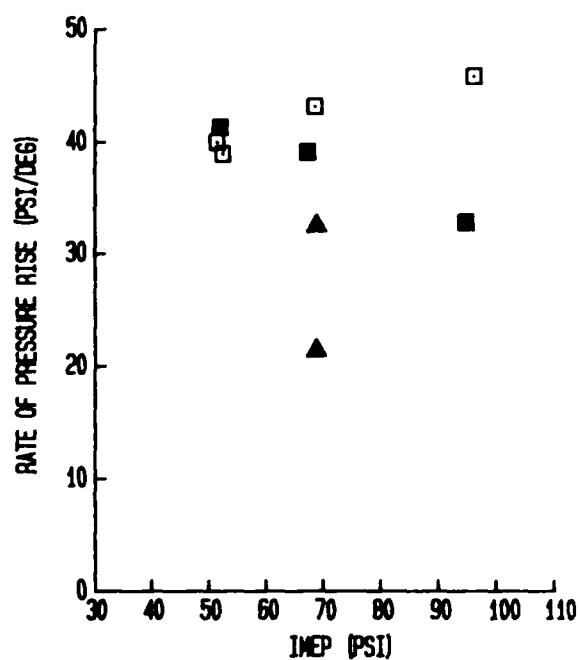
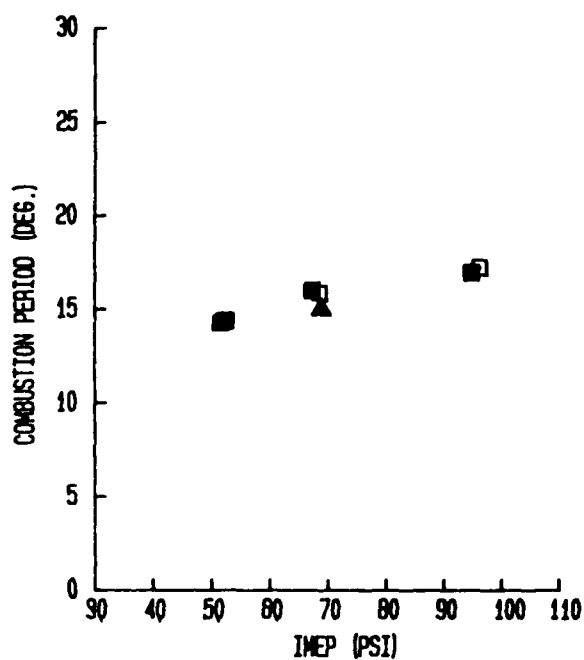


FIGURE 6-45

CETANE ENGINE

FUEL : CEC #3

COMBUSTION PARAMETERS

□ - OPTIMUM INJECTION TIMING      △ - RETARDED INJECTION TIMING      FILLED SYMBOLS = 2ND DAY DATA  
 ▽ - RETEST DATA POINT      ENGINE SPEED = 1200 RPM

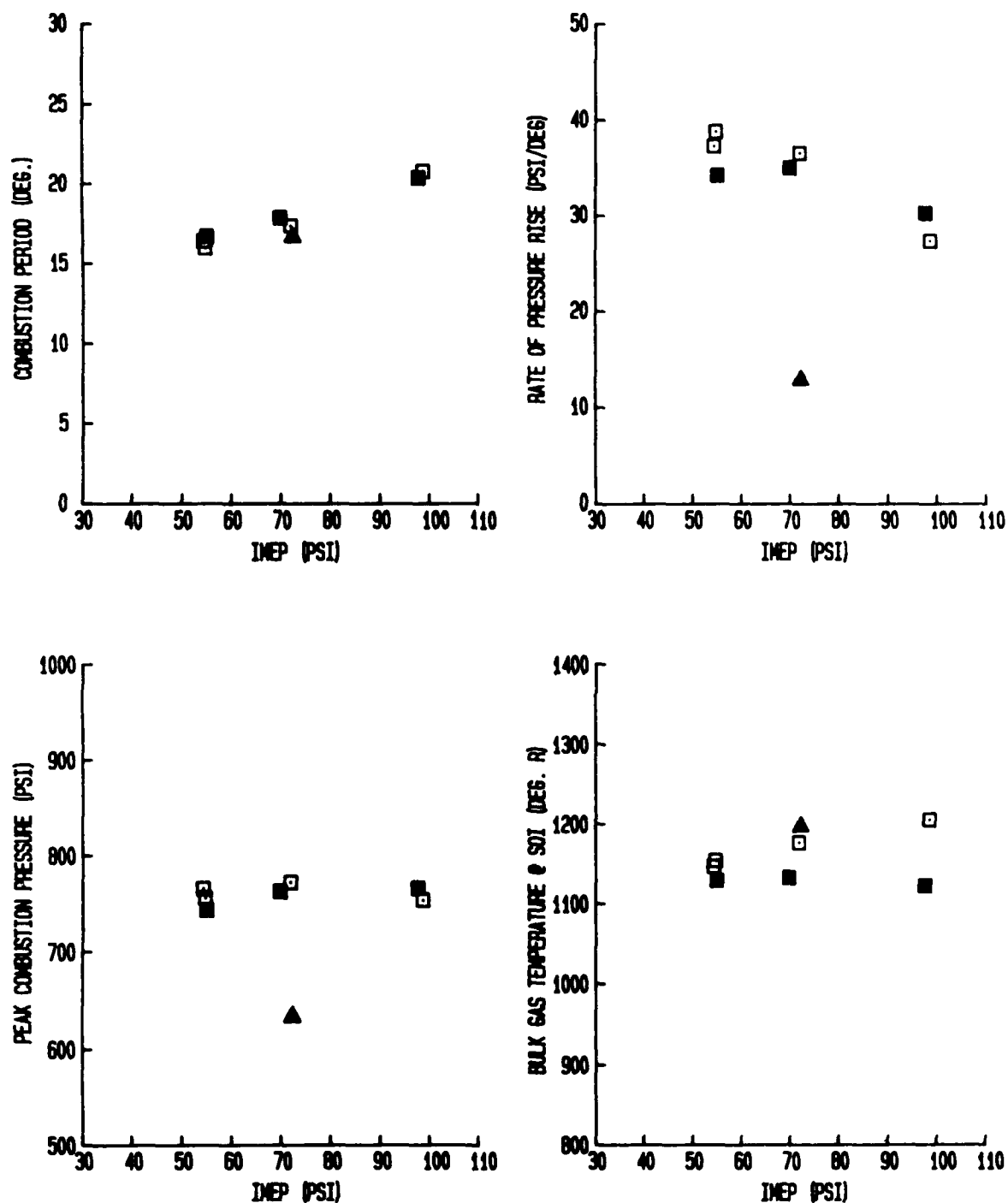


FIGURE 6-46      CETANE ENGINE      FUEL : CAPE #5  
 COMBUSTION PARAMETERS

□ - OPTIMUM INJECTION TIMING      △ - RETARDED INJECTION TIMING      ◻ FILLED SYMBOLS = 2ND DAY DATA  
 ▽ - RETEST DATA POINT      ENGINE SPEED = 1200 RPM

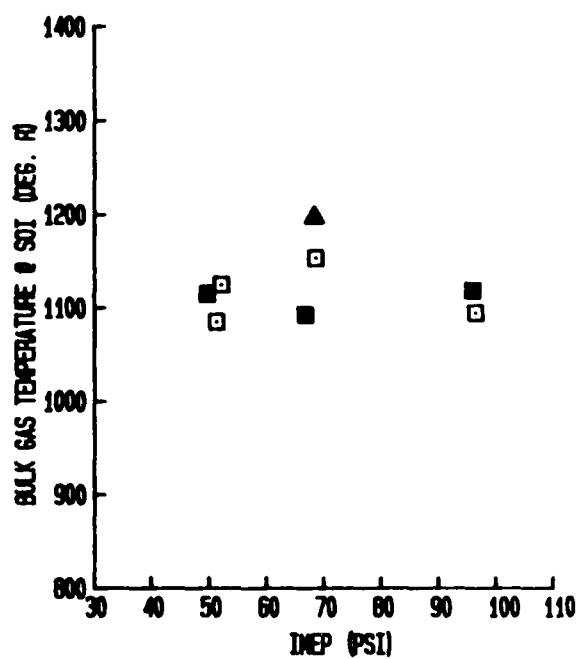
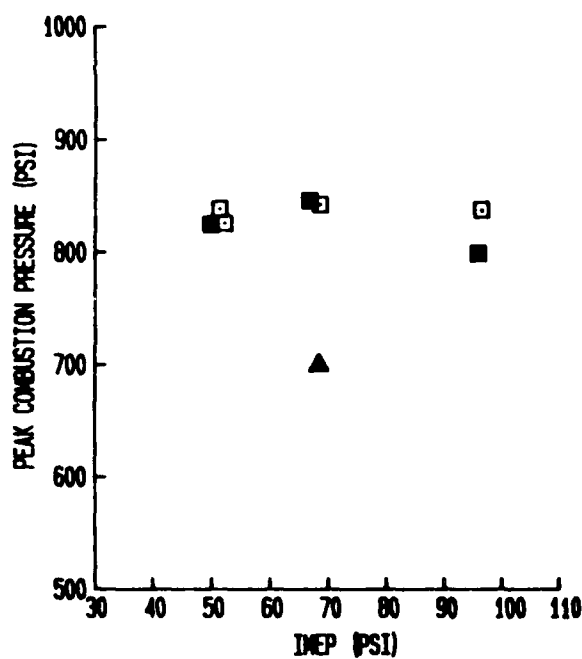
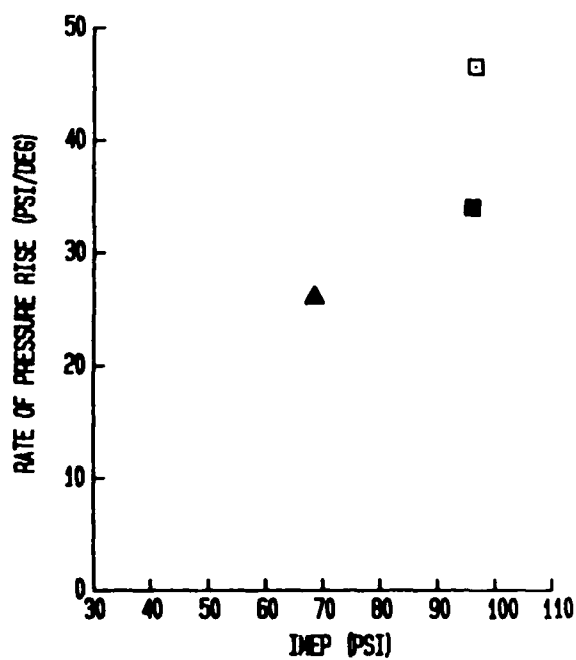
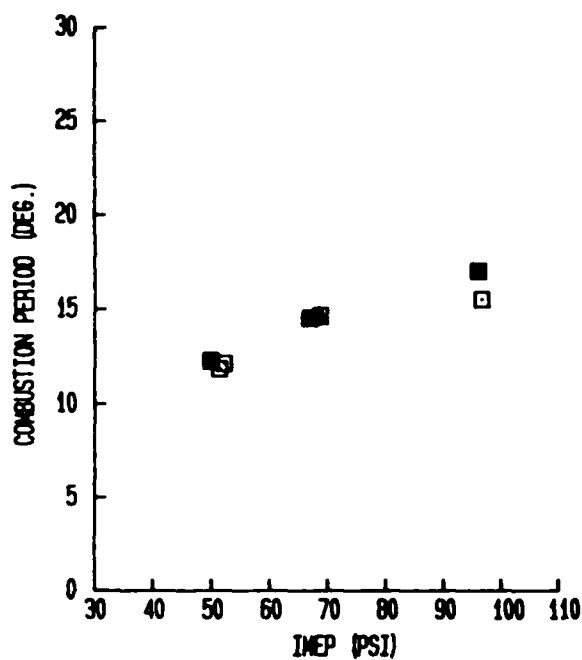


FIGURE 6-47

CETANE ENGINE

FUEL : CAPE #6

COMBUSTION PARAMETERS



discussion in the following paragraphs is based upon information contained in figures 6-48 through 6-57.

The ignition delay is relatively insensitive to load or retarded timing at the medium load condition. The poorer quality fuels (DOE #4 and CAPE #6) show the greatest sensitivity to load with noticeable increases in the ignition delay for lighter loads.

The pre-mixed combustion fraction (PCF) data demonstrated relatively large variations. It was relatively insensitive to load with the majority of fuels showing little change to a slight increase in PCF with load. Values were typically 0.10 or less. The retarded injection timing at medium load showed some tendency to increase the PCF, but it was not a strong effect. The fact that the values used to determine the PCF were relatively small compared to the total value of the variables being manipulated caused some concern about the accuracy of the PCF reported. This problem is undoubtedly reflected in the PCF data variations observed.

The pre-mixed combustion index (PCI) is quite similar to the PCF in measurement and determination and exhibits similar variations in data for the reasons just mentioned. Most, but not all, fuels show some increase with load (CAPE #6 showed no increase with load). Injection timing retard at medium load caused an increase in the PCI for several, but not all fuels.

Less data variation was noted for the diffusion combustion index (DCI) than for the PCF or the PCI. For most of the fuels tested the DCI was relatively insensitive to load. However, CAPE #6 fuel did show a definite increase with load (imep). Retarded injection timing at medium load had a tendency to increase the DCI for some, but not all the fuels.

#### 6.4.2 Fuel Effects, Cetane Engine

The previous section described the effects of engine variables and test conditions on performance, emissions, and combustion parameters. This section is devoted to describing fuel effects on these dependent variables. The approach used is to compare the behavior of the dependent variables of all other fuels to that for the DOE #1 fuel. Obvious fuel property effects will be mentioned as appropriate. The dependent variables will be discussed in the same order that they were discussed in the preceding section.

The following paragraphs contain observations developed from study and comparison of figures 6-28 through 6-37 and deal with how different fuels altered the emissions, fuel consumption, and air-fuel ratio.

For the ten fuels tested there was no observable change in the air-fuel ratio due to the use of different fuels. This result was quite predictable since the laboratory test condition was established using a nominal air-fuel ratio of 20, 30, or 40 to establish full, medium, and light load, respectively.

Indicated specific oxides of nitrogen emissions ( $ISNO_x$ ) was one of the variables more sensitive to changes in fuel. Compared to DOE #1,

□ - OPTIMUM INJECTION TIMING      △ - RETARDED INJECTION TIMING      FILLED SYMBOLS = 2ND DAY DATA  
 ▽ - RETEST DATA POINT      ENGINE SPEED = 1200 RPM

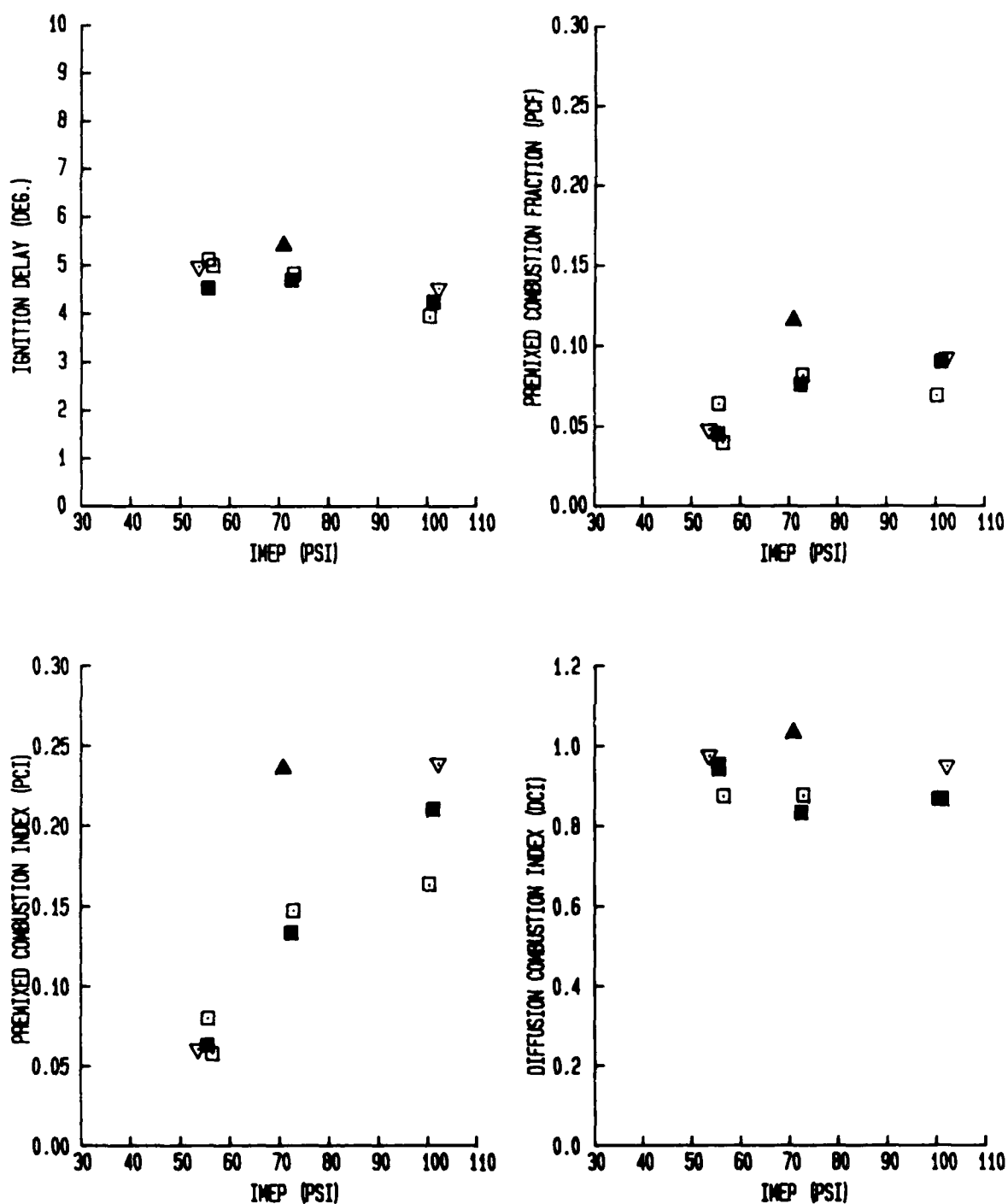


FIGURE 6-48      CETANE ENGINE      FUEL : DOE-1  
 COMBUSTION ANALYSIS PARAMETERS

□ - OPTIMUM INJECTION TIMING

△ - RETARDED INJECTION TIMING

▽ - RETEST DATA POINT

FILLED SYMBOLS = 2ND DAY DATA

ENGINE SPEED = 1200 RPM

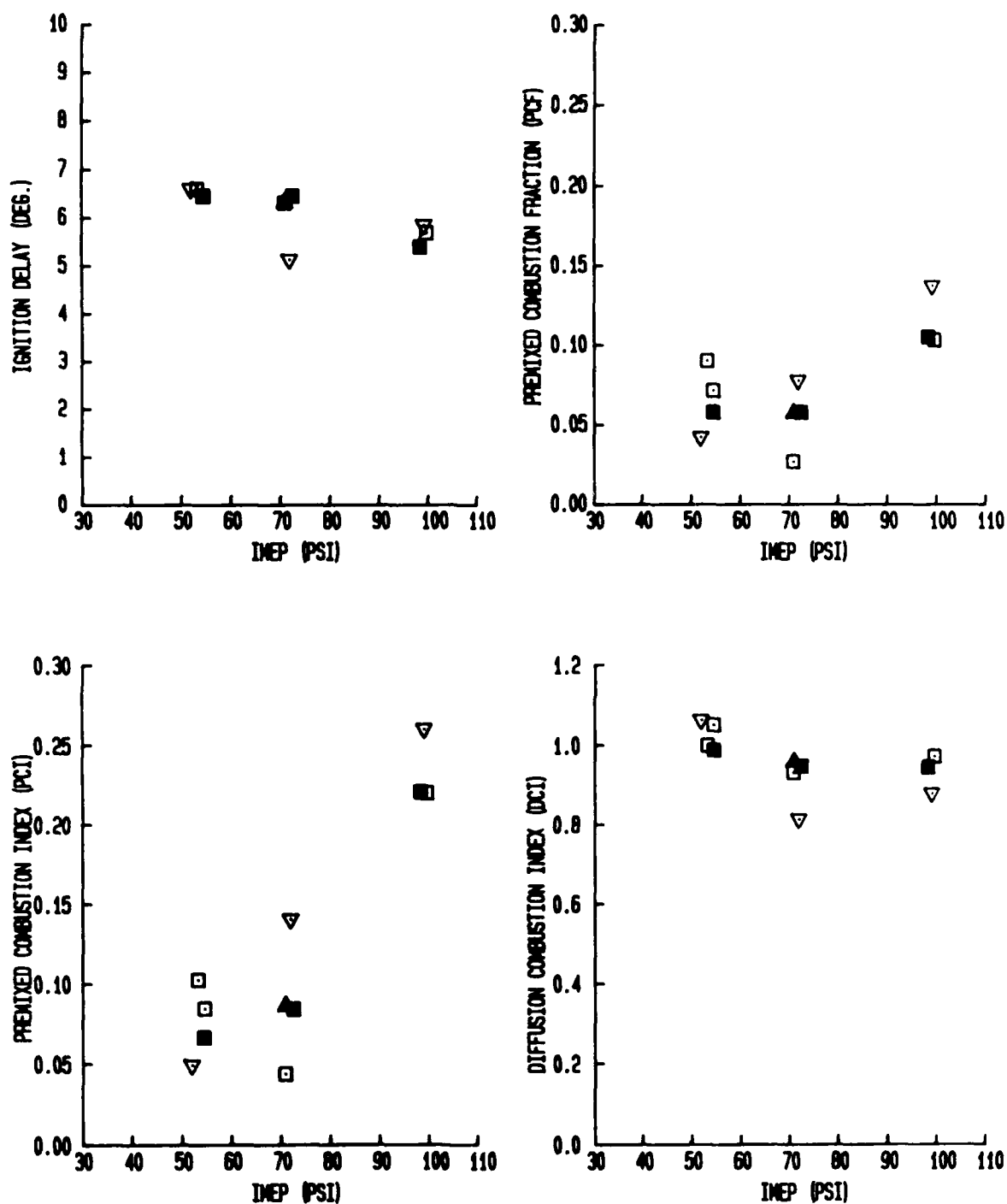


FIGURE 6-49

CETANE ENGINE

FUEL : DOE-2

COMBUSTION ANALYSIS PARAMETERS

□ - OPTIMUM INJECTION TIMING

△ - RETARDED INJECTION TIMING

FILLED SYMBOLS = 2ND DAY DATA

▽ - RETEST DATA POINT

ENGINE SPEED = 1200 RPM

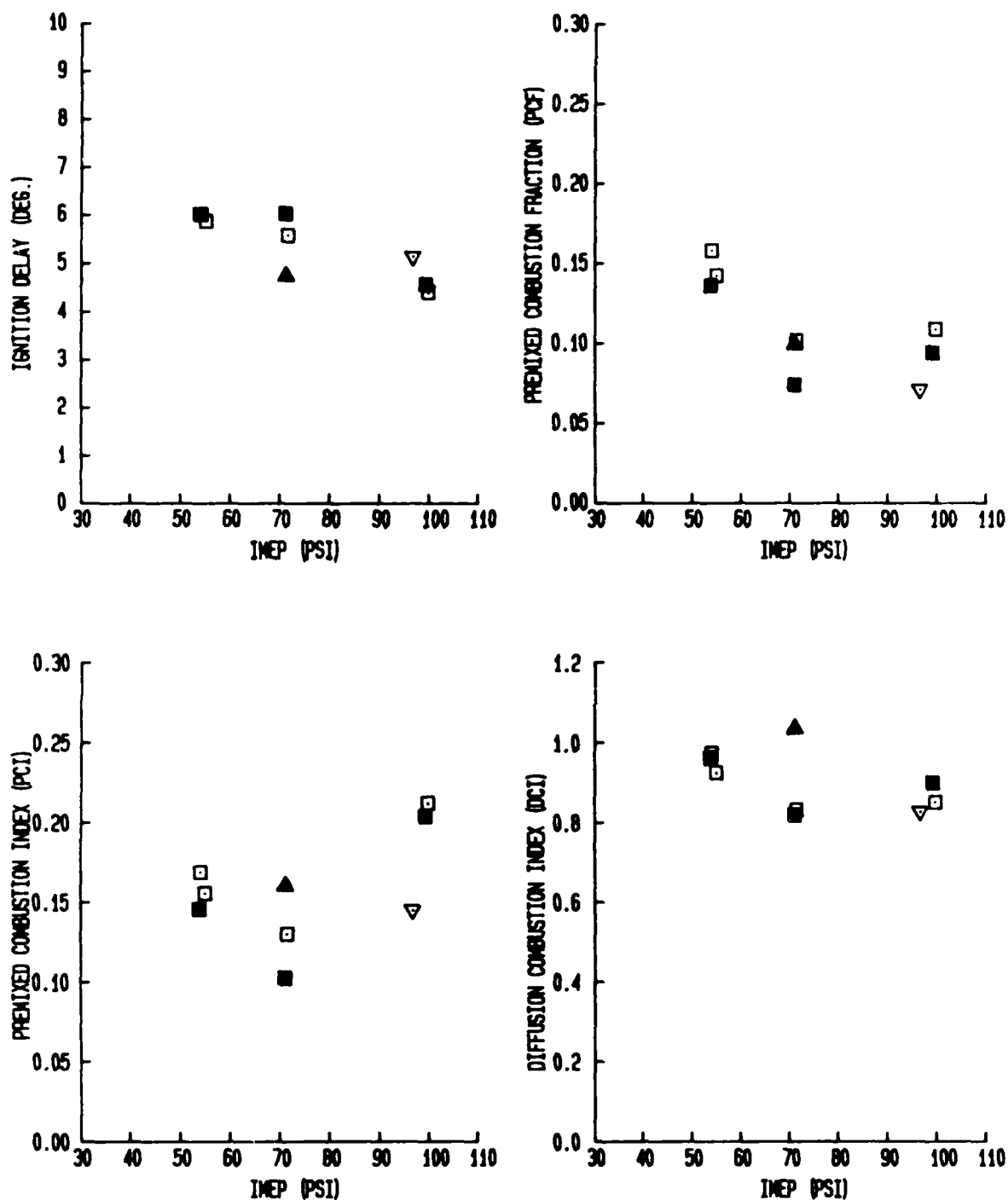


FIGURE 6-50

CETANE ENGINE

FUEL : DOE-3

COMBUSTION ANALYSIS PARAMETERS

□ - OPTIMUM INJECTION TIMING      △ - RETARDED INJECTION TIMING      FILLED SYMBOLS = 2ND DAY DATA  
 ▽ - RETEST DATA POINT      ENGINE SPEED = 1200 RPM

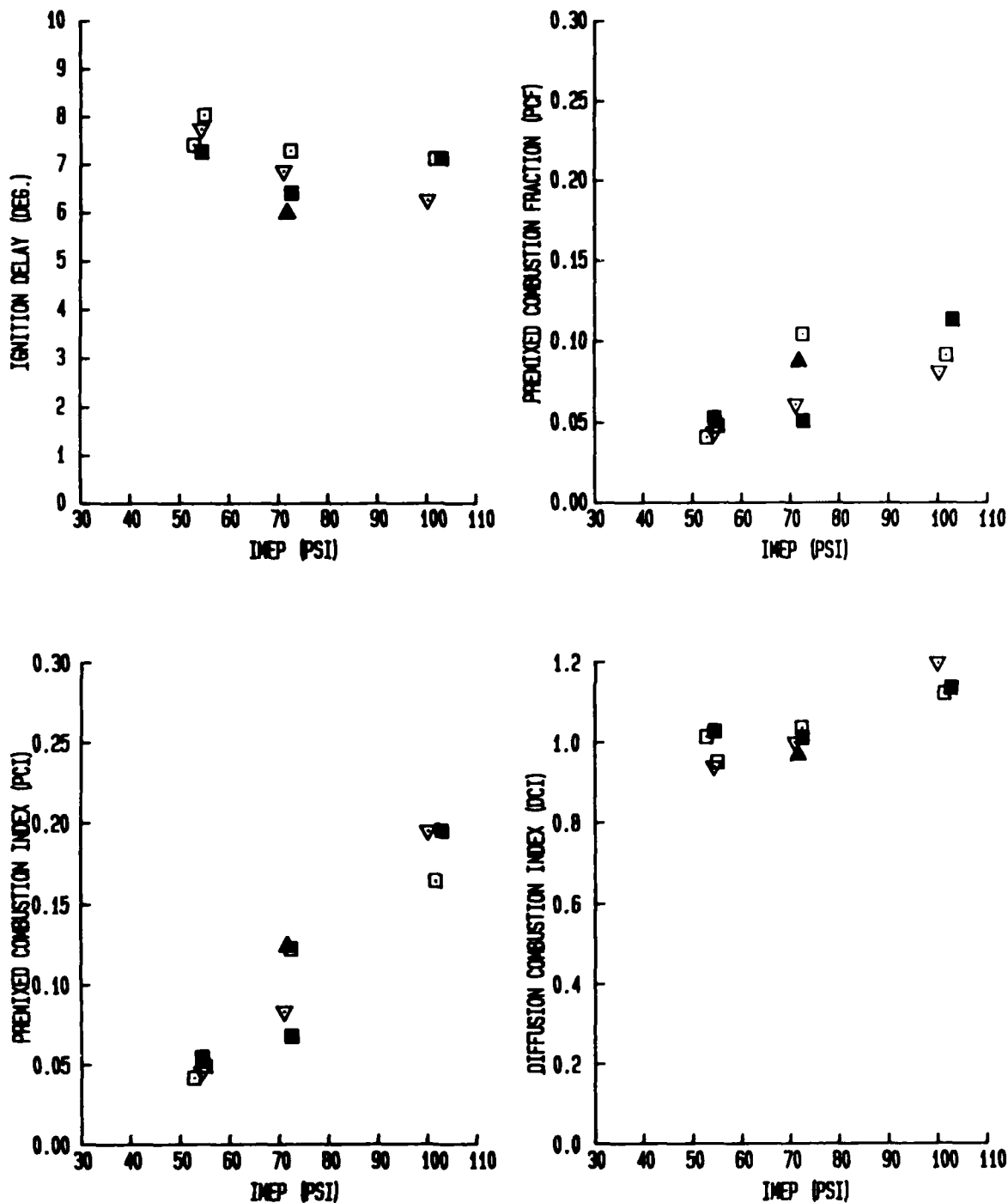


FIGURE 6-51      CETANE ENGINE      FUEL : DOE - 4  
 COMBUSTION ANALYSIS PARAMETERS

□ - OPTIMUM INJECTION TIMING

△ - RETARDED INJECTION TIMING

FILLED SYMBOLS = 2ND DAY DATA

▽ - RETEST DATA POINT

ENGINE SPEED = 1200 RPM

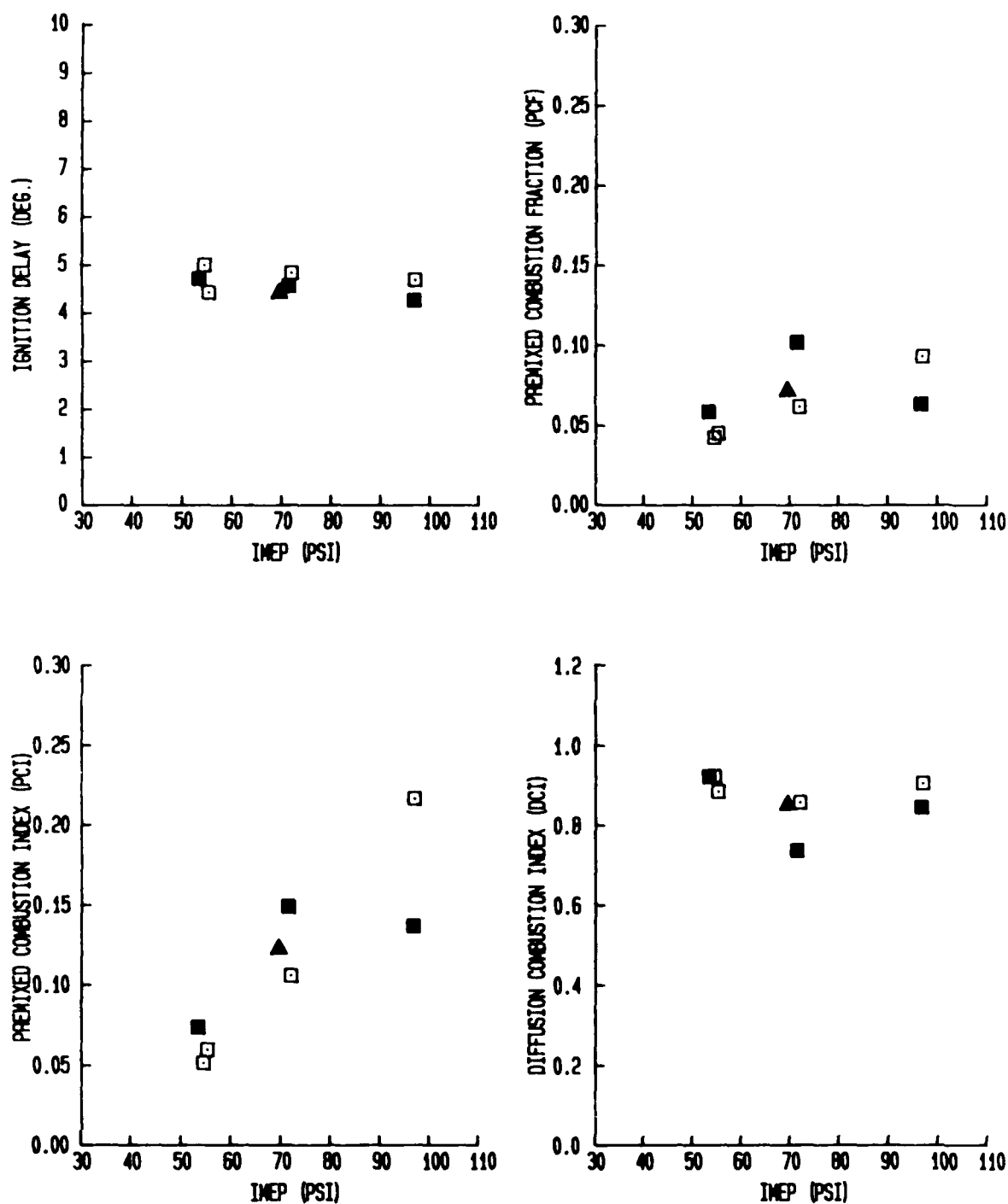


FIGURE 6-52

CETANE ENGINE

FUEL : CEC #1

COMBUSTION ANALYSIS PARAMETERS

□ - OPTIMUM INJECTION TIMING      △ - RETARDED INJECTION TIMING      FILLED SYMBOLS = 2ND DAY DATA  
 ▽ - RETEST DATA POINT      ENGINE SPEED = 1200 RPM

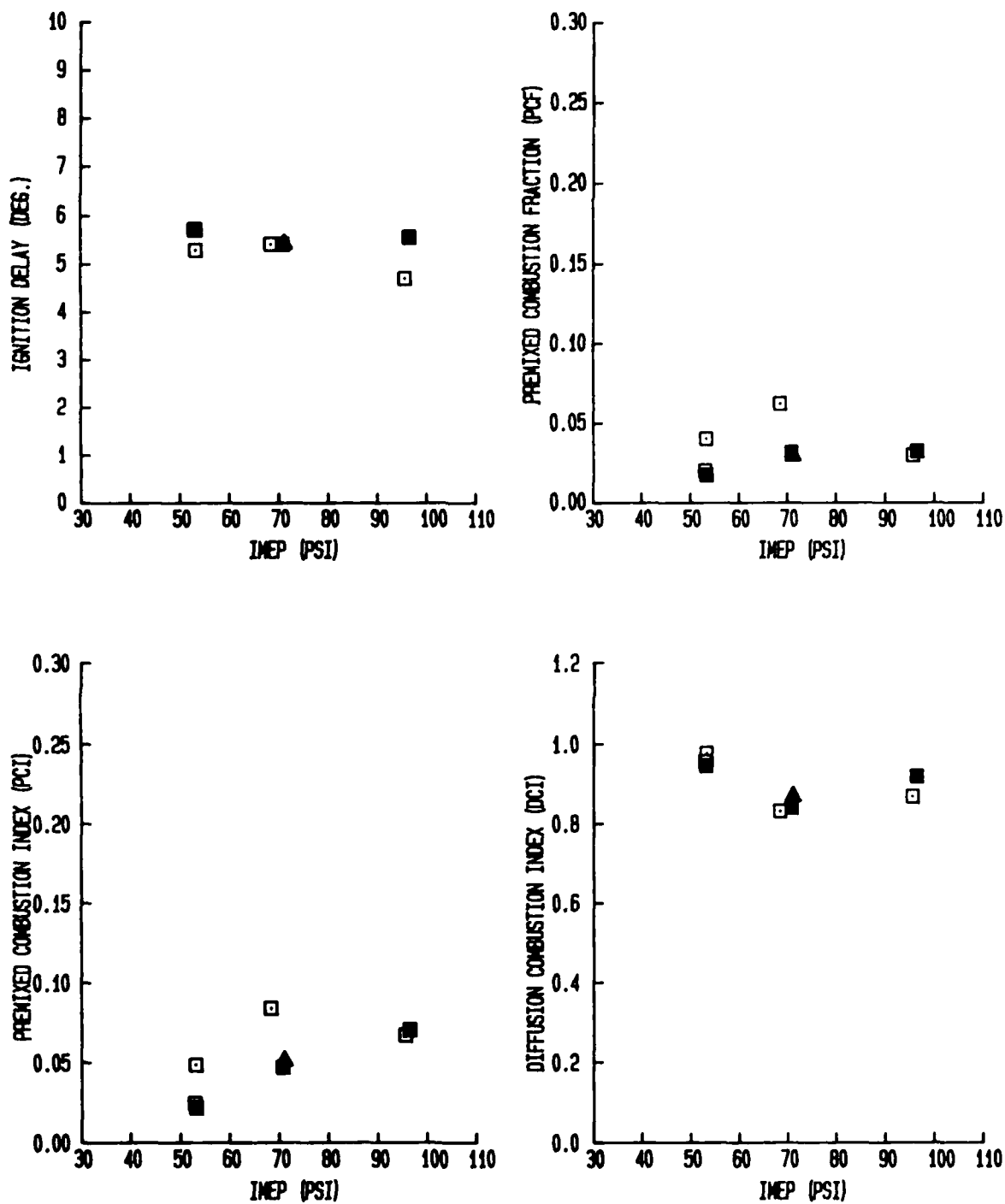


FIGURE 6-53      CETANE ENGINE      FUEL : CEC #2  
 COMBUSTION ANALYSIS PARAMETERS

□ - OPTIMUM INJECTION TIMING

△ - RETARDED INJECTION TIMING

▽ - RETEST DATA POINT

FILLED SYMBOLS = 2ND DAY DATA

ENGINE SPEED = 1200 RPM

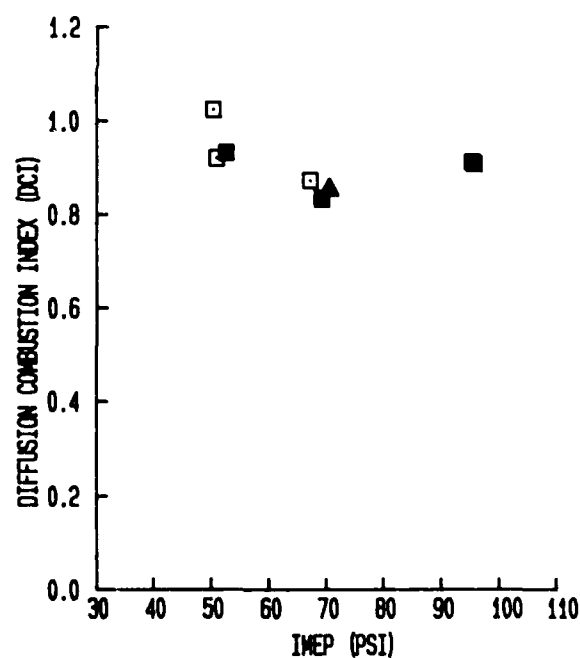
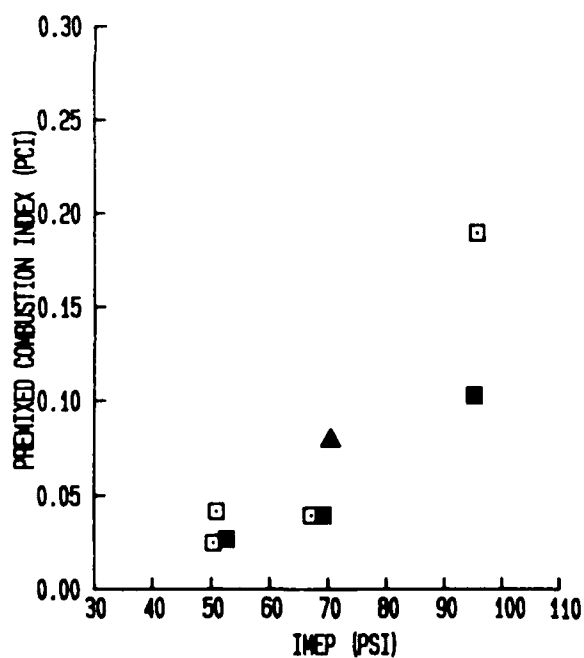
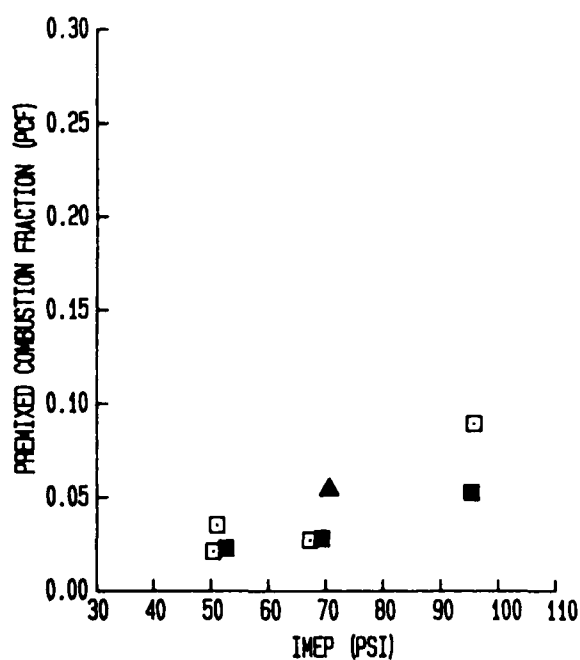
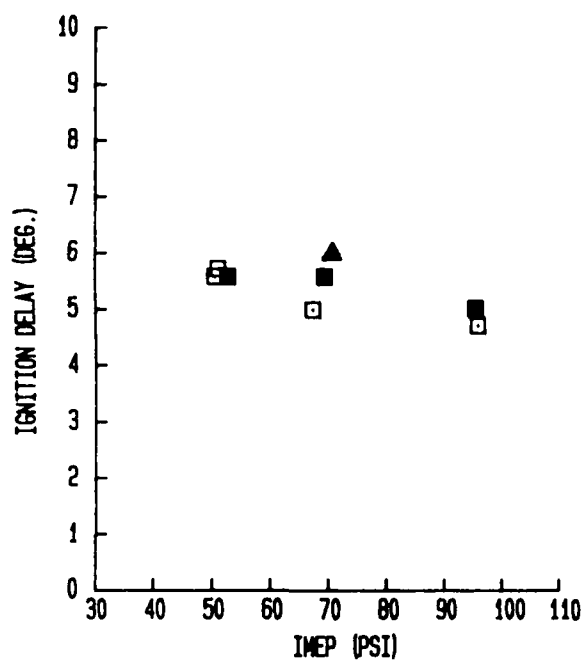


FIGURE 6-54

CETANE ENGINE

FUEL : CEC-2A

COMBUSTION ANALYSIS PARAMETERS



□ - OPTIMUM INJECTION TIMING

△ - RETARDED INJECTION TIMING

▽ - RETEST DATA POINT

FILLED SYMBOLS = 2ND DAY DATA

ENGINE SPEED = 1200 RPM

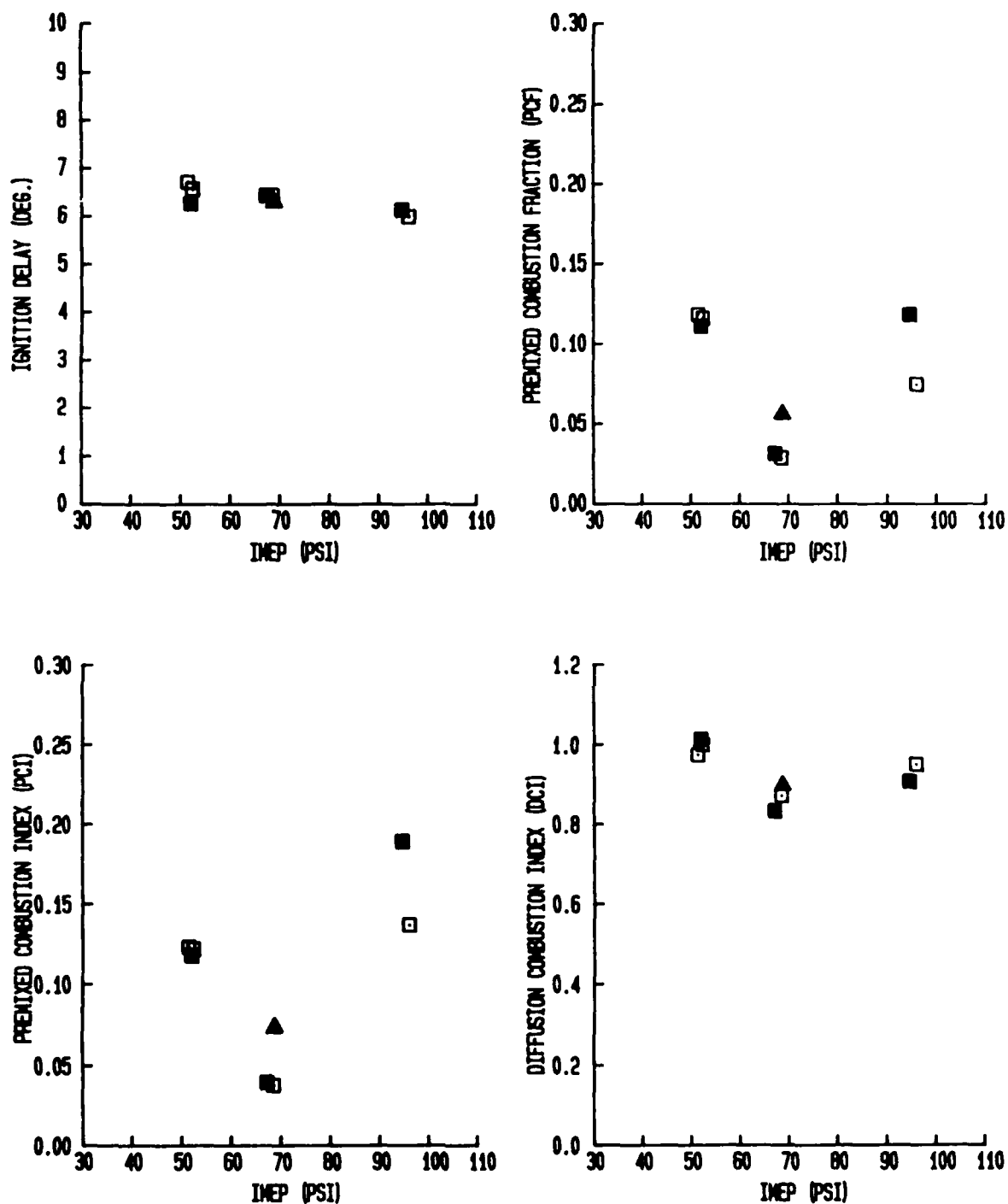


FIGURE 6-55

CETANE ENGINE

FUEL : CEC #3

COMBUSTION ANALYSIS PARAMETERS

□ - OPTIMUM INJECTION TIMING

△ - RETARDED INJECTION TIMING

FILLED SYMBOLS = 2ND DAY DATA

▽ - RETEST DATA POINT

ENGINE SPEED = 1200 RPM

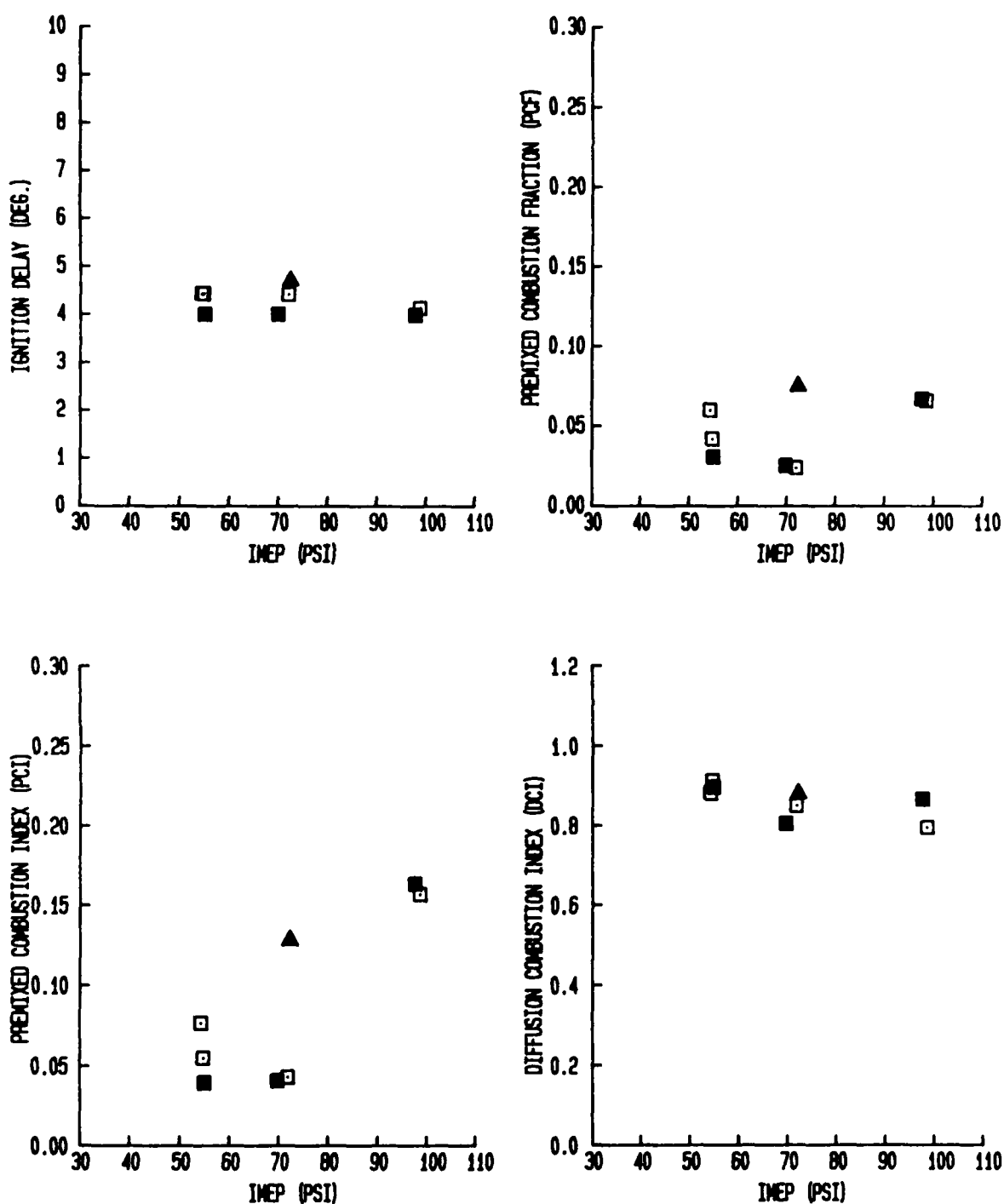


FIGURE 6-56

CETANE ENGINE

FUEL : CAPE #5

COMBUSTION ANALYSIS PARAMETERS

□ - OPTIMUM INJECTION TIMING

△ - RETARDED INJECTION TIMING

FILLED SYMBOLS = 2ND DAY DATA

▽ - RETEST DATA POINT

ENGINE SPEED = 1200 RPM

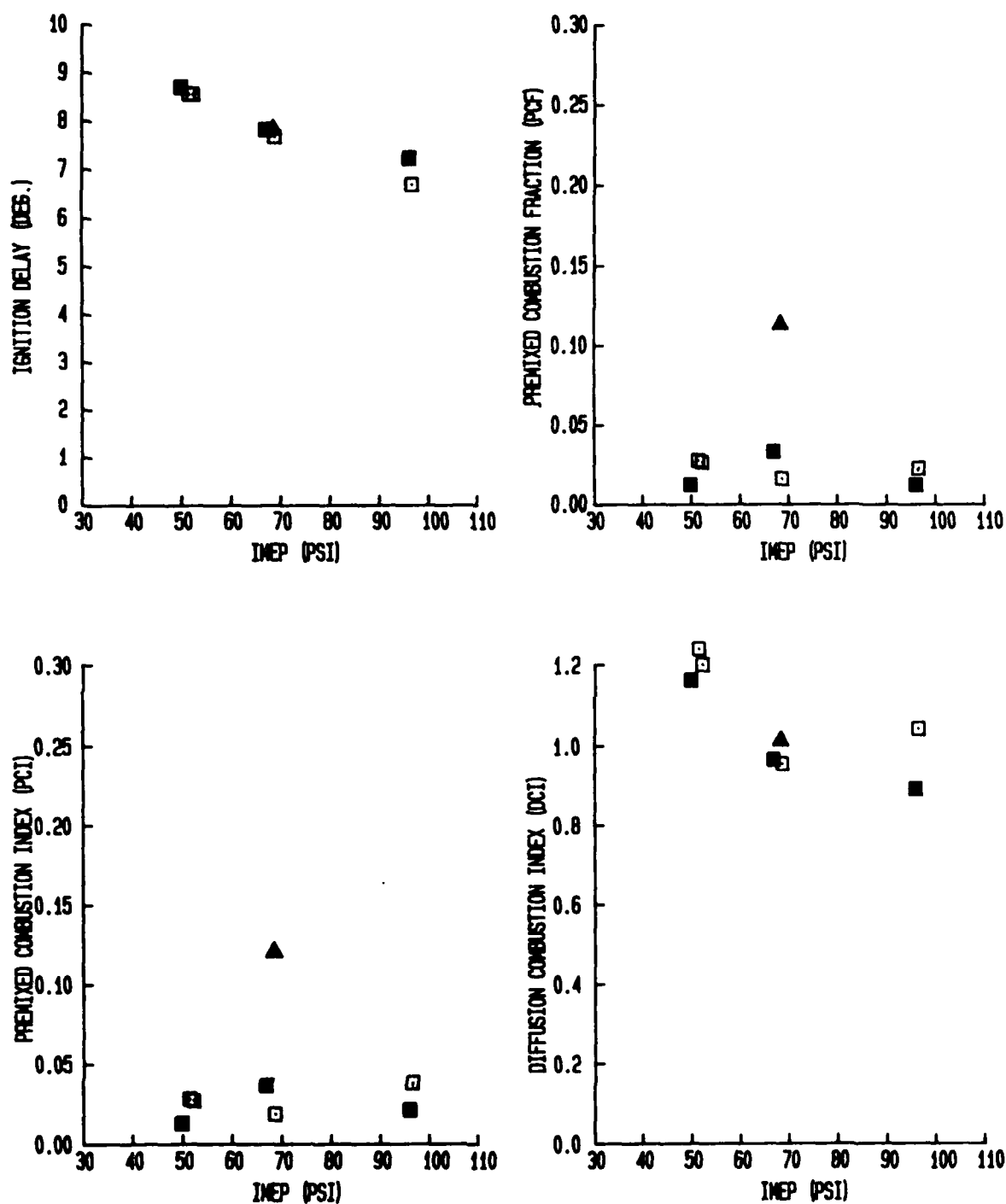


FIGURE 6-57

CETANE ENGINE

FUEL : CAPE #6

COMBUSTION ANALYSIS PARAMETERS

the lower grade mid-distillates DOE #2 and DOE #3 displayed increases in  $\text{ISNO}_x$  emissions of 10-20% and 20-30%, respectively. The increases were greater at light load for the DOE #3 fuel. Increases in  $\text{ISNO}_x$  emissions over the DOE #1 fuel were 30-50% for the broadcut DOE #4 fuel and the largest increases were at the light load conditions. For the CEC #1 fuel,  $\text{ISNO}_x$  emissions were comparable to those for DOE #1 at full load and approximately 20% higher at light load. The CEC #2 fuel behaved essentially the same as the CEC #1 fuel. Increases in  $\text{ISNO}_x$  emissions of 30 to 50% were observed for the CEC #2A fuel, with the greater increase at light load conditions. Since this fuel is CEC #3 fuel with ignition improver to bring the cetane rating up to that of the CEC #2 fuel, it was initially assumed that the ignition improver was responsible for the large  $\text{ISNO}_x$  increase. However, the CEC #3 fuel displayed essentially the same characteristics as the CEC #2A fuel, indicating that the composition of CEC #3 had more influence on the  $\text{ISNO}_x$  emissions than the presence of ignition improver. The CAPE #5 fuel is a high cetane fuel that behaved in a manner similar to CEC #1, about the same  $\text{ISNO}_x$  emissions at full load and 25% higher emissions at light load than the DOE #1 reference. The low quality CAPE #6 displayed increased  $\text{ISNO}_x$  emissions over the DOE #1 reference of 20 to 100%, with the greater increase at light load. Since optimum timing differences between all the fuels tested was only on the order of 2  $\text{CA}^\circ$ , the major change in the  $\text{ISNO}_x$  emissions is considered to be due to fuel differences.

Indicated specific fuel consumption  $\text{ISFC}$  was virtually the same for all the fuels tested except DOE #4. At light load the  $\text{ISFC}$  for DOE #4 was 5-6% higher than for DOE #1. At full load the  $\text{ISFC}$  values for both fuels were essentially the same. Virtually all the fuels exhibited the same  $\text{ISFC}$  at full load and a few exhibited very slight increases at lower loads. The  $\text{ISFC}$  for CAPE #6 was somewhat erratic due to poor operation of the engine; however, it was still about the same as that for the DOE #1 fuel.

There was a consistent tendency for the fuels considered to be of lower quality to demonstrate lower mass particulate emissions ( $\text{ISPart}$ ) than the DOE #1 reference. DOE #2 had approximately the same particulate emissions as the reference. DOE #3 had about the same particulate emissions as the reference at full load but lower at medium load. DOE #4, the broadcut fuel, was generally 50% lower in  $\text{ISPart}$  than the DOE #1 reference. CEC #1, considered a good quality fuel, had approximately the same  $\text{ISPart}$  as the DOE #1, although they were somewhat lower at medium load. The CEC #2 fuel was 20-50% lower in  $\text{ISPart}$  emissions than the reference. Interestingly enough, CEC #2A, the fuel with ignition improver, had mass particulate emissions comparable to the DOE #1 fuel. On the other hand, CEC #3, the fuel into which the ignition improver is blended to produce CEC #2A, demonstrated roughly 50% lower  $\text{ISPart}$  emissions than DOE #1. Mass particulate emissions from CAPE #5 were 20-30% lower than the reference while  $\text{ISPart}$  emissions from CAPE #6 were greater than 50% lower than the reference.

Specific hydrocarbon emissions ( $\text{ISHC}$ ) were somewhat variable, but most fuels demonstrated levels similar to the DOE #1 reference fuel.  $\text{ISHC}$  levels from DOE #4 were higher than from DOE #1, but not consistently. CEC #2 demonstrated  $\text{ISHC}$  levels 10-20% lower than those for the reference fuel while CAPE #6 demonstrated levels the same to slightly

higher. Generally, there were no major changes in the level of ISHC emissions that could be related to fuel changes.

Bosch Smoke readings for the fuels generally followed a pattern similar to ISPart, but not so pronounced. Several of the fuels had Bosch Smoke numbers similar to those for the DOE #1 reference fuel. Bosch readings for DOE #3 were the same to lower than the reference at light load. Readings for DOE #4 were 30-50% lower than the reference. Bosch numbers for CEC #3 and CAPE #5 were slightly lower, and the numbers for CAPE #6 were significantly lower than the numbers for the reference fuel.

The following paragraphs briefly describe the comparative effects of the fuels tested on the directly observable combustion parameters. Reference was made to figures 6-38 through 6-47 in the preparation of these comments.

The combustion period in CA° demonstrated some sensitivity to fuel changes. DOE #2, DOE #3, CEC #1, and CAPE #5 fuels exhibited approximately the same combustion period as the DOE #1 reference. CEC #2 demonstrated a slightly shorter combustion period, particularly at full load. Except for CAPE #6, the remaining fuels exhibited a 10-20% shorter combustion period than the reference. CAPE #6 produced 25-30% shorter combustion periods than the reference. Generally, the poorer quality fuels appeared to produce a shorter combustion period.

The rate of pressure rise of the pre-chamber pressure demonstrated fuel dependent characteristics. Generally, decreasing fuel quality led to increased rates of pressure rise. The effect was most pronounced for the DOE #4 and CAPE #6 fuels which caused increases in the rate of pressure rise of from 10 to 100% over that for the DOE #1 reference. The larger increases were at light load conditions. Most of the other fuels had rates of pressure rise that were the same to slightly higher than the reference. The increased rates were primarily at light load conditions. The CEC #3 fuel had a pressure rise rate that was from 5% to 30% higher than that for DOE #1.

The peak combustion pressure behaved in a manner similar to the rate of pressure rise for the fuels tested, although the effects were not as pronounced. Those fuels assumed to be of lower quality demonstrated somewhat higher peak combustion pressures than the DOE #1 fuel. Specifically, The DOE #4 and CAPE #6 fuels exhibited increases of 5% to 20% over the peak pressure for the reference fuel.

As might be anticipated, changes in the fuel had virtually no effect on the estimated bulk gas temperature at SOI (Start of Injection). The gas temperature should be primarily a function of the gas properties and the compression process. These results verify this characteristic.

The fuel effects on computed combustion parameters are discussed in the following paragraphs. The discussion is based on information in figures 6-48 through 6-57.

Ignition delay is one variable that is very sensitive to changes in fuel characteristics. Fuels considered to be of lower quality demon-

strated definite increases in ignition delay. The amount of increase was generally in proportion to loss of fuel quality from the reference DOE #1. DOE #4 and CAPE #6 fuels demonstrated the greatest increases in ignition delay over the DOE #1 fuel. The increases ranged from 10-75% for DOE #4 to 50-80% for CAPE #6. CEC #1 had approximately the same ignition delay as the reference and CAPE #5 exhibited a 10-20% decrease in ignition delay. The remainder of the fuels produced ignition delay increases of 10-30% over the DOE #1 reference.

The questionable accuracy of the pre-mixed combustion fraction (PCF) and pre-mixed combustion index (PCI) was discussed in the preceding section dealing with test condition and load effects. The same problem is present in determining fuel effects on these variables. For most of the fuels, the PCF and the PCI have about the same value as they do for the DOE #1 fuel. CEC #2 and CEC #2A demonstrated reduced values for the PCF of 10-50%, and the PCF for CAPE #6 increased from 50-100%, except at retarded injection timing. Compared to the values for DOE #1, the PCI for DOE #4 was 10-20% lower, about 50% lower for CEC #2, and increased by 100-300% for CAPE #6.

Only two fuels demonstrated any sensitivity to the diffusion combustion index (DCI). Compared to the values for DOE #1, the DCI for DOE #4 was 10-20% higher and approximately the same to 10% higher for CAPE #6.

#### 6.4.3 Statistical Relationships

Although not initially planned as part of this program, some statistical analysis of the data to correlate emissions, performance, and combustion variables to fuel properties was undertaken. The analysis is abbreviated and focused to show any simple linear relationship between the independent fuel properties and dependent variables such as emissions, performance, and combustion characteristics.

The analyses presented were performed using SAS\* software for the IBM personal computer. The package used included the optional statistical routines used for regression analysis.

The approach used in preparing the analyses was direct and relatively simple. Each distinctly unique test condition was assumed to be representative of a single population with fuel properties as independent variables and emissions, performance, and combustion characteristics as dependent variables. A correlation matrix for the independent variables was prepared in order to identify variables that were highly correlated so that correlated variables would not be used in the regression analysis. The four distinct test conditions were:

1. Full load, optimum injection timing
2. Half load, optimum injection timing
3. Half load, retarded injection timing
4. Light load, optimum injection timing

\* SAS Language, Version 6, SAS Institute, Inc., Box 8000, Cary, NC 27511

Review of the fuel properties table in section 6.1 indicates that several of the properties were not determined for all fuels. In order to make this statistical analysis more useful, 9 properties, that had been determined for all fuels, were selected as the independent variables. They were:

- |                                  |                           |
|----------------------------------|---------------------------|
| 1. Gravity, in °API              | 6. Saturates, in volume % |
| 2. 10% distillation point, in °F | 7. Olefins, in volume %   |
| 3. 90% distillation point, in °F | 8. Aromatics, in volume % |
| 4. Cetane number                 | 9. Sulfur, in mass %      |
| 5. Viscosity, in cSt @ 40°C      |                           |

Table 6-2 is the matrix of correlation coefficients for these 9 fuel properties. The first number at each matrix intersection is the correlation or Pearson coefficient. The second number is the significance probability under the null hypothesis that the correlation is zero. (The probability that the correlation coefficient is zero even though a value is computed.). The third number is the number of samples from which the correlations were determined. In this case, the properties for 10 different fuels were used in the determinations. Viscosity is shown in this correlation matrix. However, since only 8 values of viscosity were available, this property was not used in any of the following analyses.

In examining table 6-2 for correlations between fuel properties, correlation coefficients larger than 0.80 and significance probabilities of less than 0.01 were used as indicators that there was some reasonable correlation between the variables. For example: Viscosity and 10% point are well correlated with a coefficient of 0.925 and a significance probability of 0.001; Sulfur and 10% point are poorly correlated with a coefficient of 0.59773 and a significance probability of 0.068; and API Gravity and Cetane number are essentially uncorrelated with a coefficient of 0.09425 and a significance probability of 0.7956.

The statistical analysis of the relationship between dependent and independent variables was performed only for data from the cetane engine program. Seventeen dependent variables were chosen for analysis. They were:

- |  |   |
|--|---|
| 1. Ignition Delay                      | 10. Specific NO <sub>x</sub> (ISNO <sub>x</sub> ) |
| 2. Combustion Angle                    | 11. Mass Particulates (ISPart)                    |
| 3. Peak Cylinder Pressure              | 12. Bosch Smoke                                   |
| 4. Maximum dP/dθ                       | 13. Indicated Efficiency                          |
| 5. Pre-mixed Combustion Fraction (PCF) | 14. HC Emissions Index                            |
| 6. Pre-mixed Combustion Index (PCI)    | 15. CO Emissions Index                            |
| 7. Diffusion Combustion Index (DCI)    | 16. NO <sub>x</sub> Emissions Index               |
| 8. Specific Hydrocarbons (ISHC)        | 17. Particulate Emissions Index                   |
| 9. Specific Carbon Monoxide (ISCO)     |   |

A correlation matrix was prepared for these 17 variables for each of the four separate test conditions to determine if there were any unexpected relationships between dependent variables before a linear regression analysis was performed. The results are not included because no unexpected correlations were identified and the volume of material was substantial.

Table 6-2

Correlation Coefficients for Fuel Properties Used as Independent Variables

Correlation Coefficients / Prob >  R  under Ho: Rho=0 / Number of Observations									
	GRAVITY	_10_PCT	_90_PCT	CETANE	VISCOSTY	SAT	OLEF	AROM	SULFUR
GRAVITY	1.00000	-0.84441	-0.81705	0.09425	-0.84444	0.75466	-0.24806	-0.76094	-0.80488
	0.0000	0.0021	0.0039	0.7956	0.0083	0.0116	0.4895	0.0106	0.0050
	10	10	10	10	8	10	10	10	10
_10_PCT	-0.84441	1.00000	0.75786	0.33585	0.92500	-0.36741	0.26931	0.36123	0.59773
	0.0021	0.0000	0.0111	0.3427	0.0010	0.2963	0.4518	0.3051	0.0680
	10	10	10	10	8	10	10	10	10
_90_PCT	-0.81705	0.75786	1.00000	0.12111	0.80285	-0.66066	0.41526	0.65372	0.70967
	0.0039	0.0111	0.0000	0.7389	0.0164	0.0376	0.2327	0.0403	0.0215
	10	10	10	10	8	10	10	10	10
CETANE	0.09425	0.33585	0.12111	1.00000	0.32250	0.27124	0.57294	-0.31520	-0.26466
	0.7956	0.3427	0.7389	0.0000	0.4359	0.4484	0.0834	0.3750	0.4599
	10	10	10	10	8	10	10	10	10
VISCOSTY	-0.84444	0.92500	0.80285	0.32250	1.00000	-0.43617	0.43529	0.42908	0.53071
	0.0083	0.0010	0.0164	0.4359	0.0000	0.2800	0.2811	0.2888	0.1760
	8	8	8	8	8	8	8	8	8
SAT	0.75466	-0.36741	-0.66066	0.27124	-0.43617	1.00000	-0.47985	-0.99844	-0.70158
	0.0116	0.2963	0.0376	0.4484	0.2800	0.0000	0.1605	0.0001	0.0237
	10	10	10	10	8	10	10	10	10
OLEF	-0.24806	0.26931	0.41526	0.57294	0.43529	-0.47985	1.00000	0.43007	-0.03272
	0.4895	0.4518	0.2327	0.0834	0.2811	0.1605	0.0000	0.2148	0.9285
	10	10	10	10	8	10	10	10	10
AROM	-0.76094	0.36123	0.65372	0.31520	0.42908	-0.99844	0.43007	1.00000	0.72436
	0.0106	0.3051	0.0403	0.3750	0.2888	0.0001	0.2148	0.0000	0.0178
	10	10	10	10	8	10	10	10	10
SULFUR	-0.80488	0.59773	0.70967	0.26466	0.53071	-0.70158	-0.03272	0.72436	1.00000
	0.0050	0.0680	0.0215	0.4599	0.1760	0.0237	0.9285	0.0178	0.0000
	10	10	10	10	8	10	10	10	10



Each of the dependent variables was assumed to be related to the independent variable by a relationship of the form:

$$Y = a_0 + a_1X_1 + a_2X_2 + \dots + a_nX_n + e \quad (6.1)$$

where:  $Y$  = dependent variable  
 $a_0$  = straight line intercept  
 $X_1 \dots X_n$  = independent variables  
 $a_1 \dots a_n$  = linear regression coefficients for the independent variables  $X_1 \dots X_n$   
 $e$  = error residual

The correlation information for the independent variables was used in selecting which independent variables would be used in the regression analysis of each dependent variable. The correlation information for the dependent variables was used to reduce the number of regressions performed. Strong correlations between PCF and PCI and between ISCO and the CO emissions index were used to justify removing PCI and the CO emissions index from the dependent variable list. The regression for each of the remaining dependent variables was repeated several times in order to eliminate independent variables that did not have a statistically significant effect. The student's t test and the variance inflation factor provided by the SAS analysis software were used in this elimination process. The results of the regression analyses are shown in tables 6-3 through 6-6 for each of the four test conditions. Blanks in the tables indicate these independent variables were eliminated because they did not make a statistically significant contribution in calculating the value of the given dependent variable.

In the following descriptive paragraphs, percentages used in describing the contributions of independent variables were estimated using the nominal value of the dependent variable and the approximate change in this variable calculated using the correlation coefficient and the values of the independent variable. Thus, even though the coefficients have not been normalized, the contributions of the independent variables are described in comparable terms as a percentage change in the dependent variable.

For all four test conditions the ignition delay was a strong function of the cetane number of the fuel. For full and medium loads at optimum timing, cetane number was the only significant descriptor of ignition delay. At medium load, retarded injection timing, and light load, optimum injection timing, 10% and 90% distillation points also contributed to ignition delay; however, cetane number demonstrated the highest level of confidence in describing ignition delay.

The combustion period was also strongly related to the cetane number for all four test conditions. Only at full load, optimum injection timing conditions did another independent variable contribute measurably. The variable was aromatics content, and the contribution was on the order of 10-20% of that from the cetane number.

The cetane number was also a strong indicator of peak cylinder pressure for all test conditions, with the regression coefficients showing a high level of confidence. For medium load with retarded

Table 6-3

Linear Regression Results for Cetane Engine, Full Load Optimum Injection Timing

Independent Variable		CETANE NUMBER			AROMATICS (V%)			10% POINT (°F)			90% POINT (°F)		
Dependent Variable	INTERCEPT	coef.	t for $H_0$	prob $> t $	coef.	t for $H_0$	prob $> t $	coef.	t for $H_0$	prob $> t $	coef.	t for $H_0$	prob $> t $
Ignition Delay	5.300	-0.1476	-7.79	0.0001									
Combustion Period	19.002	0.1428	4.63	0.0001	-0.0451	-3.74	0.0012						
Peak Cyl. Pres.	801.13	-4.053	-5.12	0.0001									
Peak Pres. Rate	35.253				0.3238	4.57	0.0002				-0.0959	-3.84	0.0010
PCF	0.0785				-0.0007	-1.71	0.1015						
DCI	0.9305	-0.0089	-4.98	0.0001							-0.0014	-5.72	0.0001
ISHC	0.3147				-0.0019	-3.03	0.0063	-0.0003	-2.31	0.0312			
ISCO	2.384							0.0028	1.99	0.0596			
ISNO <sub>x</sub>	2.990	-0.0358	-4.49	0.0002	0.0096	3.03	0.0066	-0.0018	-2.83	0.0105			
ISPart	1.254	0.0259	2.34	0.0294							0.0042	2.73	0.0126
Bosch Smoke No.	4.813	0.0690	4.39	0.0002	0.0183	2.97	0.0073						
Indicated Eff.	39.942	-0.0378	-9.66	0.3301									
HC Emission Index	1.987				-0.0131	-3.74	0.0012	-0.0017	-2.60	0.0169			
NO <sub>x</sub> Emission Index	18.887	-0.2625	-5.155	0.0001	0.0413	2.04	0.0545	-0.0094	-2.38	0.0277			
Particulate Emission Index	7.978	0.1591	2.39	0.0262							0.0257	2.80	0.0107

Table 6-4

Linear Regression Results for Cetane Engine, Medium Load Optimum Injection Timing

Independent Variable		CETANE NUMBER			AROMATICS (V%)			10% POINT (°F)			90% POINT (°F)		
Dependent Variable	INTERCEPT	coef.	t for $H_0$	prob $> t $	coef.	t for $H_0$	prob $> t $	coef.	t for $H_0$	prob $> t $	coef.	t for $H_0$	prob $> t $
Ignition Delay	5.726	-.1621	-10.2	0.0001									
Combustion Period	16.71	0.1709	5.12	0.0001									
Peak Cyl. Pres.	785.03	-4.204	-6.13	0.0001									
Peak Pres. Rate	37.73	-.6844	-2.79	0.0121	0.2463	2.54	0.0206						
PCF	0.0534				-.0007	-1.89	0.0746						
DCI	0.8740	-.0074	-4.48	0.0003							-.0009	-3.57	0.0022
ISHC	0.3579				-.0014	-1.36	0.1912						
ISCO	2.261	0.0241	2.74	0.0134				0.0010	1.43	0.1713			
ISNO <sub>x</sub>	4.502	-.1092	-5.22	0.0001									
ISPart	0.6735	0.0339	4.73	0.0002				0.0030	3.36	0.0037	-.0048	-2.95	0.0090
Bosch Smoke No.	2.993	0.1189	6.68	0.0001									
Indicated Eff.	43.519	-.1759	-2.255	0.0368				0.0156	2.50	0.0221			
HC Emission Index	2.457				-.0085	-1.23	0.2355						
NO <sub>x</sub> Emission Index	30.986	-.8275	-5.56	0.0001									
Particulate Emission Index	4.621	0.2256	4.67	0.0002				0.0216	3.63	0.0021	-.0346	-3.18	0.0055

Table 6-5

Linear Regression Results for Cetane Engine, Medium Load Retarded Injection Timing

Independent Variable		CETANE NUMBER			AROMATICS (V%)			10% POINT (°F)			90% POINT (°F)		
Dependent Variable	INTERCEPT	coef.	t for $H_0$	prob > t	coef.	t for $H_0$	prob > t	coef.	t for $H_0$	prob > t	coef.	t for $H_0$	prob > t
Ignition Delay	5.808	-0.1556	-5.15	0.0013				0.0093	2.54	0.0384	-0.0150	-2.23	0.0614
Combustion Period	16.005	0.1102	3.56	0.0061									
Peak Cyl. Pres.	655.43	-4.367	-5.60	0.0005							0.2412	2.32	0.0491
Peak Pres. Rate	17.052	-0.7317	-3.42	0.0077									
PCF	0.07455												
DCI	0.94136	-0.0060	-1.92	0.0913	-0.0018	-1.48	0.1771	0.0002	1.36	0.2115	-0.0005	-1.53	0.1644
ISHC	0.52836				-0.0055	-2.60	0.0316	0.0016	-4.37	0.0024			
ISCO	2.788							0.0071	1.90	0.0950	-0.0160	-2.14	0.0650
ISNO <sub>x</sub>	3.084	-0.0853	-5.98	0.0003	0.0139	2.56	0.0336						
ISPart	1.491	0.0592	2.24	0.0520									
Bosch Smoke No.	3.875	0.1123	3.22	0.0105									
Indicated Eff.	42.455				0.0107	4.39	0.0017						
HC Emission Index	3.53				-0.0370	-2.61	0.0313	-0.0099	-3.98	0.0040			
NO <sub>x</sub> Emission Index	20.729	-0.5547	-5.43	0.0006	0.1034	2.66	0.0289						
Particulate Emission Index	10.060	0.4091	2.28	0.0483									

Table 6-6

Linear Regression Results for Cetane Engine, Light Load Optimum Injection Timing

Independent Variable		CETANE NUMBER			AROMATICS (V%)			10% POINT (°F)			90% POINT (°F)		
Dependent Variable	INTERCEPT	coef.	t for $H_0$	prob $> t $	coef.	t for $H_0$	prob $> t $	coef.	t for $H_0$	prob $> t $	coef.	t for $H_0$	prob $> t $
Ignition Delay	6.093	-0.2094	-16.59	0.0001				0.0038	2.50	0.0186	-0.0079	-2.78	0.0096
Combustion Period	14.815	0.1732	7.73	0.0001									
Peak Cyl. Pres.	773.93	-4.904	-9.11	0.0001	-0.5498	-2.62	0.0138						
Peak Pres. Rate	40.895	-1.258	-5.27	0.0001									
PCF	0.0588										0.0002	1.39	0.1748
DCI	0.9821	-0.0132	-8.90	0.0001				0.0008	4.32	0.0002	-0.0007	-2.07	0.0479
ISHC	0.4463	-0.0085	-3.80	0.0007	-0.0024	-2.75	0.0101						
ISCO	3.159				-0.0493	-3.98	0.0004	0.0024	2.62	0.0138			
ISNO <sub>x</sub>	5.227	-0.1062	-6.16	0.0001									
Bosch Smoke No.	1.685	0.0504	4.16	0.0002									
Indicated Eff.	44.044							0.0117	2.48	0.0189			
HC Emission Index	3.096	-0.0549	-3.69	0.0009	-0.0156	-2.68	0.0119						
NO <sub>x</sub> Emission Index	36.294	-0.7012	-6.29	0.0001									

injection timing, 90% point also contributed to peak cylinder pressure on the order of 30-40%. For light load and optimum injection timing, aromatics content contributed to peak cylinder pressure on the order of 5%. In both cases the confidence level for the cetane number regression coefficient was at least two orders of magnitude higher than that for the 90% point or the aromatics content.

Interestingly enough, the peak pressure rate was not as strong a function of the cetane number as the peak cylinder pressure. At full load and optimum injection timing conditions the peak pressure rate was a function of aromatics and 90% point with virtually no contribution from cetane number. For medium and light loads, however, cetane number was the major descriptor for peak pressure rate. Aromatics content also contributed to the peak pressure rate for medium and light load test conditions with optimum injection timing. For the medium load retarded injection timing case, cetane number was the only important variable. These results are useful in that they lend substance to the theory that cetane number or fuel combustion quality is more critical for medium and light load operation than it is for full load operation.

The Pre-mixed Combustion Fraction (PCF) did not demonstrate a strong sensitivity to any of the independent fuel variables used in the analysis. For full load and medium load with optimum injection timing, the fuel aromatic content was identified by regression analysis as a possible descriptor for PCF. For medium load with retarded injection timing, the independent variables identified were 10% and 90% points, while for light load and optimum timing, 90% point was identified. For all cases, the confidence of the accuracy of the coefficient determined was low, particularly compared to confidence levels demonstrated for some of the dependent variables examined up to this point. Thus, even though linear regression coefficients have been determined, the relationship between the independent variables involved and the dependent variable being examined was not strong.

Diffusion Combustion Index (DCI), on the other hand, showed a strong relationship to cetane number. Cetane number was one of the variables identified for all four test cases with a high degree of confidence. Other variables also contributed significantly, but at different test conditions. 90% point was identified as a contributing variable for all conditions except retarded injection timing at medium load. For that case, aromatic content was identified as a contributing variable, although not at a very high confidence level. 10% point was identified as contributing at light load. The result points to cetane number as a major indicator of diffusion combustion; however, other fuel properties will also play a role of varying importance, depending on engine operating conditions.

Hydrocarbon emissions, as indicated by ISHC and HC Emission Index (gm/kg fuel), obviously depend on the aromatic content of the fuel. Fuel aromatics were the fuel property that influenced ISHC and HC emission index for all test conditions. The slopes represented by the regression coefficients were not large, nor always consistent in sign. Also, the confidence levels associated with the regression coefficients were not as high as for many of the coefficients determined. Cetane number and 10% point were also identified as contributing variables for

some of the test conditions. None of these variables, however, had a consistent effect on the ISHC and HC Emission Index for all test conditions.

ISCO emissions do not demonstrate a strong dependency on any of the independent fuel variables used in this analysis. Cetane number, aromatic content, 10% point, and 90% point could be related to the ISCO in different combinations at different test conditions.

The ISNO<sub>x</sub> and NO<sub>x</sub> Emission Index (gm/kg fuel) were both a strong function of cetane number for all test conditions. At full load aromatic content and 10% were also minor contributors to the two NO<sub>x</sub> terms. Aromatics content was also a minor contributor to NO<sub>x</sub> at the medium load retarded injection timing condition.

Cetane number was the major independent variable describing ISPart emissions and Particulate Emission Index (gm/kg fuel) for all test conditions for which particulate measurements were made. 10% and 90% points also contributed at different test conditions.

Cetane number was also the major independent variable describing Bosch Smoke Number for all test conditions. At full load conditions, fuel aromatic content also contributed.

Indicated Efficiency was not described well by any of the independent variables examined. Regression coefficients for cetane number and fuel aromatic content were determined in different combinations for different test conditions. None of the coefficients demonstrated high confidence factors in their determination.

## 6.5 Summary Graphical Results for Ricardo Engines

The data provided from Ricardo Consulting Engineers, combined with the DOE/Ricardo report, yielded four different fuels and four different operating conditions for each engine. Although this was not as much information as that developed for the cetane engine, it is still a substantial number of pages to examine and comprehend. Thus, summary graphical results, similar to those for the cetane engine, were prepared. In fact, the results were placed in a format as identical as possible to that for the cetane engine to aid in comparing results between engines.

The summary data are plotted using the same three separate pages for information - one for engine performance and emissions, a second for direct combustion parameters, and a third for computed combustion parameters. Since there were only four test conditions and four fuels, separate plots for each fuel were not prepared, and symbols were used to identify test results for each different fuel. A separate set of figures was prepared for each of the two Ricardo engines tested. The figures have been paired to facilitate comparison between the two engines. Figures 6-58, 6-60, and 6-62 are for the Ricardo IDI engine while figures 6-59, 6-61, and 6-63 are for the Ricardo DI engine. In some instances the scales of the plots shown on each figure have been changed from those for the cetane engine. This reflects significant changes in the range of the variables being examined. Whenever possible,

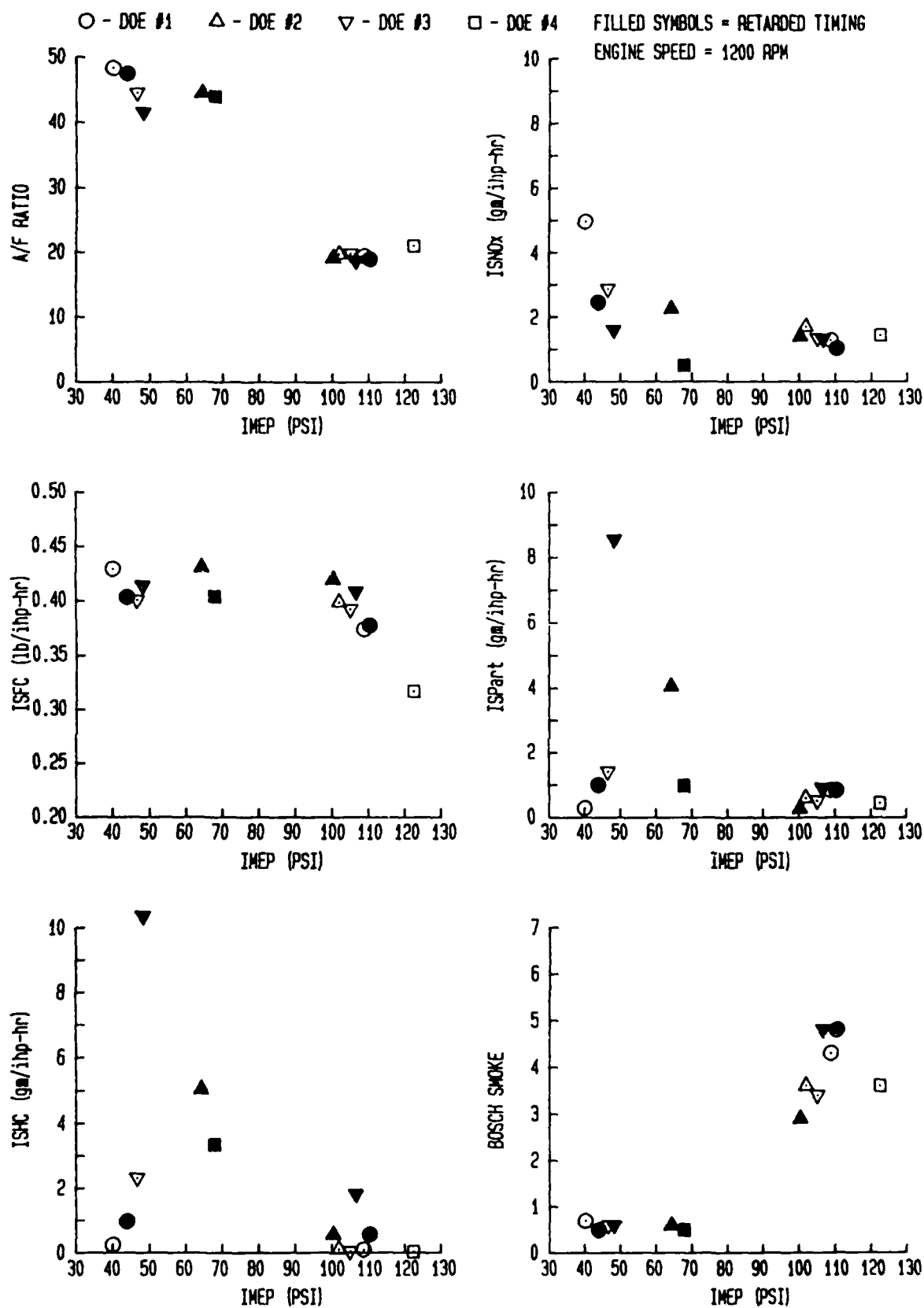


FIGURE 6-58 DOE/RICARDO IDI ENGINE FUELS: DOE #1 - #4  
EMISSIONS, FUEL CONSUMPTION, AND AIR/FUEL RATIO



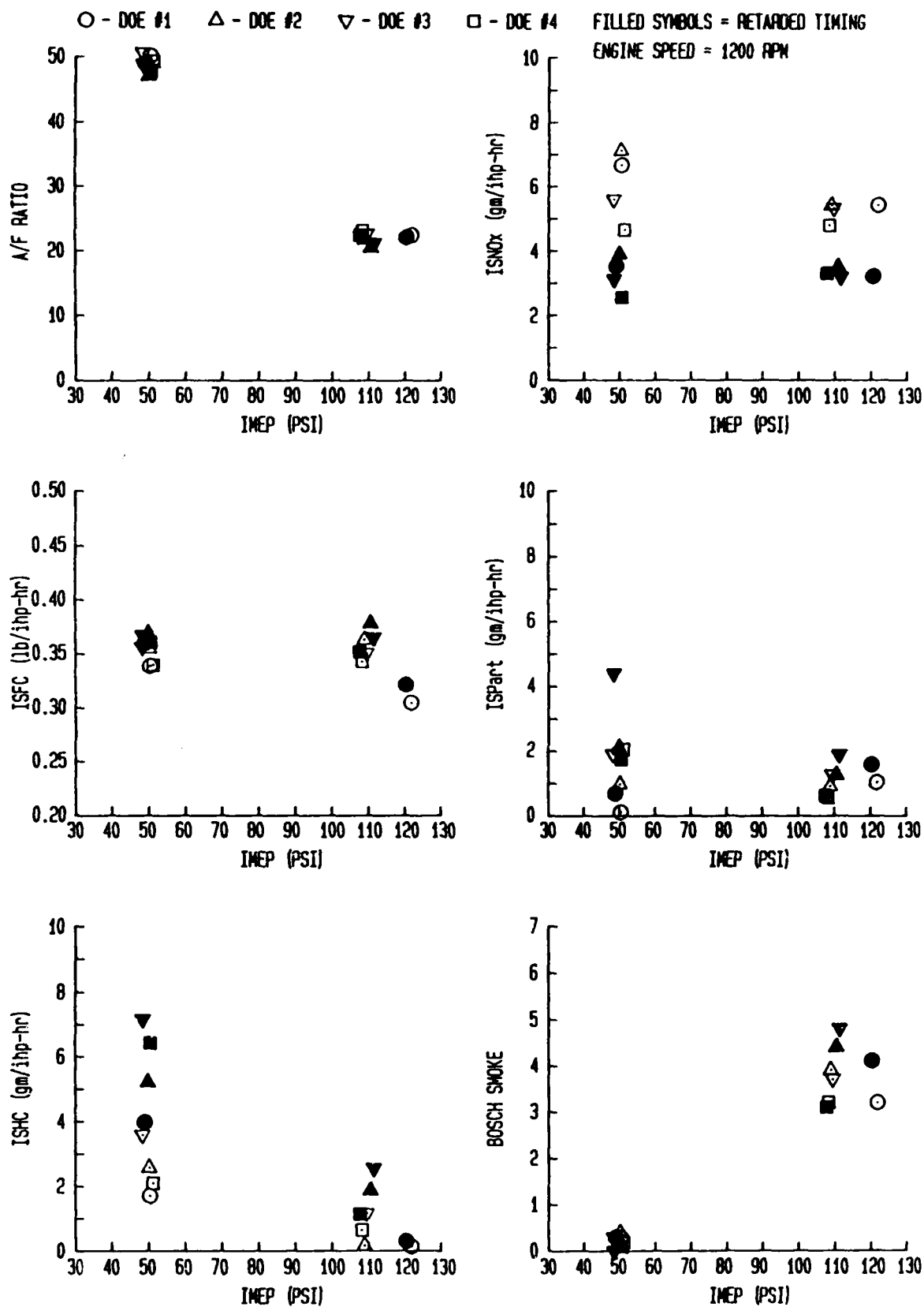


FIGURE 6-59 DOE/RICARDO DI ENGINE FUELS: DOE #1 - #4  
EMISSIONS, FUEL CONSUMPTION, AND AIR/FUEL RATIO

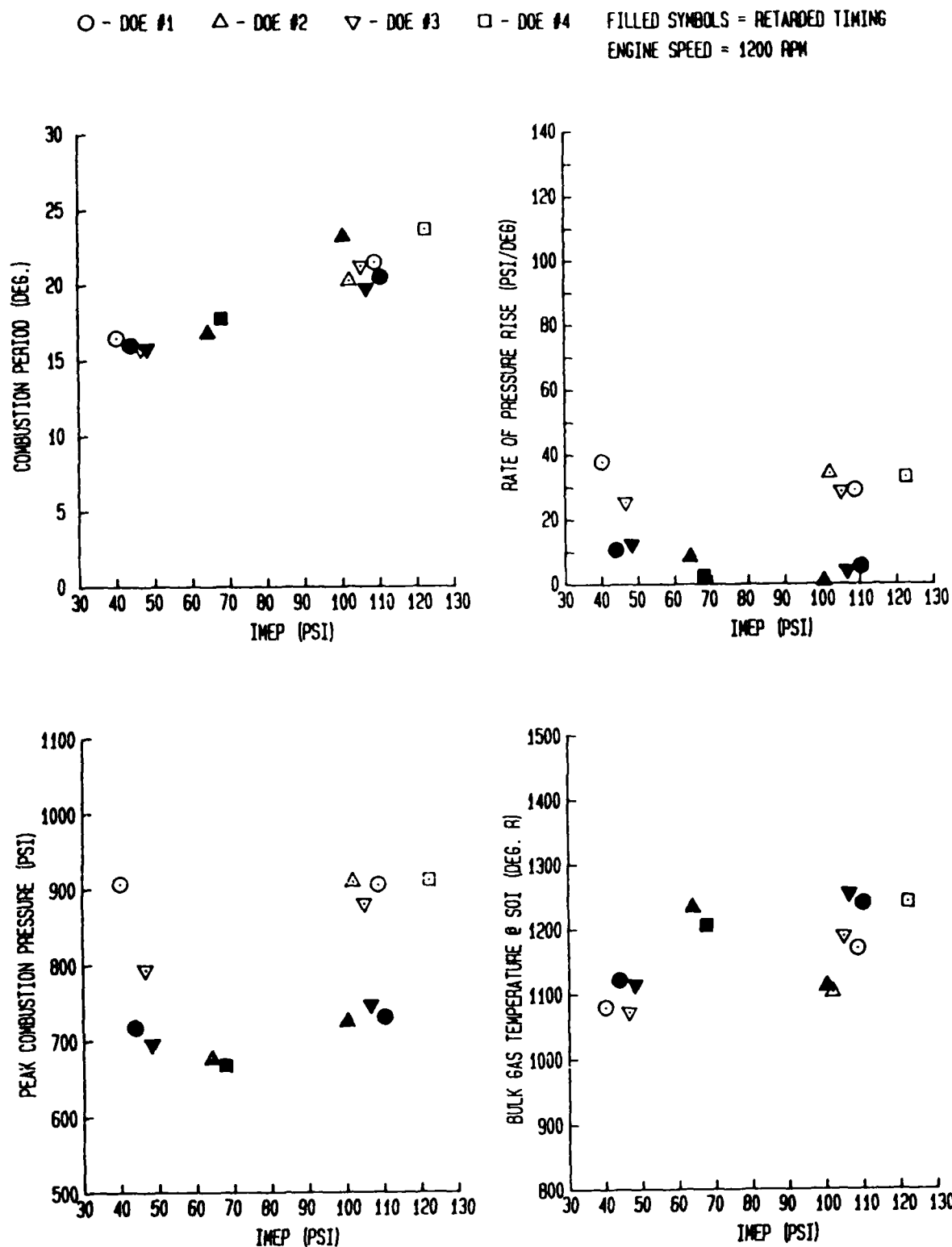


FIGURE 6-60 DOE/RICARDO IDI ENGINE FUELS: DOE #1 - #4  
COMBUSTION PARAMETERS

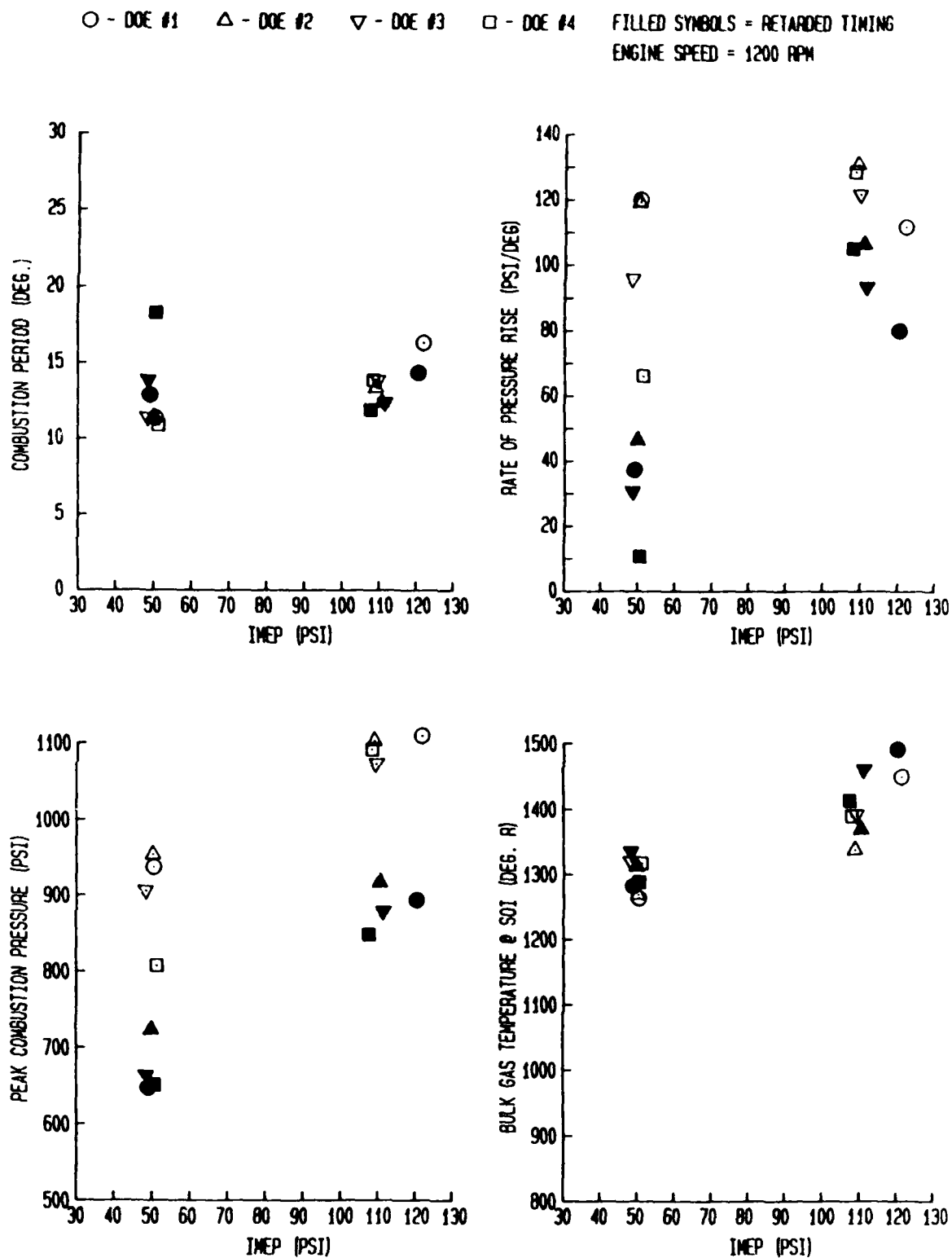


FIGURE 6-61 DOE/RICARDO DI ENGINE FUELS: DOE #1 - #4  
COMBUSTION PARAMETERS

○ - DOE #1    △ - DOE #2    ▽ - DOE #3    □ - DOE #4    FILLED SYMBOLS = RETARDED TIMING  
ENGINE SPEED = 1200 RPM

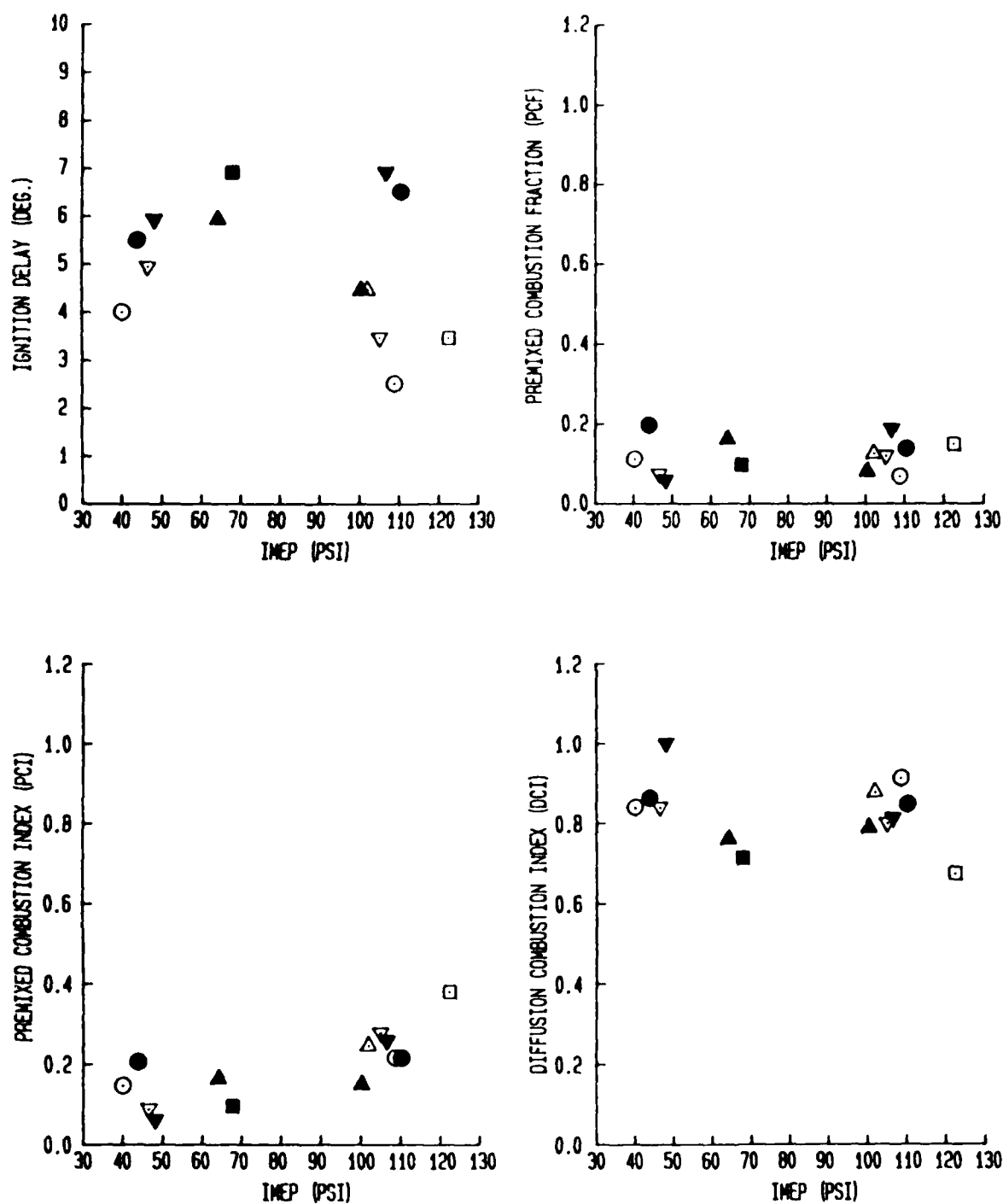


FIGURE 6-62 DOE/RICARDO IDI ENGINE FUELS: DOE #1 - #4  
COMBUSTION ANALYSIS PARAMETERS

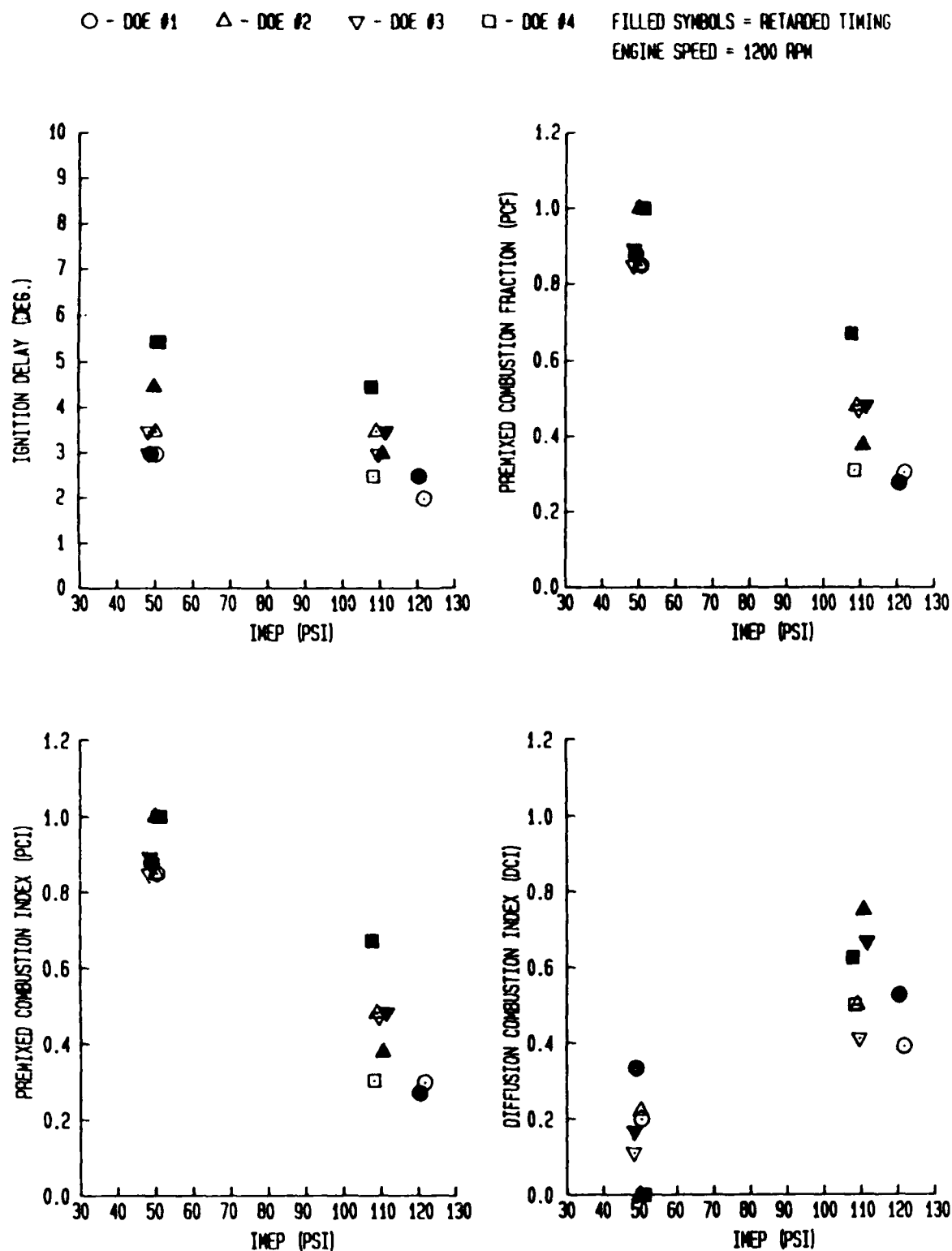


FIGURE 6-63 DOE/RICARDO DI ENGINE FUELS: DOE #1 - #4  
COMBUSTION ANALYSIS PARAMETERS

the variable ranges were not changed so that direct comparison of the Ricardo engine and cetane engine data would be more convenient.

#### 6.5.1 Test Condition and Engine Variable Effects, Ricardo Engines

The information used to prepare the following paragraphs is displayed in figures 6-58 through 6-63. These figures include data for both the IDI and the DI engine. In the discussion, effects that are general for both engines are described without specific mention of an engine. If an effect is specific to one engine, the engine is named.

The air-fuel ratio behaves as anticipated - decreasing with increasing imep. This result directly correlates with the fact that, at a given speed, diesel engine power is controlled almost entirely by fuel flow. Since air flow is virtually fixed with engine speed, air-fuel ratio must reflect changes in fuel flow or power output. There are two possible discrepancies for the IDI engine results at 70 and 125 imep. There may be some question concerning these imep values, which were determined from the area under the P-V data. However, since there is no reason to reject these points, they have been kept in the data set.

The ISNO<sub>x</sub> emissions showed similar trends for both engines. There was a slight tendency toward reduced ISNO<sub>x</sub> emissions at higher load for diesel type fuels. The broadcut fuel showed no change to a slight increase in ISNO<sub>x</sub> with increasing load. Retarded timing generally reduced ISNO<sub>x</sub> emissions for both engines.

There was a wide variation in data for indicated specific fuel consumption (ISFC), particularly for the IDI engine. A check of the imep computation from the area under the P-V data indicates that reasonable phasing errors do not account for the differences. The most probable error is the assumption that the bmep = 2 bar, as indicated in the DOE/Ricardo report. Since all the DOE/Ricardo data is reported on a brake specific basis, an accurate value for bmep is needed for conversion to imep. Trials with bmep = 3 bar for two questionable points in the area of 65-70 psi imep puts the ISFC at a level more comparable to other data points. The BSFC data for these points from the DOE/Ricardo report is comparable to other data points with no changes. Examination of the ISFC data with these facts in mind leads to the general trend for both engines that the ISFC declines very slightly with increasing imep, particularly with the better quality fuels. Injection timing retard generally results in a slight increase in ISFC.

Mass particulates data (ISPart) demonstrated a wide variation. There was no consistent trend discernable for all fuels. Retarded injection timing tends to increase ISPart emissions for most fuels, particularly at light load conditions.

Specific hydrocarbon emissions (ISHC) tended to decrease with increasing imep for all fuels. Retarded injection timing caused significant increases in ISHC emissions in several cases. The effect was particularly noticeable at light load.

The Bosch Smoke number clearly increased with load (imep) for all fuels. Retarded injection timing tends to increase the smoke somewhat at full load.

The combustion period in  $CA^\circ$  generally increased with load (imep) for both engines and all fuels at optimum injection timing. The effect was more pronounced for the IDI engine. Also, for the IDI engine, the influence of injection timing retard was not significant. For the DI engine, retarded injection timing tended to lengthen the combustion period at light load and to reduce combustion period at full load.

The rate of pressure rise was substantially different for the DI and IDI engines. The most obvious difference was that the rates for the DI engine were on the order of 5 to 10 times larger than those for the IDI engine. This, of course, is indicative of the major difference in these two combustion systems. For the IDI engine, rate of pressure rise was relatively insensitive to load (imep). Retarding the injection timing noticeably reduced rate of pressure rise for all fuels in the IDI engine. The rate of pressure rise data for the DI engine demonstrated wide variation, although for most of the fuels there was an increase at full load. Retarded injection timing noticeably reduced the rate of pressure rise for all fuels in the DI engine also.

For both engines the peak cylinder pressure demonstrated an increase with load (imep). For the IDI engine the increase was slight but observable. For the DI engine the increase was significant and on the order of 100 to 150 psi. In both cases, retarded injection timing significantly reduced the peak cylinder pressure. For the IDI engine the reduction was approximately 100-200 psi. For the DI engine, the reduction was typically 150-300 psi. Similar behavior was observed for all fuels.

There was noticeable variation in the estimated bulk gas temperature for the IDI engine. The general trend was to increase slightly with load (imep). Retarded injection timing had a very slight tendency to raise the temperature. The bulk gas temperature estimate for the DI engine was reasonably consistent, generally increasing with load. Retarded injection timing consistently caused a small increase in the temperature. The estimated temperature for the DI engine was significantly higher than that for the IDI engine. This result is due to the fact that the DI engine has a larger value for the compression index than the IDI engine. Reduced heat transfer losses during compression probably account for this result.

Ignition delay data showed some variation. For optimum timing, both engines showed essentially no sensitivity of ignition delay to load. Retarded injection timing showed a tendency to increase ignition delay. The effect was more pronounced for the IDI engine.

Pre-mixed Combustion Fraction (PCF) and Pre-mixed Combustion Index (PCI) demonstrated different characteristics for the IDI and DI engines. For the IDI engine the data was variable and there was no obvious trend with load or retard. The values of PCF and PCI for the IDI engine were also small, indicating that a relatively small fraction of the combustion process occurred in the pre-mixed mode. The data for PCF and PCI

for the DI engine demonstrated a pronounced trend of lower values with increased load. The values for PCF and PCI were much larger for the DI engine than for the IDI engine, indicating a larger fraction of the combustion process for the DI engine occurred in the pre-mixed mode. Retarded injection timing did not have a consistent effect on values of PCF and PCI for the DI engine.

There was wide variation in the data for diffusion combustion index (DCI) for both the IDI and DI engines. For the IDI engine, there were no obvious effects due to load or injection timing retard. Large values for DCI indicate, as expected, a large diffusion combustion component for the IDI engine. The DCI data for the DI engine also showed wide variation with a trend to increase with load. Injection timing retard generally caused an increase in DCI for the DI engine. The combustion process for the DI engine demonstrated a large pre-mixed fraction as indicated by the values for PCF and PCI. The fact that the values for DCI were significantly lower than those for the IDI engine indicate that the anticipated reduction in the diffusion fraction did occur.

#### 6.5.2 Fuel Effects, Ricardo Engines

The preceding section characterizing the cetane engine described the effects of the different fuels on the dependent variables by comparing results for each fuel to those for the DOE #1 fuel. The same approach is used for characterizing fuel performance in the Ricardo engines. The following paragraphs contain observations developed from examination and comparison of figures 6-58 through 6-63 and deal with how different fuels altered engine performance, emissions, and combustion characteristics. Unless a specific mention of IDI or DI engine is made, comments are meant to apply to both engines.

Air-fuel ratio has little sensitivity to the fuel being used. This result was expected since all the fuels have similar mass energy content, and diesel engine power output is controlled by fuel flow.

ISNO<sub>x</sub> emissions for the two engines give some indication that the DOE #3 and DOE #4 fuels might contribute to a reduction in these emissions, particularly at light load conditions. The reduction may not be as great as indicated by the graphical summary data since there are differences of several CA° in the injection timing for different fuels. However, all data are at optimum injection timing or a fixed retard in that injection timing; thus, ISNO<sub>x</sub> sensitivity to injection timing might not be as significant a factor as with a timing change for a given fuel.

Data variability for ISFC was not large on a percentage of value basis; however, it was sufficient to preclude drawing firm conclusions concerning fuel effects on ISFC. Discrepancies between relative values for ISFC and BSFC (from the DOE/Ricardo report) again lead to the question of the accuracy of the value for bmep given in the DOE/Ricardo Report. The discrepancies do not appear to be large, but they are significant enough to preclude detecting minor changes in ISFC due to fuel differences.

Mass particulate emissions (ISPart) were sensitive to fuel and load. At full load, DOE fuels 2, 3, and 4 demonstrated mass particulate emis-



sions comparable to or lower than those for the DOE #1 reference fuel. This relationship also existed for retarded injection timing at full load. At light load, the relationship reversed, and the mass particulate emissions for DOE fuels 2, 3, and 4 were comparable to or higher than those for the reference fuel. DOE #3 had substantially higher (factors of 5 and 10) ISPart emissions than the reference fuel for light load and retarded injection timing. The light load, retarded injection timing test condition seemed to create the greatest change in the ISPart emissions with fuel quality changes. Both the IDI and the DI engine provided similar results, although the magnitude of the changes observed was different.

Unburned hydrocarbon emissions (ISHC) behave in a fashion similar to the mass particulate emissions. The differences in ISHC emissions between DOE fuels 2, 3, and 4 and those for the DOE #1 reference fuel are smaller at full load conditions than at light load. Compared to the reference fuel, for the IDI engine at full load, fuels 2, 3, and 4 produced lower ISHC emissions with optimum injection timing and higher ISHC emissions at retarded injection timing. For the DI engine at full load, the emissions for fuels 2, 3, and 4 were greater than those for the reference fuel, both for optimum injection timing and for retarded injection timing. At light load the ISHC emissions for fuels 2, 3, and 4 were significantly greater than those for the reference fuel, both at optimum and retarded injection timing and for both engines. Retarded injection timing at light load produced increased ISHC emissions for DOE #3 fuel of approximately 200% for the DI engine and 1000% for the IDI engine.

DOE fuels 2, 3, and 4 did not appear to cause any major changes in the Bosch smoke measurement, compared to the DOE #1 fuel. The DOE #4 fuel yielded consistently lower results than the other fuels for both engines. No similar conclusion could be drawn for the other fuels.

There was no clear indication that any of the test fuels had a major influence on the combustion period. In the IDI engine, combustion period was relatively insensitive to the fuel being used. The DI engine seemed to have some sensitivity to fuel type at retarded injection timing conditions. For full load operation of the DI engine with retarded timing, the combustion period decreased for the DOE fuels 2, 3, and 4 compared to the combustion period for the DOE #1 fuel. At light load operation of the DI engine with retarded timing, the effect appeared to be reversed, and fuels 2, 3, and 4 had significantly longer combustion periods than the DOE #1 fuel.

For the IDI engine there were no pronounced changes in the rate of pressure rise due to fuel type. The DI engine, on the other hand, demonstrated some fuel sensitivity in this variable. At full load conditions for the DI engine, DOE fuels 2, 3, and 4 demonstrated increased rates of pressure rise over the DOE #1 fuel, both for optimum and retarded timing. Light load operation of the DI engine produced an inverse effect. Generally, the DOE fuels 2, 3, and 4 caused a reduced rate of pressure rise compared to the reference DOE #1, both for optimum and retarded timing. The DOE #2 fuel did not follow this trend, and the rate of pressure rise was comparable to or somewhat greater than the rate for DOE #1.

The peak combustion pressure results were somewhat similar to those for rate of pressure rise. For the IDI engine, peak combustion pressure was relatively insensitive to different fuels, although there was evidence of reduced peak pressure for DOE #2 over DOE #1 at light load. The peak pressure showed relative insensitivity to fuel type for the DI engine at full load, both for optimum and retarded timing. At light load and optimum timing, however, DOE fuels 3 and 4 demonstrated reduced peak pressure from that for DOE #1. Light load and retarded timing for the DI engine did not seem to produce a fuel sensitivity result for peak combustion pressure.

Even though there is some data variability, the estimated bulk gas temperature does not appear to demonstrate any significant fuel type effects for either the DI or the IDI engine. This result was expected since the estimate of this temperature should depend primarily on the starting temperature and the compression index.

As with the cetane engine, ignition delay was one of the variables most sensitive to fuel changes. For virtually all cases, DOE fuels 2, 3, and 4 demonstrated longer ignition delays than the DOE #1 reference fuel. The effect was slightly more pronounced at the retarded injection timing conditions. DOE fuel #2 was the exception and had a shorter ignition delay when operated in the IDI engine at full load and retarded injection timing conditions. It was also noted that the increases in ignition delay for fuels 2, 3, and 4 over the reference fuel were more consistent at the light load condition, both for optimum and retarded injection timing.

Pre-mixed Combustion Fraction (PCF) and Pre-mixed Combustion Index (PCI) behaved in a comparable fashion for each engine; however, behavior in the IDI engine was quite different than behavior in the DI engine. In the IDI engine the values for PCF and PCI were low, and there did not appear to be a clear relationship between the value of the variable and the fuel type. The DI engine, on the other hand, demonstrated significantly higher values for PCF and PCI, and the values for DOE fuels 2, 3, and 4 were comparable to or greater than the values for DOE #1. In fact, the relative changes were quite similar to the relative changes exhibited by the ignition delay for the DI engine.

The Diffusion Combustion Index (DCI) behaved differently for the IDI and DI engines. For the IDI engine values of DCI were relatively high. There was some indication that DOE fuels 2, 3, and 4 tended to have lower values for DCI than DOE #1; however, this was not true in all cases. Results for the DI engine seemed to reverse with load (imep). At full load there was a trend for the DCI for fuels 2, 3, and 4 to increase over that for DOE #1, both at optimum and retarded injection timing. At light load conditions, this behavior was essentially reversed and DCI values for fuels 2, 3, and 4 were comparable to or lower than the values for DOE #1.

#### 6.6 Comparison of Results from Cetane and Ricardo Engines

The air-fuel ratio for all three engines was a function only of engine load as anticipated, and no further comparison is needed. The general trend of the ISNO<sub>x</sub> emissions was similar for all three engines.

In the cetane engine there were obvious increases for DOE fuels 2, 3, and 4 over DOE #1. The Ricardo IDI and DI engines exhibited similar, but less pronounced behavior for these fuels. Some of the differences are attributed to injection timing differences between fuels observed with the Ricardo Engines.

There were obvious differences between the ISFC characteristics for the cetane engine and those for the Ricardo engines. ISFC tended to increase with load for the cetane engine while the Ricardo Engines showed decreases with load. This difference is thought to be related to the very high internal friction of the cetane engine. There were slight differences in ISFC for different fuels; however, there were no obvious trends for any of the three engines.

There were some similarities between engines for ISPart emissions; however, only a slight increase in level at retarded injection timing for light loads could be compared. The DOE #4 fuel showed consistently lower ISPart levels than DOE #1 for all engines. There was no consistent behavior for the DOE #2, and #3 fuels for all engines.

There was generally similar behavior for ISHC emissions between engines. These emissions tended to decrease with increasing load (imep) and to increase with retarded injection timing. As mentioned in an earlier section, there was significant variability in the ISHC data and the results were too inconsistent to draw any conclusions about fuel effects between the engines.

Bosch smoke numbers displayed a very similar behavior for all three engines; increasing with load and showing slight increases for cases with retarded injection timing. The DOE #4 fuel demonstrated a consistently lower Bosch smoke number than the DOE #1 fuel when used in the cetane engine. This was not the case for either of the Ricardo engines. There were no consistently identifiable changes in Bosch smoke number for DOE fuels 2 and 3 compared to DOE #1, either for the cetane engine or for the Ricardo engines.

The combustion period behaved similarly for all three engines; increasing with load. The DOE #4 fuel demonstrated a 10-20% shorter combustion period over DOE #1 in the cetane engine. There was no comparable effect for the Ricardo engines. No other fuel related effects were noticed.

The rate of pressure rise for the cetane engine was similar to that of the Ricardo IDI engine; relatively insensitive to load. For all three engines the rate of pressure rise was reduced with retarded injection timing. The DOE #4 fuel demonstrated rates of pressure rise 10-100% higher than those for DOE #1 in the cetane engine at light load. Neither Ricardo engine showed a similar effect. In fact, the rate of pressure rise for DOE #4 fuel in the DI engine was actually 50% lower than that for DOE #1 at light load conditions.

The cetane engine and the Ricardo IDI engine demonstrated similar peak cylinder pressure characteristics; a slight increase with engine load. All three engines demonstrated a significant drop in peak pressure with retarded injection timing. The DOE #4 fuel produced 10-20%

higher peak pressures than DOE #1 in the cetane engine. No similar effect was observed for the Ricardo engines.

Both Ricardo engines demonstrated a slight increase in the estimated bulk gas temperature with engine load. This effect was not observed in the cetane engine. The estimated bulk gas temperature was primarily a function of the inlet air temperature and the compression index. Different fuels had virtually no effect on this variable.

The ignition delay for all three engines demonstrated insensitivity to load (imep). The Ricardo engines showed a slight sensitivity to retarded injection timing that was not obvious for the cetane engine. All three engines exhibited increasing ignition delay for DOE fuels 2, 3, and 4 over DOE #1. The IDI engine demonstrated the greatest sensitivity and the DI engine the least sensitivity. The cetane engine seemed to produce results that were more consistent with other fuel characteristics. For example, DOE #4, the fuel with the lowest cetane number, had the longest ignition delay at light load condition in the cetane engine.

The cetane engine and the Ricardo IDI engine demonstrated similar results for the calculated combustion parameters PCF and PCI. The values were small (less than 0.2) and relatively insensitive to engine load or injection timing retard. The Ricardo DI engine demonstrated substantially larger values for PCF and PCI, and there was a pronounced trend to lower values with increased load. The only observed fuel effect was for DOE #4 in the cetane engine. The value for PCI was typically 10-20% lower than that for the DOE #1 reference fuel. There were no strong fuel related trends for the Ricardo engines.

The cetane and Ricardo IDI engines also demonstrated similar behavior for the calculated combustion parameter DCI. The data had noticeable variation and were relatively insensitive to engine load and retarded injection timing. The relatively large values of DCI (typically greater than 0.8) indicated significant diffusion burning in these engines. The Ricardo DI engine also demonstrated a wide variation in data; however, an increase in DCI with load was obvious. Also, retarded injection timing caused an increase in DCI. There were not pronounced effects for fuel changes in any of the three engines. The most noticeable change was an increase in the DCI of 10-20% for DOE #4 fuel over DOE #1 in the cetane engine. The DOE #4 fuel exhibited generally lower values for DCI compared to DOE #1 in both Ricardo engines.

## 6.7 Ranking of Fuels

Ranking of the fuels was done using only the information from the cetane engine test program since this was the only data that contained results for all ten test fuels. The fuel related effects described in section 6.4.2 were reviewed, and those results having some consistent change due to fuel were identified. A crude matrix of the fuels and these variables was prepared and is shown in table 6-7. The change in the variable from the DOE #1 fuel is shown as N for nominal or no change, + for an increase in the variable, and - for a decrease in the variable. The number of + or - signs is indicative of the size of the change.

The variables  $dP/d\theta$  and ignition delay (IGN. DEL.) were weighted most heavily in the fuel ranking process.  $ISNO_x$  was also used as a strong indicator, and the remaining variables were used in making decisions between fuels that were otherwise closely ranked. Increases in  $dP/d\theta$ , ignition delay, and  $ISNO_x$  were considered indications of poorer fuel quality. A shorter combustion period (COMB. PER.) coupled with a longer ignition delay was also considered to be an indication of poorer combustion of the fuel. Using these criteria, the ranking shown in table 6-8 was established from the information in table 6-7. It should be noted that the ranking process was based entirely on the output results from the engine and not on the measured fuel properties. The cetane number of the ranked fuels is shown for reference information only. It was not used in ranking the fuels.

Table 6-7

Fuels - Results Matrix for Use in Ranking\* Fuels

Fuel	$dP/d\theta$	IGN. DEL.	COMB. PER.	PCF PCI	DCI	$ISNO_x$	ISPart	Bosch NO
DOE #1	N	N	N	N	N	N	N	N
DOE #2	+	++	N	N	N	+	N	N
DOE #3	++	++	N	N	N	++	N to -	N
DOE #4	+++	+++	--	-	+	+++	---	--
CEC #1	N	N	N	N	N	N to +	N to -	N
CEC #2	+	++	-	--	N	N to +	---	N
CEC #2A	+	++	--	--	N	+++	N	N
CEC #3	+	++	--	N	N	+++	---	-
CAPE #5	N	--	N	N	N	N to +	--	-
CAPE #6	+++	+++	---	+++	+	++++	---	---

\*Referenced to DOE #1, N = no change, + = increase, - = decrease

Table 6-8

## Ranking of Ten Test Fuels

RANK	FUEL	CETANE <sup>1</sup> NUMBER	NOTES
1	CAPE #5	53.1	These fuels were obviously the best and easily ranked in this order.
2	CEC #1	49.8	
3	DOE #1	50.1	
4	CEC #2	48	These fuels demonstrated roughly similar behavior and considerably more judgement was used in the ranking process.
5	DOE #2	41.6	
6	CEC #2A	43.2	
7	DOE #3	40.7	
8	CEC #3	39.3	
9	DOE #4	36.2	These fuels were obviously the worst and easily ranked in this order.
10	CAPE #6	33.9	

<sup>1</sup> Cetane Number included for reference only, it was not used in ranking the fuels.

## 7. Conclusions and Recommendations

Although this program involved significant time and effort, the conclusions that can be drawn from the results are relatively short and direct. The major conclusions are:

1. The cetane engine can be operated at conditions more representative of commercial design diesel engines and can provide consistent results for engine performance, emissions, and combustion characteristics. Considerably more effort and attention to detail in operating and maintenance procedures is required for using the cetane engine in this manner than for diesel engines of current design.
2. The results obtained from the cetane engine test program indicate that cetane number is a good indicator of fuel behavior in the cetane engine. High cetane number fuels had good combustion and performance characteristics, and low cetane fuels had poor combustion and performance characteristics.
3. For the comparisons possible, the emissions, performance, and combustion characteristics of the cetane engine were not readily comparable to those of the Ricardo engines. Thus, even though consistent results were obtained with the cetane engine, their ability to predict fuel behavior in current design engines is questionable.
4. The results from the cetane engine test program showed similarities to results obtained from the Ricardo IDI engine. The similarities were not sufficient to provide accurate predictions about fuel behavior in the Ricardo IDI engine from the cetane engine results.
5. The results from the cetane engine test program showed few similarities to results obtained from the Ricardo DI engine. Major discrepancies were noted. It was obvious that some of these discrepancies were related to the difference in combustion for DI and IDI engines.

These conclusions are based upon a very restricted comparison between the results from the cetane engine test program and some of the results from the DOE/Ricardo program. They should not be considered representative of conclusions that might be drawn from comparison of the cetane engine data with results from a wider variety of engine tests done under similar conditions. Recommendations to be considered are:

1. Reduce the remaining DOE/Ricardo engine data for different speed and load conditions to determine if this larger data base will confirm or alter the conclusions reached concerning comparison with cetane engine data.
2. Obtain and reformulate engine test results from the CEC program so that comparisons can be made directly with the cetane engine data.

3. Refine and improve the data reduction and analysis process for the cetane engine data to improve consistency and accuracy of results, particularly in the area of apparent heat release computations and determination of combustion parameters.
4. Investigate testing conditions with the cetane engine using refrigerated intake air to simulate cold weather operating conditions. The test would be more severe at light load conditions. The relative behavior of the primary and secondary reference fuels should also be investigated at this low temperature test condition.
5. Investigate ways in which the large amount of detailed cetane engine data generated for this project can be made more readily available for analysis by other interested parties.



## References

- 1-1 Baker, Q. A., "Alternate Fuels for Medium-Speed Diesel Engines", Society of Automotive Engineers Paper 80030, February, 1980.
- 1-2 Tuteja, A. D., and Clark, D. E., "Comparative Performance and Emission Characteristics of Petroleum, Oil Shale and Tar Sands Derived Diesel Fuels", Society of Automotive Engineers Paper 800331, February, 1980.
- 1-3 Ryan, III, T. W., Storment, J. O., Wright, B. R., and Waytulonis, R., "The effect of Fuel Properties and Composition on Diesel Engine Exhaust Emissions - A Review", Society of Automotive Engineers Paper 810953, 1981.
- 1-4 Hardenberg, H. O., and Ehnert, E. R., "Ignition Quality Determination Problems with Alternative Fuels for Compression Ignition Engines", Society of Automotive Engineers Paper 811212, 1981.
- 1-5 Trevitz, S. S., Lestz, S. S., and Taylor, W. D., "Single-Cylinder Diesel Engine Study of Several Shale and Coal-Derived Fuels", Society of Automotive Engineers Paper 841333, 1984.
- 1-6 Webster, G. D., Chiappetta, S. J., Neill, W. S., Glavincevski, B., and Strigner, P. L., "High Speed Diesel Performance/Combustion Characteristics Correlated with Sturctural Composition of Tar Sands Derived Experimental Fuels", Society of Automotive Engineers Paper 850240, February, 1985.
- 1-7 Gilder, O. L., Glavincevski, B., and Burton, G. F., "Ignition Quality Rating Methods for Diesel Fuels - A Critical Appraisal", Society of Automotive Engineers Paper 852080, 1985.
- 1-8 Needham, J. R., and Doyle, D. M., "The Combustion and Ignition Quality of Alternative Fuels in Light Duty Engines", Society of Automotive Engineers Paper 852101, 1985.
- 1-9 Siebers, D. L., "Ignition Delay Characteristics of Alternative Diesel Fuels: Implications on Cetane Number", Society of Automotive Engineers Paper 852102, 1985.
- 1-10 Neill, W. S., Wolf, W. M., and Webster, G. D., "Cold Temperature Diesel Performance/Combustion with Canadian Low Ignition Quality Fuels", Society of Automotive Engineers Paper 860251, 1986.
- 1-11 Ryan, III, T. W., "Diesel Fuel Ignition Quality as Determined in a Variable Compression Ratio, Direct-Injection Engine", Society of Automotive Engineers Paper 870585, February, 1987.
- 1-12 Doyle, D. M. and Needham, J. R., "Investigation Into Alternative Fuel Rating Techniques", Final Report for U.S. Department of Energy contract DE-AC01-83CE50010, Document Number DOE/CE/50010-1, November, 1985.

### References (Continued)

- 1-13 Hare, C. T., "Study of the Effects of Fuel Composition, and Injection and Combustion System Type and Adjustment, on Exhaust Emissions from Light-Duty Diesels", Final Report for Coordinating Research Council project CAPE-32-80, April, 1985.
- 3-1 MacDonald, J. S., Plee, S. L., D'Arcy, J. B. and Schreck, R. M., "Experimental Measurements of the Independent Effects of Dilution Ratio and Filter Temperature on Diesel Exhaust Particulate Samples", Society of Automotive Engineers Paper 800185, February, 1980.
- 4-1 Johnson, R. T. , Freeburg, S. E. and Stoffer, J. O., "Alcohol Petroleum Systems as Fuels for Diesel Engines", U.S. Department of Energy report DOE/CS/50026-1 (DE82020752), June, 1982.
- 4-2 Johnson, R. T. and Stoffer, J. S., "Single Cylinder Engine Evaluation of Stabilized Diesel Fuels Containing Alcohols", Society of Automotive Engineers Paper 830559, March, 1983.
- 4-3 Johnson, R. T. and Stoffer, J. S., "Performance of Stabilized Diesel Fuels Containing Alcohols and Water in Single and Multicylinder Direct Injection Engines", Society of Automotive Engineers Paper 830557, March, 1983.
- 5-1 Stivender, D.L., "Development of a Fuel Based Mass Emission Measurement Procedure", Society of Automotive Engineers paper 710604, 1971.
- 5-2 Douaud, A. and Eyzat, P., "DIGITAP - An On-Line Acquisition and Processing System for Instantaneous Engine Data - Applications", Society of Automotive Engineers paper 770218, February, 1977.
- 5-3 Rassweiler, G.M., and Withrow, L., "Motion Pictures of Engine Flames Correlated with Pressure Cards", Society of Automotive Engineers Transactions, Vol 42, No. 5, pp185-204, 1938.
- 5-4 Wade, W.R., White, J.E., Jones, C.M., Hunter, C.E., and Hansen, S.P., "Combustion, Friction and Fuel Tolerance Improvements for the IDI Diesel Engine", Society of Automotive Engineers paper 840515, February, 1984.
- 6-1 Telephone and letter correspondence with Mr. D. M. Doyle of Ricardo Consulting Engineers, Ltd., England.

END

DATE

FILMED

8-88

DTIC